NASA CR-72564
APS-5286-R

FINAL REPORT
1200-HZ BRAYTON ELECTRICAL RESEARCH COMPONENTS

Prepared Under Contract NAS3-9427
by
AiResearch Manufacturing Company of Arizona
A Division of The Garrett Corporation
for
National Aeronautics and Space Administration

NOTICE

Requests for copies of this report should be referred to

National Aeronautics and Space Administration
Office of Scientific and Technical Information
Attention: ATSS
Washington, D.C. 20546

AIRESEARCH MANUFACTURING COMPANY OF ARIZONA
A DIVISION OF THE GARRETT CORPORATION

NASA CR-72564
APS-5286-R

FINAL REPORT
1200-HZ BRAYTON ELECTRICAL RESEARCH COMPONENTS

Prepared Under Contract NAS3-9427
by
AiResearch Manufacturing Company of Arizona
A Division of The Garrett Corporation
March 19, 1969
for
National Aeronautics and Space Administration
Lewis Research Center

Technical Management

Space Power Systems Division
James H. Dunn

ABSTRACT

The AiResearch Manufacturing Company of Arizona, A Division of The Garrett Corporation, designed and fabricated the electrical components for a 1200-Hz Brayton energy conversion system. These components consist of a high efficiency Rice four-pole brushless 10.5-KW alternator, a voltage regulator/exciter, and a parasitic load-type speed control. Together, these three units comprise the alternator research package (ARP). The alternator was designed with oil-mist lubricated ball bearings. However, the specifications require the minimization of the magnetic load unbalance on the bearings to permit the future application of gas lubricated bearings.

Both series and shunt field control are provided in the voltage regulator/exciter to maintain steady-state regulation within ±1 percent of rated voltage with loads from 10 to 100 percent at 0.75 lagging power factor. The speed control is designed to maintain speed (frequency) regulation of 1200 Hz ±1.0 percent under steady-state conditions.

TABLE OF CONTENTS
ALTERNATOR RESEARCH PACKAGE FINAL REPORT

TABLE OF CONTENTS (Contd.)

LIST OF FIGURES

LIST OF FIGURES (Contd.)

Page

LIST OF FIGURES (Contd.)

LIST OF TABLES

LIST OF APPENDICES

AIRESEARCH MANUFACTURING COMPANY OF ARIZONA
A DIVISION OF THE GARRETT CORPORATION

FINAL REPORT
1200-HZ BRAYTON ELECTRICAL RESEARCH COMPONENTS

by

AiResearch Manufacturing Company of Arizona

SUMMARY

The electrical components for a 1200-Hz Brayton energy conversion system have been designed and fabricated. The components consist of a brushless alternator having a rated output of 10.5 KW and the electrical power system controls, consisting of an alternator voltage regulator, a series controller, and a parasitic-type speed controller.

The alternator is a 36,000 rpm four-pole Rice machine designed for a power output range of 2.25 to 10.5 KW. The magnetic load unbalance in the alternator has been held to a minimum to permit the future use of gas lubricated bearings. However, the bearings incorporated into this machine are oil-mist lubricated.

The control devices which utilize static components were designed and fabricated as breadboard units. The control units are designed to provide system voltage regulation of ±1 percent, speed regulation of ±1 percent, maximum response times for voltage and speed of 1/4 and 1 sec., respectively. The voltage regulator operates in a switching mode. Multiple-speed controllers are provided. The components were designed to operate at the highest practical efficiency.

1.0 INTRODUCTION

NASA is currently engaged in a program to develop a prototype Brayton energy conversion system. The electrical components, as discussed in this report, were designed and fabricated to facilitate early evaluation of components of this energy conversion system. The purpose of this program is to establish the performance characteristics of an alternator and associated electronic controls which would electrically and magnetically satisfy the needs of a space power conversion system.

This power conversion system utilizes electrical components similar in configuration to those used in previous systems with the exception that the rotor speed and gas characteristics are different. These differences tend to increase the alternator windage losses.

For instance, the system gas pressure, compared to the previous two-spool Brayton conversion system, is approximately four times greater; the gas molecular weight is twice as large, and the speed is three times greater at basically the same power level. These differences result in a need for a rotor design which minimizes the windage loss. The alternator design used is based on the Rice patent. Windage losses are reduced to approximately 30 percent of those which would result were the homopolar induction alternator design used. This latter type of alternator has been used in various power conversion systems developed at NASA-Lewis. The electrical components were designed by the AiResearch Manufacturing Company, A Division of The Garrett Corporation, while the component development is being conducted at the NASA-Lewis Research Center.

2.0 SPECIFICATIONS

Specifications for the electrical components were established by NASA Contract NAS 3-9427, Exhibit "A", as revised in Supplemental Agreement dated July 6, 1967.

2.1 Alternator Specifications

(a) Alternator to be radial-gap type with stationary excitation coil
(b) Alternator to be capable of motoring
(c) Unbalanced magnetic forces to be minimized
(d) Rated frequency: 1200 Hz at 36,000 rpm (four poles)
(e) Maximum operating speed: 43,200 rpm (120 percent of design)
(f) Continuous rating:
    12.6 KVA at 0.85 pf
    14.3 KVA at 0.75 pf
(g) Five-second rating:
    21.3 KVA at 0.75 pf
(h) Voltage: three-phase, 120/208 V ±1 percent from 10 to 100 percent load.
(i) Requirements of MIL-G-6099A (ASG) apply to:
    (1) Waveform, paragraph 4.5.16, except total RMS harmonic content of line-to-neutral voltage with 10 to 100 percent pure resistive load shall be less than 5 percent
    (2) Phase Balance, paragraphs 4.5.10, 4.5.10.1, and 4.5.10.2, except individual phase voltage deviation is 1.5, 3, and 6 percent as appropriate in paragraph 4.5.10.1.
    (3) Output Voltage Modulation, paragraph 4.5.13, except limit is 0.5 percent.

2.2 Voltage Regulator/Exciter (VRE) Specifications - The following paragraphs define the requirements for the voltage regulator/exciter:

(a) Voltage Regulation - Plus or minus 1 percent for combined 10 to 100 percent load and ±10 percent speed variation at 0.75 lagging power factor.

(b) Voltage Drift - The voltage drift is specified as 1.0 V maximum at any fixed load between 10 and 100 percent at 0.75 lagging power factor (voltage to remain within the 2 percent band defined in the preceding paragraph).

(c) Applicable Requirements of MIL-G-6099A

Voltage Excursion - In accordance with Figure 3 of MIL-G-6099A except that the recovery time to within 5 percent of nominal voltage may be 0.25 sec.

Voltage Adjustment - In accordance with paragraph 3.3.5.1 of MIL-G-6099A.

Short-Circuit Capacity - In accordance with paragraph 4.5.12 of MIL-G-6099A.

(d) Abnormal Operating Conditions - Electrical components shall perform as specified in the following under abnormal operating conditions indicated.

Under abnormal system operating conditions, the VRE shall not be the limiting element.

The system shall operate for at least 5 sec. at an overload of 21 KVA at rated voltage, 0.75 lagging power factor, applied at rated speed and at stabilized rated-load temperature.

At 1800 Hz (1.5 times rated speed) and zero to rated load, the output voltage is to differ from nominal by no more than 5 percent.

At 600 Hz (half-rated speed) and zero load, the output voltage is to differ from nominal by no more than 40 percent.

Temperature was not specified for the research VRE package. A temperature range of -25° to +75°C was selected. The upper limit was selected on the basis of an expected future cold-plate temperature of 65°C. The lower limit was chosen arbitrarily, based on the -18°C specifications commonly used for this type of equipment in other space programs.

(e) Components - Components are to be selected to be replaceable with types suitable for flight without circuit changes. Actual hardware is to be fabricated of military components and of high-quality, reliable commercial parts.

(f) Electrical Interference - The VRE shall be designed to meet the requirements of MIL-STD-826.

(g) Parts Interchangeability - All parts shall be interchangeable in accordance with the requirements of paragraph 3.4 of MIL-G-6099A (ASG).

(h) Packaging - The VRE shall be mounted on a chassis attached to standard 19-in. rack panels. Components and terminations shall be readily accessible for modification, repair, and instrumentation. Although the package will essentially be a breadboard, all components shall be based on flight environmental requirements stated herein--notably heat transfer. In subsequent flight models, all heat shall be transferred by conduction to heat sinks which shall not exceed 150°F.

2.3 Speed-Control Specifications

(a) Speed-Control Type - The speed (frequency) control shall be of the parasitic-loading type.

(b) Frequency Regulation - Frequency regulation shall be as specified in the following:

(1) Steady-state regulation shall be 1200 Hz ±1 percent for a change in load from 10 percent to full load.

(2) Under transient conditions, regulation shall be 1200 Hz ±2 percent with a recovery time of 1.0 sec. (the

frequency shall return and remain within the 2-percent band specified in paragraph (1)), with no sustained oscillations, when tested under step application and removal of one per unit-load.

(3) Modulation shall not exceed ±2 Hz under any load condition from 10 to 100 percent, under all environmental conditions. The frequency shall remain within the 2-percent band specified in paragraph (1).

(4) The drift shall not exceed ±2 Hz at any fixed load from 10 to 100 percent load. The frequency shall remain within the 2-percent band specified in paragraph (1).

(c) Electrical Interference - The speed-control shall be designed to meet the requirements of MIL-STD-826.

(d) No-Load Losses - Special effort shall be made to minimize losses in the control device when the demand for parasitic load is zero.

(e) Harmonic Distortion - Special effort shall be made to minimize the effect of the control device on the harmonic content of the alternator voltage and current.

(f) Control Characteristics - In addition to the frequency regulation specified in paragraph (b) above, the control shall permit the system to start and reach operating speed and shall provide full load to the system for all speeds up to at least 150 percent of design speed to ensure control in case of an accidental overspeed condition.

(g) Voltage Sensitivity - The speed-control sensing device shall be independent of voltage at any steady-state or transient voltage within specifications.

(h) Parts Interchangeability - All parts shall be interchangeable in accordance with the requirements of paragraph 3.4 of MIL-G-6099A (ASG).

(i) Packaging - The speed-control device shall be mounted on a chassis attached to standard 19-in. rack panels. Components and terminations shall be readily accessible for modification, repair, and instrumentation. Although the package will be essentially a breadboard, all components shall be based on flight environmental requirements stated herein--notably heat transfer. In subsequent flight models, all heat shall be transferred by conduction to heat sinks which shall not exceed 150°F.

3.0 DESCRIPTION OF ALTERNATOR

The objective in developing this alternator was to create a component for a practical space power system capable of operating on gas bearings for support of the rotating elements. The running gear is designed for low bearing losses and the package includes complete temperature and pressure instrumentation for performance evaluation. This alternator, however, used an oil-mist lubricated ball bearing system. System considerations established these design criteria for the alternator:

(a) High efficiency (to reduce overall system weight)
(b) Minimum rotor size (to reduce windage loss and bearing load)
(c) Maximum reliability

Evaluation of the applicable system specifications and the various design criteria pertaining to the application of this alternator led to the selection of the Rice configuration (Figures 3-1 and 3-2). AiResearch has considerable experience with the fabrication of Rice alternators. The physical configuration of the alternator is shown on Drawings 699650 and 699651, Appendix II.

The Rice alternator is a brushless, nonrotating coil synchronous alternator (Figure 3-3). The stator has a conventional three-phase winding. In the normal synchronous machine, the field winding is on the rotor and produces a multipolar d-c rotating field. The d-c power is brought to the rotor by slip rings or a rectified rotary exciter. Because of its wound rotor construction, the normal synchronous machine is speed-limited.

The Rice Machine also has a d-c multipolar construction. However, to improve the speed characteristics, the field excitation coil is stationary, and the flux is carried to the rotor through two auxiliary

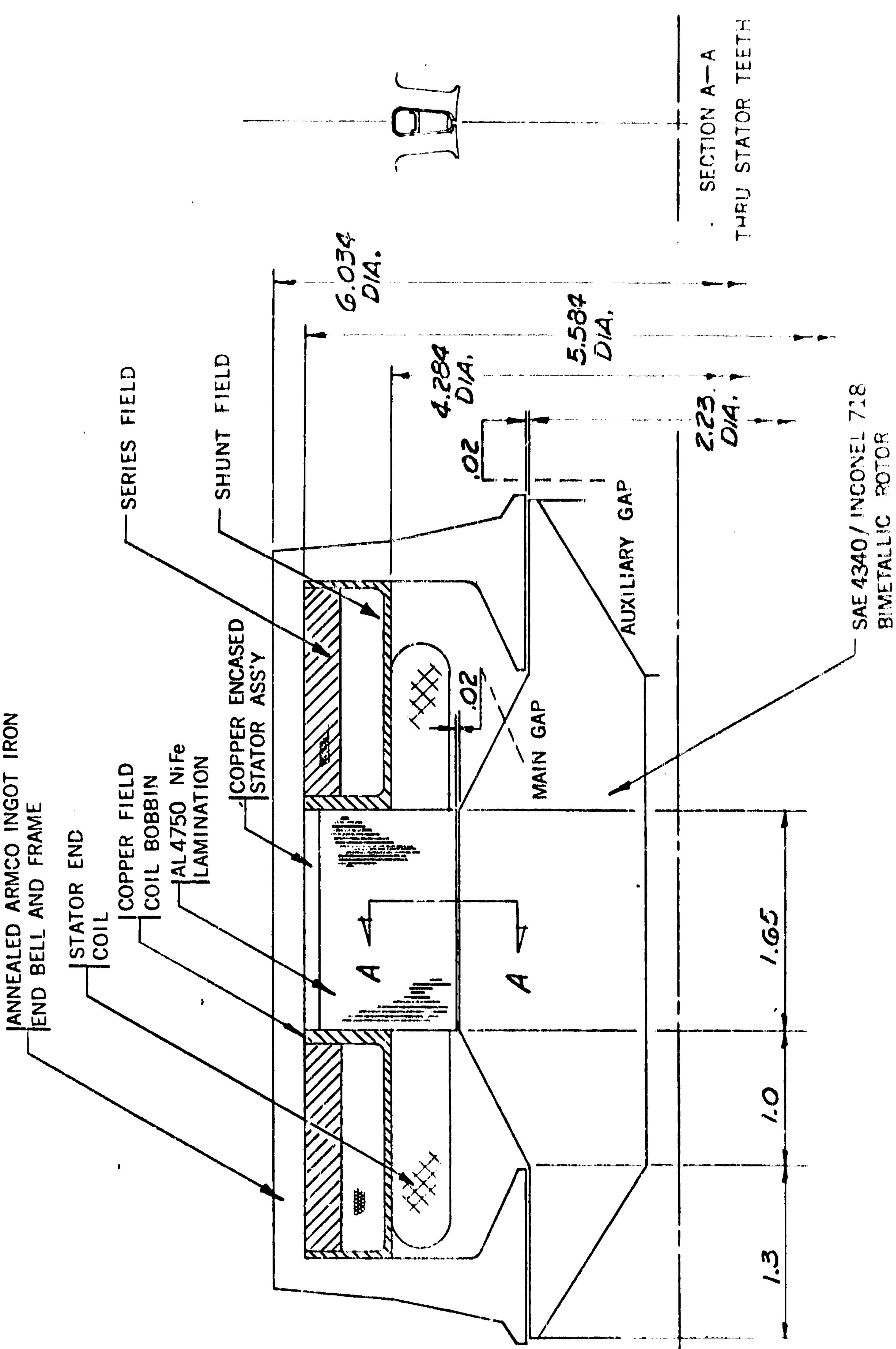

ALTERNATOR SKETCH

FIGURE 3-1

ALTERNATOR RESEARCH PACKAGE COMPONENTS

FIGURE 3-2

RICE ALTERNATOR

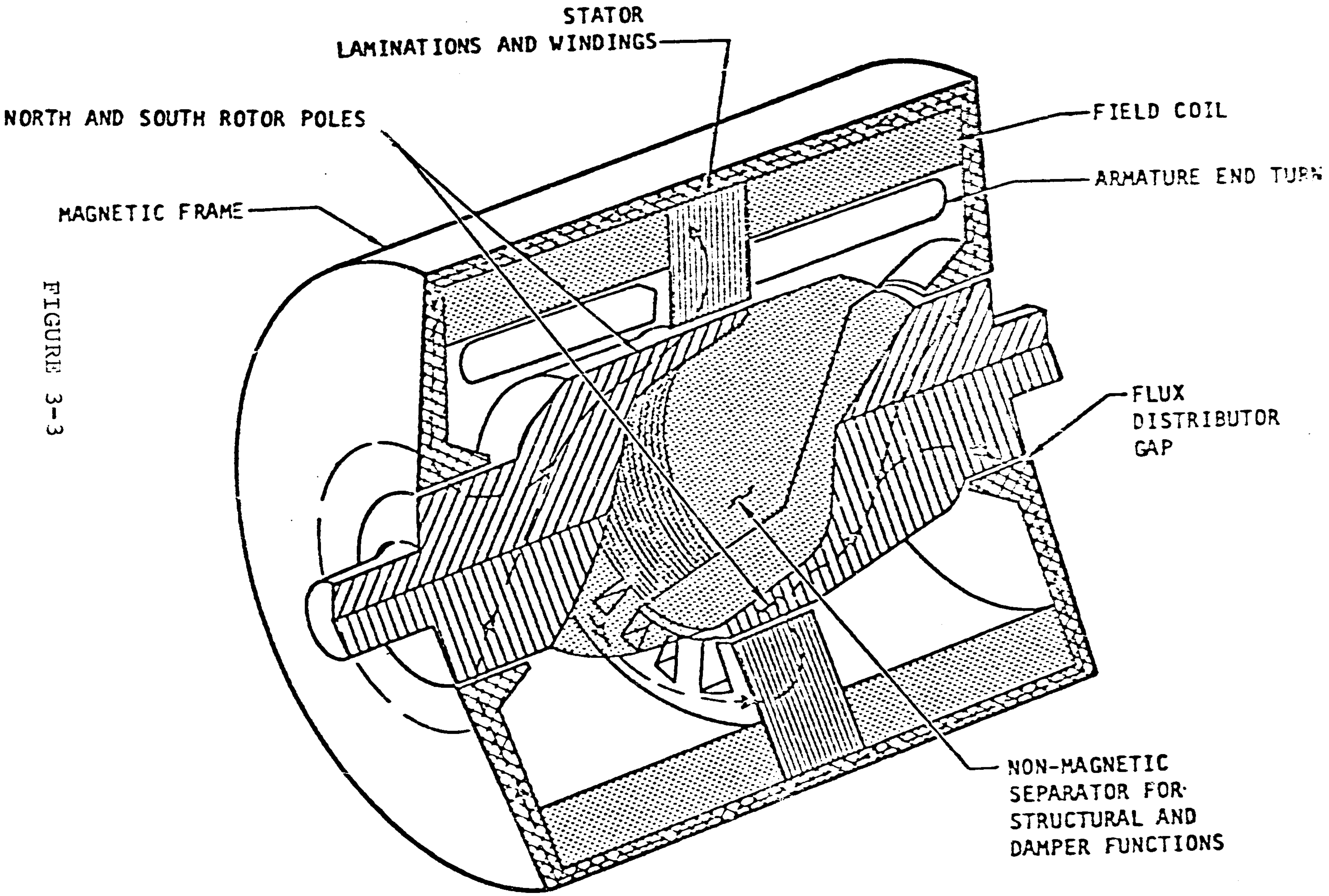

FIGURE 3-3

air gaps at each end of the rotor (Figure 3-1). The north and south pole elements of the rotor conduct flux to the stator windings; the main flux flows through paths of least-magnetic reluctance. The flux is established by the magnetomotive force of stationary excitation coils in the frame of the machine. The magnetically conductive portions of the rotor are separated by a nonmagnetic separator which is primarily a structural element to provide strength, or rigidity, and pole separation in the rotor (Figure 3-4). The separator has secondary functions of windage loss reduction and electromagnetic damping to minimize the flux variations.

The stator laminations are supported in a copper cage to:

(a) Achieve good heat removal to the frame, which is fluid-cooled.
(b) Minimize flow of flux from the stator to the frame and, thus, reduce the possibility of magnetic unbalanced forces arising due to unsymmetrical flux distribution in the air gap.
(c) Hold the stack laminations together without the use of bonding cement or back-iron weldment.

Other significant features of the Rice configuration are:

(a) The alternator frame serves both as a structural member and as a part of the magnetic circuit. The frame and end plates have two functions in addition to their structural function. First, they provide the necessary low-reluctance magnetic circuit for the excitation coils conducting the flux around the fields to the flux collectors or auxiliary gaps at each end of the rotor. Second, they provide a means of conducting heat from the alternator parts to the cooling fluids.

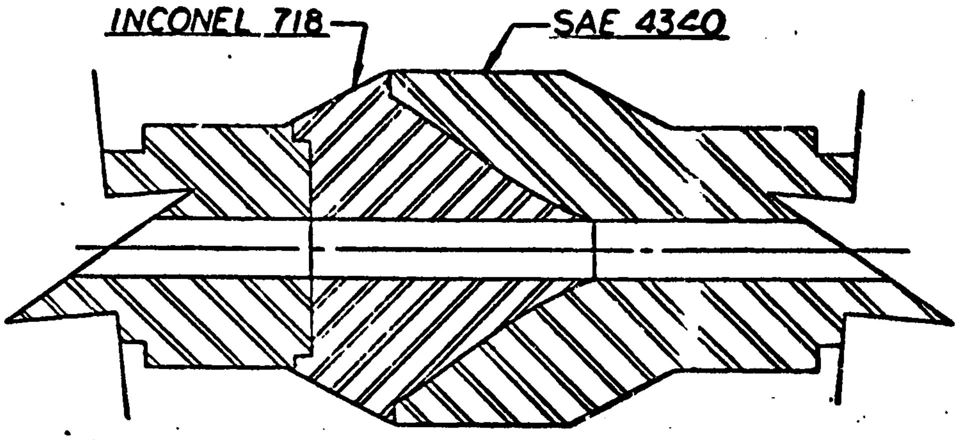

SECTION A-A

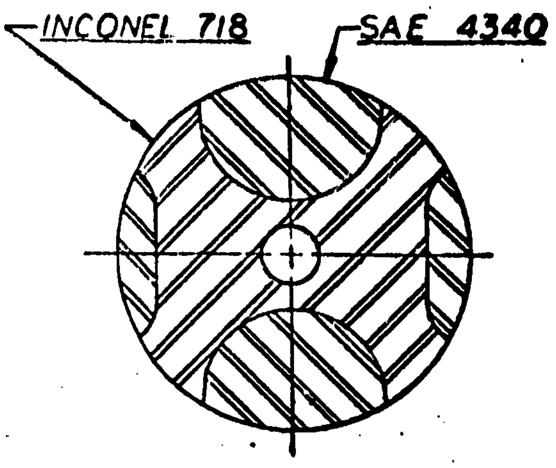

SECTION D-D

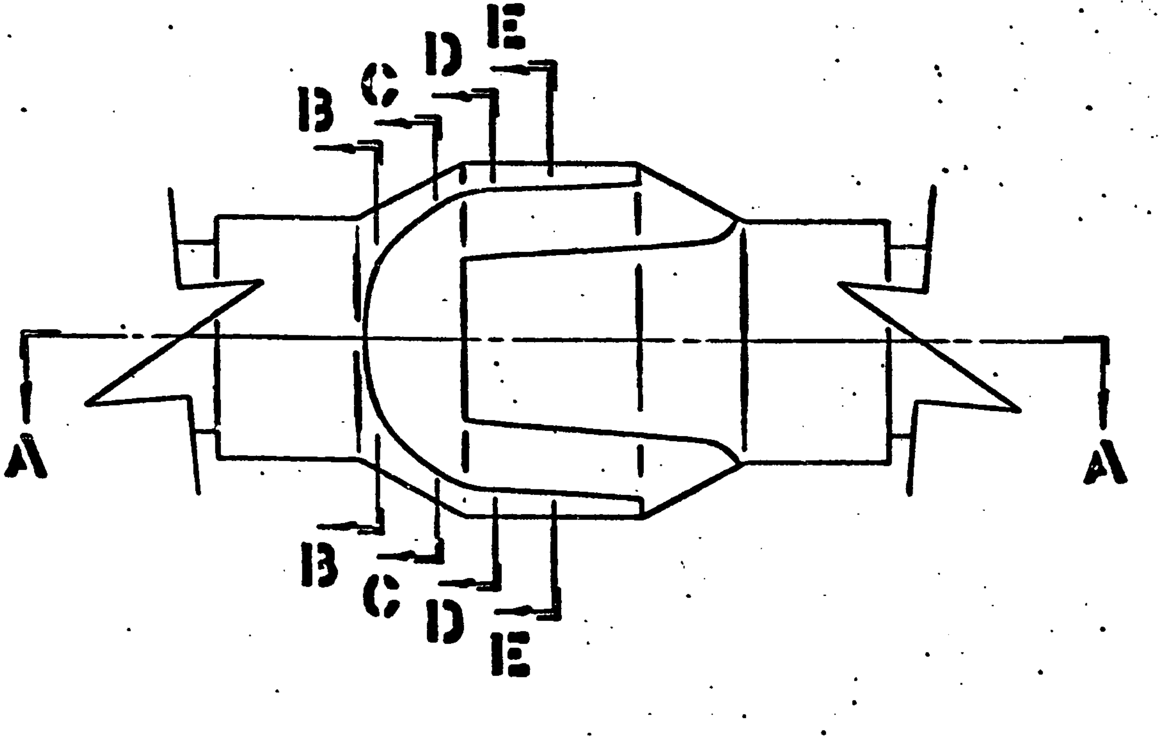

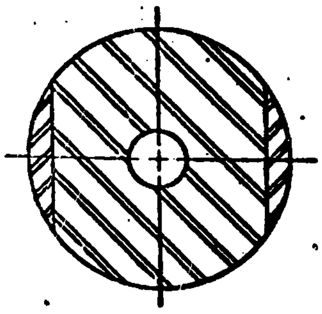

SECTION B-B

FOLDOUT FRAME

FOLDOUT FRAME

UNLESS OTHE
THIS DRAWIN
THIS ITEM SHA
WITH AIRESEA
SC-5535, STAN
TERPRETATIONS

REVISIONS

ZONE	LTR	DESCRIPTION	DATE	APPROVED

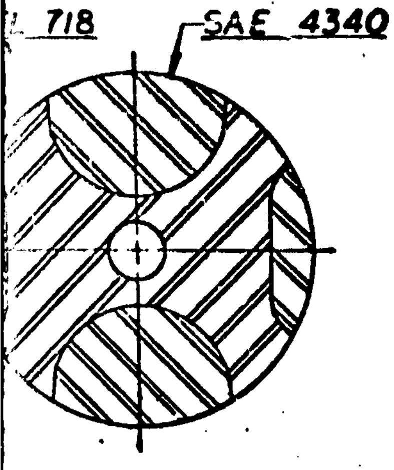

SECTION D-D

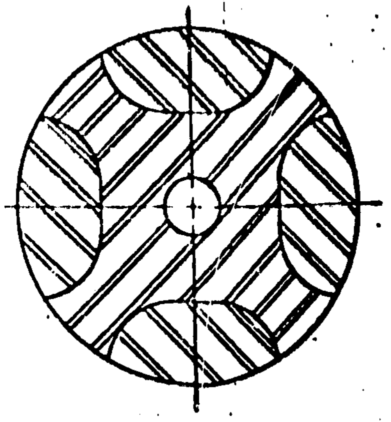

SECTION E-E

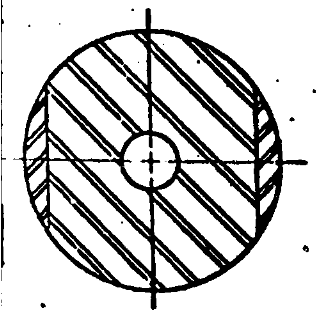

SECTION B-B

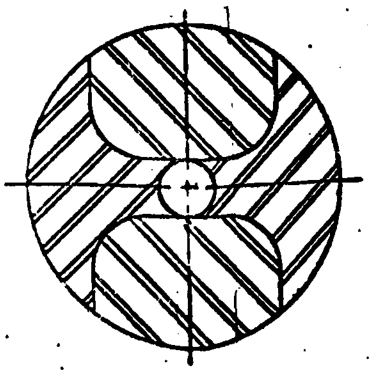

SECTION C-C

FIGURE 3-4

APS-5286-R
Page 3-6

QUANTITY REQD	ITEM NO	PART NO.	SYM	DESCRIPTION	CODE IDENT	MATERIAL AND SPECIFICATION	ZONE
	←ASSY			LIST OF MATERIAL			

UNLESS OTHERWISE SPECIFIED ON THIS DRAWING, FABRICATION OF THIS ITEM SHALL BE IN ACCORDANCE WITH AIRESEARCH SPECIFICATION SC-5535, STANDARD DRAWING INTERPRETATIONS.

REQD	NEXT ASSY	USED ON
HEAT TREATMENT		PROCESS
HARDNESS AND SPEC		NAME AND SPEC

SIGNATURES	DATES
DFT	
CHK	
ENG	
MATL	
STRESS	
ENG	
APPD	
APPD	
ACTIVITY APPD	
OTHER ACTIVITY APPD	

AIRESEARCH MANUFACTURING COMPANY OF ARIZONA
A DIVISION OF THE GARRETT CORPORATION
PHOENIX ARIZONA

DWG TITLE
ALTERNATOR ROTOR ASSEMBLY, B.R.U.

SIZE	CODE IDENT NO	DWG NO
D	99193	SKP 18036
SCALE	WT	SHEET OF

FOLDOUT FRAME

(b) Field coils are located adjacent to the frame and stator, facilitating heat transfer of the field losses. The field or excitation coils at each end of the alternator are simple bobbin-wound coils. Each coil has two sections--a series section and a control (shunt) section. The series coils provide excitation from current transformers in the leads to the load. This excitation is proportional to load current. The control coils provide excitation from the voltage regulator as necessary to maintain constant voltage regardless of load, speed, or temperature variation in the system. The excitation coils are supported in copper bobbins which provide good heat conduction from the coils to the frame. The copper bobbins also facilitate cooling at the end turns of the stator winding.

(c) The rotor is a composite structure of magnetic and nonmagnetic materials. Both casting and brazing techniques are readily available for ensuring high strength for this member. The nonmagnetic material between the poles acts as an electromagnetic damper during motor and generator action.

3.1 Electrical Analysis of the Alternator

One of the primary design objectives for the alternator is maximum efficiency. Because of this, the electromagnetic weight of the alternator (Table 3-1) is rather high when compared to lower efficiency machines where minimum weight has been emphasized. To obtain high efficiency, the current densities in the windings must be low. Thus, the heat generation and resultant temperature rises should be low, even at the 21-KVA overload conditions, since the densities at that condition are:

Armature winding current density	9350 amp/in.^{2}
Field current density	2900 amp/in.^{2}

TABLE 3-1

ALTERNATOR ELECTROMAGNETIC WEIGHTS

Component	Lbs.
Rotor	10.70
Stator Back-Iron	3.67
Teeth	1.19
Windings	1.88
Field Coils	6.59
End-Bells and Frame	9.75
Core Spacer	1.00
TOTAL	34.78

Another design objective was that the rotor should be small. A minimum-sized rotor is desirable to provide lower windage losses for bearing design considerations. However, in establishing rotor proportion, judgment must be used to allow adequate separation of the rotor poles to maintain an acceptably low leakage permeance in the rotor structure.

The flux leakage was determined by flux plotting. Because the accuracy of these determinations may be in error by as much as 20 percent, tolerance factors of 1.2 and 1.25 were applied to these permeances, respectively. Since the rotor iron is operated at less than 86 kilolines/in^2. for all conditions except 21 KVA, the design is conservative for all steady-state load conditions. At 21 KVA, the rotor pole and shaft densities are both 100 kilolines/in^2. These are easily within the capabilities of the excitation system and the selected materials.

Pole Shape Determination - A harmonic analysis of various pole configurations was undertaken, with results as shown in Table 3-2. For rectangular poles, the lowest tabulated harmonic content is 0.268 at 135°, corresponding to a pole embrace of 0.75. For trapezoidal poles with a pole embrace of 0.667, the lowest harmonic content is 0.215 at 120° ±10°. This data is a useful guide to establish a practical pole configuration in conjunction with other criteria. Excessive leakage between the poles in the rotor can be caused by a large pole embrace; thus, in the interest of obtaining the minimum rotor size, it is believed that a pole embrace of 0.667 would be the better choice. Fringing is present from the pole sides up to the stator, causing the effective pole embrace to be higher than 0.667; the more optimum value is approached without incurring the higher rotor leakage.

The evaluation shows that the trapezoidal pole shape is evidently quite effective in reducing harmonic distortion. However, the trapezoidal shape increases the effective air gap and/or tooth saturation because all of the flux from the wide section of a pole cannot enter the correspondingly narrow section of the adjacent pole. Thus, part of the pole flux must traverse axially across the back-iron. This feature is undesirable because the iron stacking factor is only 90 percent; that is, an air gap of 0.1 in. must be traversed by the axial component of the flux for every inch of the axial path.

All factors considered, it was decided that a good compromise would be a trapezoidal pole shape of 120° ±5. This minimizes slot ripple, and the axial flux component in the stator is relatively low.

Magnetic circuit data is presented in Table 3-3 and demonstrates the conservative flux densities expected in the unit operation. A no-load saturation voltage of 1.3 p.u. V is shown. Performance above this voltage level was not predicted because magnetizing data for AL 4750 stator iron was not readily available at higher densities. In

TABLE 3-2

POLE CONFIGURATION EFFECT UPON HARMONIC CONTENT

Pole Configuration	Harmonic Distortion $= \frac{1}{a_1}\sqrt{a_2^2 + a_3^2 = \text{----}\ a_n^2}$
I RECTANGULAR	

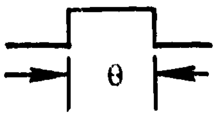

θ = 100°	0.389
105	0.356
110	0.328
120	0.288
135	0.268
140	0.272

II TRAPEZOIDAL

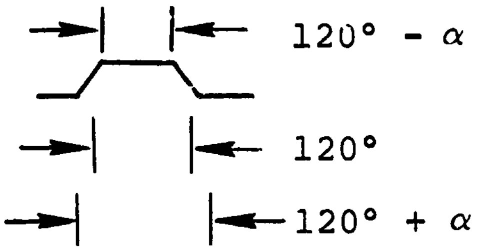

120° ±1.735°	0.2837
120° ±5.0°	0.2614
120° ±7.5°	0.2380
120° ±10.0°	0.2150

TABLE 3-3

MAGNETIC CIRCUIT DATA--KILOLINES PER SQUARE INCH

Load Conditions	No-Load 1.0 p.u. V	No-Load 1.3 p.u. V	7210 VA 0.85 pf	12,600 VA 0.85 pf	14,300 VA 0.75 pf	21,300 VA 0.75 pf
Main Gap	33.5	-	34.8	36.5	39.2	42.5
Teeth	75	-	78	81.8	87.9	95.3
Back-Iron	59	-	61.1	64.5	68.9	75
Pole	61.5	86.2	70.1	79.3	86.5	100
Shaft	59.4	86.4	68.5	78.4	85.5	100
Auxiliary Gap	24.1	33.4	27.8	31.8	34.6	40.5
Frame	57.8	80.1	67.5	77.5	84.6	100

the determination of pole flux under load conditions, only 93 percent of the direct axis voltage drop was subtracted from the total internal generated voltage. This conservatively allowed for the possibility of flux wave distortion at high saturation density in the teeth. In establishing flux density in the back iron, pole flux was used. Since low weight was not a prime requirement, the refinement of subtracting the armature winding leakage flux in the back iron (due to slot permeances) was neglected. This provided a more conservative design.

Series and shunt field characteristics for the stator are shown in Table 3-4 for the load and short-circuit conditions.

Criteria for the selection of the structural and magnetic materials were availability, previous successful usage, and compatibility with the design for high efficiency.

TABLE 3-4
SERIES AND SHUNT FIELD CHARACTERISTICS

Load	Field NI		Load Amps	Watts	
	Series	Shunt	I_L	Series	Shunt
No-Load	0	1102	0	0	35.4
3 p.u. short circuit	3300	0	105	300	0
7,210 VA (0.85 pf)	629	995	20	10.8	29
12,600 VA (0.85 pf)	1100	1036	35	33.2	31.3
14,300 VA (0.75 pf)	1250	1194	39.7	43	41.7
21,300 VA (0.75 pf)	1860	1650	59.2	95	79.5

An evaluation of certain variations in the alternator configuration was undertaken to determine if some trade-offs could be established to provide a relatively constant efficiency versus load. Some drop in efficiency at light loads is unavoidable in view of the relatively fixed iron losses. For the design under consideration, losses expressed as a percent of the output are shown in Table 3-5.

Variations in the configuration of the alternator were evaluated for areas where certain losses are predominant, such as back-iron, tooth, and pole losses. The effects are described in Table 3-6.

Predicted Alternator Performance- Figure 3-5 presents the predicted electrical characteristics of the alternator design at no-load, short-circuit, overload, and at three design-point conditions. Table 3-7 gives the calculated alternator losses in watts and the electromagnetic efficiencies, predicted from the loss analysis for this design, at various load conditions. Total losses plotted against the KVA output are shown in the graph of Figure 3-6. It can be seen that there is potential margin in the design efficiency which is in the range of

TABLE 3-5

ALTERNATOR LOSSES, PERCENT

	2.25 KW	10.7 KW
Back-Iron	3.690	0.890
Tooth	2.044	0.542
Armature Copper	0.356	1.600
Fields	1.070	0.598
Pole Face	5.780	1.400
Strays	0.266	1.170
TOTAL	13.206	6.200

TABLE 3-6

LOSS PARAMETER EFFECTS

Loss Parameter	Action	Effect
Tooth	Reduce to 1% at 2.25-KW load condition	Increases copper losses by 0.7 percent. Creates net efficiency loss of 1.33 percent at 10.7 KW. Almost doubles the temperature rise, reducing reliability and the expected winding life.
Back-Iron	Increase section	Little or no reduction in losses when the theoretical core density is reduced below 60 kilolines (design value). Adds weight. Increases thermal conduction path and results in a greater temperature rise.
Pole Face	a. Bridge slot openings	Reduces slot ripple
	b. Increase main gap	Increases excitation power requirement
	c. Increase pole surface resistance	Reduces the damping of the magnetic variations due to eccentricity of the rotor.

I_B = 35 AMPS
V_B = 120/208

SERIES FIELD TO BE
1100 NI AT 1 PU (33.2W)

SHUNT FIELD TO BE
1036 NI AT 12,600 VA (31.3W)

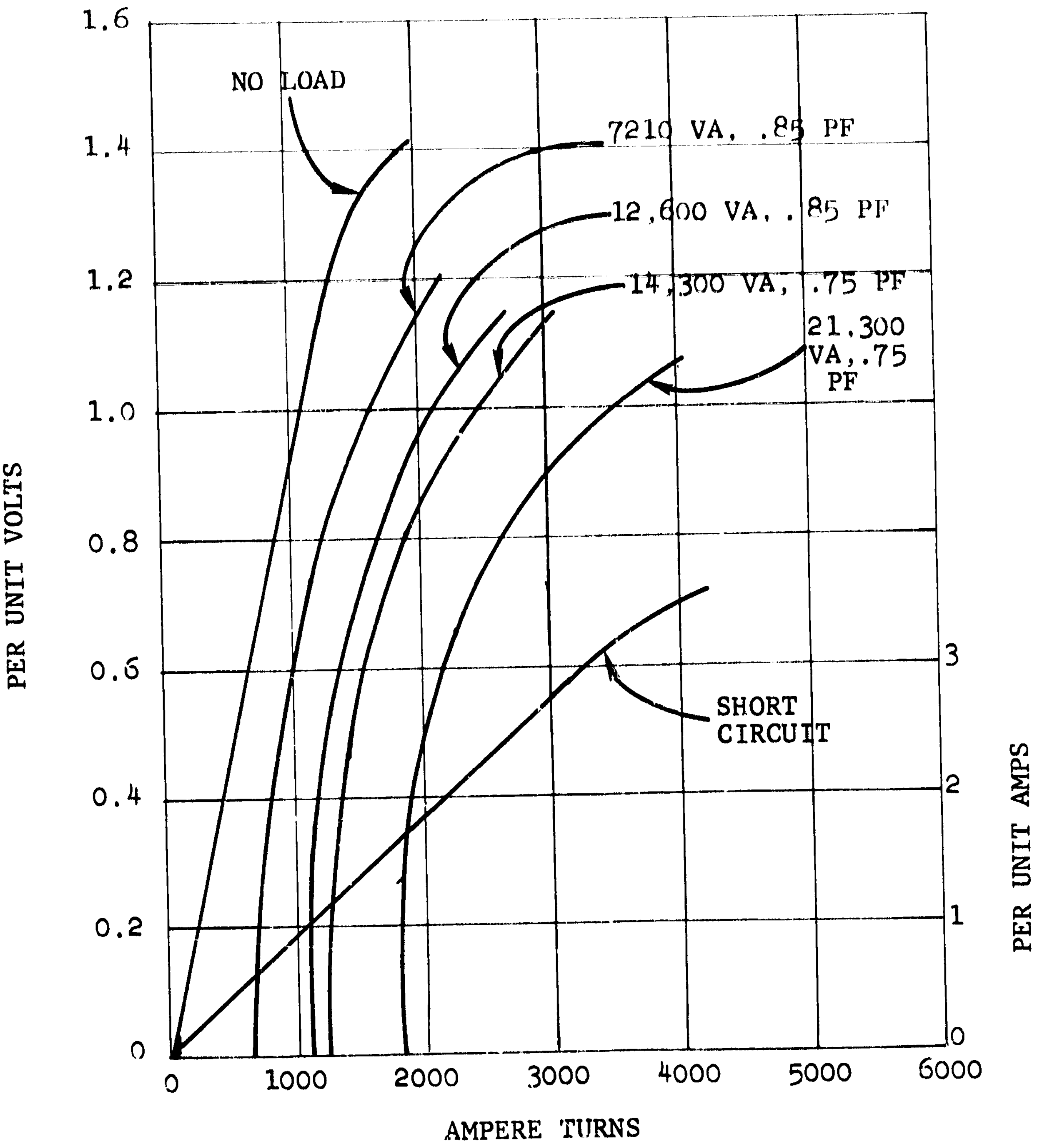

PREDICTED ALTERNATOR ELECTRICAL
CHARACTERISTICS

FIGURE 3-5

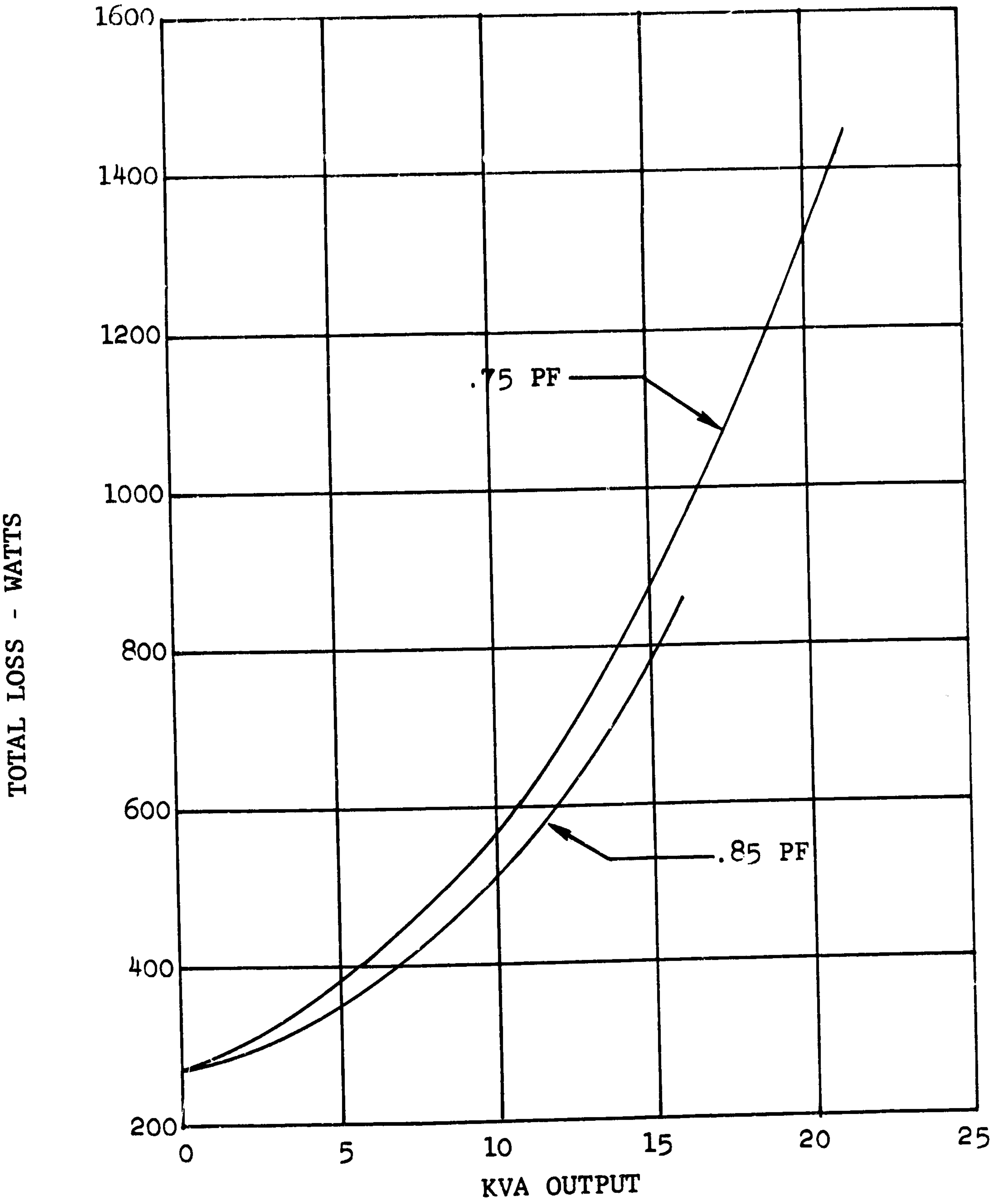

TOTAL LOSS VS KVA OUTPUT
BRU ALTERNATOR PRELIMINARY DESIGN

FIGURE 3-6

TABLE 3-7

ALTERNATOR LOSS SUMMARY
(All Losses in Watts)

Loss	No-Load	2.650 KVA 0.85 pf	7.210 KVA 0.85 pf	12.600 KVA 0.85 pf	14.300 KVA 0.75 pf	21.300 KVA 0.75 pf
Back-Iron	80	83	85	96	118	114
Teeth	43	46	51	58	71	86
Armature Copper	0	8	56	171	220	490
Field Copper	17	24	37	64	84	174
Pole Face	126	130	136	150	172	203
Stray Load	0	6	41	126	162	360
Total	266	297	406	665	827	1,457
Input	266	2547	6536	11,370	11,530	11,460
Output	0	2250	6130	10,700	10,700	16,000
E.M. Efficiency	0	0.883	0.938	0.941	0.927	0.916
System Rating, KW	0	2.250	6.000	10.500	--	--

0.85 to 0.92 E.M. efficiency over a power-output range of 2.25 to 10.7 KW, respectively.

3.1.1 <u>Summary of Electromagnetic Force Considerations as Related to Gas Bearing Application</u> - The ultimate use of this alternator is in the BRU, which is gas-bearing-supported. The primary concern, therefore, is that the gas bearings are capable of supporting not only the dynamic loads but also the electromagnetic loads. Studies of the unbalanced electromagnetic forces have now been completed for the following conditions:

(a) Normal alternator operation at full speed
(b) Unbalanced electrical loads
(c) Short-circuit conditions
(d) Operation as a motor

It has been concluded that bearing loads due to magnetic unbalance should not be a problem within the normal range of operating speeds.

Evaluation of the Effect of Unbalanced Alternator Electrical Load - The studies to date on unbalanced magnetic forces have been based on the assumed worst-case condition of no-load, 1.3 p.u.V. A survey was conducted of the effect of unbalanced electrical loads on the machine in accordance with MIL-G-6099, paragraph 4.5.10.1.

The symmetry of the machine was first evaluated. The location and distribution of the stator windings in the four-pole alternator is designed so that, when energized, they create a symmetrical magnetomotive force (MMF). With Figure 3-7 considered as typical of the machine under consideration, it may be noted that even if an unbalanced load is applied to the three-phase winding, symmetry is still maintained with respect to the rotor, and this is true for any position of that rotor. Each phase thus creates symmetrical MMFs around the rotor, but variations in load in the phases will vary the total MMF in the relative windings. Thus, it may be deduced that there will be no significant magnetic unbalance because of symmetry and, therefore, the magnitude of the MMFs in the windings at unbalanced load conditions is the important consideration.

MMF magnitudes were determined by the vectorial method for symmetrical components and then compared to known balanced-load conditions.

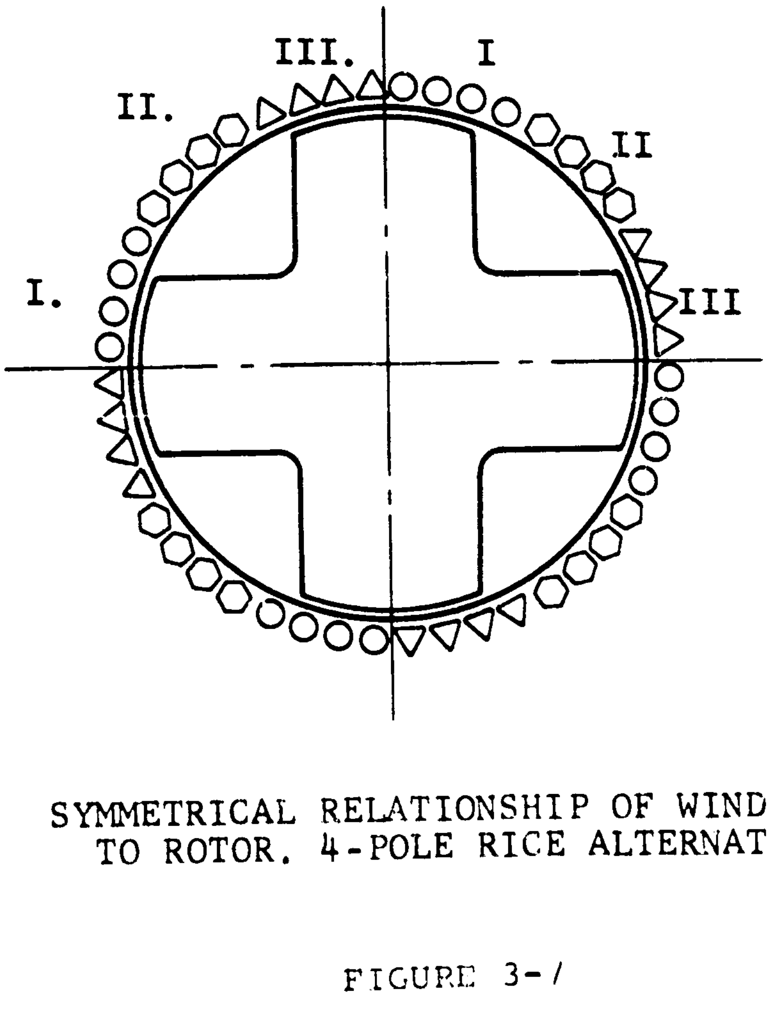

SYMMETRICAL RELATIONSHIP OF WINDINGS
TO ROTOR. 4-POLE RICE ALTERNATOR

FIGURE 3-1

Since the amplitude of the resultant MMF of a symmetrical three-phase system is 1.5 times the amplitude of a single-phase system, the in-phase sum of the vectors of the unbalanced system does not exceed unity and, thus, does not exceed the MMF at rated balanced-load.

Since the rated balanced-load condition is not the "worst-case" condition for electromagnetic unbalance, it can be confidently concluded that unbalanced electrical loads will have much less effect upon the gas bearing system than the no-load, 1.3-p.u.V condition previously reviewed.

Effects of Negative Sequence Reactance on Voltage Unbalance with Unbalanced Loads - The effect of unbalanced load on unbalanced voltage as a function of negative sequence reactance was investigated, and the results are shown in Figure 3-8. The method of solution utilized unbalanced load impedance rather than unbalanced load currents, and in consequence a slightly optimistic result is presented. This method avoided the use of a difficult iterative analysis, yet provided adequate results.

The maximum permissible value of X_2, the negative sequence reactance, is 0.3 p.u. or 2.38 X_1, where X_1 is the armature winding leakage reactance. While this appeared to lie in the range of X_2 attainable in solid pole-face machines without the use of damper bars, a test on the ARP resulted in an X_2 value of 0.38 p.u. Unless absolutely necessary, the use of pole-face dampers should be avoided in order to simplify construction of the unit. However, if it is determined that the voltage unbalance is higher than anticipated, pole-face dampers can be added without much difficulty to overcome the problem. Motor starting and unbalanced magnetic forces are two other considerations that could also require rotor modification to include damping.

LOAD IMPEDANCES:
Z_A = (3 + j0) p.u.
Z_B = (3 + j0) p.u.
Z_C = (1 + j0) p.u.
BASE OHMS = 3.43

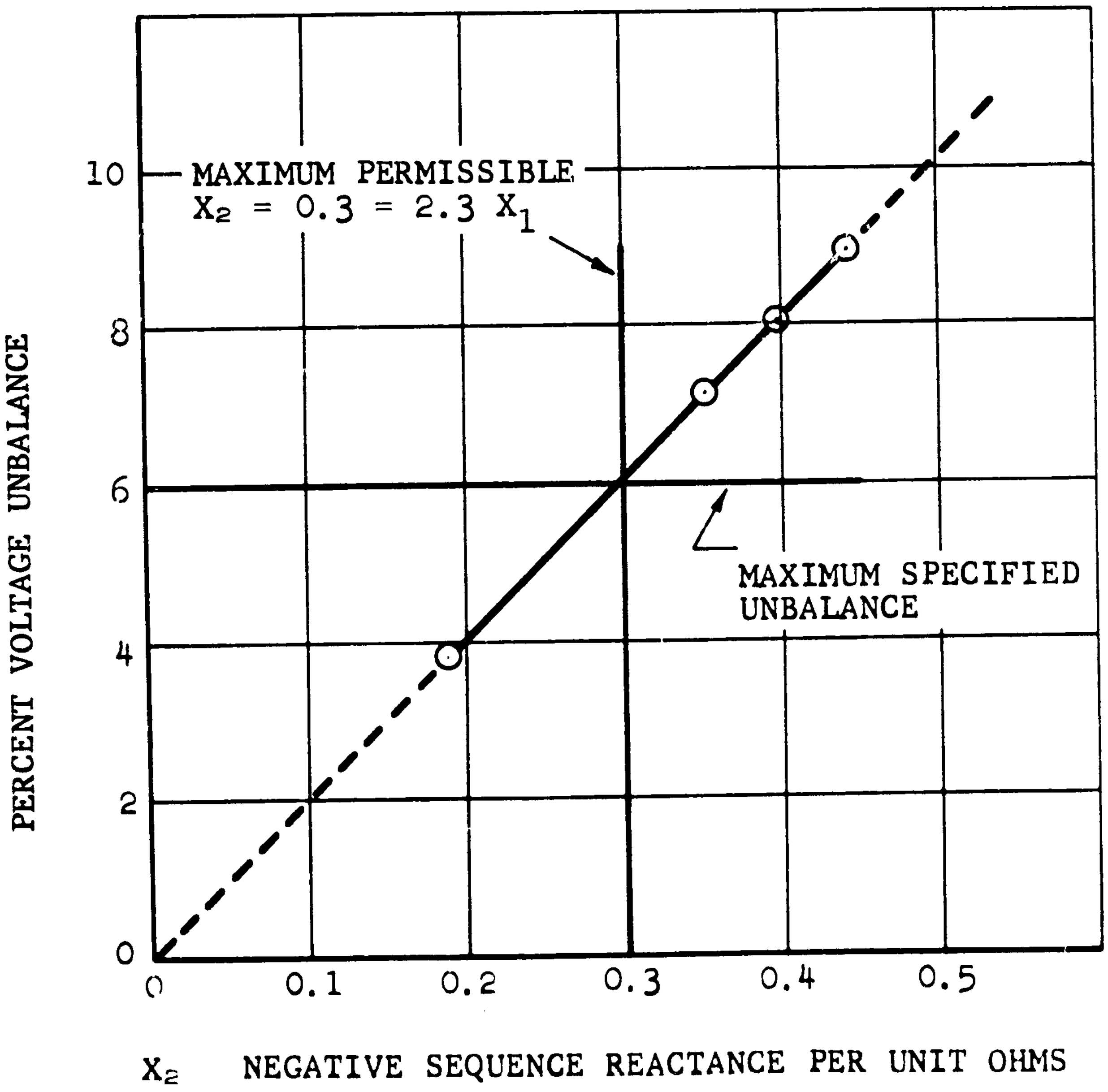

PERCENT VOLTAGE UNBALANCE VS.
NEGATIVE SEQUENCE REACTANCE AT
VARIOUS LOAD IMPEDANCES

FIGURE 3-8

Evaluation of Electrical Short-Circuit Effects on the Electromagnetic Forces Imposed on the Bearings - Under conditions specified by MIL-G-6099, paragraph 4.5.12, at 3-p.u.V short-circuit current, the flux in the main air gap is proportional to the voltage drop ($I_{sh.c}Z_a$) in the armature winding and approaches 50 percent of rated voltage. Auxiliary air-gap flux under the same conditions is increased because the field winding ampere-turns are almost at the maximum value, and leakage flux is also a considerable portion of this air-gap total flux at short-circuit. In the analysis of the alternator, 1624 field ampere-turns are present at short-circuit. At overload conditions, 1755 ampere-turns are present at 21.3 KVA, 1.0 p.u.V.

Thus, it may be concluded that the short-circuit condition does not represent an electromagnetic force problem for the bearings and will be considerably less severe than the no-load 1.3 p.u.V case chosen.

Evaluation of Electromagnetic Forces on the Bearings Due to Operation of the Alternator as a Motor - Initial studies of the electromagnetic effect on the loading of the gas bearings have indicated that, when utilizing the alternator as a motor for starting purposes, loads were established as follows:

Main flux gap	2.3 lbs.
Auxiliary flux gaps	0.54 lb. each

The above represents a distributed load, per bearing, of 1.69 lbs. Assumed conditions were as follows:

(a) Across-the-line start at 600 Hz and rated volts per cycle - i.e., 60 V
(b) No eddy-current damping
(c) Rotor is considered stationary
(d) 0.002-in. magnetic rotor eccentricity

One additional check-point was taken at a low rotational speed, and the loads indicated a diminishing trend as was expected. Further studies will be undertaken in this area, and these will include various starting frequency levels. However, it is considered that the initial trends, as established, signify that bearing forces should not create problems of operation during motor-start conditions.

Motoring Start Capability - The performance of the MTU as a motor was investigated. Under locked-rotor conditions, the torque was 5 to 7 lbs.-in. at 35 amps stator current, 16.5 V a-c, 400 Hz. The torque variation was due to rotor saliency.

This data can be projected to show 34 lbs.-in. at rated volts per cycle (40 V, 400 Hz) with stator current of 83.5 amps (2.38 p.u. based on 35 amps rated-load current). This would indicate that the alternator, as a motor, would perform much more satisfactorily than initially expected.

3.2 Mechanical Analysis

Dynamic Analysis of the ARP (Critical Speed Analysis) - The rotor of this machine (Figure 3-9) is a furnace-brazed bimetallic, solid-metal part having a smooth, compact configuration possessing stiffness and strength required for this rotational speed and bearing application.

Ball bearings were selected on the basis of digital computer analysis. The bearings should meet the design objective of a TBO of 300 hrs. minimum when using an oil-mist lubrication (MIL-L-7808). The major characteristics of the bearings are:

Bore diameter	25 mm
Outside diameter	47 mm

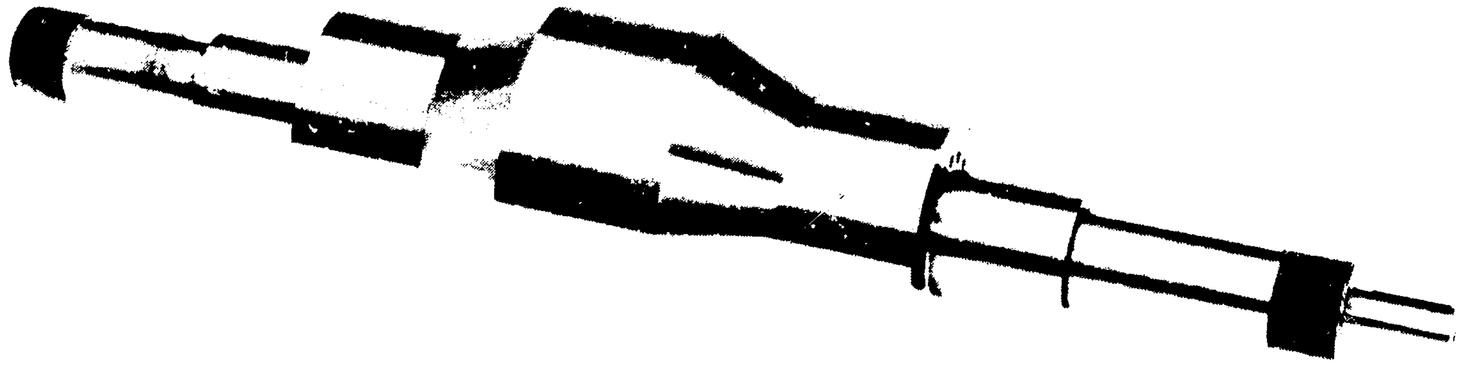

ALTERNATOR RESEARCH PACKAGE ROTOR

FIGURE 3-9

Width	12 mm
Number of balls	13
Ball diameter	1/4 in.
Inner-race curvature	52-53 percent of ball diameter
Outer-race curvature	52-53 percent of ball diameter
Contact angle	20°
Ring and ball material	Consumable-electrode vacuum-melted M-50 tool steel
Separator material	Iron-silicon-bronze, silver-plated

The axial length of the main and auxiliary flux gaps, rotor flux leakage considerations, and requirements for instrumentation and bearing supports defined the bearing center-to-center distance and acted as restraints in analysis of critical speed performance for the shaft. The stator end-plates were utilized to mount the speed sensing and orthogonal proximity probes and to mount the bearing carrier supports.

Operating clearances at the main and auxiliary flux gaps (Figure 3-1) were designed to be 0.020 in. A limited radial travel of 0.002 in. was allowed between shaft and stator centers. This minimized the unbalanced electromagnetic loads on the bearings, yet imposed design restraints on the method of mounting the bearings.

Figure 3-10 presents a cross-sectional view of the alternator research package (ARP). The unit consists basically of the same alternator electromagnetic configuration and cooling system that is to be utilized in the Brayton rotating unit (BRU) but mounted on oil-mist-lubricated ball bearings. A buffer seal arrangement at the rotor cavity and an external gas supply fitting is provided so that BRU alternator cavity ambient conditions can be simulated during alternator performance evaluation. Drawings of the bearings and seal arrangement are included in Appendix II. The ARP is driven with a turbine assembly

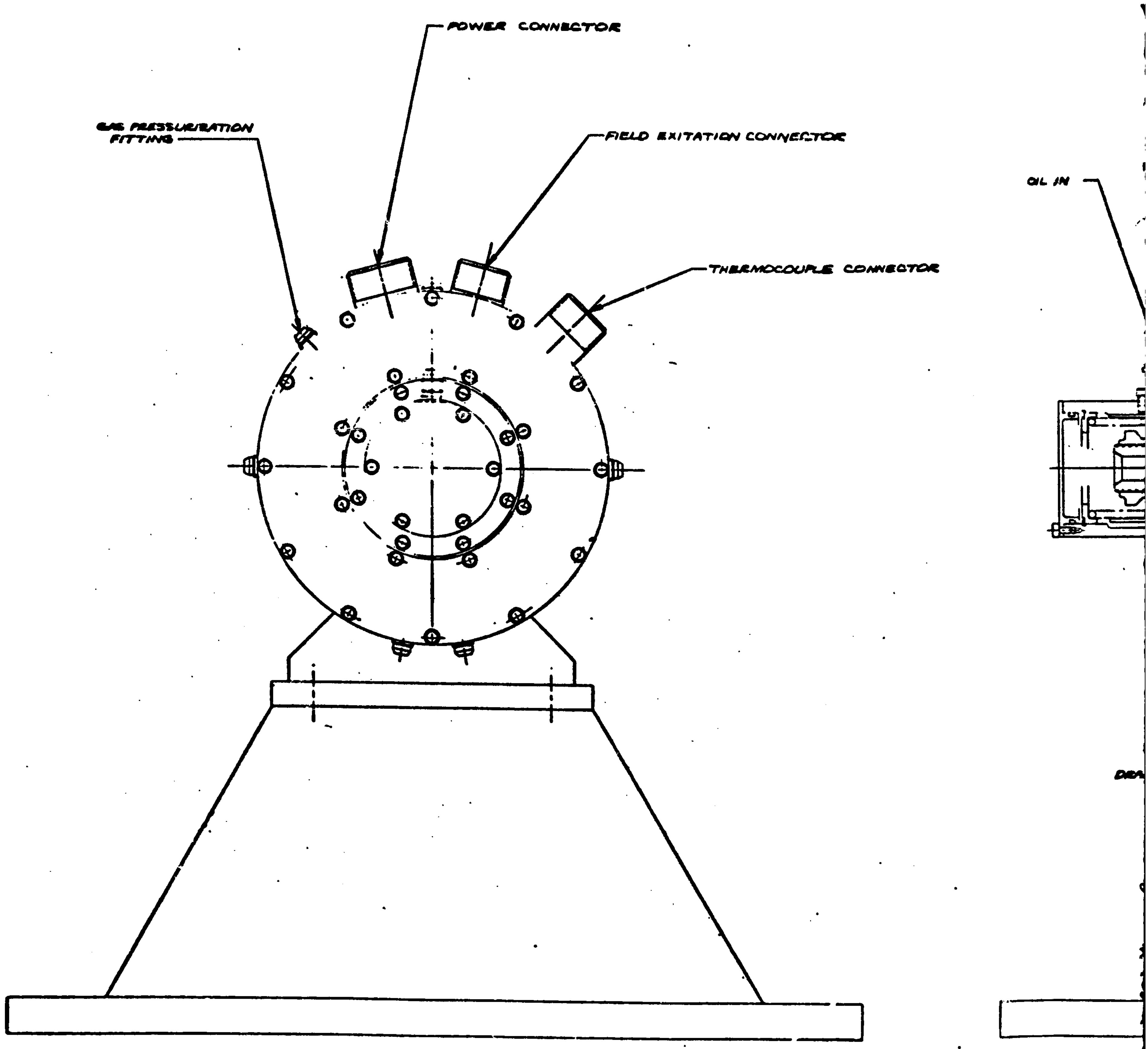

ALTERNATOR RESEARCH PACKAG

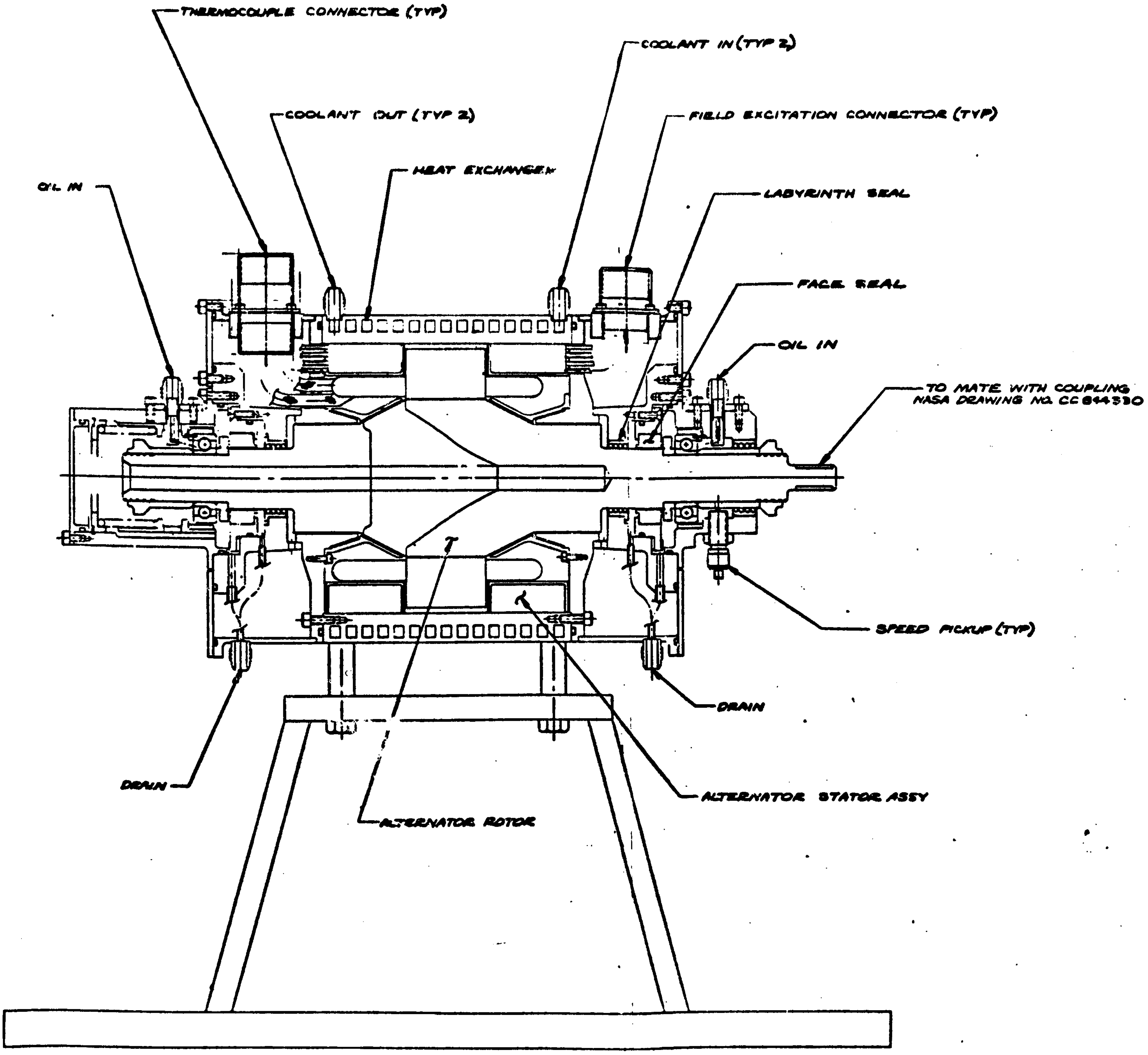

ESEARCH PACKAGE

FIGURE 3-10

through a special, balanced coupling as shown in Figure 3-10. This coupling is detailed in Drawing 699667, Appendix II.

The hole through the axial center of the alternator rotor simulates the tie-bolt hole, which is required in the BRU. A nonmagnetic tie-bolt is used in the BRU to avoid the magnetic leakage that a magnetic bolt would create.

The elastic and mass models of the rotating assembly used for the critical speed analysis are shown in Figure 3-11. The rotating assembly critical speeds plotted as a function of bearing resilient-mount spring-rate are shown in Figure 3-12. This shows that the use of 20,000-ppi resilient mounts at each bearing mounting will permit operation at the design operating speed of 36,000 rpm. Bearing loads at 36,000 rpm, with the 20,000 ppi resilient mounting system, are shown to be in the order of 5 to 7 lbs. at an assumed rotor c.g. eccentricity of 0.0002 in. (Figure 3-13).

The bearing system life, B_1, for a preferred preload of 30 lbs., a 6.6-lbs. unidirectional radial load per bearing, and dynamic loads of 5 to 7 lbs. is shown to be in excess of 2400 hrs. (Figure 3-14). The horsepower loss per bearing under these conditions (Figure 3-15) is approximately 0.215. The bearing requirements are shown in AiResearch Source Control Drawing 358498, Appendix II.

The proposed carbon-face contact seal for the alternator package application is shown on AiResearch Source Control Drawing 699652, Appendix II.

Thermal Analysis - A thorough thermal analysis was performed on the alternator research package. Journal bearing heat losses utilized the auxiliary gaps to transfer their shaft heat, by convection, to the end-plates. Rotor heat was removed at the main gap. Windage and convection shields were attached to the inside of the end plates to direct

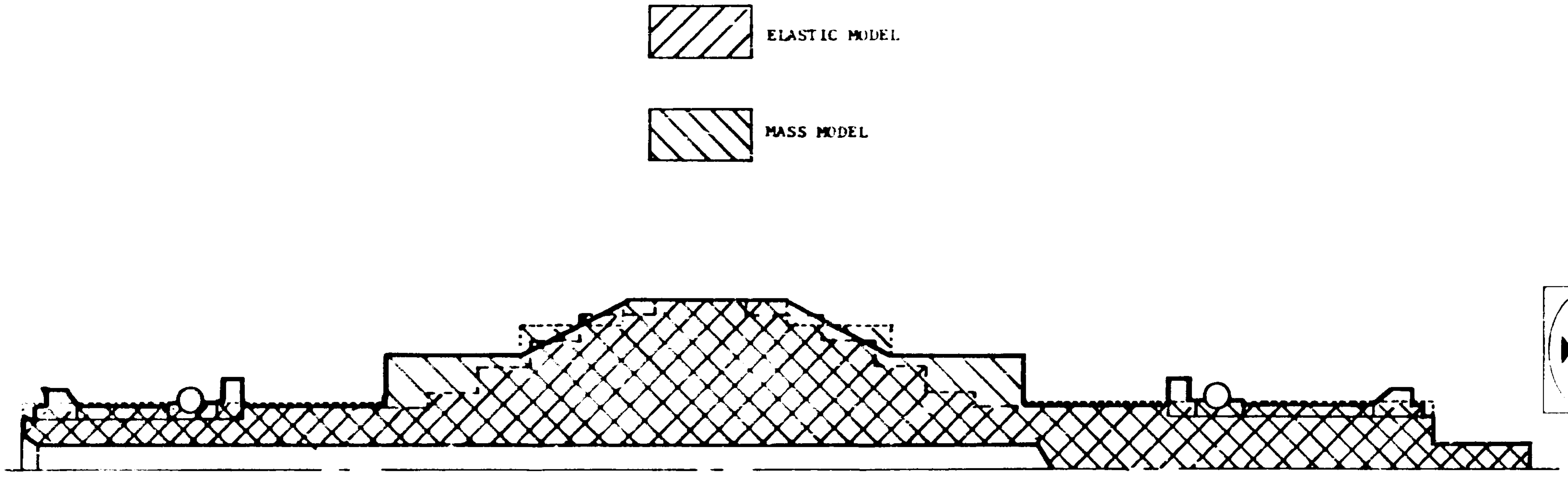

APPROX. SCALE

1 INCH

NOTES:

1. SYSTEM ANALYZED IS DEFINED BY BROAD OUTLINE
2. MASS MODEL ASSUMED IS THAT BELOW DOTTED LINE AND CROSSHATCHED AS INDICATED
3. ELASTIC MODEL ASSUMED IS THAT BELOW DASHED LINE AND CROSSHATCHED AS INDICATED, E 2.9 10^{7} LB IN^{2} THROUGHOUT

NOTES: (1) REF. A33383
(2) BOTH BEARINGS EQUALLY MOUNTED

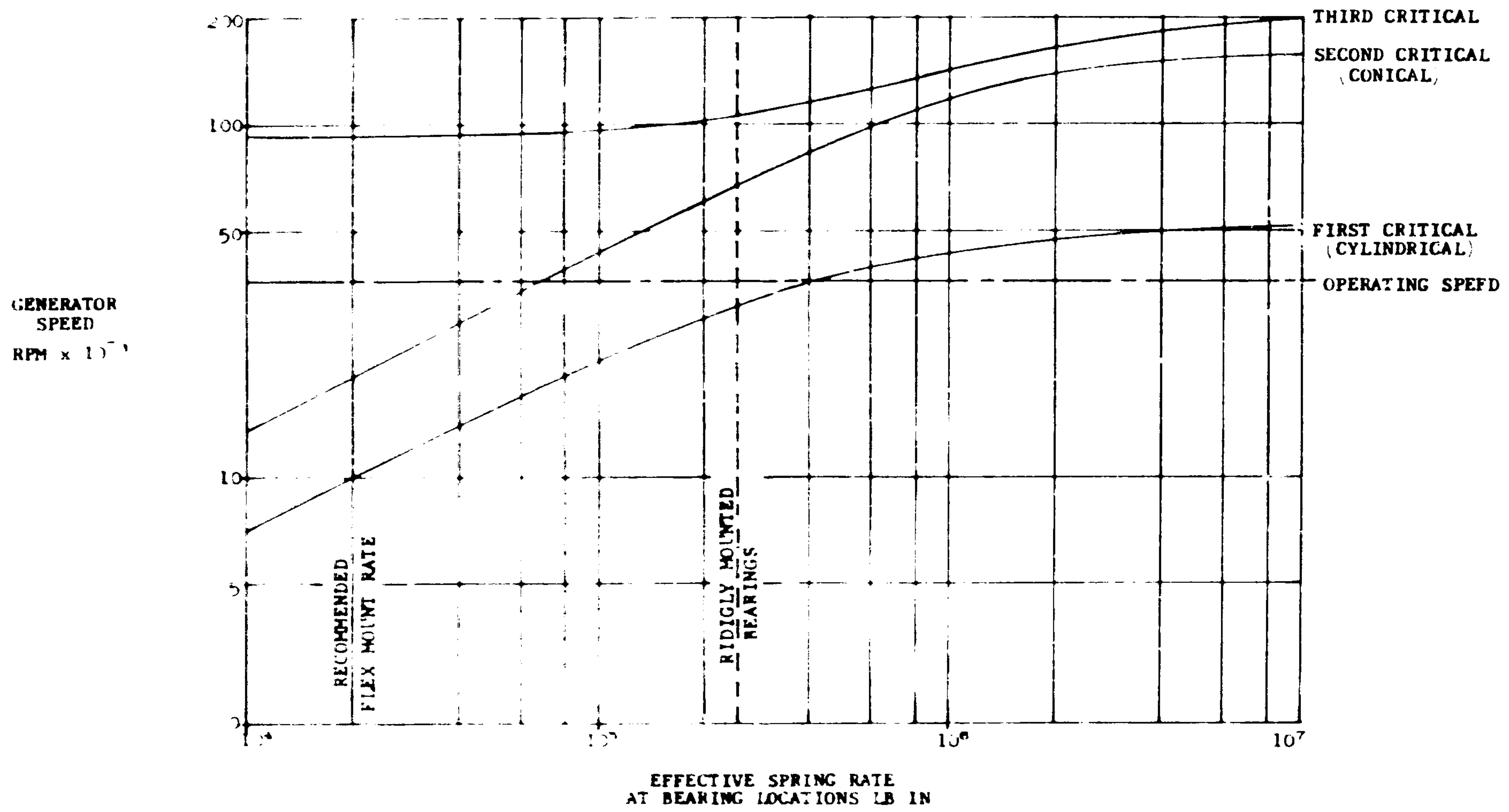

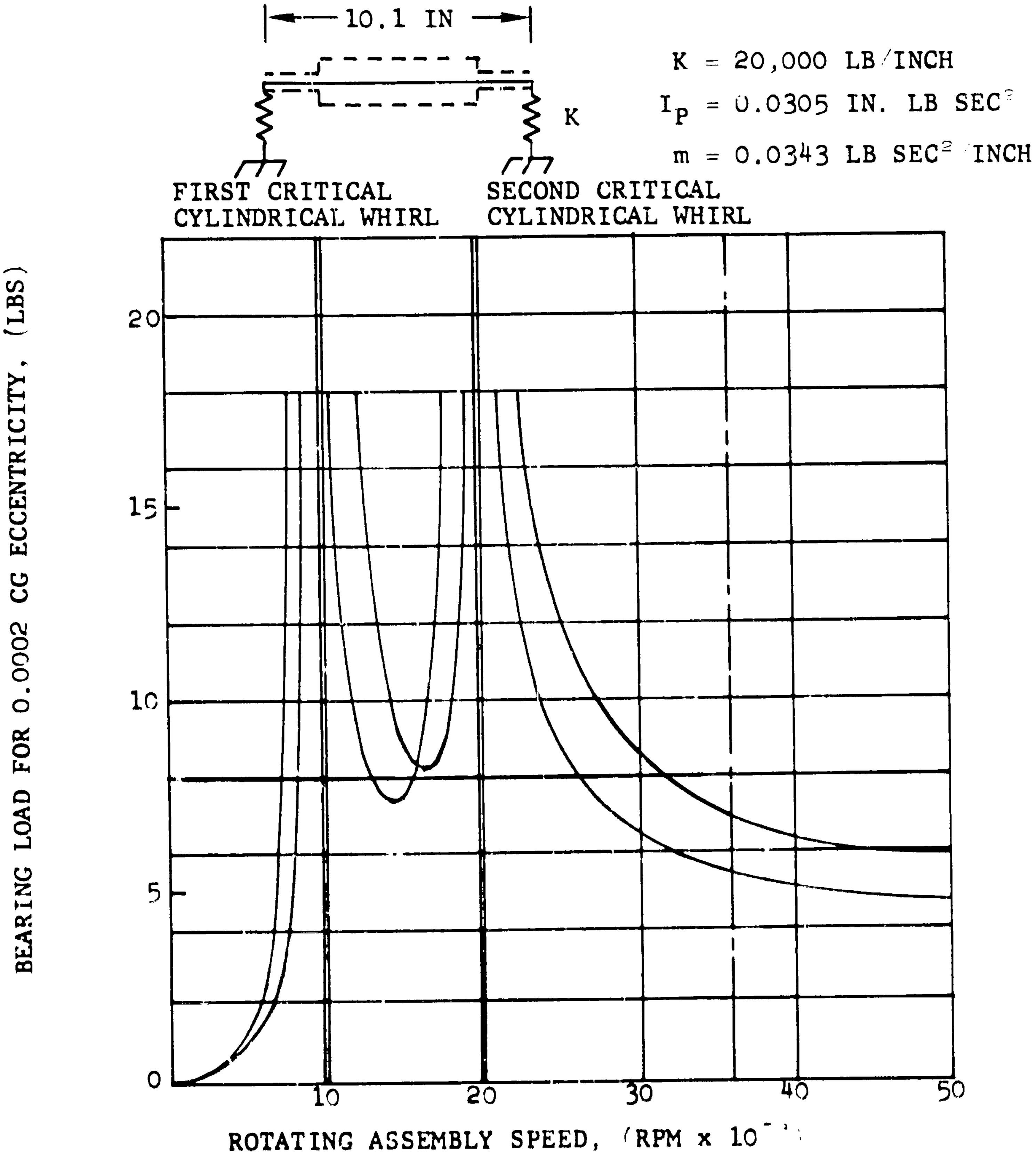

FIGURE 3-13

ALTERNATOR RESEARCH PACKAGE
FIRST AND SECOND CRITICAL
DEFINITION

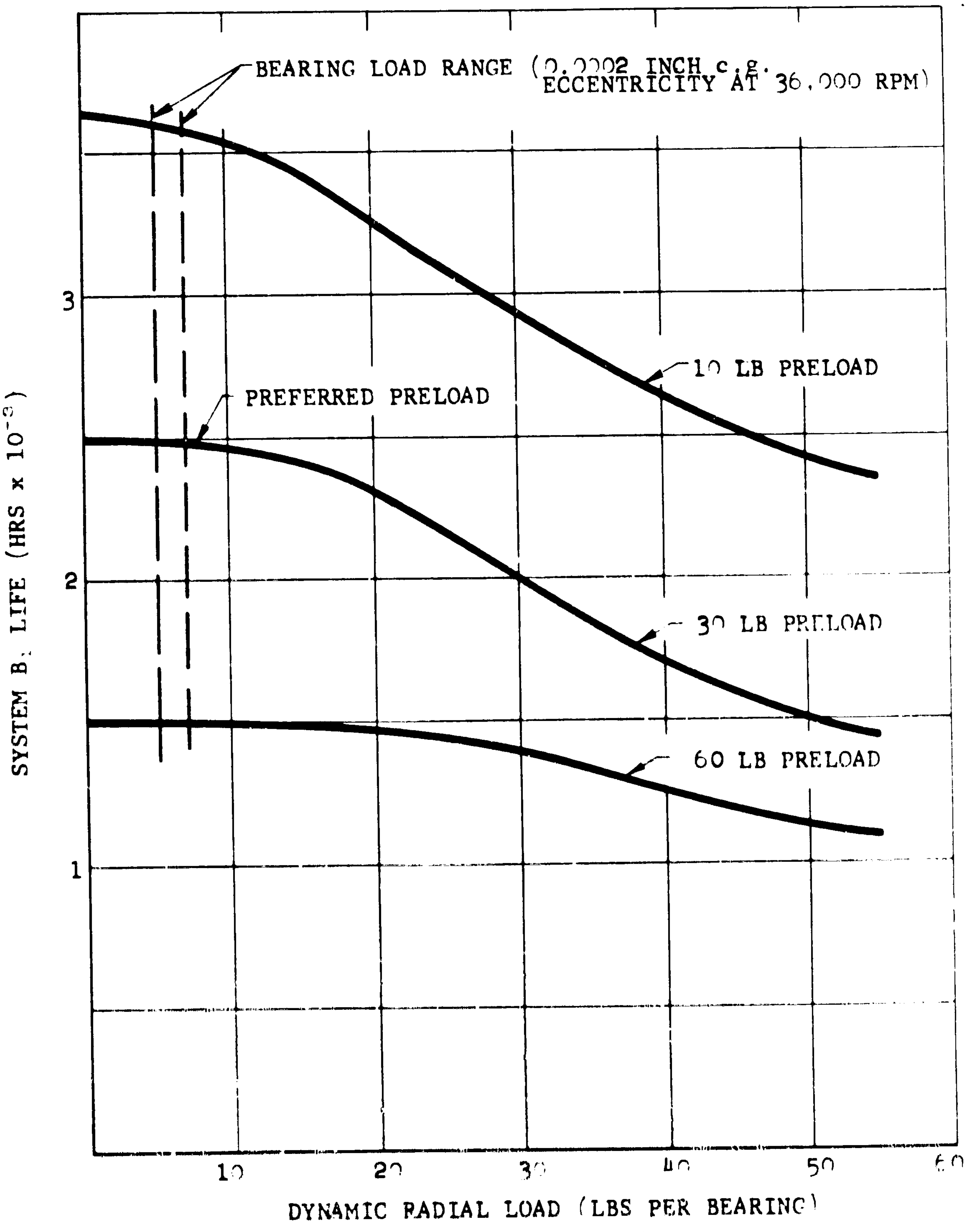

FIGURE 3-14

BEARING SYSTEM LIFE FOR NASA BRU ALTERNATOR RESEARCH PACKAGE USING CEVM M-50

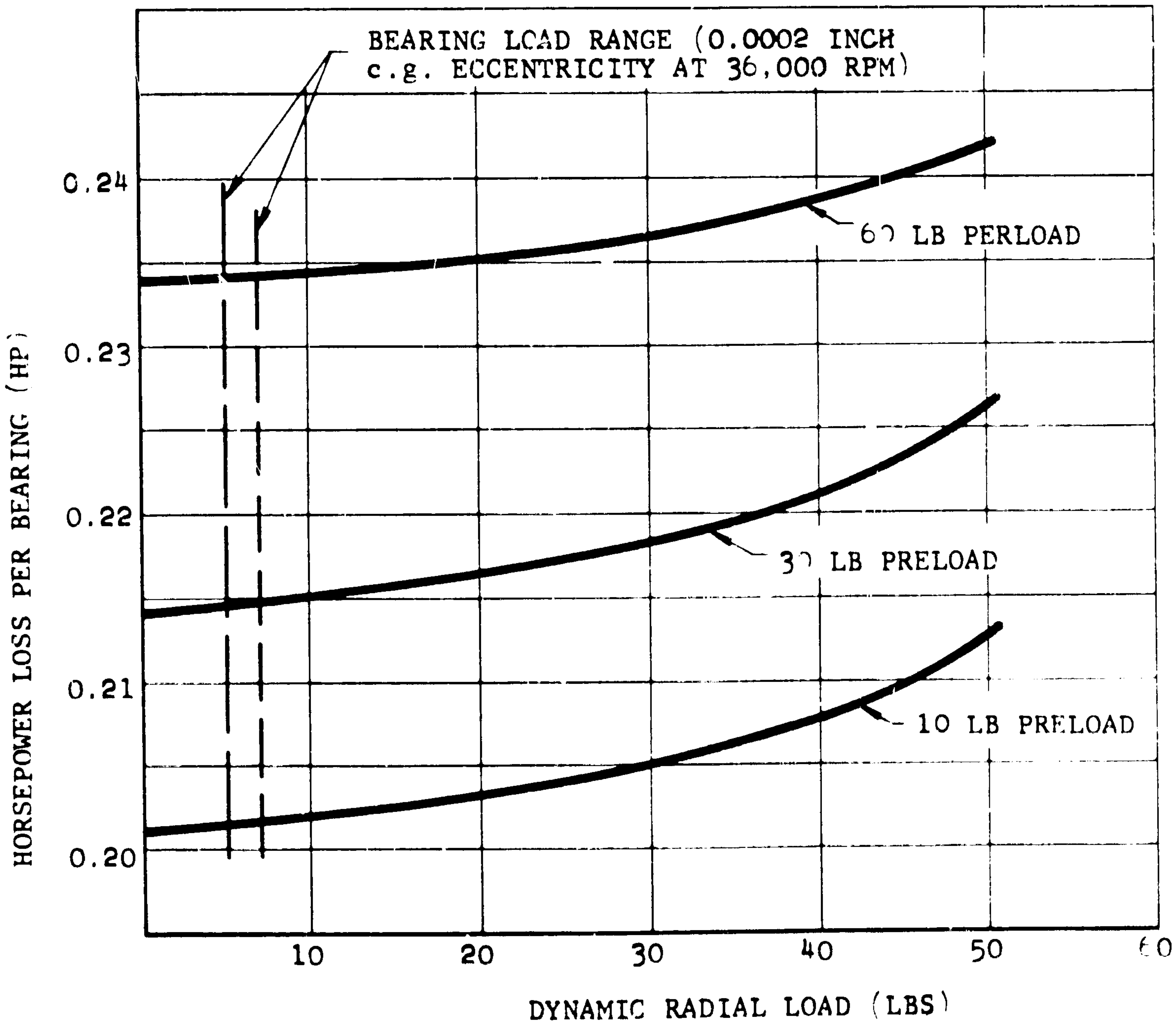

FIGURE 3-15

BEARING POWER LOSS FOR NASA BRU ALTERNATOR RESEARCH PACKAGE the heat to the flux gaps mentioned. The cooling jacket around the stator was thus employed to remove the generated waste heat and also limit the heating of the stator coils to safe operating levels.

The liquid-coolant heat exchanger utilized for cooling the alternator consists of a double helix machined onto the outer frame assembly of the alternator stator (Figure 3-16).

The coolant passage cross-sectional dimensions are 0.20 in. wide by 0.25 in. deep and the thread lead is 0.667 in. Each helical passage is independently supplied with coolant to provide the required coolant system redundancy.

The specified coolant is Dow-Corning 200, blended to yield, at 770°F, a viscosity of 2.0 centistokes. The recommended coolant flow rate, determined from heat-transfer analysis on the BRL, is 0.12 lb./sec. Estimated pressure drop, including inlet and discharge disturbances, is 7.5 psi.

Results of the thermal analysis are presented in Figure 3-17. Based on these results, thermocouple locations in the ARP were assigned as in Figure 3-18.

3.2.1 <u>Rotor Fabrication</u> - The major problems encountered during the fabrication of the alternator were the development of a satisfactory braze technique for the rotor and an acceptable heat-treatment procedure.

In its final form, the rotor is a solid structure made by brazing three separate pieces together. Figure 3-4, SKP 18036, depicts the rotor and shows the nonmagnetic metal separator (Inconel 718) that is brazed to the two magnetic (SAE 4340) pole pieces. As shown, the mating surfaces have a complex shape, and development of the proper

ALTERNATOR RESEARCH PACKAGE
MAIN FRAME ASSEMBLY
DETAIL PARTS PRIOR TO BRAZING

FIGURE 3-16

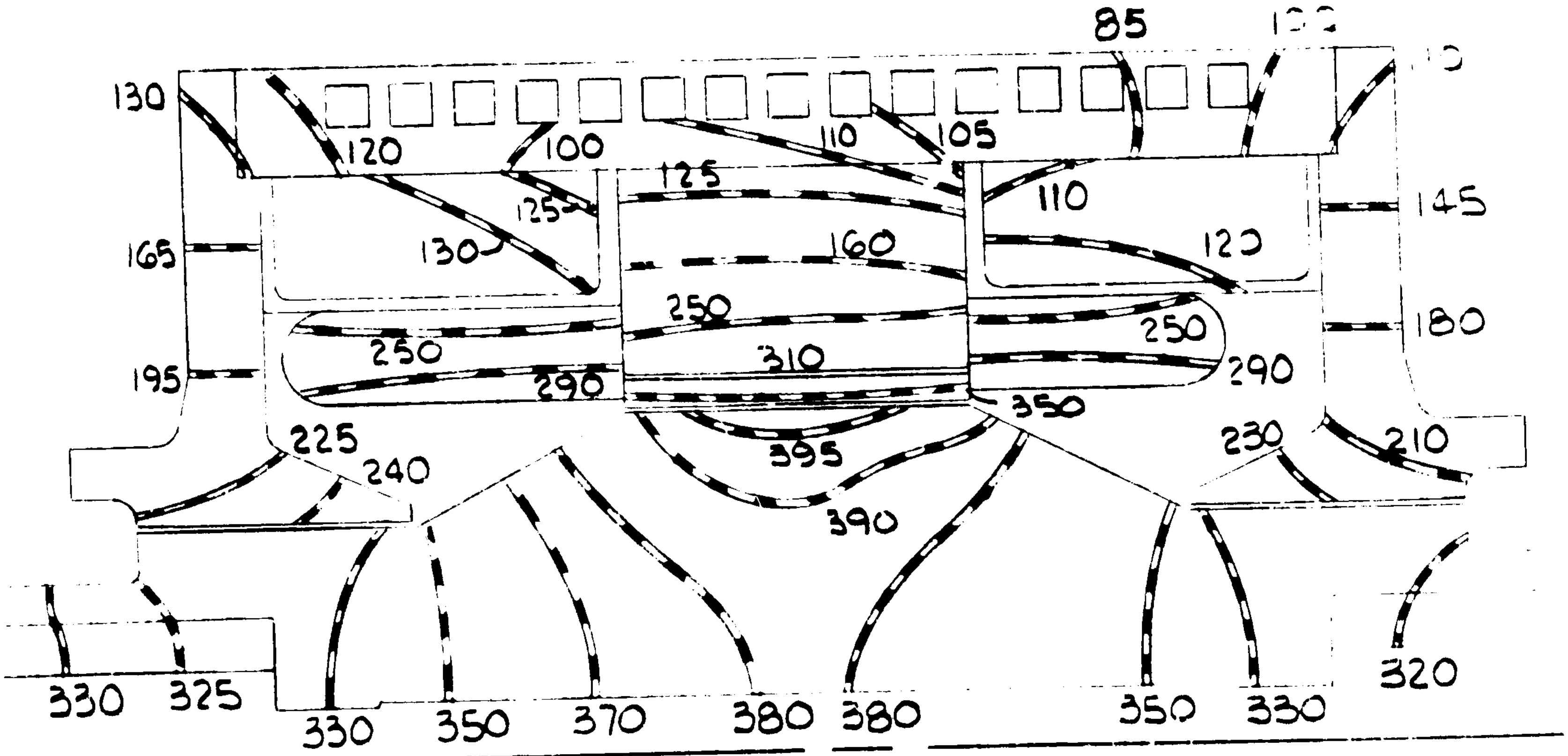

ALTERNATOR ELECTROMAGNETIC LOSSES	665 WATTS
ALTERNATOR WINDAGE LOSS	429 WATTS
TURBINE JOURNAL BEARING LOSS	45 WATTS
COMPRESSOR JOURNAL BEARING LOSS	45 WATTS
ALTERNATOR COOLANT - DOW CORNING 200	
COOLANT FLOW RATE	0.12 LB/SEC
COOLANT INLET TEMPERATURE	70°F

FIGURE 3-17

ALTERNATOR THERMAL ANALYSIS ISOTHERMS WITH OUTPUT OF 10.5 KW AT 0.85 PF

A33193, Rev.1

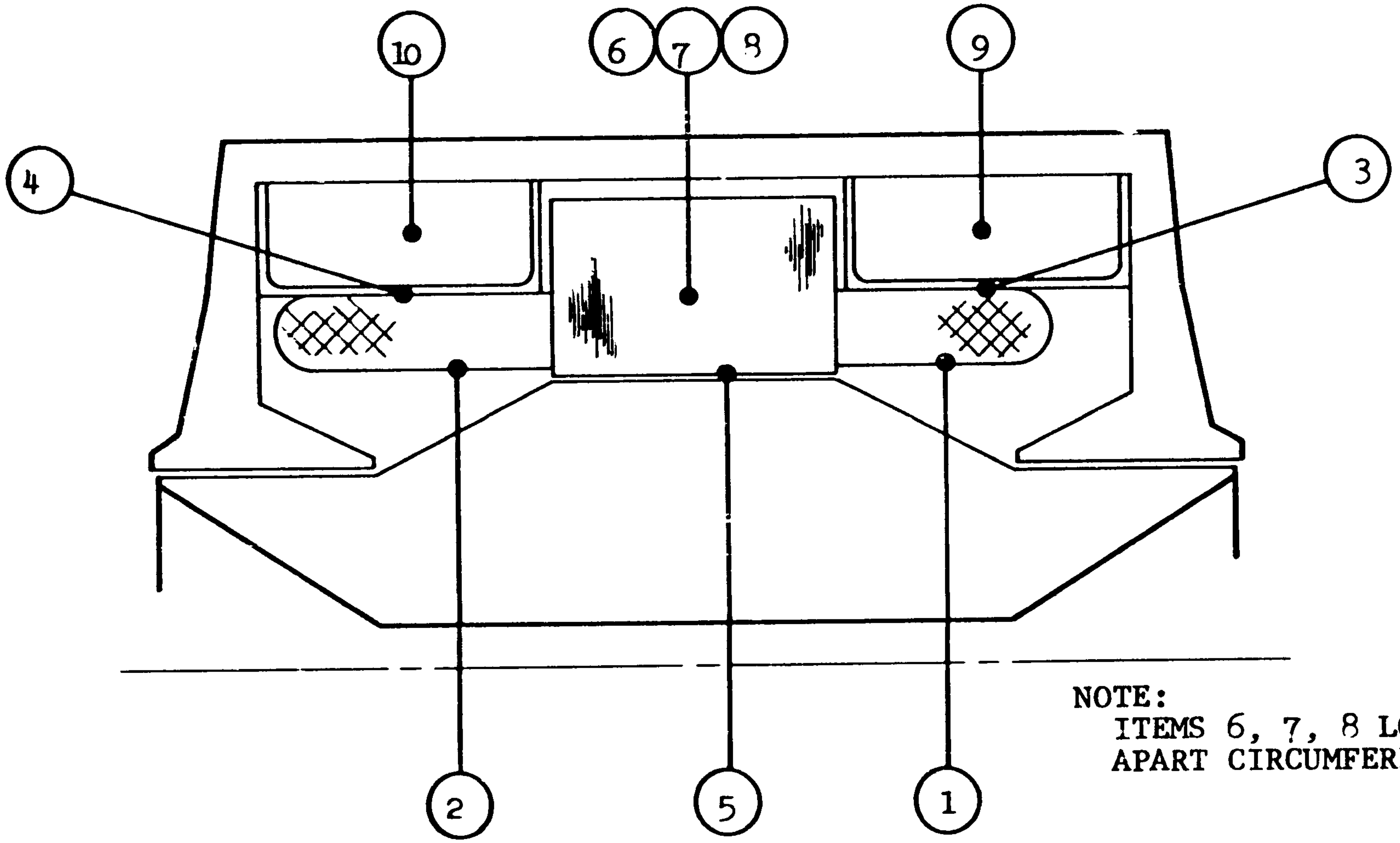

NOTE:
ITEMS 6, 7, 8 LOCATED 12
APART CIRCUMFERENTIALLY

ALTERNATOR STATOR THERMOCOUPLE LOCATIONS
FOR RESEARCH PACKAGE AND DYNAMIC SIMULATOR

FIGURE 3-18

brazing technique was required. In this respect, metallurgical and process problems were resolved and sound rotors were produced.

The rotor pole pieces are machined from bar stock. The Inconel separator is first cast and then finish-machined to match the pole pieces using the "Elox" process. The three parts of the rotor, prior to brazing, are shown in Figure 3-19. The brazed rotor prior to final machining is shown in Figure 3-20. Figure 3-9 shows a typical spin test rotor after final machining. Spin testing (on the test rig, Figure 3-21) at speeds up to 50,000 rpm is used as a method of determining braze integrity.

A considerable effort was expended in developing the brazing procedure. Sample parts were prepared and brazed in accordance with a schedule of different techniques. These parts were subsequently sectioned to permit inspection of the integrity of the braze for evaluation of the process.

To determine the heating and cooling cycles required for brazing the rotors, a dummy assembly was prepared. This was made of SAE 4340 bar-stock identical in size and shape with the braze assembly. The dummy assembly was then provided with thermocouples at eight locations throughout its mass. It was run through a trial cycle in the brazing furnace. During the entire cycle, an eight-point recorder continuously monitored and recorded the temperatures. Since the furnace used was of the vacuum-hydrogen-purged, sealed-retort type, very close control could be maintained over the rate of heating and cooling by regulating the flow of hydrogen purge through the sealed retort as well as by controlling the furnace heaters. Response time of the heavily thermocoupled dummy assembly determined the heating rates to which actual assemblies would be subjected. The spread between readings of the eight thermocouples monitoring the temperatures was held to ±10°F.

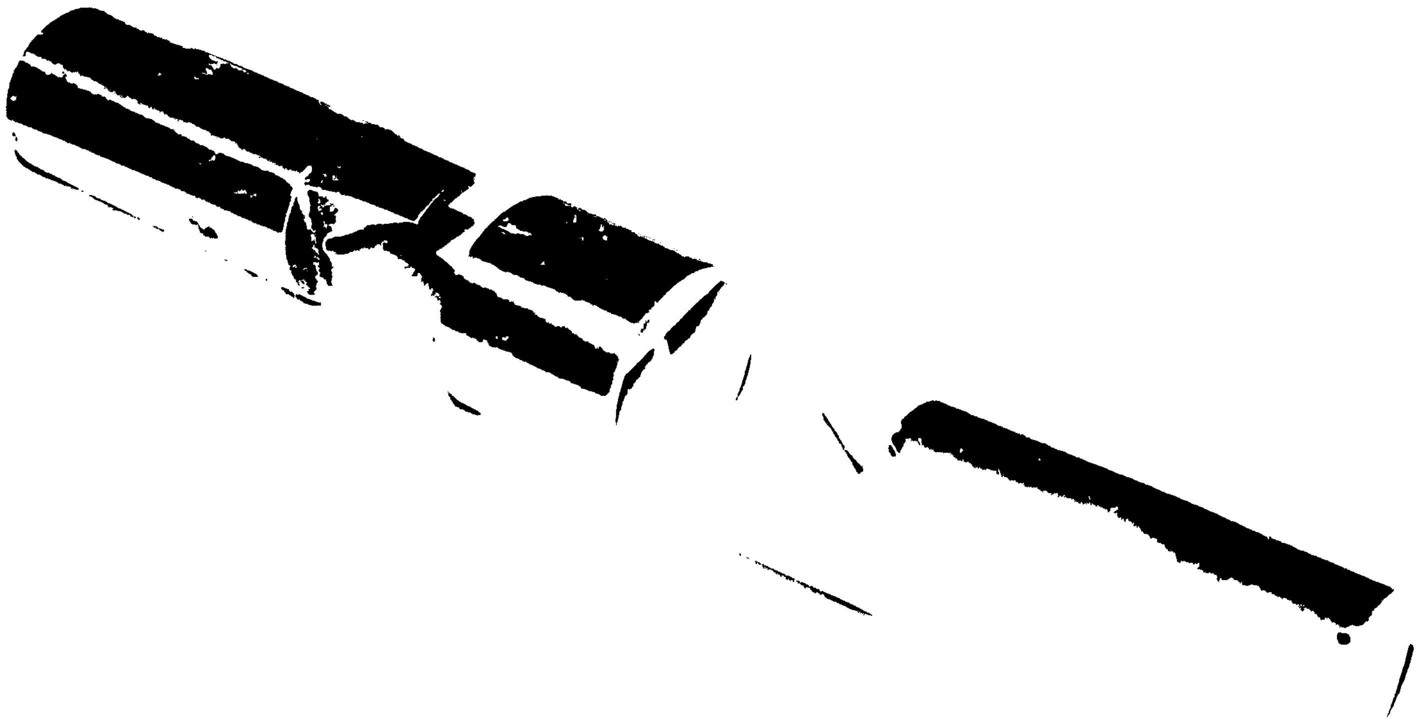

ROTOR POLES AND SEPARATOR PRIOR TO BRAZING

FIGURE 3-19

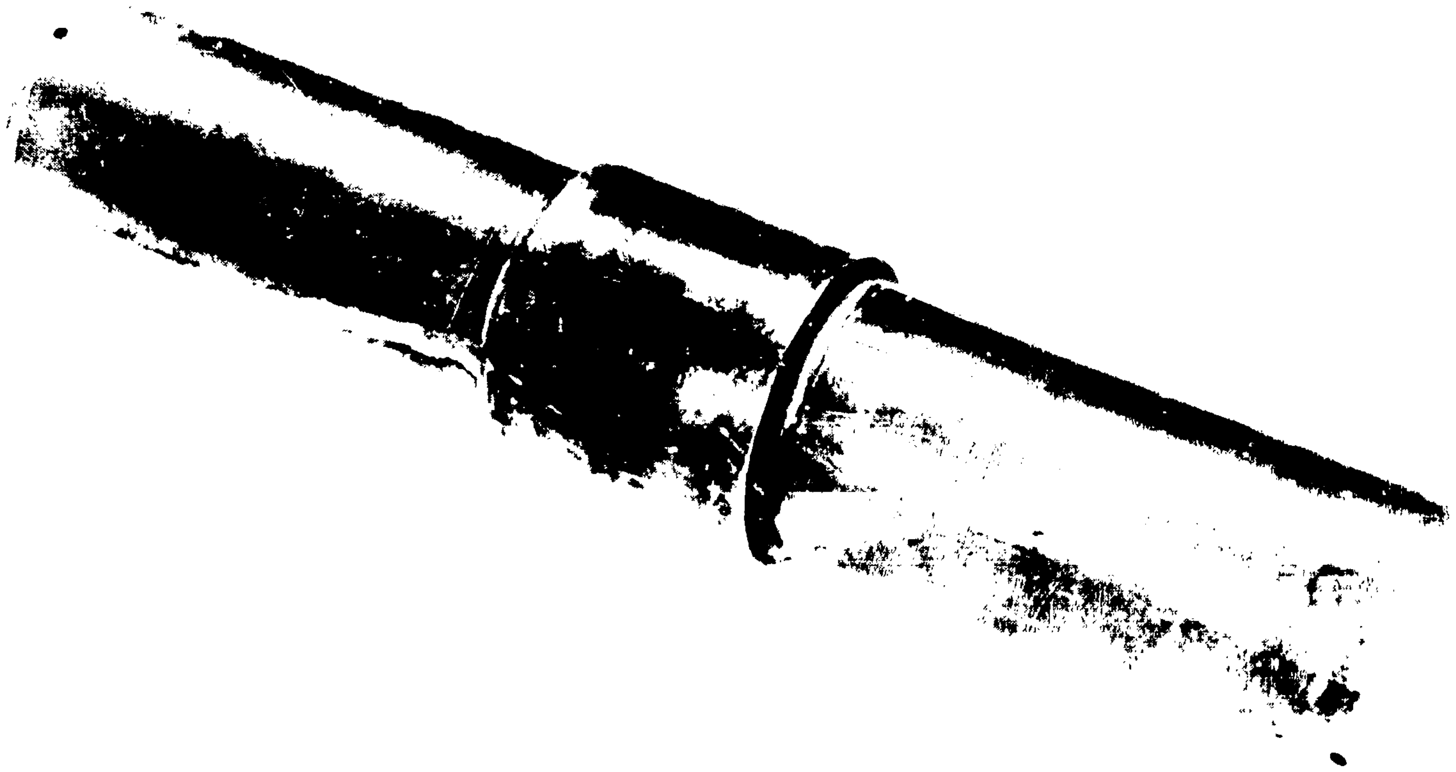

ALTERNATOR RESEARCH PACKAGE
BRAZED ROTOR ASSEMBLY

FIGURE 3-20

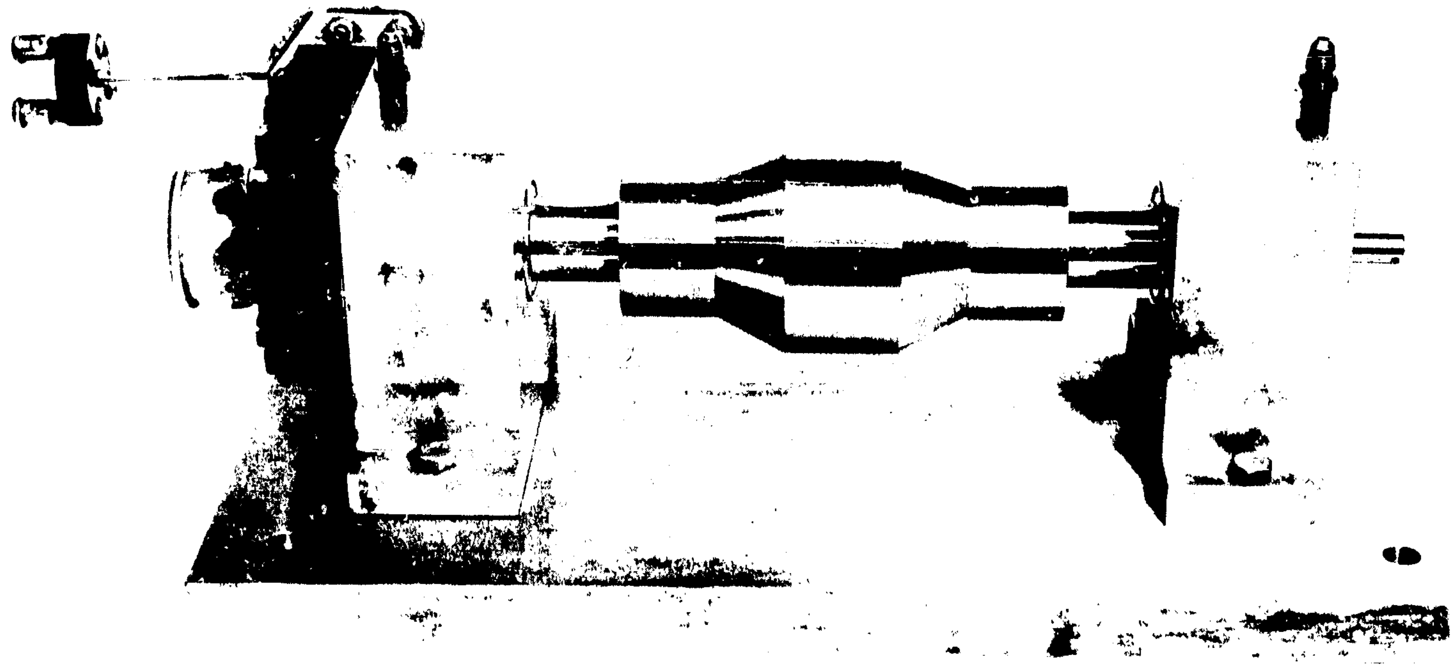

ALTERNATOR RESEARCH PACKAGE ROTOR
PART NO. 699531-1, SERIAL NO. 7X102
SHOWN IN ROTOR SPIN TEST RIG

FIGURE 3-21

From metallurgical examination and spin testing of sample rotors, a process specification was developed. Briefly, the specification calls for preparation of the braze joint surfaces of all three pieces by a steel grit blast. They were then given a nickel-plated flash, which was followed by plating with 0.0002-in. electrolytic gold. Due to its excellent wetting and strength characteristics for the type of alloy under consideration, Palnioro-7 was used for the braze alloy. Pieces of the alloy, formed from foil, were preplaced over the entire joint area prior to assembly of the rotor pieces. Intimate fit of the foil to the Eloxed joint surfaces, and of the pieces to each other, was accomplished by subjecting the three assembled parts to the force of a hydraulic press. Additional filler alloy in the form of wire and powder supplemented the in-joint foil.

The investigation into the rotor heat treatment required to produce satisfactory rotors involved some seven different heat-treat cycles. These cycles ranged over the austenizing temperature range of the 4340 material. It was determined that the length of time at 1200°F during the heat-treat cycle was a critical factor. Too short a time at this temperature allowed a significant amount of austenite to be retained at room temperature, which was then transformed into martensite or bainite. The resultant structure was notch-sensitive and subject to crack propagation.

To summarize, the brazing and heat-treat sequence involves the following steps:

(a) Heat to 1980°F at 350 to 400 deg/hr.
(b) Hold at 1980°F for 15 min. brazing time
(c) Furnace-cool to 1700°F at 200 deg/hr.
(d) Furnace-cool to 1400°F as fast as the furnace will permit
(e) Hold at 1400°F for 5 hrs. minimum - heat-treat time for Inconel 718

(f) Furnace-cool to 1165°F at 100 deg/hr.

(g) Hold at 1165°F for 8 hrs. heat-treat time for wrought 4340

(h) Rapid-cool to room temperature

Table 3-8 indicates the latest available data obtained on the rotor materials following subjection to representative braze and heat-treat cycles. In the case of the wrought 4340, the heat-treat cycle was generated by sample test to provide the results tabulated. Minimum rotor requirements are based upon design analysis, experience in braze development, and the stresses to be incurred in overspeed tests (50,000 rpm). The overspeed tests are required for quality control purposes.

Materials selected for the alternator construction are tabulated in Table 3-9.

TABLE 3-8
ROTOR MATERIAL DATA AFTER REPRESENTATIVE BRAZE AND HEAT TREATMENT CYCLES

	Minimum Rotor Requirements	Wrought 4340	Cast Inco 718
Retained Austenite - %	1.0	0.3	-
Yield Strength - ksi	50	65.4	110
Ultimate Strength -ksi	100	114.4	143.6
Elongation - %	10	23.5	11.0
Hardness - Rockwell C	15-20	17-18	-
Notch Sensitivity - Charpy V - ft.-lb.	20	22-24	-
Heat-treat		8 hrs. at 1165° ±15°F	5 hrs. at 1400°F plus 8 hrs. at 1165°F

TABLE 3-9

Component	Material	Basis for Selection
Frame and End Plates	Annealed Ingot Iron	High saturation-density at relatively low magnetizing intensity; good availability.
Rotor	4340 Nickel Chrome Alloy Steel and Inconel 718	The 4340 has desirable magnetic and structural properties. The nonmagnetic Inconel 718 is a good thermal match for use in this bimetallic structure. Previous good experience in furnace-brazing Rice rotors of smaller size using these materials was an all-important factor in this selection.
Laminations	AL* 4750, 0.004 in.	This 48 percent nickel alloy was selected to obtain low tooth and core loss. Since saturation density is lower than for silicon steels, a weight disadvantage is incurred. Laminations were treated to produce a No. 11 oxide film.
Magnetic Wire	Heavy ML Insulated Copper	Class 220°C insulation provides reliable, long-life operation with good margin for thermal overloads.
Stator Winding Varnish	Westinghouse Doryl B109-3	Class 220°C varnish with good build and toughness.
Field Coil Impregnant	Epoxylite 108	Class 180°C impregnant. Successfully used in similar applications.
Slot Insulation	Triple Ply (3-3-3) of Nomex, H-Film, and Nomex	Class 220°C materials with good physical and dielectric properties.
Top Stick		Micarta Doryl laminate

---

*Allegheny Ludlum

Figure 3-2 shows the ARP disassembled. The calculated weight of the electromagnetic components of the ARP is tabulated in Table 3-1.

3.3 Test Results

By contract, the usual component development tests would be performed by NASA rather than by the contractor. Under these conditions, it was also the intent of NASA to match the alternator with the first VRE and speed-control. However, to assure proper functioning of the components, certain functional tests were performed.

3.3.1 Alternator Research Package Rotor Spin Test Rig - A simple test rig (Figure 3-21) utilizing antifriction bearings for support was designed and fabricated for rotor spin testing. This rig was designed to accommodate all rotors, whether for BRUs or the research package. Before use in machines, all rotors were subjected to this spin test to demonstrate integrity. Overspeed of 50,000 rpm subjects the rotor to approximately twice the design stress levels and was used to prove rotor integrity.

3.3.2 ARP Alternator Evaluation - Prior to the system tests using the Alternator Research Package, the voltage-regulator/exciter, and the speed control, a performance scan test was run on the ARP alternator unit. To obtain an early assessment of the electromagnetic performance of the alternator components, a magnetic test unit (MTU) was fabricated early in the development program. The stator, field coils, and rotor were magnetically the same as their counterparts in the ARP and BRU. The frame and end-plates were magnetically similar to the ARP and BRU counterparts, but differed physically because of design simplifications. Low-speed bearings were substituted for the oil-mist or gas bearings.

The load and short-circuit characteristics for the ARP are shown in Figure 3-22 which compares the test data with the design predictions. These tests reveal appreciable differences between the predicted ARP alternator performance and the results of low-speed tests undertaken previously on the MTU (Figure 3-23). The saturated no-load voltage obtained with the MTU (Figure 3-24) was 1.82 p.u. as compared to 1.4 for the ARP (30-percent low). The no-load performance of the ARP was rechecked at 36,000 and 3600 rpm to rule out the possibility of test-meter error and also to determine if there was a speed effect on saturation voltage due to poor interlamination resistance of the stator stack. Results indicated that initial saturation data results for the ARP were valid and also that the speed effect was slight. At the same time, a no-load saturation test was again conducted on the MTU, using different instruments. These results confirmed the original MTU value. In addition to the above-mentioned dynamic tests, static tests were made to obtain a flux survey of the machine. These tests check the accuracy of the leakage flux calculations. Results showing the total flux crossing the auxiliary gap plotted against excitation are shown in Figure 3-25. Hence, it was concluded that there were, in fact, performance differences between the MTU and ARP magnetic systems.

A review of possible causes for the indicated discrepancy disclosed the following three items worthy of consideration:

(a) The rotor used in the MTU was one of the first three ever made. Although defective in the brazed joint, the rotor had been satisfactorily heat-treated and considered safe to spin in the MTU test fixture up to 6000 rpm. The ARP rotor had been subjected to a revised heat treatment, then finish-machined. Metallurgical examination of later rotors (double-braze group) showed that following the second braze cycle, approximately 8 percent austenitic iron had been

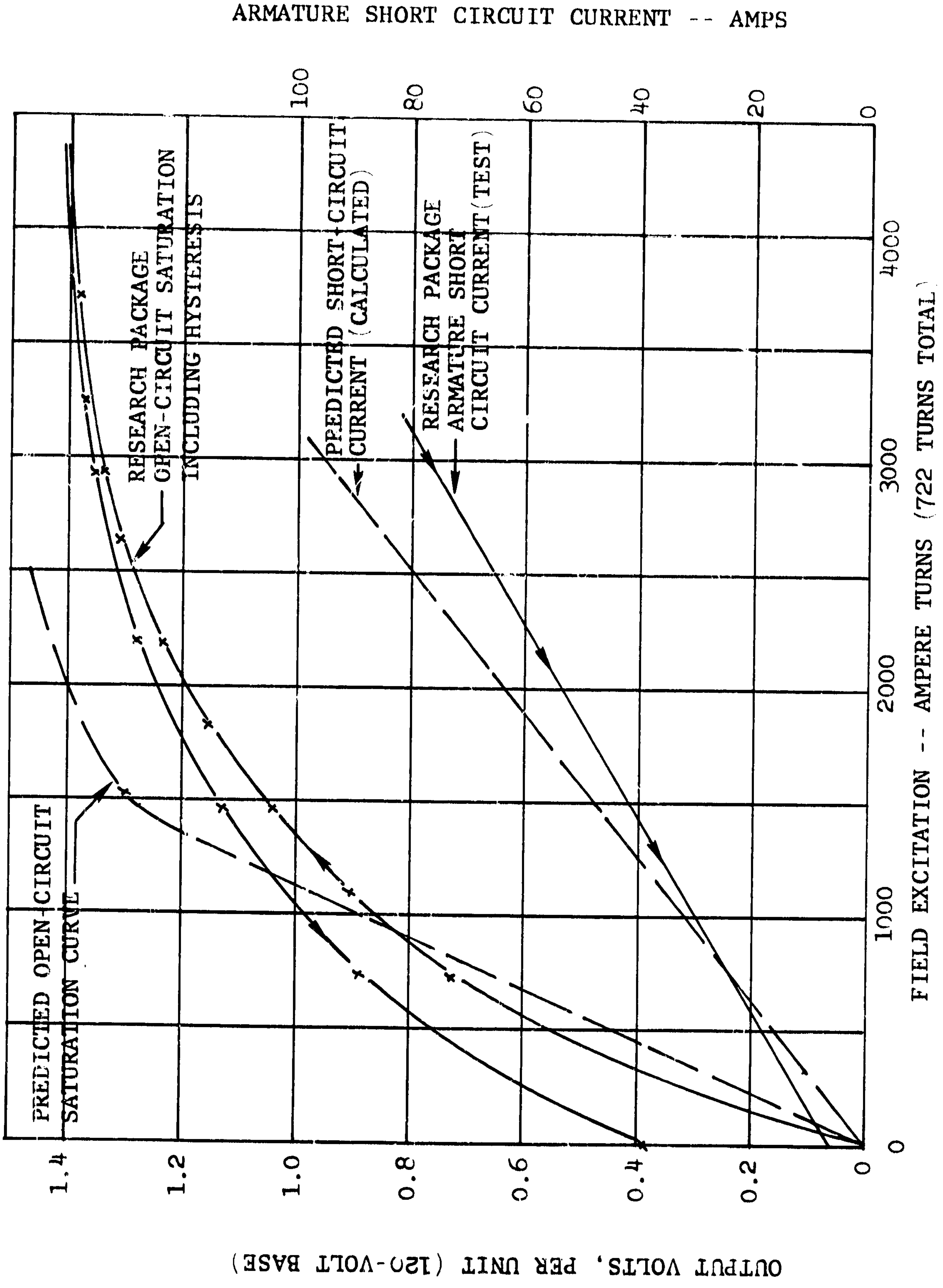

NO-LOAD SATURATION CHARACTERISTICS
ALTERNATOR RESEARCH PACKAGE
AT 100 PERCENT SPEED (36000 RPM)

FIGURE 3-22

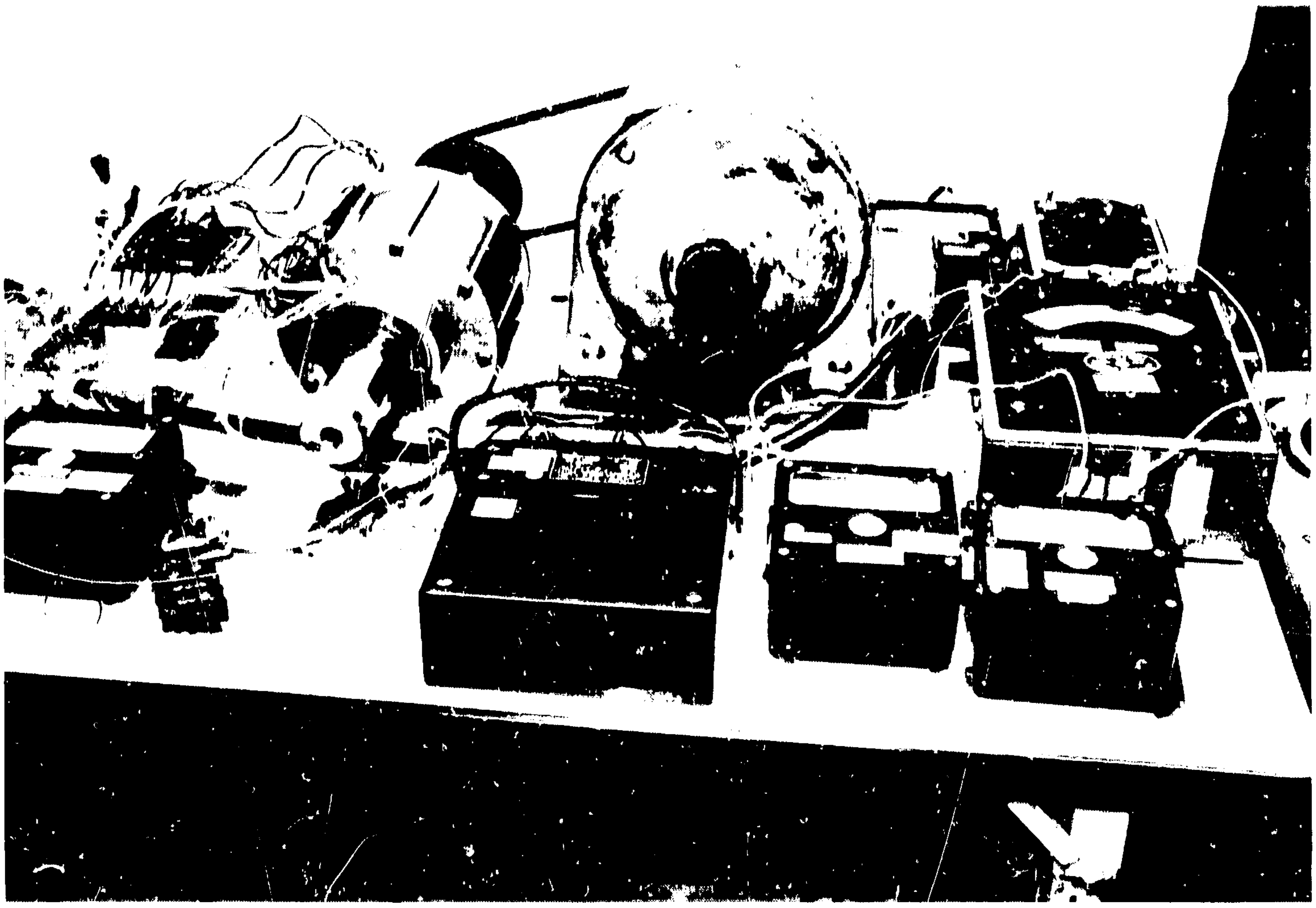

ELECTROMAGNETIC TEST RIG

FIGURE 3-23

SATURATION CHARACTERISTIC
FOR BRU ALTERNATOR PART 518606
TESTED 6-27-60

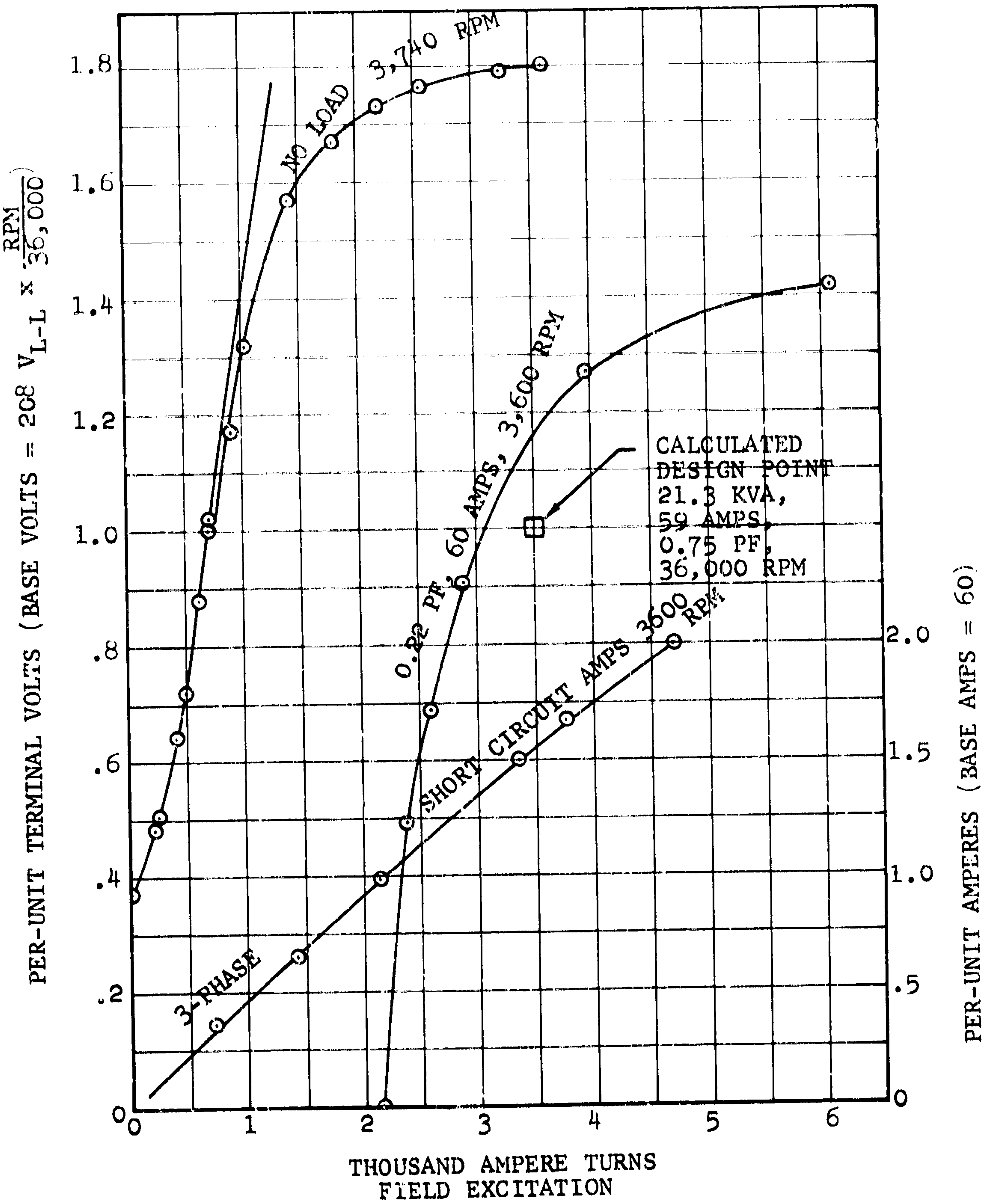

FIGURE 3-24

TOTAL FLUX AT THE AUXILIARY GAP
VERSUS
TOTAL FIELD EXCITATION
BRU ALTERNATOR PART 518606

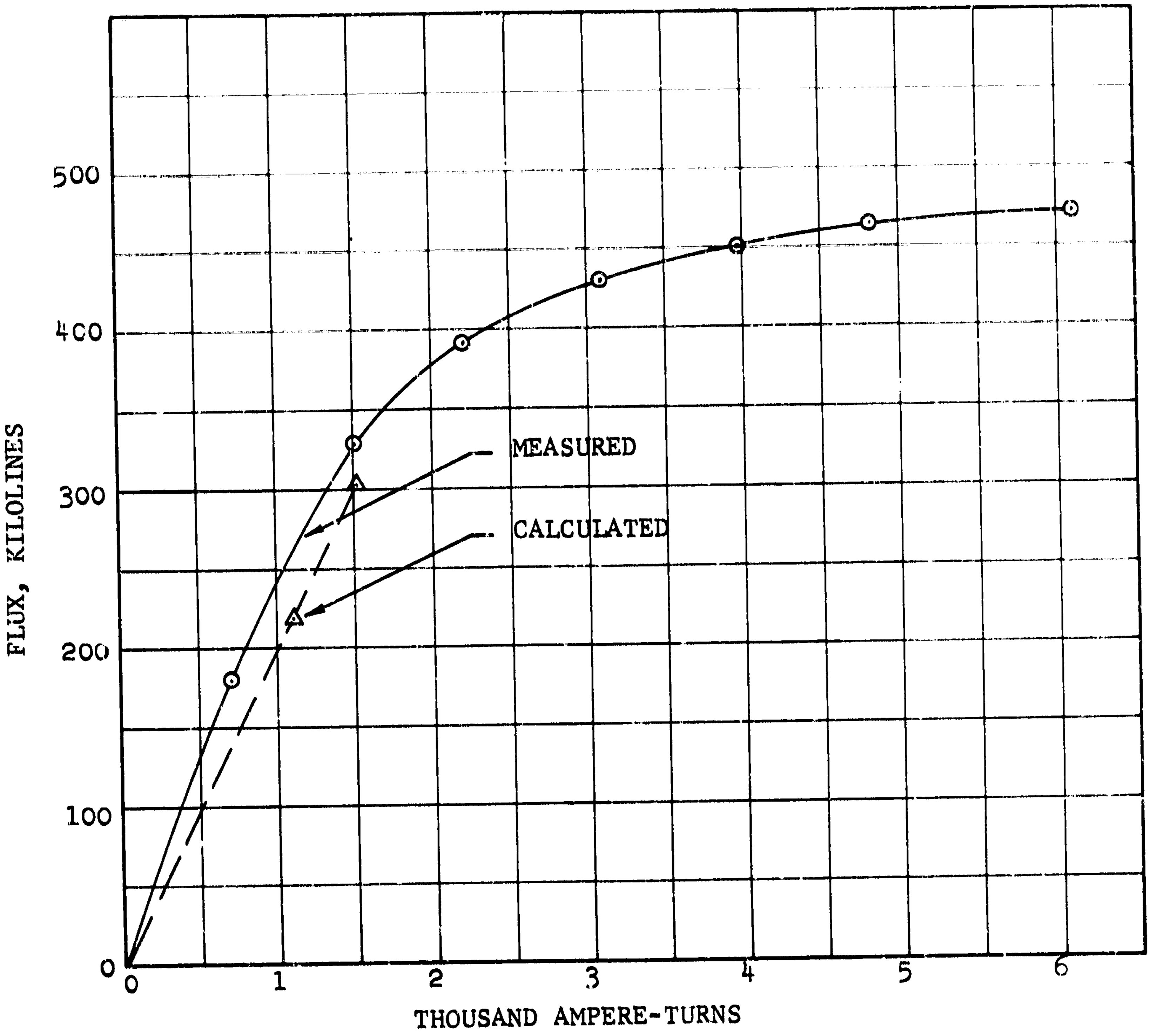

FIGURE 3-25

retained. To obtain removal of the retained austenite in the ARP rotor would have required tempering. Since the rotor had been finish-machined, tempering was not attempted because it was believed that distortion might occur. A cold-soak to -30°F for 1 hr. and subsequent heating to +350°F had been undertaken in order to physically stabilize the rotor as much as possible with minimum distortion.

(b) Stator laminations had been heat-treated in two groups, and the MTU and research package stacks differed in this respect. Poor annealing or handling abuse during stacking could have affected the performance.

(c) Investigation of the laminations in the two groups also indicated that the insulation resistance of the No. 11 film was poor, particularly on those representative of the ones used in the research package.

Because all of the above possible causes were determined on the basis of the tests conducted on the ARP, further investigation and corrective action was initiated as follows:

Rotor - To determine the effect of retained austenite, the backup rotor, ARP Serial No. 2 (with identical fabrication processes and heat treatment) was adapted to fit the MTU. Comparison check runs were made. (A replacement rotor is in process for the delivery ARP. Note that in Section 3.2.1 in the discussion of the rotor heat treatment, processing was established for all future rotors, insuring the percentage of retained austenite is held to an acceptably low level.)

These tests showed that the Serial No. 2 rotor had a saturation voltage of only 1.63 p.u. compared with 1.82 for the original MTU rotor. Tempering of Serial No. 2 rotor at 1200°F for 2 hrs. was then successfully attempted with only slight growth or distortion of the part. When the Serial No. 2 rotor was again tested in the MTU, the saturation voltage increased to 1.76 p.u. This indicated that the basic cause of poor performance (low saturation voltage) was austenite-retention in the rotor. This problem should not exist in future units.

Stator Laminations - Future stator laminations will receive a high-temperature insulating film treatment in lieu of the No. 11 oxide film originally specified.

With the design and fabrication of the ARP completed and the unit due to be delivered, the ARP was shipped to the NASA-Lewis Research Center where development tests could indicate other areas of possible deficiency in that unit. In its present condition, the ARP is expected to display a lower overall efficiency than predicted, and additional excitation power will be required at the 21.3-KVA overload condition. A replacement rotor to correct these deficiencies will soon be available for installation in the ARP.

3.3.3 Functional Test of the Components - Prior to the acceptance of the alternator research package, the VRE and speed-control were connected with the ARP and briefly checked to assure compatibility between the components. This could not be determined conclusively, however, because of the filter problem noted in the speed-control section. When the VRE and the alternator were connected and the speed-control disconnected, the operation was stable. When the speed-control was connected without filtering, there was some interaction between the VRE and the speed-control at conduction angles near 90° due to the transient noise generated. Proper filtering probably would remove this interaction.

The VRE and the alternator were stable when an air turbine drive system was used. The speed control demonstrated capability of attaining the specified limits of 1200 Hz ±1 percent from zero to 10.5 KW with 0.75 pf lagging vehicle load. It cannot be concluded from this, however, that the entire system will be stable when operated with a much stiffer drive system.

ARP Acceptance Test - The ARP was operated through the entire speed range while the bearing temperatures, vibration levels, and operational characteristics were observed. The acceptance test was witnessed and approved by NASA representatives. Included in the tests were a critical speed survey, 30 min. operation at the design speed of 36,000 rpm, and 10 min. operation at 120-percent speed (43,200 rpm). During these tests, temperatures and vibration levels were recorded.

4.0 DESCRIPTION OF THE VOLTAGE REGULATOR/EXCITER (VRE)

The voltage regulator/exciter is designed as a breadboard unit utilizing high reliability components. It is designed for maximum flexibility during development testing and includes such features as provisions for either internal or external voltage sensing and a removable series field module.

A block diagram of the VRE and of its loops is shown in Figure 4-1. This diagram is also used to define the major symbols used in this report. Capital letters denote d-c or rms quantities, as appropriate, and lower case letters denote instantaneous quantities.

For all specified lagging load conditions the excitation provided by the series field is less than the total required alternator excitation. The shunt field regulator supplies the required incremental excitation upon demand as determined by the voltage loop. Operation at leading power factors, when the series field excitation may be in excess of the total requirement, is not within the capability of this system.

Table 4-1 is a summary of the alternator field excitation requirements. This information is derived from the predicted alternator performance curves shown in Figure 4-2. Total excitation requirements at short circuit and various other operating points are obtained directly from the graph. The available series field excitation is linearly extrapolated from the short-circuit requirements, and the difference is then assigned to the shunt field.

It may be noted that, for example, at 12.6 KVA and 1800 Hz (equivalent to 0.667 p.u. voltage on Figure 4-2), the total excitation requirement is only 1500 ampere turns, of which at least 1100 ampere turns are supplied by the series field. Clearly the overspeed

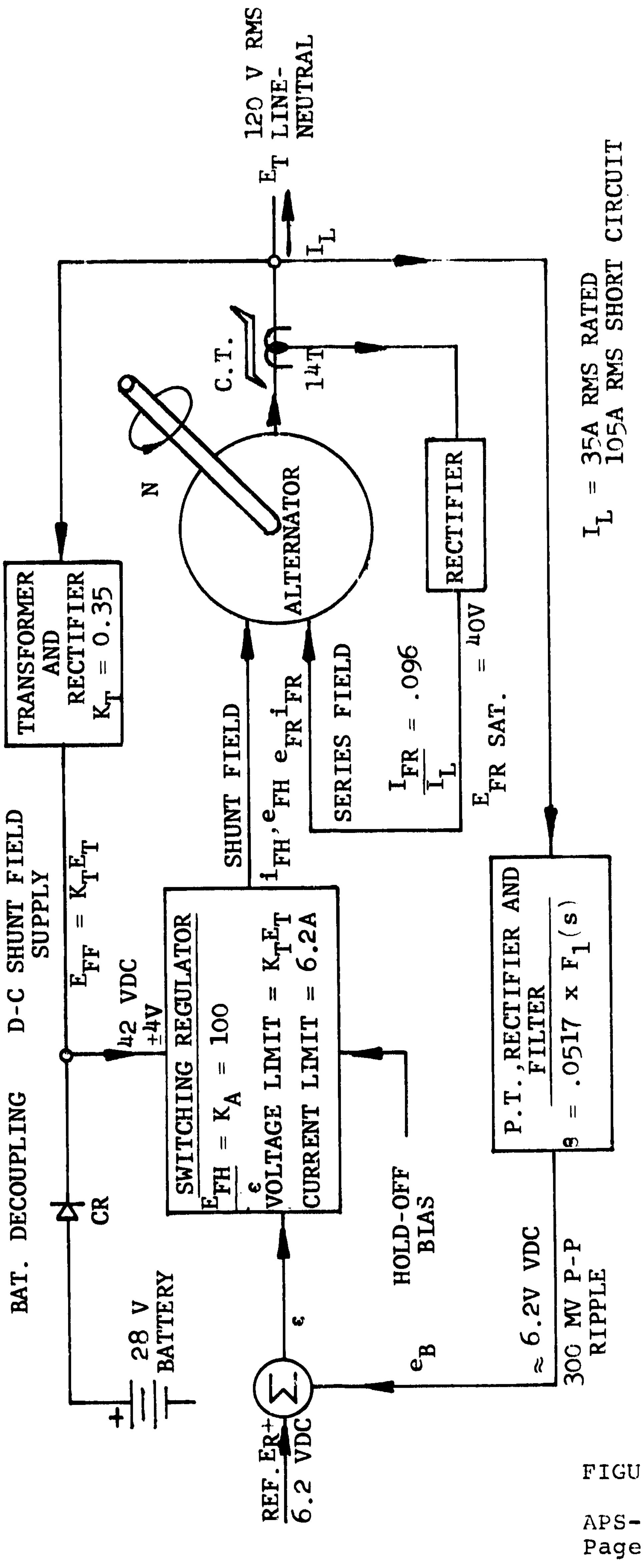

BLOCK DIAGRAM, BRAYTON ROTATING UNIT
VOLTAGE-REGULATOR/EXCITER UNIT

FIGURE 4-1

NOTE: THIS CHART IS CHANGED FROM PREVIOUS EDITION

TABLE 4-1
FIELD EXCITATION REQUIREMENTS

N_{FH} = 364T R_{FH} = 4.0 Ω N_{FR} = 358T R_{FR} = 4.40 Ω

RESISTANCES AT 177°C (DIV. BY 1.6 FOR 22°C VALUE)

TERMINAL VOLTAGE 120 V RMS L-N

KVA	0	2.65	7.21	12.6	14.3	21.3 ①	SHORT	
P.F.	-	0.85	0.85	0.85	0.75	0.75	-	
I_L	0	7.37	20.0	35.0	39.7	59.1	105	A RMS
NI at 1.2 KC	1100	1300	1625	2136	2444	3510	3300	AT
$(NI)_R$	0	232	629	1100	1257	1860	3300	AT
I_{FR}	0	0.647	1.76	3.07	3.49	5.20	9.20	ADC
E_{FR}, 177°C	0	2.85	7.75	13.5	15.4	22.8	40.5	VDC
E_{FR}, 22°C							25.3	VDC
$(NI)_H$	1100	1068	995	1036	1194	1630	0	AT
I_{FH}	3.02	2.94	2.73	2.84	3.2[illegible]	4.53	0	ADC
E_{FH}, 177°C	12.2	11.8	10.9	11.4	13.1	18.2	0	VDC
E_{FH}, 22°C	(7.56)	(7.35)	(6.82)	(7.10)	(8.20)	(11.4)	0	VDC
NI at 1.08 KC	1225	1550	1900	2500	2980	SATURATED	(3650)	AT
$(NI)_H$	1225	1318	1271	1400	1630		0	AT
I_{FH}	3.36	3.62	3.49	3.85	4.48		0	ADC
E_{FH}, 177°C	13.4	14.5	14.6	15.4	17.9	▼	0	VDC
E_{FH}, 22°C							0	VDC
NI at 1.32 KC	1000	1200	1450	1950	[illegible]	[illegible]	(2000)	AT
$(NI)_H$	1000	968	821	850	[illegible]	[illegible]		AT
I_{FH}	2.75	2.66	2.26	2.34	2.77	[illegible]	0	ADC
E_{FH}, 177°C	11.0	10.7	9.03	9.4	11.[illegible]	12.[illegible]	0	VDC
E_{FH}, 22°C			(5.65)				0	VDC

SUBSCRIPTS: H SHUNT (CONTROL) FIELD, R IS SERIES FIELD

① 2 p.u. LOAD, 5 SEC. RATING

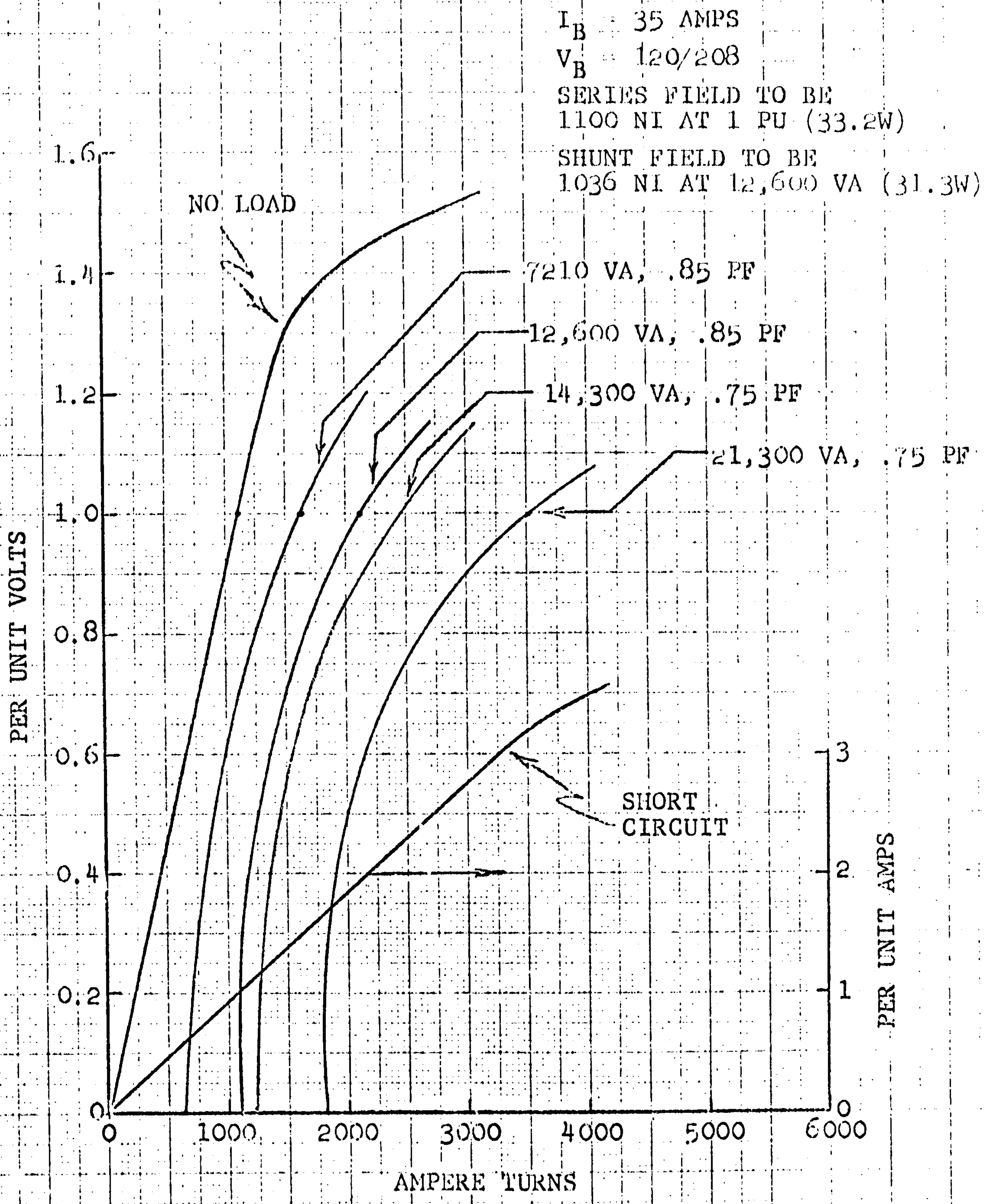

ALTERNATOR ELECTRICAL CHARACTERISTICS

FIGURE 4-2

operational requirement is only marginally controllable, and only a bare minimum of excess series field capacity may be allowed to cover design tolerances.

4.1 Series Field Controller (Exciter) Analysis

The series field circuit is schematically shown in Figure 4-3. The output of three line current transformers is rectified and fed to the field. The purpose of the capacitor is to eliminate the high voltage pulses which, in its absence, would appear across the field and the rectifiers; it also serves to control the magnitude of transient field voltage resulting from a step-load application. The required design equations are derived below and are followed by detail numerical information.

Figure 4-3 is used to define the nomenclature. The symbol I_L is used for the rms magnitude of the line currents.

Current Transformer Derivations - The rectifier output current is shown in Figure 4-4c. It is assumed that its a-c component flows in the capacitor only. By inspection, the d-c component is the field current, given by:

$$I_{FR} = \frac{3}{\pi} \int_{\pi/3}^{2\pi/3} \sqrt{2}\, \frac{I_L}{N} \sin\theta \, d\theta = 1.35 \frac{I_L}{N} \qquad (4\text{-}1)$$

where N is the turns ratio (number of secondary turns) of the transformer. The d-c voltage is simply given by

$$E_{FR} = I_{FR} R_{FR} = 1.35 \frac{I_L}{N} R_{FR} \qquad (4\text{-}1a)$$

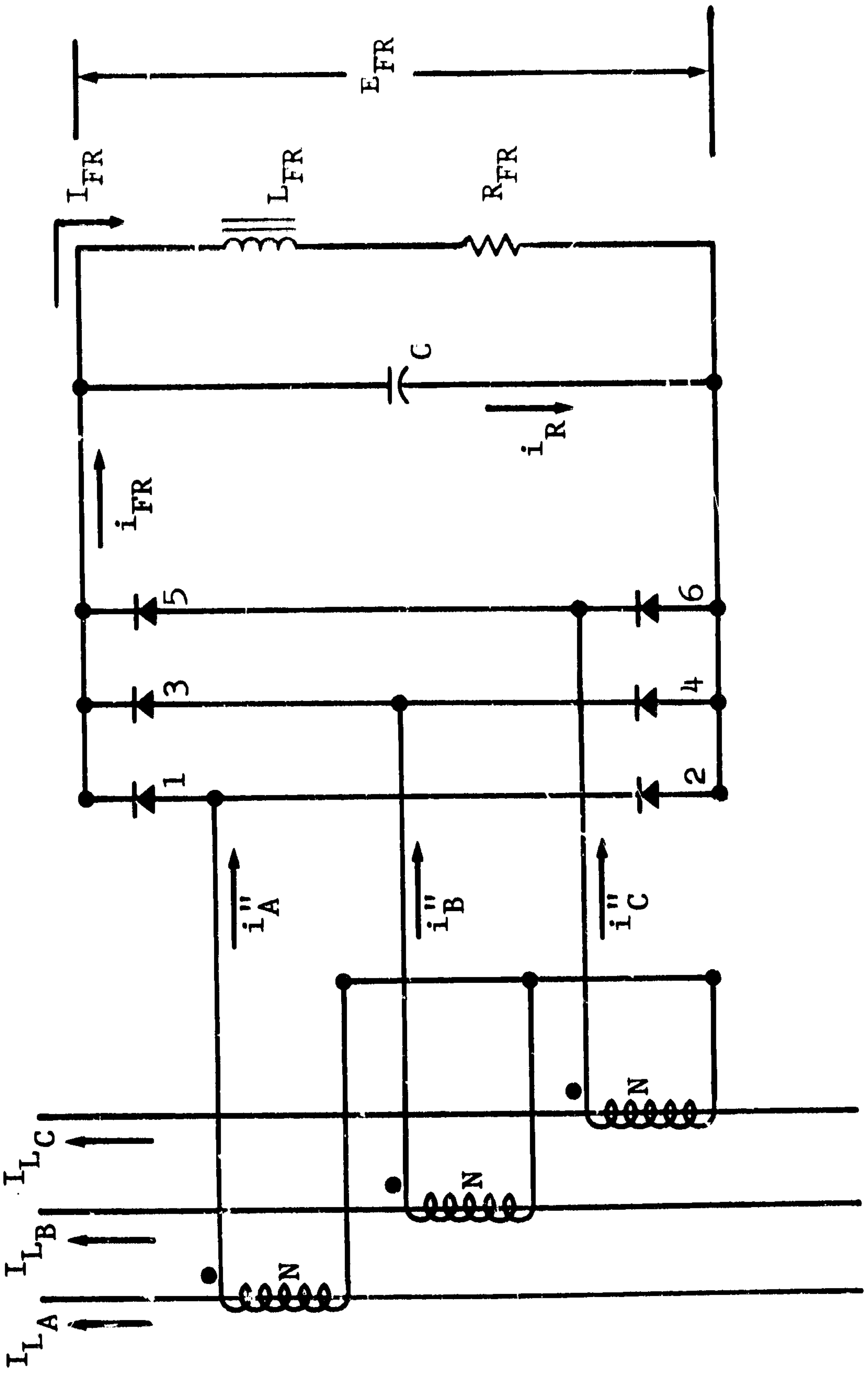

FIGURE 4-3
SERIES FIELD CIRCUIT

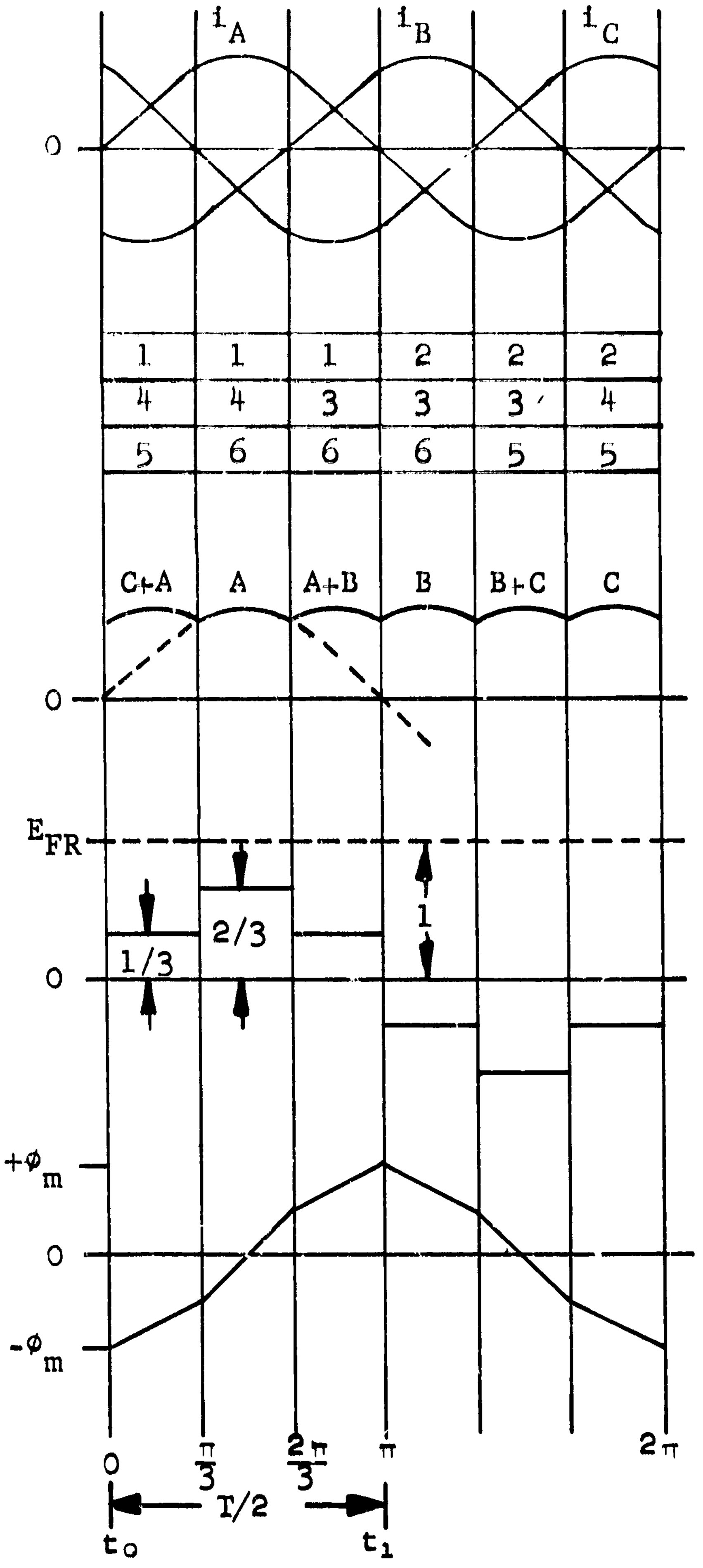

FIGURE 4-10a

PRIMARY LINE CURRENTS
OR SECONDARY PHASE CURRENTS

FIGURE 4-10b

CONDUCTING RECTIFIER

FIGURE 4-10c

RECTIFIER OUTPUT CURRENT, i_{FR}, AND ITS COMPOSITION

FIGURE 4-10d

SECONDARY VOLTAGE OF PHASE A TRANSFORMER SCALED WITH RESPECT TO D-C FIELD VOLTAGE

FIGURE 4-10e

FLUX OF PHASE A TRANSFORMER

FIGURE 4-4

SERIES FIELD WAVE FORMS

Although the transformer secondary currents are essentially sinusoidal, the secondary voltages are not. The secondary voltages are determined by the series field voltage, as the secondaries are sequentially clamped to the field by the rectifiers. For ideal rectifiers, zero magnetizing current and a large filter capacitor, the transformer secondary voltage is as shown in Figure 4-4d.

The transformer flux, as related to the voltage, is shown in Figure 4-4e. From Faraday's Law:

$$e\,dt = 10^{-8}\ N\ d\phi \qquad (4\text{-}2)$$

Dividing both sides of the equation by the half-period T/2 and integrating between appropriate limits:

$$\frac{2}{T}\int_{t_o}^{t_1} e\,dt = \frac{2}{T}\int_{-\phi_M}^{+\phi_M} 10^{-8}\ N d\phi \qquad (4\text{-}3)$$

The left-hand member of this expression is recognized to be the half-cycle average value of the voltage; and, thus, by inspection (Figure 4-4d):

$$\frac{4}{9}\,E_{FR} = \frac{2}{T} \times 10^{-8}\ N \times 2\phi_M$$

The total flux is replaced by $\phi_M = B_M A_C$ and the expression is solved for A_C:

$$A_C = \frac{10^8\ E_{FR}}{9N\ B_M f} \qquad (4\text{-}4)$$

where f is in Hertz, B_M in kilogauss, and A_C in square centimeters.

By substituting Eq. 4-1 into 4-4, another form is obtained:

$$A_C = \frac{10^8 \times E_{FR} \times I_{FR}}{12.15 \times B_M \times I_L \times f} \qquad (4-5)$$

which simply states that, for a given line current, the cross-sectional area of the core is determined by the series field power requirement. In practical computation, the 2-V drop of the rectifiers is lumped into the E_{FR} of the above equations.

The waveform shown in Figure 4-4d is not seen in practice due to the superposition of a ripple voltage generated by the a-c component of the rectifier output current. When the peak of this ripple voltage is smaller than E_{FR}, its average over the integration period is zero, and the results are not affected. If E_{FR} tries to go negative during parts of a cycle due to high ripple voltage, the rectifier free-wheels at those times. The effect is an increase in average field current, approaching the peak of the a-c current. In a three-phase circuit, this effect is negligible since the peak a-c current is less than 5 percent higher than the average.

The magnetizing current of the CT is considered with the aid of Figure 4-5 in which the usual B-H curve is replaced by the flux-current loop of the particular transformer. The idealized loop shown is considered sufficiently accurate for the materials used. The peak magnetizing current, referred to the secondary, is then given by:

$$I_M = \frac{H_c l_c}{0.4\pi N} \qquad (4-6)$$

where H_c is the coercive force in question, and l_c is the magnetic path length in centimeters.

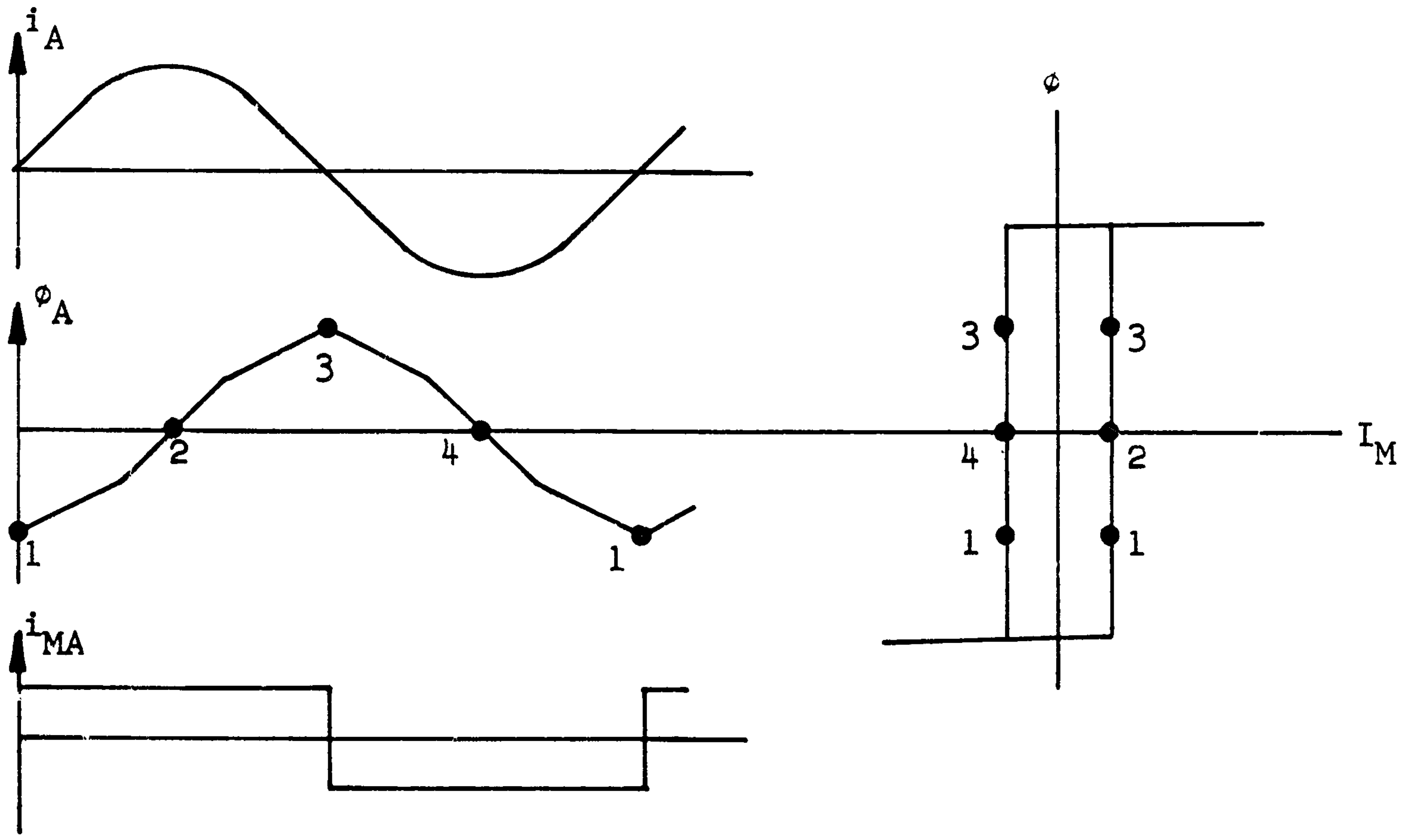

CURRENT TRANSFORMER MAGNETIZING CURRENT

FIGURE 4-5

This magnetizing current is accounted for by adding it to the field current required by the alternator.

Series Field Transfer Function - Figure 4-6 depicts the static transfer function of the series field during a three-phase short-circuit. The shunt field contributes nothing during a short. The "required" curve shows the alternator short-circuit test characteristics. This curve does not pass through the point of origin due to residual magnetism. The "supplied" curve indicates the design requirements. To provide short-circuit current capability, the twc curves must intersect above the minimum specified fault-current.

Nonsinusoidal Alternator Load - It is instructive to look at a condition of nonsinusoidal alternator loading. Figure 4-7 presents waveforms associated with a rectifier load having a large choke input filter. The amplitude of the line current is equal to the d-c load current I_D. Clearly, if N is the current transformer (C.T.) turns ratio

$$I_{FR} = \frac{I_D}{N} \tag{4-7}$$

However, the RMS line current is given by:

$$I_L = 0.816 I_D \tag{4-8}$$

Thus,

$$I_{FR} = \frac{1.225\ I_L}{N} \tag{4-9}$$

The transformer voltage waveform is shown in Figure 4-7c. Clearly, the transformer has to support only one-third of the half-cycle field

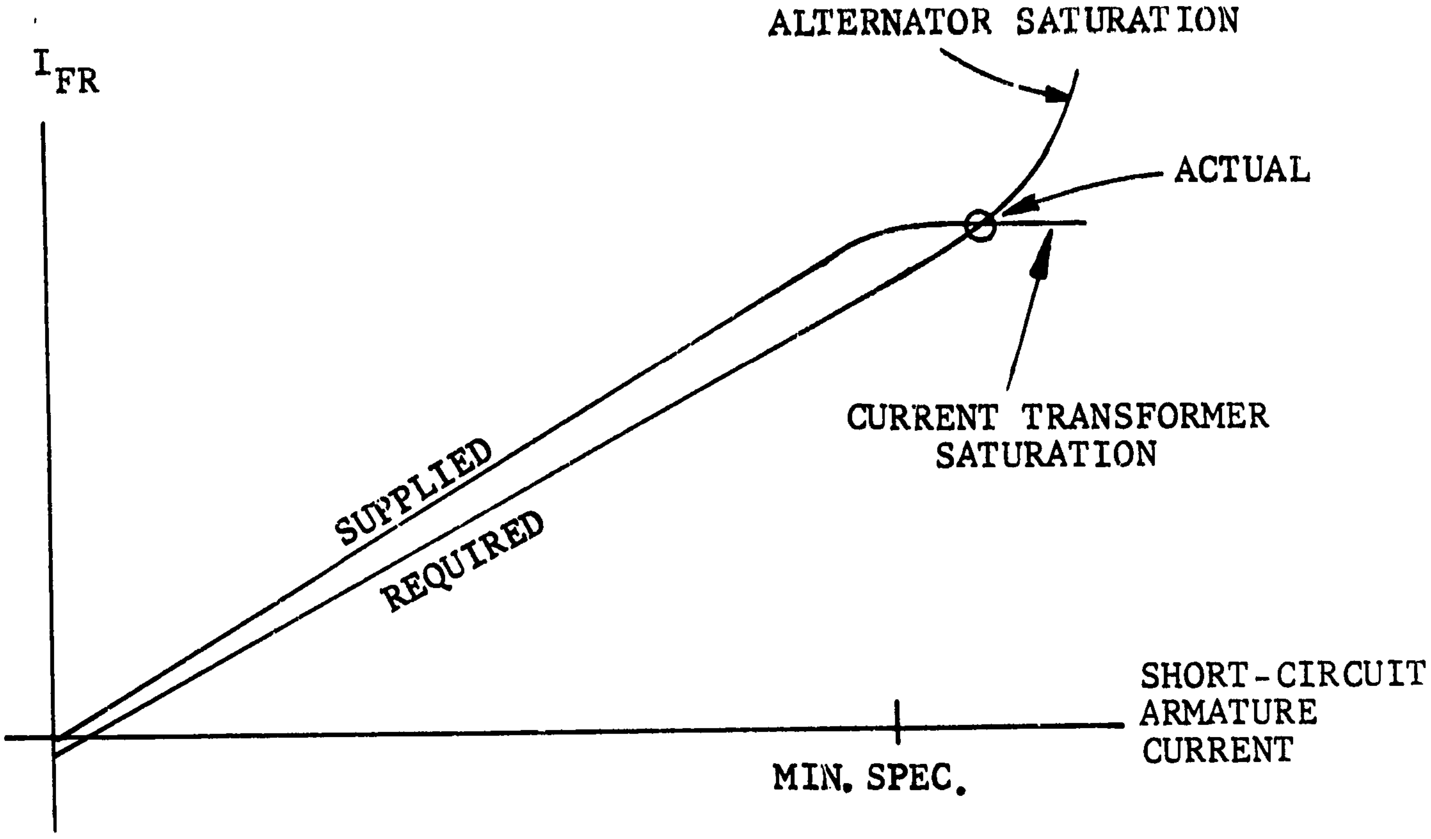

SERIES FIELD STATIC CONTROL CHARACTERISTICS

FIGURE 4-6

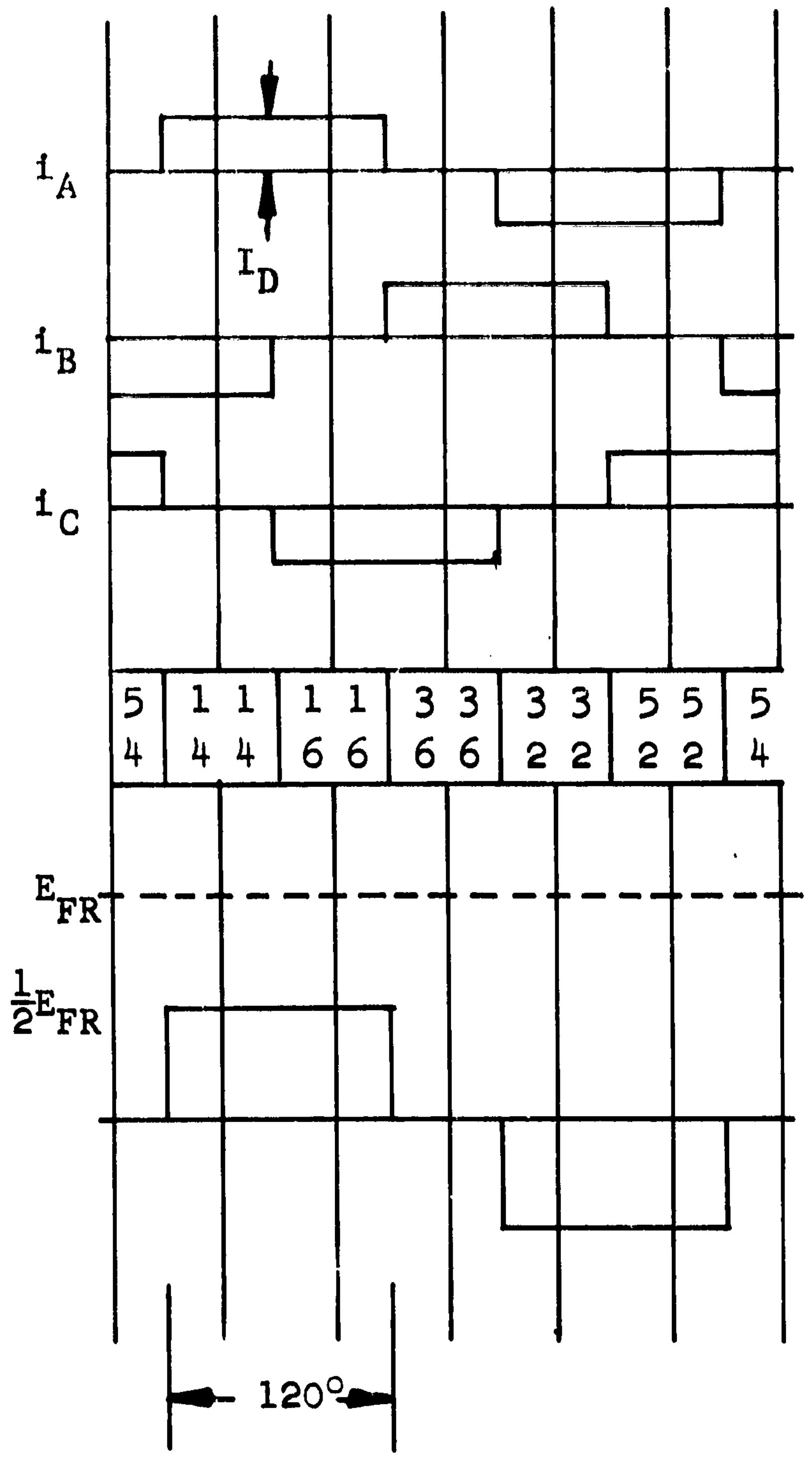

FIGURE 4-14a

PRIMARY LINE CURRENTS OR SECONDARY PHASE CURRENTS

FIGURE 4-14b

CONDUCTING RECTIFIER

FIGURE 4-14c

PHASE A TRANSFORMER SECONDARY VOLTAGE

FIGURE 4-7

WAVE FORMS FOR NON-SINUSOIDAL LINE CURRENTS volt-seconds as compared to four-ninths in the sinusoidal case. The corresponding transformer equations become

$$A_C = \frac{10^8 \times E_{FR}}{12N\ B_M f} = \frac{10^8 \times E_{FR} \times I_{FR}}{14.7 \times B_M \times I_L \times f} \qquad (4\text{-}10)$$

Evidently, if the transformer is sized for the sinusoidal case, there is now more field current flowing per RMS line current--i.e., the shunt field has less work. Moreover, the core can support a higher short-circuit current due to the reduced volt-second demand.

Capacitor Derivation - The function of the capacitor is to limit the surge voltage upon application of transient loading. A simplified analysis is based on the equivalent circuit and waveforms shown in Figure 4-8. Initial conditions are assumed to be zero. When a step-current is applied to the circuit, the field voltage will tend to ring up sinusoidally to a peak determined by the surge impedance and the magnitude of the current. At the time t_1, however, the current transformer saturates and ceases to supply current. Whatever current has been established in the inductor by that time "free-wheels" down by way of the rectifiers.

The field volt-seconds represented by the shaded area are approximately

$$(ET)_{FR} = \frac{E_{pk} \cdot t_1}{2} \qquad (4\text{-}11)$$

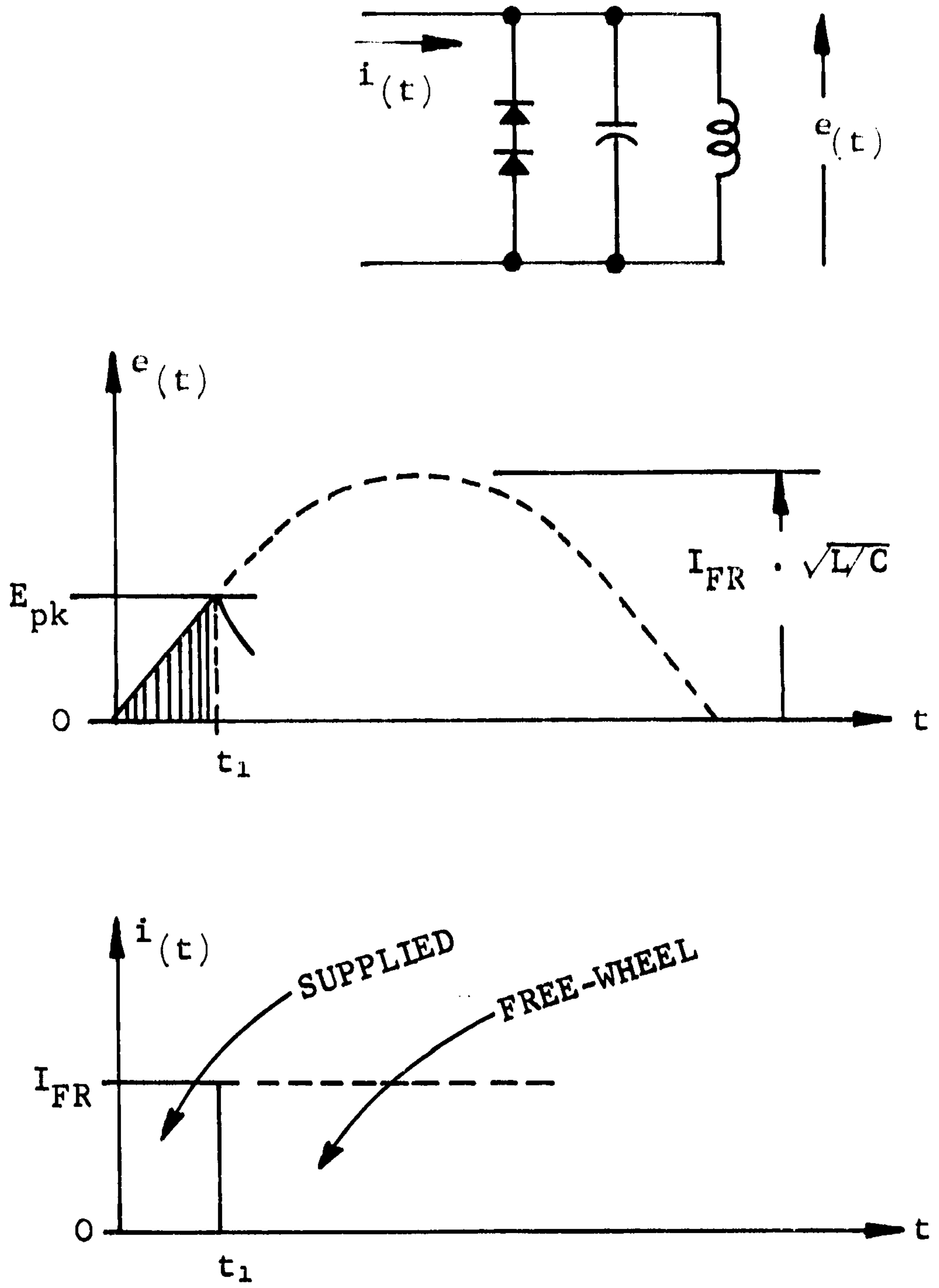

SERIES FIELD SURGE VOLTAGE

FIGURE 4-8

If the flux in the transformer traversed from negative to positive saturation during this time, then according to the transformer equation, it absorbed the following volt-seconds:

$$(ET)_T = 2NA_cB_s \cdot 10^{-8} \qquad (4\text{-}12)$$

However, as previously shown, each core absorbs only four-ninths of the field volt-seconds; thus:

$$\frac{4}{9} \cdot \frac{E_{pk} \cdot t_1}{2} = (ET)_T \qquad (4\text{-}13)$$

During the first part of the cycle the majority of current flows into the capacitor. Therefore, one can write

$$E_{pk} = \frac{I_{FR}}{C} \cdot t_1 \qquad (4\text{-}14)$$

or

$$t_1 = \frac{E_{pk} \cdot C}{I_{FR}} \qquad (4\text{-}15)$$

Substituting Eq. (4-15) into (4-13):

$$E_{pk} = \sqrt{\frac{9}{2} \cdot (ET)_T \cdot \frac{I_{FR}}{C}} \qquad (4\text{-}16)$$

or

$$C = \frac{4.5 \cdot (ET)_T \cdot I_{FR}}{E_{pk}^2} \qquad (4\text{-}17)$$

Since $(ET)_T$, the transformer volt-seconds, is determined by other considerations, Eq. (4-16) and (4-17) establish a trade-off between surge voltage and capacitor value.

Ripple current (or voltage) rating must be considered during capacitor selection. Since the waveforms are analogous to those shown for standard rectifiers, the following is presented without further proof.

For X_C much smaller than X_L (at the ripple frequency), the total RMS current in the capacitor is given by

$$I_r, \text{ (RMS)} = 0.042\ I_{FR} \tag{4-18}$$

If ripple voltage is desired, it can be approximated by its fundamental:

$$E_r, \text{ (RMS)} = \frac{0.040\ I_{FR}}{12\pi f C} \tag{4-19}$$

where f is the line frequency. Equations (4-18) and (4-19) assume a balanced three-phase system.

It should be noted that the series field module contains no protection in case of open-circuit series field wiring. A protective circuit can be added in the future; however, due to the high energy levels and high transient voltages involved, such a circuit is not simple.

4.1.1 Design of the Series Field Controller

DATA: I_{FR} = 9.2 amps minimum at 105 amps short-circuit line current

R_{FR} = 4.4 ohms maximum at 177°C

The series field resistance R_{FR} was predicted at 4.1 ohms. However, a value of 4.4 ohms is used to provide a 7-percent safety factor for tolerances and bus drops. A similar safety factor is used for the control field.

Allowing a 10-percent margin to assure an intersection (Figure 4-6), the secondary turns are, by Eq. (4-1):

$$N = \frac{1.35\ I_L}{I_{FR}} = \frac{1.35 \times 105}{1.1 \times 9.2} = 14 \text{ turns}$$

The average d-c voltage at 177°C, including a 2-V allowance for the rectifiers, is:

$$E_{FR} = I_{FR}R_{FR} + V_D = [1.1 \times 9.2 \times 4.4] + 2 = 46 \text{ V}$$

Selecting a 4-mil-grain oriented silicon steel toroid for the current transformer core, $B_{(SAT)}$ is 17.6 kilogauss; and according to Eq. (4-4), the required cross-sectional area is

$$A_c = \frac{10^8 E_{FR}}{9NB_M f} = \frac{10^8 \times 46}{9 \times 14 \times 17.6 \times 10^3 \times 1.2 \times 10^3} = 1.75 \text{ cm}^2$$

With allowance for a stacking factor of 90 percent, the gross core area becomes 1.95 cm.^{2} minimum. Since standard cores having such an area are large, a special core was designed. It is specified in AiResearch Drawing 521258 (Appendix II) and has a magnetic path length of 7.6 cm. The coercive force is estimated at 1.0 oersted; thus, the magnetizing current, referred to the secondary, is given by Eq. (4-6):

$$I_M = \frac{H_c I_c}{0.4\pi N} = \frac{1.0 \times 7.6}{0.4\pi \times 14} = 0.43 \text{ amp}$$

The maximum cross-sectional area of the core is 2.2 cm^2 and the maximum saturation flux density is estimated to be 20 kilogauss. According to Eq. (4-12), the volt-seconds are

$$(ET)_c = 2NA_cB_s x10^{-8} = 2x14x2.2x20x10^3x10^{-8} = 1.23x10^{-2}$$

For a capacitor of 2 Mfd and a step current of 10 amps, the surge voltage, per Eq. (4-16), is:

$$E_{PK} = \sqrt{\frac{9}{2} \times (ET)_c \times \frac{I_{FR}}{C}} = \sqrt{\frac{9}{2} \times 1.23 \times 10^{-2} \times \frac{10}{2 \times 10^{-6}}} = 525 \text{ V}$$

This is within the capability of the selected rectifiers and within the surge rating of the capacitor.

The RMS ripple current is computed by Eq. (4-18) for a 3.1-amp field current (nominal condition):

$$I_r(RMS) = 0.042 \, I_{FR} = 0.13 \text{ amp}$$

which also is well within the continuous rating of the selected capacitor.

4.2 Shunt Field Voltage Regulator Analysis

The alternator output voltage is regulated by controlling the average shunt field current. This is accomplished by a transistorized switching regulator (chopper). The average field current is determined by the duty cycle (ON-time with respect to the OFF-time) of the chopper, which, in turn, is a function of the error voltage.

The normal field supply voltage is supplied by rectifiers taking power from the alternator output. The system battery is gated into the field circuit by a diode and supplies field current until the rectifier output (E_{FF}) exceeds the battery voltage, thereby reverse-biasing the diode. Since the battery by itself can supply the rated 1.0 p.u. excitation requirements, no field-flashing is needed to assure build-up. The excess E_{FF} over battery voltage provides a source for field-forcing.

The dynamic response of the alternator output is principally determined by the simple shunt field time-constant and, to a lesser degree, by the machine subtransient response. The contribution of the feedback signal rectifier filter $F_{(s)}$ is small. The response to load application is faster than the response to load removal due to the availability of field-forcing voltage. Response to load removal can be improved at the expense of extra power dissipation.

Provisions are made for the injection of a hold-off bias derived from the battery which disables the shunt field regulator during alternator acceleration in order to minimize prime mover loading. It should be noted that some excitation will still be available from the series field unless an external short circuit is placed across the series field terminals by the system controller.

The switching regulator also incorporates a current limit designed to protect the field against overheating during prolonged fault conditions. It should be noted that this feature will not protect the VRE output transistor in case of a shorted shunt field bus because the circuit depends upon the field inductance to limit the rate of current rise. Protection against a bus short, however, can be added if so desired.

A block diagram of the shunt field regulator is shown in Figure 4-9. Briefly, the regulator consists of the following functional sections:

(a) A transformer-rectifier/filter circuit to provide power for the shunt field regulator
(b) A transformer-rectifier/filter circuit to sense the alternator output voltage
(c) A shunt field current switching circuit to meter power from the power supply to the shunt field
(d) A voltage reference and error detector
(e) A shunt field current level detector and a circuit to protect the switching transistors as well as the field by providing a current limited mode of operation
(f) An OR-gate circuit to provide a smooth transition from voltage regulation to the current limit mode of operation
(g) An auxiliary power supply for the regulator electronics
(h) A battery gating-circuit to assure alternator buildup in lieu of field flashing (Figure 4-10)

Shunt Field Transfer Function - The shunt field transfer function is derived with the aid of Figure 4-11. Symbols and terminology correspond with the definitions presented in Figure 4-1. The switch (SW) represents the action of the solid-state regulator.

When the switch is closed, the total supply voltage is applied to the field, causing current to build up. Diode D is reverse-biased and nonconducting. When the switch is opened, current continues to flow in the field circuit due to the effect of the field inductance. This current is in the direction of diode forward conduction; thus, the voltage across the field terminals becomes reversed in polarity and limited in magnitude to the forward voltage drop of the diode. The current then decays according to the field time-constant until the

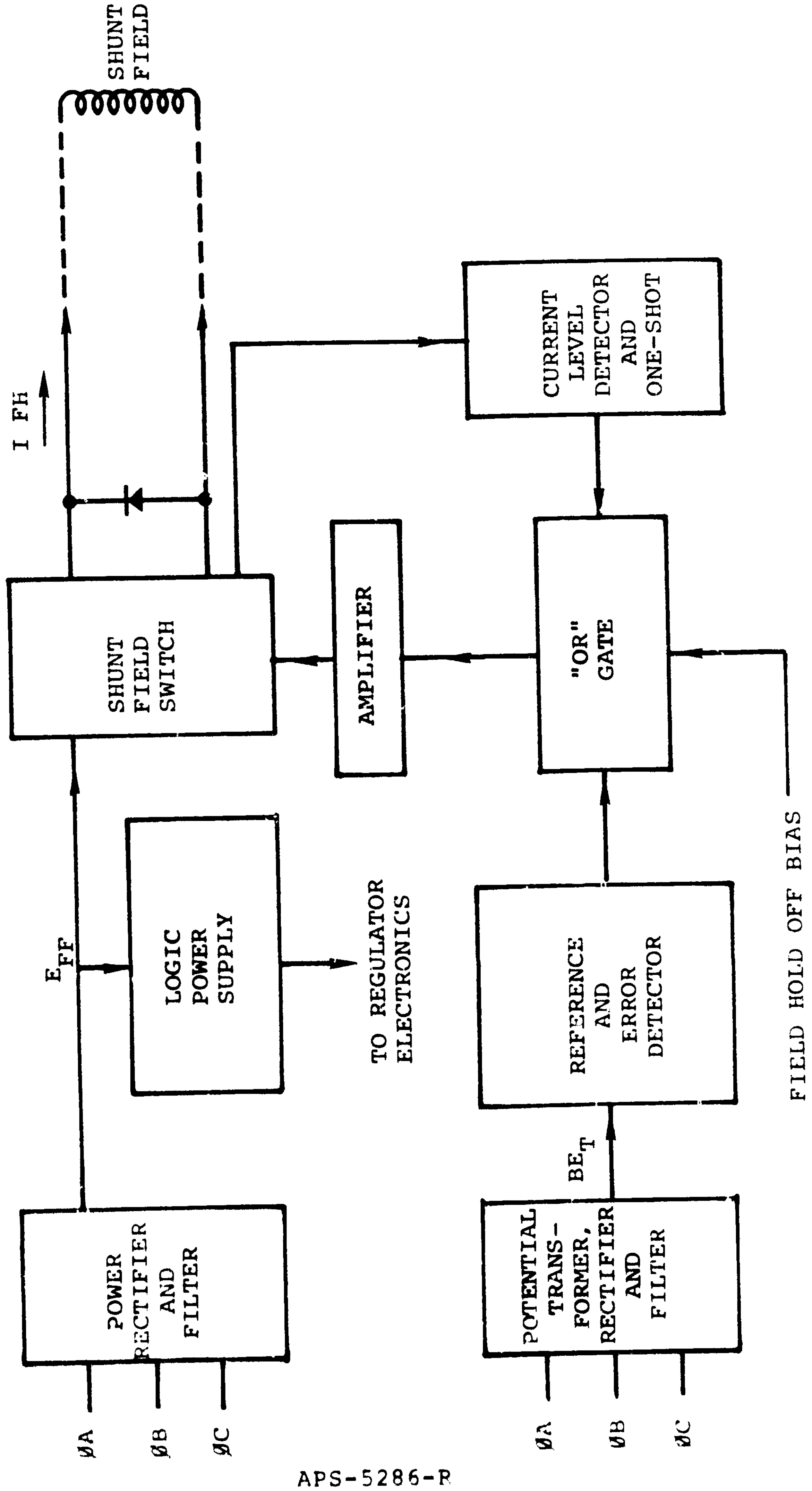

BLOCK DIAGRAM OF SHUNT FIELD REGULATOR

FIGURE 4-9

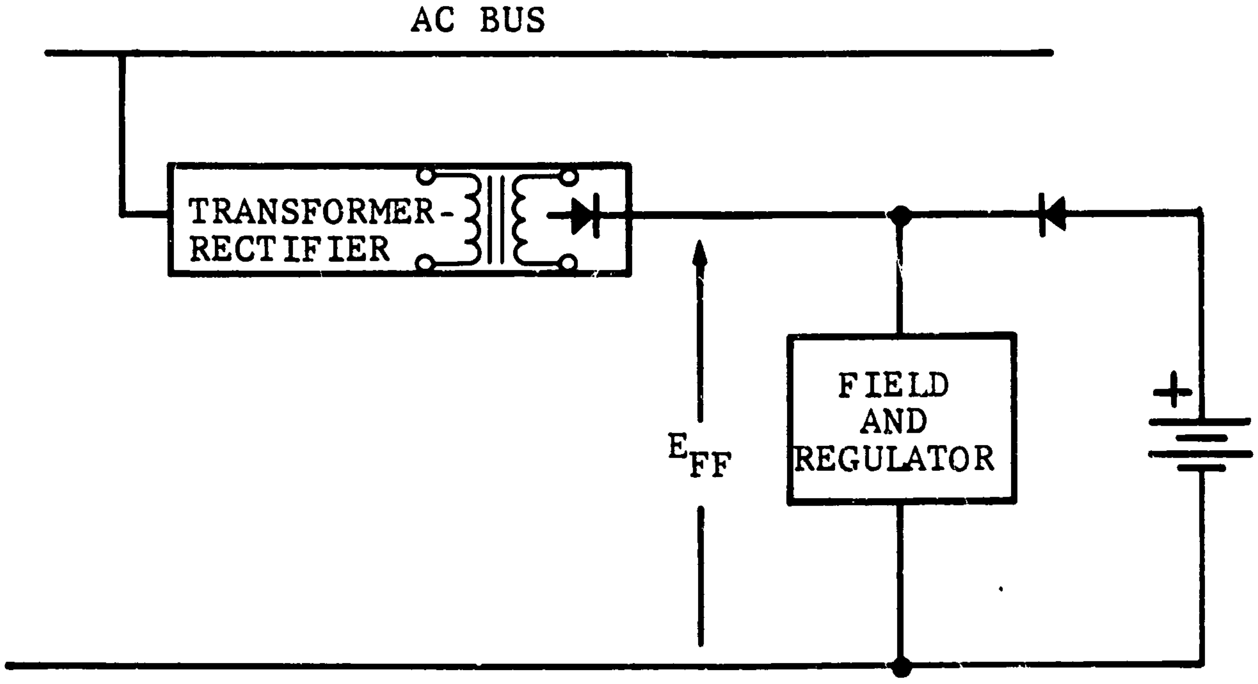

BATTERY ASSISTED START UP

FIGURE 4-10

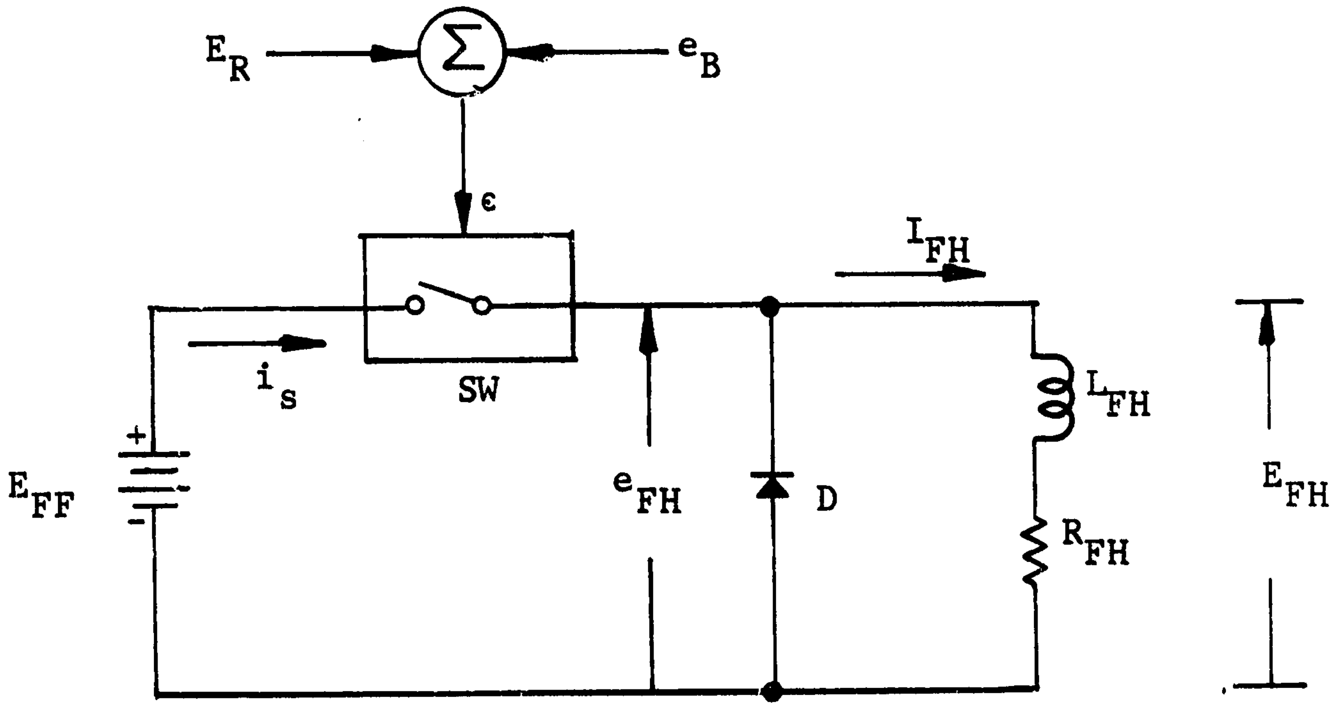

SWITCHING REGULATOR

FIGURE 4-11

switch is again closed to initiate a current buildup. The duty cycle of this switching action determines the average field current. The resultant field voltage and current waveforms are shown in Figures 4-12c and 4-12d, respectively, drawn with the free-wheeling diode and switch considered ideal. By inspection, it can be seen that the average field voltage is given by:

$$E_{FH} = E_{FF} \cdot \frac{T_c}{T} \qquad (4\text{-}20)$$

and that the average field current is given by

$$I_{FH} = \frac{E_{FH}}{R_{FH}} \qquad (4\text{-}21)$$

If the current ripple is very low, then I_{FH} is also equal to the peak value of the power supply current pulse, i_s.

The switching action is controlled at the summing junction in the manner shown by Figure 4-12a. This point has two inputs: a d-c reference (E_R), and a feedback signal (e_B). The feedback signal consists of a d-c level (E_B), with a proportional superimposed ripple at three times line frequency if α is the constant of proportionality:

$$e_B = E_B + [\alpha E_B]_{(t)} \qquad (4\text{-}22)$$

This signal is obtained from the alternator output voltage by the sensing transformer rectifier; since $E_B = \beta E_T$, one can write

$$e_B = \beta \left\{ E_T + [\alpha E_T]_{(t)} \right\} \qquad (4\text{-}23)$$

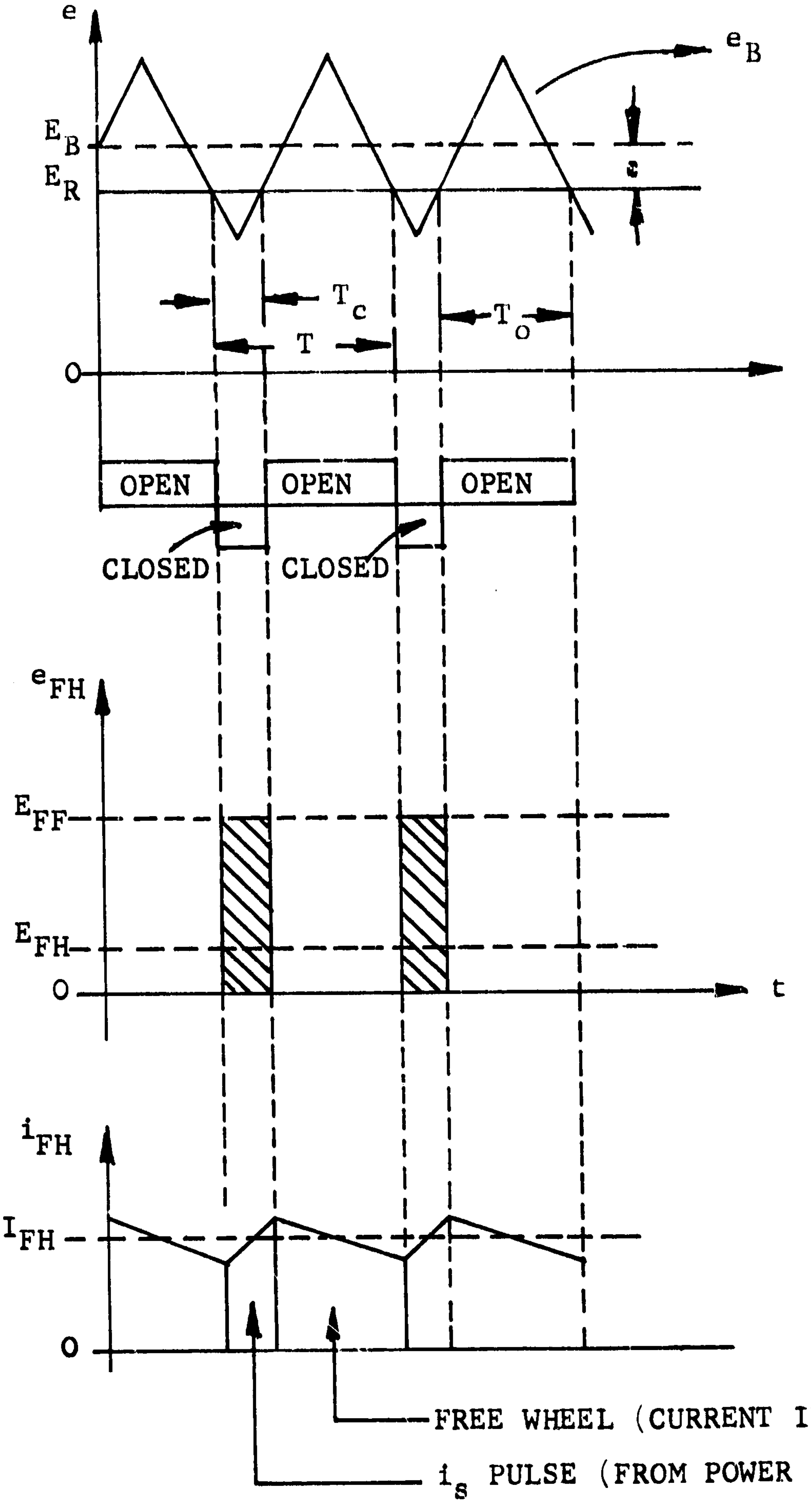

FIGURE 4-19a
SUMMING JUNCTION

FIGURE 4-19b
SWITCHING ACTION

FIGURE 4-19c
FIELD VOLTAGES

FIGURE 4-19d
FIELD CURRENTS

FREE WHEEL (CURRENT IN DIODE, D)

i_s PULSE (FROM POWER SUPPLY, E_{FF})

SHUNT FIELD WAVE FORMS

FIGURE 4-12

The switch is actuated by the relationship between E_R and the instantaneous level of e_B as shown in Figure 4-12b. The switch is open for $e_B > E_R$ and closed for $e_B < E_R$. The error (ϵ) indicates that, at the illustrated operating point, closed-loop equilibrium demands that $T_o > T_c$ for $E_{FF} > 2\ E_{FH}$; this is the "gain error" of a Type-Zero loop. The triangular ripple is a close approximation to actual circuit waveforms. In fact, the detail design of the voltage sensing circuit filter shapes the ripple to this desired waveform. The field supply voltage is proportional to the alternator line voltage; thus, it can be written (referring to Figure 4-1)

$$E_{FF} = K_T E_T \tag{4-24}$$

The transfer function can now be derived. When the error is positive and equal to half the peak-to-peak amplitude, the troughs of e_B cease intersecting with E_R, and E_{FH} goes to zero. When the error is negative and equal to half the peak-to-peak amplitude, the peaks of e_B cease intersecting with E_R and the switch goes fully on--i.e., $E_{FH} = E_{FF}$. For the triangular ripple this change is linear; thus, if $\left[\alpha E_B\right](t)$ is the peak-to-peak ripple, then:

$$\frac{\Delta E_{FH}}{\Delta \epsilon} = \frac{E_{FF} - 0}{\left[\alpha E_B\right](t)} = \frac{K_T E_T}{\alpha\beta E_T} = \frac{K_T}{\alpha\beta} \tag{4-25}$$

Equation (4-25) is the open-loop gain (K_A) of the amplifier. K_T is fixed by the field voltage requirements, and β is simply the ratio between E_R and E_T. Obviously, the gain is a function of the ripple amplitude only--whence the name "ripple regulator".

4.2.1 Detail Design of the Shunt Field Regulator - According to Table 4-1, the shunt field voltage requirement at rated-overload and

177°C copper temperature is 18 V. For fast response, twice this voltage should be available for field forcing. If a 2-V series drop is assigned to the regulator,

$$E_{FF}\ (\mathrm{MIN}) = 2 \times 18 + 2 = 38\ \mathrm{V}$$

Allowing a 10-percent design tolerance on this supply, E_{FF} becomes

$$E_{FF}\ (\mathrm{NOM}) = 42\ \mathrm{V}$$

From Eq. (4-24),

$$K_T = \frac{E_{FF}}{E_T} = \frac{42}{120} = 0.350$$

which determines the design of the field supply transformer-rectifier.

The selected zener reference voltage is 6.2 nominal, thus

$$\beta = \frac{E_R}{E_T} = \frac{6.2}{120} = 0.052$$

According to Paragraph 2.2a, a total operating band of 2-percent is permitted. This corresponds to 124 mv referred to the reference. The 1.0 V allocated for drift corresponds to 52 mv referred to the reference. Thus the regulation error becomes 72 mv.

According to Table 4-1, between zero and 12.6 KVA and ±10-percent speed, the shunt field has to swing a maximum of 6.4 V (at 177°C) for zero error. From this,

$$K_A = \frac{\Delta E_{FH}}{\Delta \epsilon} = \frac{6.4}{72 \times 10^{-3}} = 89$$

A design gain of 100 is chosen to allow for worst-case K_T and E_R. The required ripple can now be computed from the gain expression (4-25) and from the ripple definition (4-22)

$$\alpha\beta = \frac{K_T}{K_A} = \frac{0.35}{100} = 0.0035$$

$$\beta\left[\alpha E_T\right](t) = 0.0035 \times 120 = 0.420 \text{ V P-P}$$

In practice, a ripple of exactly triangular waveform cannot be realized. To compensate for the resultant rounded corners, a smaller ripple amplitude is required. From experience, a factor of 0.7 applies and, thus, the required ripple becomes 300 mv P-P. This defines the filter of the feedback rectifier and also its frequency dependence $F_1(s)$. Due to the low open-loop gain, the lags associated with $F_1(s)$ and with the switching transport lag are negligible in comparison with the principal time constant, e.g., the field L/R; therefore, the regulator loop is stable. Provisions have to be made to add a stabilizing network if such is required to enhance system stability.

Due to lack of pertinent data, it is difficult to predict conformance to the drift specification of paragraph 2.2b. However, the drift due to field warmup corresponds to and estimated ΔE_{FH} of 4.3 V, which would reflect to the alternator output as a line voltage shift of approximately 1.0 V RMS.

4.2.2 Detail Circuit Description

The schematic of the shunt field regulator is shown in Figure 4-13.

Voltage Regulator Power Supply - Power for the shunt field regulator is derived from an unregulated power supply comprising transformer T1, bridge rectifier CR1, and filter capacitor C5. The transformer was designed in the delta-delta configuration to increase the reliability of the unit, should it be forced to operate in the open-delta configuration due to an open-type failure in one of the coils. The transformer was designed to have tightly balanced coils to minimize circulating currents.

Switching Circuit - The basic field current switching function is performed by Transistor Q5. Transistor Q4 is a Darlington driver to increase the gain of the switching circuit. Resistor R13 provides the base current drive for Transistor Q4, which is normally in the ON-condition when Q3 is OFF. Transistor Q3 is driven ON by Q2. This drive can be overridden by the inhibit circuit comprising R34, R35, CR7, and CR8 permitting the shunt field to be shut off during engine start-up. Zener Diode CR7 provides approximately 6 V of noise immunity for the inhibit circuit.

Voltage Loop - Voltage regulation is performed by comparing a d-c feedback voltage to a reference voltage. The resulting error voltage is amplified and used to control the basic switching function. The feedback voltage is derived from the voltage sensing transformer T2 and the bridge rectifier CR3, CR4, and CR5. This feedback voltage is fed into the "left" base of the differential amplifier Q1 and is compared to the reference voltage established by zener diode CR10. Potentiometer R3 adjusts the level of the feedback voltage and, therefore, determines the alternator output voltage. Capacitors C1, C2,

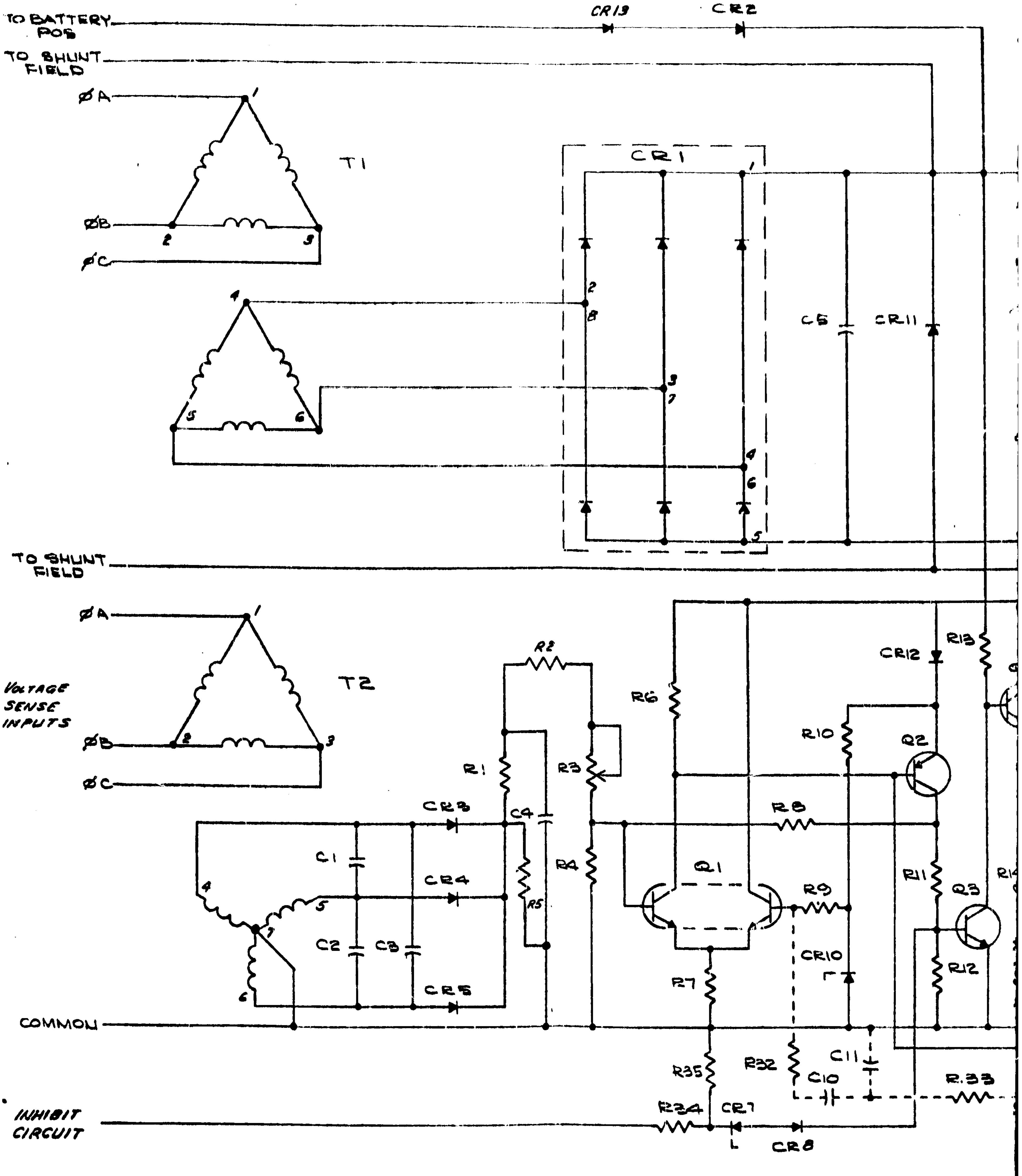

FOLDOUT FRAME

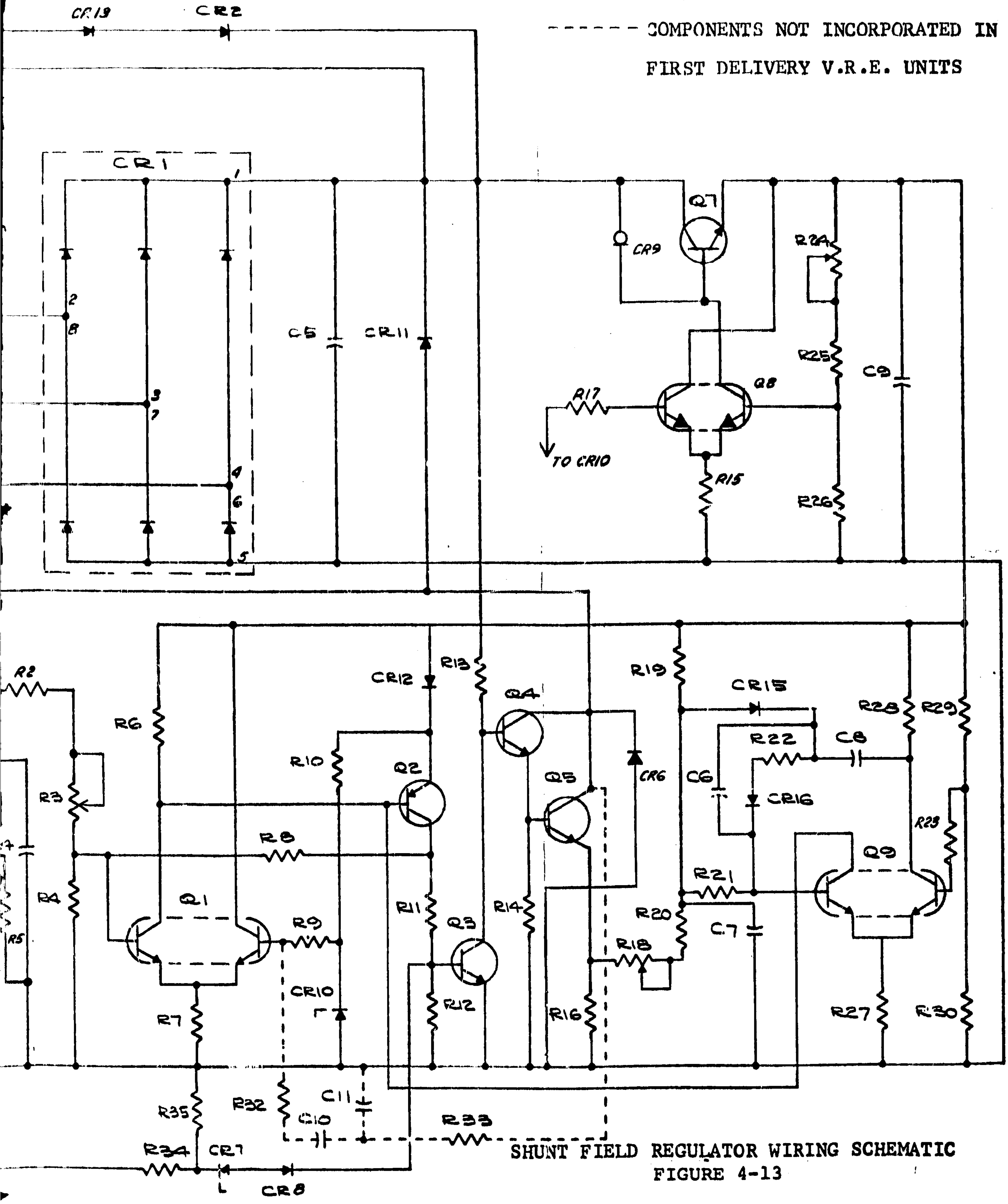

------ COMPONENTS NOT INCORPORATED IN FIRST DELIVERY V.R.E. UNITS

SHUNT FIELD REGULATOR WIRING SCHEMATIC
FIGURE 4-13

and C3 filter high-frequency noise spikes on the sensing transformer output windings. Resistor R8, which is coupled from the output of the OR-gate (Q2) to the input to the differential amplifier, provides positive feedback that decreases the rise time of the switching transistors and gives a more positive switching action by the introduction of a small amount of hysteresis. Resistor R5, the final value of which has not been determined, is used to match the diode temperature coefficient to the temperature coefficient of the transformer winding resistance; theoretically a value can be chosen to make the net temperature coefficient zero. Capacitor C4 controls the ripple amplitude and hence the loop gain.

<u>OR-Gate Circuit</u> - Transistor Q2 is an OR-gate that is driven from the voltage level detector when the alternator voltage is in the normal regulation band but is overridden by the current detector circuit whenever the output voltage is substantially below normal.

<u>Current Level Detector</u> - During a cold start, the shunt field resistance can be as low as half the hot resistance. The fact that the resistance is low and that a two-times forcing voltage is provided would require the switching transistor to be capable of conducting several times the normal operating current. The current limit circuit protects the shunt field winding and the switching transistors from a possible overcurrent condition when a low output voltage would otherwise command maximum available current flow.

The shunt field current is detected by measuring the voltage developed across Resistor R16. This voltage is compared to a reference voltage determined by Resistors R29 and R30. The peak voltage across R16 is coupled to the "left" base of the differential amplifier Q9. If the voltage exceeds a preset level, the "left" transistor turns ON and, thus, the "right" transistor is turned OFF. A positive feedback current is coupled back to the "left" base through C8 and R22. This holds it in the ON-condition for a period determined by the time-constant of C8 and R22. As the "left" transistor of Q9 is turned ON, the OR-gate (Q2) is also turned ON, which turns the field current switch (Q5) OFF. The field current free-wheels down due to the winding inductance until the end of the above-mentioned one-shot period. At that time the "left" transistor of Q9 turns OFF, allowing Q5 to turn ON again. When Q5 turns ON, field current increases until it reaches the current limit point, and the cycle repeats. Operation of this circuit requires a certain minimum of series inductance and will not provide field bus short-circuit protection unless an inductor is added inside the VRE. Capacitor C7 filters the high-frequency clearing spike generated by the free-wheeling diode CR11 at the instant it recovers from a free-wheeling condition. Diode CR15 provides a fast recovery path for the one-shot timing circuit.

Figure 4-14 depicts the field current and the alternator output voltage for a typical start-up condition. The internal ΔT_1 (Figure 4-14) is the time-constant of the current limit circuit. During this time, the field current is decaying according to the L/R time constant of the shunt field. Interval ΔT_2 is the time required for the current to build back-up to the current limit point. The slope of the current ripple is a function of the field inductance and the supply voltage and is determined by

$$\frac{di}{dt} = \frac{E_{FF}}{L_{FH}} \qquad (4-26)$$

As the output voltage crosses the 100-percent point (Point A on Figure 4-14), the field current control shifts to the voltage loop and decreases to the normal operating current. The output voltage can overshoot somewhat due to the excess stored energy in the field, but this is small compared to the overshoots seen in the absence of current

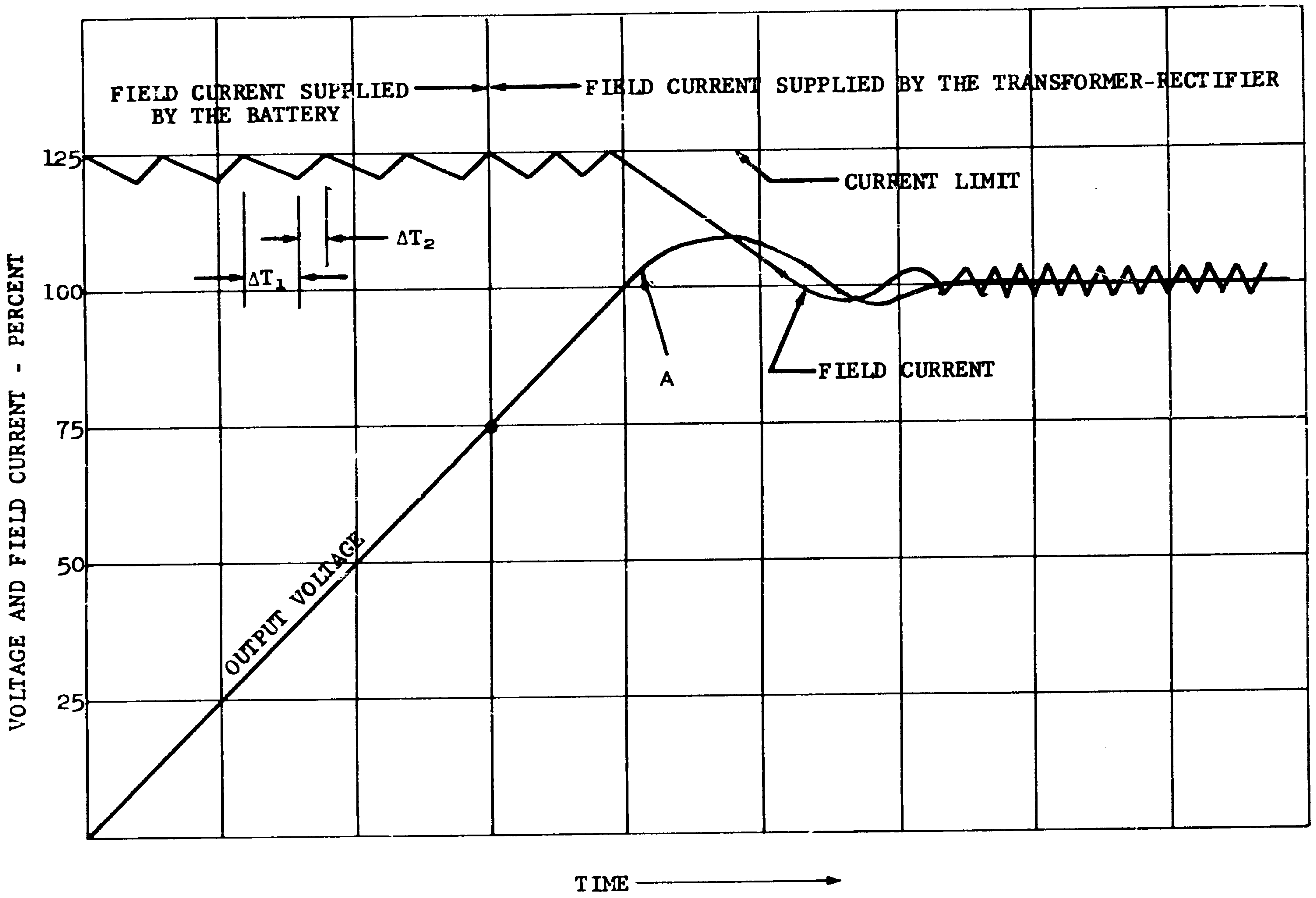

FIELD CURRENT AND OUTPUT VOLTAGE DURING START-UP

FIGURE 4-14

limiting. The current limit point is adjusted by potentiometer R-18.

Logic Power Supply - The current-limit circuit is sensitive to power-supply changes; and in order to assure operation of the power transistor well within its safe operating area, reasonably accurate power supply performance is required. This power supply accuracy also contributes the basic simplicity of the overall circuit and minimizes the use of zener diodes.

The logic power supply is composed of Transistors Q7 and Q8 and their associated components. The output voltage is compared to zener reference CR10 by differential amplifier Q8. Field effect diode CR9 supplies a constant base drive current to the series regulating Transistor Q7. With the assumption that the differential amplifier is operating normally, an increase in the power supply output voltage will cause the "right"-hand transistor of Q8 to increase its collector current, which reduces the available base drive current to Q7. The output voltage will therefore decrease to the normal value. Resistor R24 is used to adjust the power-supply voltage.

Although the field effect diode is a new and unproven device, the simplifications afforded by its use make it an excellent candidate for widespread future application. The diodes shipped in the VRE have been subjected to a fairly severe screening and burn-in program at AiResearch and are, therefore, considered sufficiently reliable for this application. The worst-case analysis of the power supply allows for a 2:1 change in the field effect diode characteristics without degradation of the power supply performance.

4.2.3 Worst-Case Analysis

This section provides a brief summary of the voltage regulator worst-case analysis and the ground rules on which it is based. The analysis shows the maximum and minimum limits of major circuit parameters due to component tolerances, temperature effects, and aging.

The basic design of the shunt field regulator, in conformance to the established ground rules, does not lend itself readily to a fail-safe "fail-off" configuration. In a "HI-REL" end application, additional external protection devices are mandatory.

Ground Rules - Supply voltage is 42 nominal, with 80 V transient peaks, transient dips to 22 V; the ambient temperature range is established as -25°C to +75°C. In general, component design tolerances are derived from MIL-HDBK-217A. Some component tolerances are shown in Table 4-2, and include long-term drifts when available.

Current Limit Circuit - The worst-case analysis of the current limit circuit shows the change in the current limit as a result of temperature, power supply drift, and aging of components. Due to the method used to sense the control field current, differential voltage changes between the voltage reference divider and the current sense divider are reflected directly to the current sense resistor. The current limiter has a sensitivity of 5 ma/mv. Since the actual current limit is not critical, this circuit was preferred over more accurate ones because of its simplicity and the small number of components.

	Current Change, amp ±	Percent* Change ±
Variable		
Power supply drift (±0.5 V)	0.2	3.2
Temperature Effects		
Voltage reference	0.055	0.9
Current sense circuit	0.075	1.2

TABLE 4-2
VRE COMPONENT TOLERANCES

1. Resistors

Type	Tol., %	Design Tol., %*	T/C, PPM/°C	Specification
Metal film	±1	±5	200	MIL-R-10509
Metal film	±2	±6	200	MIL-R-22684
Wire Wound, power	±1	±7	50	
Wire Wound, precision	±0.1	±1	30	MIL-R-93
Wire Wound, variable	--	±3	50	MIL-R-27208

2. Reference Diode

Type	V_z Min	V_z Max	Test Current	Dynamic Impedance	T/C %/°C
IN827A	5.8	6.6	7.5 ma	10Ω	±0.001

3. Signal Transistors

Type	H_{FE} min at -25°C	V_{CE}(sat) max	V_{BE}(sat) max
2N2060	30	1.2	1.0
2N2219	35	1.0	1.2
2N3251	60	0.7	1.2

Supplemental data 2N2060 differential amplifier:

H_{FE2}/H_{FE1}: 9 min. 1.0 max ΔV_{BE}: 5 mv and 10 μV/°C

*Initial tolerance plus allowances for aging and temperature coefficients.

	Current Change, amp ±	Percent* Change ±
Temperature Effects (CONT)		
Differential amplifier base emitter offset voltage	0.003	
Differential amplifier base current offset	0.018	0.3
Aging Effects		
Voltage reference resistors	0.35	5.6
Current sense circuit resistors	0.55	8.8
TOTAL Drift	±1.25	±20.0

The minimum current limit is established at 5 amp to allow some margin with respect to the 4.5-amp maximum required field current. Consequently, the initial setting must be 5.00 + 1.25 = 6.25 amp and the maximum current is 6.25 + 1.25 = 7.5 amp.

Power Amplifier - The current handling capability of the output Transistor Q5 and of its drive Q4 is analyzed with respect to transistor parameter changes, power supply voltage extremes, temperature fluctuations, and resistor tolerances. Power dissipation in the main power transistor, Q5, is calculated under worst-case operating conditions; however, data to derive worst-case switching losses is not available and, thus, these losses were estimated from breadboard measurements.

The results of the analysis may be summarized as follows:

Q5

(a) Steady state	7.5 amp
(b) Transient peak	11.5 amp

---

*Based on 6.25 amp nominal current limit.

Transient peak is 0.2-μsec long during recovery of CR11

(c) Maximum power dissipation:

Due to switching losses	3.5 W
Due to ON conditions	6.4 W
Total	9.9 W

(d) Maximum steady-state voltage drop, collector to emitter: 1.32 V

(e) All switching transitions are estimated as less than 6-μsec duration and thus, well within safe-operating regions of second breakdown curves.

Q4

(a) Maximum collector current:

Steady state	0.5 amp
Transient peak	11.5 amp

(b) Maximum steady-state voltage drop collector to emitter: 0.2 V

(c) All switching transitions are well within the safe operating area of second breakdown curves.

Q3

(a) Maximum collector current: 96 ma

(b) Minimum overdrive

$$\frac{\beta I_B}{I_C} = 2.7$$

Nominal overdrive = 5.3

Error Detector and Amplifier - The stability and sensitivity of the error amplifier (comprising Transistors Q1 and Q2 and associated circuitry) are analyzed with respect to variations of critical circuit parameters, including initial parameter variations within manufacturer tolerances and changes due to aging and temperature effects.

Changes in the d-c feedback voltage at the input to the amplifier are expressed as percentages of nominal and are reflected as changes in the a-c output voltage on a 1:1 basis.

	Percent Change in Input	
Variable	Due to Time and Temp, %	Due to Temp Only, %
Resistor-divider ratio	+2.26, -2.17	±0.26
Combined input offset	±0.15	±0.42
Reference diode voltage changes as function of:		
(a) Bias and load changes	±0.16	
(b) Temperature coefficient of reference diode	±0.08	
Amplifier gain change	±0.032	
TOTAL (sum of changes)	+2.68 -2.59	±0.68

Sensing Transformer - The sensing transformer presents a rather complex picture as a function of temperature. The change in copper resistance drop is opposite to the change in diode voltage drop. In addition, since the magnetizing and iron loss currents are significant with respect to the load current, they reflect an additional component into the primary voltage drop. This is further complicated by the discontinuous nature of the load current. It is often possible to select a load resistor to minimize the net effects of temperature variations. A "ball-park" value has been calculated and was used to establish the voltage divider resistors; it requires experimental verification and adjustment. Provisions have been made for additional loading for compensation purposes (R5).

Power Supply - The logic power supply analysis is based on a 50-ma essentially constant load and includes combined effects of temperature and aging. The correct initial setting is 15.0 V.

Variables	Output Voltage, mv	
Input line voltage	± 50 (estimate)	
Gain and current source variations	±100	
Reference and ΔV_{BB}	- 10	
Bridge resistors	+310,	-350
TOTAL Design Tolerance:	+470,	-510

4.2.4 Failure Rate Analysis

Wherever feasible, components have been initially selected from the "JPL Approved Parts List". However, following an investigation into the availability and cost of such components, the selection requirements were clarified and redirected. For fabrication purposes, "commercial equivalent" or military parts were used. Table 4-3 is a list of the parts actually used for the regulator.

Potentiometers have been selected for use where adjustment is needed for component tolerances, since the values are unknown until final adjustment. "Select at Test" procedures would have resulted in excessive procurement delays.

A failure rate analysis for the shunt field is summarized in Tables 4-4 through 4-11. It is based on the following criteria:

(a) Data in accordance with MIL-HDBK-217A when available
(b) Ambient and mounting-base temperature of 70°C
(c) No allowance for increased reliability due to screening of the power transistors, transformers, and the constant current

TABLE 4-3

VRE COMPONENT LIST

Part 543936-1-1

Component Designation Shunt Field	Manufacturer	Part Number	Rating	Approved Standard
R1	Sprague	RB54CE698ROF	698Ω, 0.25W, 1%	MIL-R-93B
R2	Sprague	RB54CE15000F	1500Ω, 0.25W, 1%	MIL-R-93B
R3	Bourns	224L-500-202	2000Ω, 0.5W,	
R4	Sprague	RB54CE750ROF	750Ω, 0.25W, 1%	MIL-R-93B
R5	Sprague	RW69V	(1) 3W	MIL-R-26C
R6	Corning Glass	RL07S272G	2700Ω, 0.25W, 2%	MIL-R-22684B
R7	Corning Glass	RL07S562G	5600Ω, 0.25W, 2%	MIL-R-22684B
R8	Corning Glass	RL20S474G	470K, 0.5W, 2%	MIL-R-22684B
R9	Corning Glass	RL07S621G	620Ω, 0.25W, 2%	MIL-R-22684B
R10, 12	Corning Glass	RL07S102G	1000Ω, 0.25W, 2%	MIL-R-22684B
R11	Corning Glass	RL20S162G	1600Ω, 0.5W, 2%	MIL-R-22684B
R13	Sprague	RW67V911	910Ω, 6.5W, 5%	MIL-R-26C
R14	Corning Glass	RL07S101G	100Ω, 0.25W, 2%	MIL-R-22684B
R15	Corning Glass	RL07S821G	820Ω, 0.25W, 2%	MIL-R-22684B
R16	Dale	RE70NR200	0.2Ω, 0.25W, 1%	MIL-R-18546
R17	Corning Glass	RL07S751G	750Ω, 0.25W, 2%	MIL-R-22684B
R19, 29	Sprague	RB54CE18000B	1800Ω, 0.25W, 0.1%	MIL-R-93B
R20	Sprague	RB54CE562ROF	562Ω, 0.25W, 2%	MIL-R-93B
R21, 23	Corning Glass	RL07S222G	2200Ω, 0.25W, 2%	MIL-R-22684B
R22	Corning Glass	RL07S362G	3600Ω, 0.25W, 2%	MIL-R-22684B
R24, 18	Bourns	224L-500-102	1000Ω, 0.5W	
R25, 26	Sprague	RB55CE12100F	1210Ω, 0.15W, 1%	MIL-R-22684B
R27	Sprague	RB55CE20000B	2000Ω, 0.15W, 0.1%	MIL-R-93B
R28	Sprague	RB55CE27100B	2710Ω, 0.15W, 1%	MIL-R-93B
R30	Sprague	RB54CE12100B	1210Ω, 0.25W, 0.1%	MIL-R-93B
R32, 33	Sprague	RW69V	(1)	MIL-R-26C
R34	Sprague	RW69V152	1500Ω, 3W, 5%	MIL-R-26C
R35	Corning Glass	RL07S202G	2000Ω, 0.25W, 2%	MIL-R-22684B
C1, 2, 3	Sprague	196P10492S4	0.1 MFD, 200V, 10%	
C4	Sprague	150D105X9075B2	1 MFD, 75V, 10%	
C5	GE	69F116G2	440 MFD, 100V	
C6	Corning Glass	CY10G221J	220pF, 300V	MIL-C-23269
C7	Corning Glass	CY30G103J	10000pF, 300V	MIL-C-23269

TABLE 4-3 (CONT)
VRE COMPONENT LIST
Part 543936-1-1

Component Designation	Manufacturer	Part Number	Rating	Approved Standard
C8	Sprague	196P223925 4	0.022 MFD, 200V	
C9	Sprague	137D946X0050A2	94 MFD, 50V	
C10	Sprague	137D	(1)	
C11	Sprague	137D	(1)	
CR1	Varo	45524-200	250V, 15 amp	
CR2, 6, 11, 13	GE	JAN IN 1206	600V, 12 amp	MIL-S-19500/160
CR3, 4, 5, 8, 12, 15, 16		JAN IN 485B	180V, 100 ma	MIL-S-19500/118B
CR7	Motorola	JAN IN 753A	6.2V ±5%	MIL-S-19500/127
CR9	Motorola	IN5308	100V, 2.7 ma	
CR10	Motorola	IN827A	6.2V, ±5%	MIL-S-19500/159
Q1, 8, 9	FAS, TI	JAN 2N2060	Silicon NPN Dual	
Q2	Motorola	JAN 2N3251A	Silicon PNP	
Q3	Motorola	JAN 2N2219	Silicon NPN	
Q4, 5, 7	AiResearch	521246-1	Silicon NPN Power	
T1	AiResearch	521259-1		
T2	AiResearch	521260-1		
Series Field				
C1, 2	Marshall	HL4-105(ISC)	1 MFD, 400V	
CR1, 2, 3, 4, 5, 6	[illegible]	IN4507	400V, 12 amp	
T1, 2, 3	AiResearch	521247-1		

NOTE: (1) Component values to be selected as required during development tests at Lewis Research Center.

TABLE 4-4

FAILURE RATE CALCULATION FOR DIODES (FIG. 7.4.3 MIL-HDBK-217A)

Module BRU

Lower Card Assy

Part	Type and No.	P_{Jmax} W *MA	P_J mW *MA	T_{Jmax} °C	T_s °C	θ_{JA} $\frac{T_{Jmax}-T_s}{P_{Jmax}}$ (°C/mW)	T_A °C	$T_J = T_A + \theta_{JA} P_J$ °C	$T_n = \frac{T_J - T_s}{T_{Jmax} - T_s}$	Base Failure Rate (10^{-6})	K	Total Failure Rate (10^{-6})
(1) CR1	45524-200	-	10W	165	75	5°C/W	70	110	0.39	0.620	6.0	3.720
(2) CR2	IN1206	-	0	200	25		70	70	0.26	0.005	1.0	0.005
CR3	IN485B	200*	5*	200	25	0.875°C/MA	70	74	0.28	0.255	1.5	0.372
CR4	IN485B	200*	5*	200	25		70	74	0.28	0.255	1.5	0.372
CR5	IN485B	200*	5*	200	25		70	74	0.28	0.255	1.5	0.372
CR6	IN1206	-	0	200	25		70	70	0.26	0.340	1.0	0.340
CR7	IN753A	400	0	200	25		70	70	0.26	0.670	1.0	0.670
CR8	IN485B	200*	0	200	25		70	70	0.26	0.222	1.5	0.333
(3) CR9	IN5308	-	80	200	25	0.250	70	90	0.37	0.870	1.0	0.870
CR10	IN827A	400	46	200	25	0.44	70	90	0.37	0.980	1.0	0.980
CR11	IN1206	-	3W	200	25	3°C/W	70	79	0.36	0.515	1.0	0.515
CR12	IN485B	200*	20*	200	25	0.875°C/MA	70	87.5	0.36	0.290	1.5	0.435
(2) CR13	IN1206	-	-	-	-	-	-	-	-	-	-	-
CR15	IN485B	200*	~0	200	25	-	70	70	0.026	0.222	1.5	0.333
CR16	IN485B	200*	~0	200	25	-	70	70	0.026	0.222	1.5	0.333
												9.650

(1) Integrated bridge, six rectifiers
(2) Redundant pair
(3) Field effect constant current diode. Used Zener failure rate.

TABLE 4-5

FAILURE RATE CALCULATION FOR TRANSISTORS (FIG. 7.4.4 MIL-HDBK-217A)

Module BRU
Lower Card Assy

Part	Type and No.	P_{Jmax} W	P_J *W	T_{Jmax} °C	T_s °C	$\theta_{JA} \frac{T_{Jmax}-T_s}{P_{Jmax}}$ (°C/mW)	T_A °C	$T_J=T_A+\theta_{JA}P_J$ °C	$T_n = \frac{T_J-T_s}{T_{Jmax}-T_s}$	Base Failure Rate (10^{-6})	K	Total Failure Rate (10^{-6})
Q1	2N2060	0.5	9	200	25		70	73	0.27	0.222	1.5	.333
Q2	2N3251A	.36	15	200	25		70	77	0.30	0.670	1.5	1.005
Q3	2N2219	0.8	180	200	25		70	110	0.48	0.410	1.5	.615
Q4	521246	70	1*	200	25		70	74	0.28	0.510	1.0	.510
Q5	521246	70	11*	200	25		70	114	0.51	0.820	1.0	.820
Q7	521246	70	1.5*	200	25		70	76	0.29	0.510	1.0	.510
Q8	2N2060	0.5	66	200	25		70	91	0.39	.325	1.5	.487
Q9	2N2060	0.5	27	200	25		70	79	0.31	.255	1.5	.337
												4.617

TABLE 4-6

FAILURE RATE CALCULATION FOR CAPACITORS

Part	Type	Value	V_r Volts	V_a Volts	Stress Factor V_a/V_r	Base Failure Rate (10^{-6})	K	App. Failure Rate (10^{-6})
C1	196 p (paper)	0.1 Mfd	200v	40v pk	.20	.0079	1.3	0.01027
C2	196 p (paper)	0.1 Mfd	200v	40v pk	.20	.0079	1.3	0.01027
C3	196 p (paper)	0.1 Mfd	200v	40v pk	.20	.0079	1.3	0.01027
C4	Solid Tant.	1 Mfd	75	25	.3	.0270	3x.07	0.00567
C5	GE 95F (Tant Slug)	440 Mfd	100v	42	.42	.2300	0.5	0.11500
C6	CY 10G (Glass) (2)	220 pF		15	.05	.0002	1.0	0.00020
C7	CY 30G (Glass) (2)	10000 pF		15	.05	.0002	1.0	0.00020
C8	196 p (paper)	.022 Mfd		15	.075	.0024	1.3	0.00312
C9	137 D (Tant Slug)			15	.30	.0170	0.5	0.08500
								0.2400

1. C10 and C11 to be used in stabilization network if required, and are not included here.
2. Mfg. Data.

TABLE 4-7

FAILURE RATE CALCULATION FOR (WIRE WOUND) RESISTORS

Part	Type	Value Ohms	P_r W *	F_a W	Stress Factor P_a/P_r	Base Failure Rate (10^{-6})	K	App. Failure Rate (10^{-6})
R1	RB54C	698	.81	.048	.06	1.13	1.0	1.13
R2	RB54C	1500	.81	.102	.125	1.13	1.0	1.13
R4	RB54C	750	.81	.051	.063	1.13	1.0	1.13
R19	RB54C	1.80K	.81	.045	.056	1.13	1.0	1.13
R20	RB55C	562	.49	.014	.029	1.13	1.0	1.13
R25	RB55C	1.21K	.49	.032	.065	1.13	1.0	1.13
R26	RB55C	1.21K	.49	.032	.065	1.13	1.0	1.13
R27	RB55C	2.00K	.49	.018	.037	1.13	1.0	1.13
R28	RB55C	2.71K	.49	.030	.061	1.13	1.0	1.13
R29	RB54C	1.8K	.81	.045	.056	1.13	1.0	1.13
R30	RB55C	1.21K	.49	.032	.056	1.13	1.0	1.13
								12.43

*Extrapolated from 125 Rating to 70 C base temperature. Used for stress calculation only.

TABLE 4-8
FAILURE RATE CALCULATION FOR METAL FILM RESISTORS

PART	TYPE	VALUE OHMS	P_r W	P_a W	STRESS FACTOR P_a/P_r	BASE FAILURE RATE (10^{-6})	K	APP. FAILURE RATE (10^{-6})
R6	MIL-R-22684	2.7K	0.25	--	(0.1)	0.250		
R7		5.6K	0.25	0.0064	0.026	0.250		
R8		470K	0.50	--	(0.1)	0.250		
R9		620	0.25	--	(0.10)	0.250		
R10		1000	0.25	0.08	0.32	0.310		
R11		1600	0.50	0.12	0.24	0.300		
R12		1000	0.25	0.001	(0.1)	0.250		
R14		100	0.25	0.05	0.20	0.300		
R15		820	0.25	0.044	0.176	0.300		
R17		750	0.25	--	(0.1)	0.250		
R21		2.2K	0.25	--	(0.1)	0.250		
R22		3.6K	0.25	0.0045	0.018	0.250		
R23		2.2K	0.25	--	(0.1)	0.250		
R35*		2.0K	0.25	0	0	0 3.46	0.3	1.038

*Normally not stressed. For signaling noise immunity only.

TABLE 4-9
FAILURE RATE CALCULATION FOR POWER RESISTORS AND POTENTIOMETERS

PART	TYPE	VALUE OHMS	P_r W	P_a W	STRESS FACTOR P_a/P_r	BASE FAILURE RATE (10^{-6})	K	APP. FAILURE RATE (10^{-6})
R5	MIL-R-26	(1)						
R13	MIL-R-26	910	6.5W	2.0	0.31	0.016	10	0.160
R34 (1)	MIL-R-26	1500	3.0W	0	0	0		
R3	POT, 224L	2000	0.5	0.130	0.260	0.068		0.068
R18	POT, 224L	1000	0.5	0.013	0.026	0.068		0.068
R24	POT, 224L	1000	0.5	0.025	0.050	0.068		0.068 0.364

(1) Failure does not affect normal operation.

TABLE 4-10
FAILURE RATE CALCULATION FOR
TRANSFORMERS SEC. [illegible] MIL-HDBK-217A)

	TRANS-FORMER	INSU-LATION CLASS	TEMP. RISE AT RATED LOAD ΔT_R, °C	RATED VOLT AMP. VA_R	ACTUAL VOLT AMP. VA_a	ACTUAL TEMP. RISE °C ΔT (*)	ACTUAL TEMP. $T_a = T_{amb} + \Delta T$ °C	λ Base (10^{-6})	K	λApp. (10^{-6})
T.	521259	T	40°C	220 VA	220 VA	ESTIM.) 40°C MAX.	110°C	0.20	1.5	0.30
T.	521260	T	40°C	4.4 VA	4.4 VA	ESTIM.) 40°C MAX.	110°C	0.20	1.5	0.30 0.60

TABLE 4-11
SUMMARY OF FAILURE-RATE CALCULATIONS FOR
VOLTAGE-REGULATOR/EXCITER

Part Name		Total Application Failure Rate (10^{-6})
Resistors	(Table 4-8)	1.038
Resistors	(Table 4-7)	12.430
Resistors	(Table 4-9)	0.364
Capacitors	(Table 4-6)	0.240
Transformers	(Table 4-10)	0.600
Transistors	(Table 4-5)	4.617
Diodes	(Table 4-4)	9.650
TOTAL		$\lambda = 28.939 \times 10^{-6}$/hr.
		MTBF = 34,550 hr.

diode. (It should be noted that the screening has proven very effective in removing weak power transistors and constant current diodes.)

The resultant overall failure rate is 29 × 10^{-6}/hr., corresponding to an MTBF of 34,500 hrs. This appears encouraging, since it is based on standard military and commercial components. With flight-type components, at least a tenfold improvement is anticipated. The two largest contributors to the present failure-rate evaluation results are the diodes (including rectifiers), and the precision wire-wound resistors. Simple semiconductor screening to Jan TX specifications is claimed to reduce failure rates by one order of magnitude. In addition, if the precision wire-wound resistors are replaced by precision, established-reliability film resistors purchased to Level P of

MIL-R-55182, a 40-times reduction in the predicted failure rate may well be possible.

4.3 Mechanical Description

The VRE is packaged in a 19-in. rack panel chassis. The chassis is mounted on slides to provide convenient access to the electrical components. The basic mechanical concept was to provide a packaged breadboard where components are conveniently located and, at the same time, to maintain quality workmanship. The series field module can be removed from the VRE chassis and located remotely if desired. Terminal junctions are located on the inside of the back panel to allow for the following optional wiring configurations:

- (a) Local or remote voltage sensing
- (b) Local or remote power pickup
- (c) Local or remote series field location

The optional wiring schedule, Drawing 521301 (Appendix IV) contains detailed instructions for reconnecting the terminal junctions. A set of jumper leads and special tools for wire installation and removal are provided with each unit. Note that in order to use the "Local" wiring option, the alternator output must be routed through the VRE chassis. The VRE is delivered prewired in the local configuration.

CAUTION: The machine may not be operated under any circumstance with P2 and/or P7 disconnected (Series Field Open) when current flows in the current transformer primary. This primary consists of three wires routed through holes in the series field module.

The physical configuration of the VRE is shown on Drawing 543936 (Figure 4-15) and the location of the various components and modules is shown on Drawing 543937, Figure 4-16. Photographs of the actual hardware are presented in Figures 4-17, 4-18, and 4-19. Figure 4-20 is the system wiring diagram of the BRU alternator, VRE, and speed control.

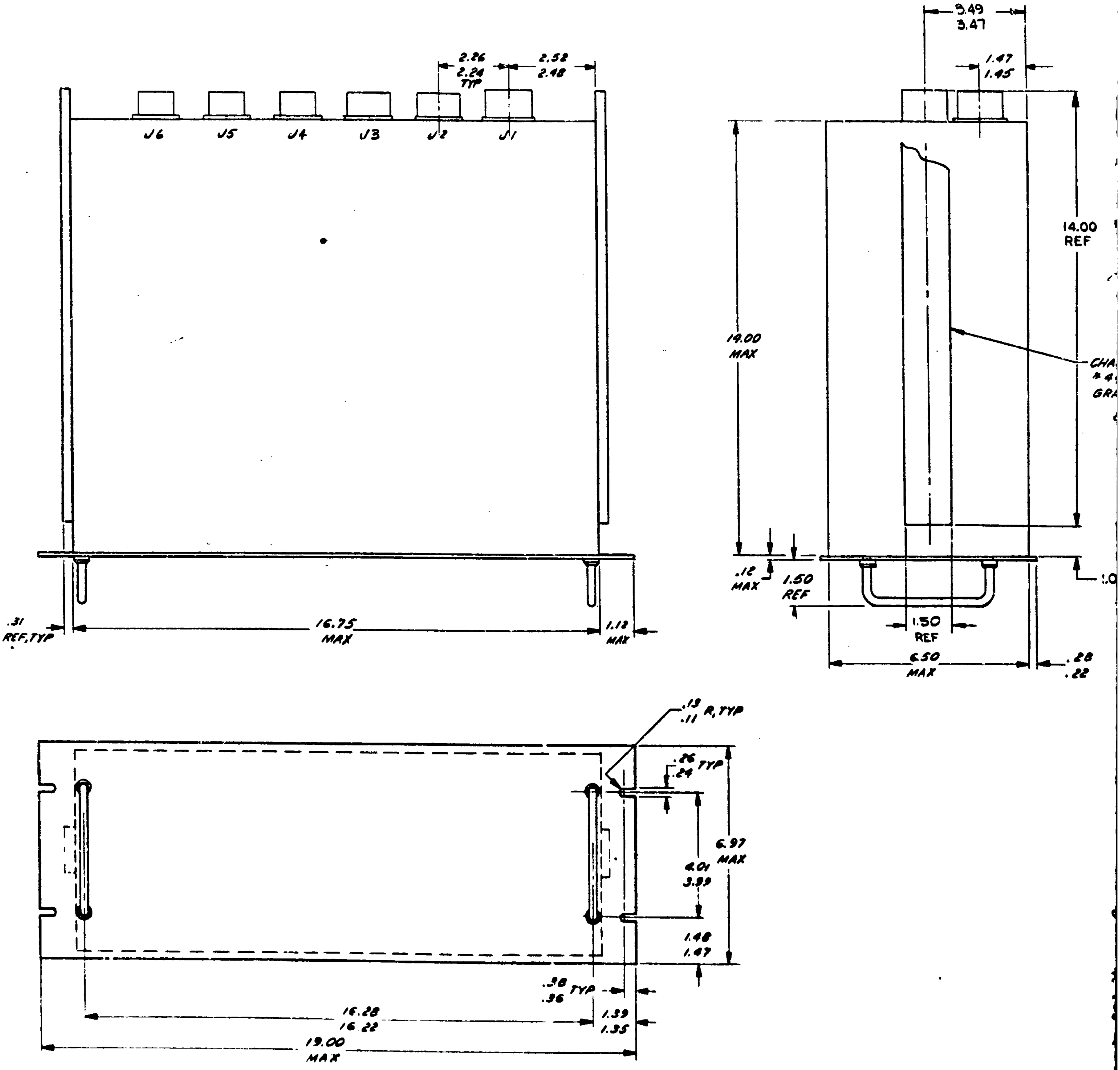

2. FOR SYSTEM WIRING DIAGRAM SEE DRAWING 521219.

1. FOR SCHEMATIC DIAGRAM SEE DRAWING 521169.

NOTES: UNLESS OTHERWISE SPECIFIED

FOLDOUT FRAME

REVISIONS			
LTR	DESCRIPTION	DATE	APPRO
A	SEE REVISION NOTICE	9-13-67	

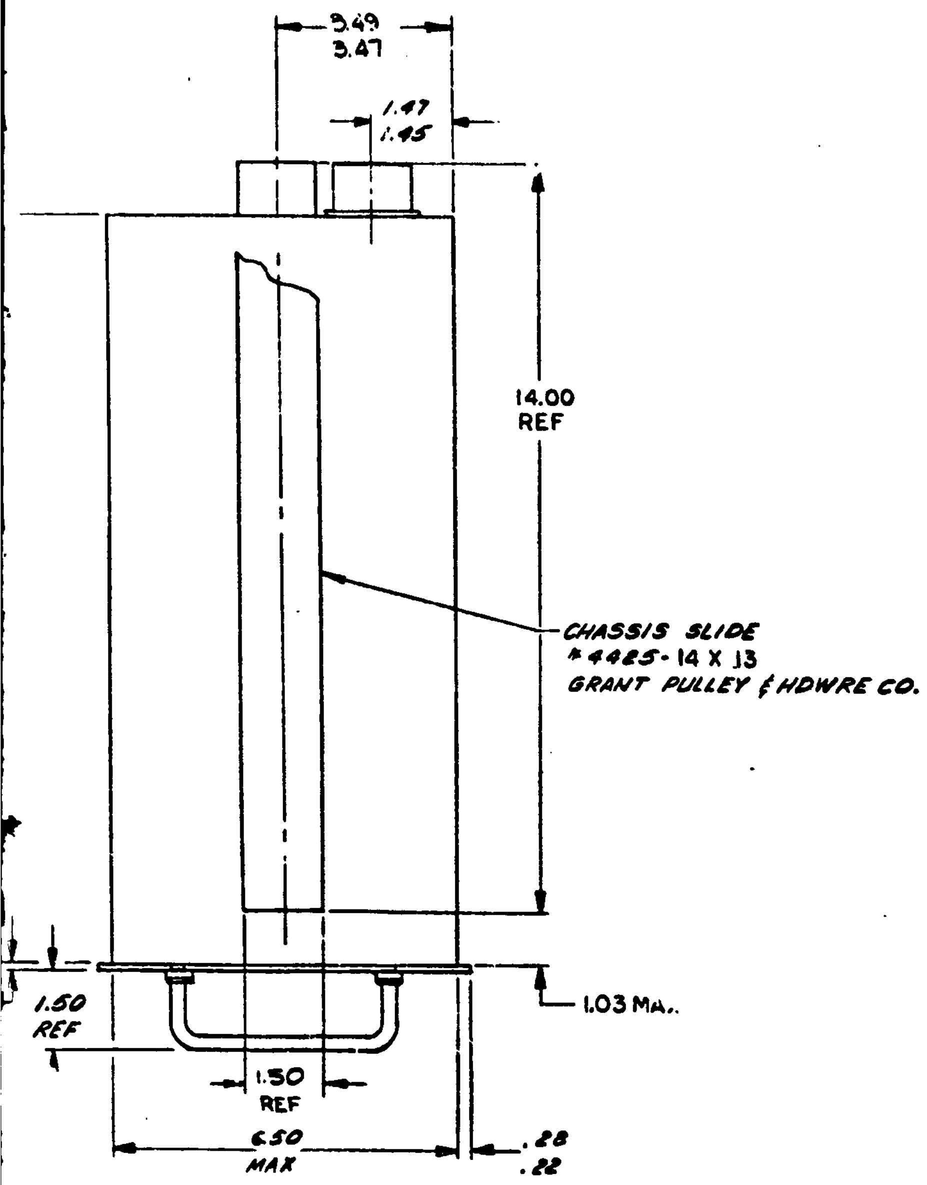

FIGURE 4-15

APS-5286-R
Page 4-54

2. FOR SYSTEM WIRING DIAGRAM SEE DRAWING 521219.

1. FOR SCHEMATIC DIAGRAM SEE DRAWING 521169.

NOTES: UNLESS OTHERWISE SPECIFIED

	FINAL	
REQD	NEXT ASSY	USED ON
APPLICATION		

543936-1-1	543937-1					
PART NO.	ASSY NO.					
QTY REQD	ITEM NO.	PART NO.	SYM	DESCRIPTION	CODE IDENT	MATERIAL AND SPECIFICATIO
←ASSY				LIST OF MATERIAL		

UNLESS OTHERWISE SPECIFIED:
DIMENSIONS ARE IN INCHES
MACHINE FILLET RADII .015-.030
SURFACE ROUGHNESS PER MIL-STD-10
BURR CONTROL PER SO-50
DIMENSION LIMITS HELD AFTER PLATING
IDENT MARKING PER MC38
DIMENSIONING AND TOL PER MIL-STD-8

HEAT TREATMENT	PROCESS
HARDNESS AND SPEC	NAME AND SPEC

SIGNATURES	DATES
DFT V P King	2-6-67
CHK	6-16-67
VALUE ENGR	
MATL	6-28-67
STRESS	6-?-67
APPD	6-19-67
APPD	6-30-67
AIRESEARCH APPD	
OTHER ACTIVITY APPD	

AIRESEARCH MANUFACTURING COMPA
A DIVISION OF THE GARRETT CORPORATION
LOS ANGELES, CALIFORNIA

REGULATOR-EXCITER OUTLINE,
VOLTAGE, ALTERNATOR

NEW ISSUE 6-29-67

SIZE	CODE IDENT NO.	DWG NO.
D	70210	543936
SCALE 1/2		SHEET 1 OF

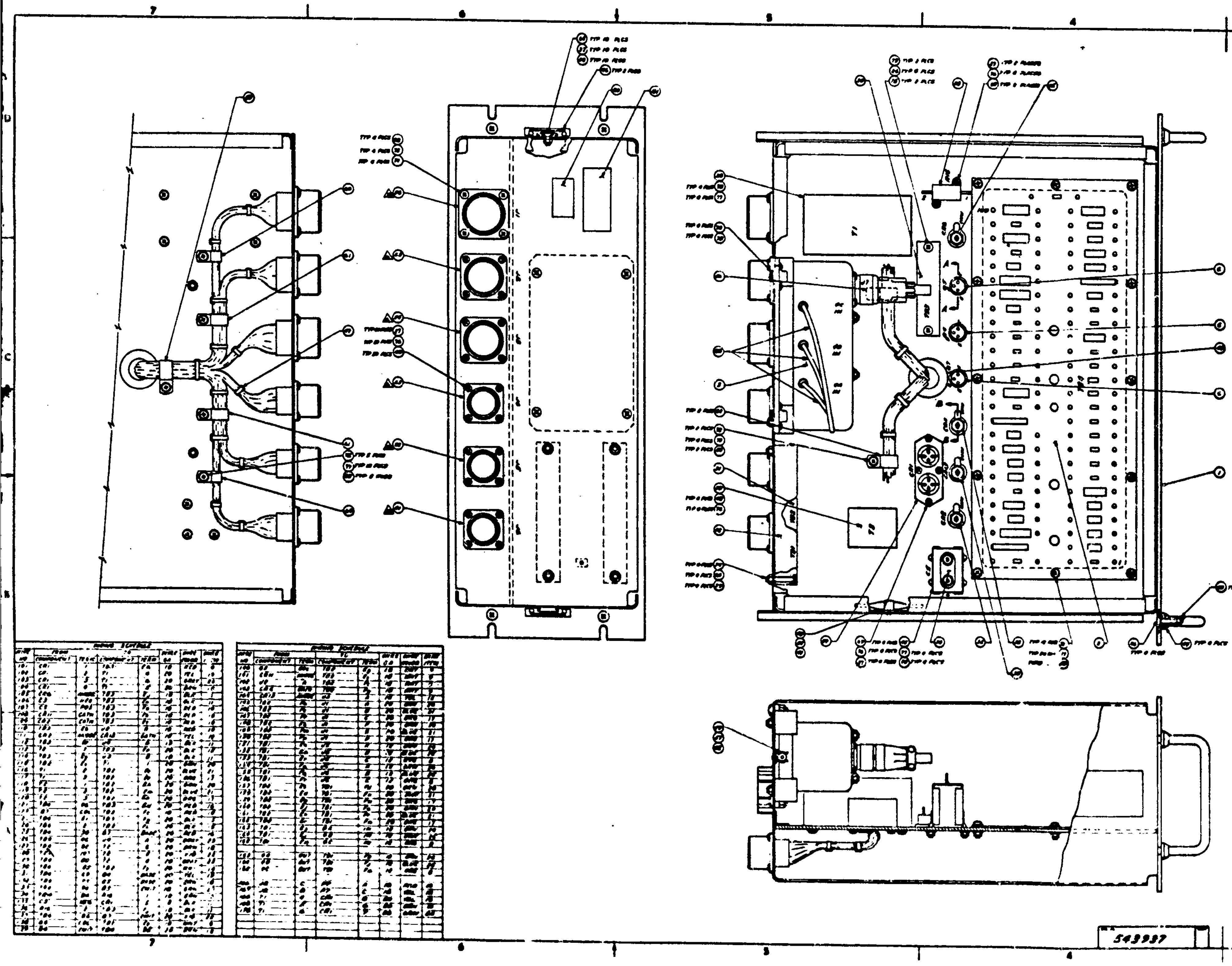

FOLDOUT FRAME

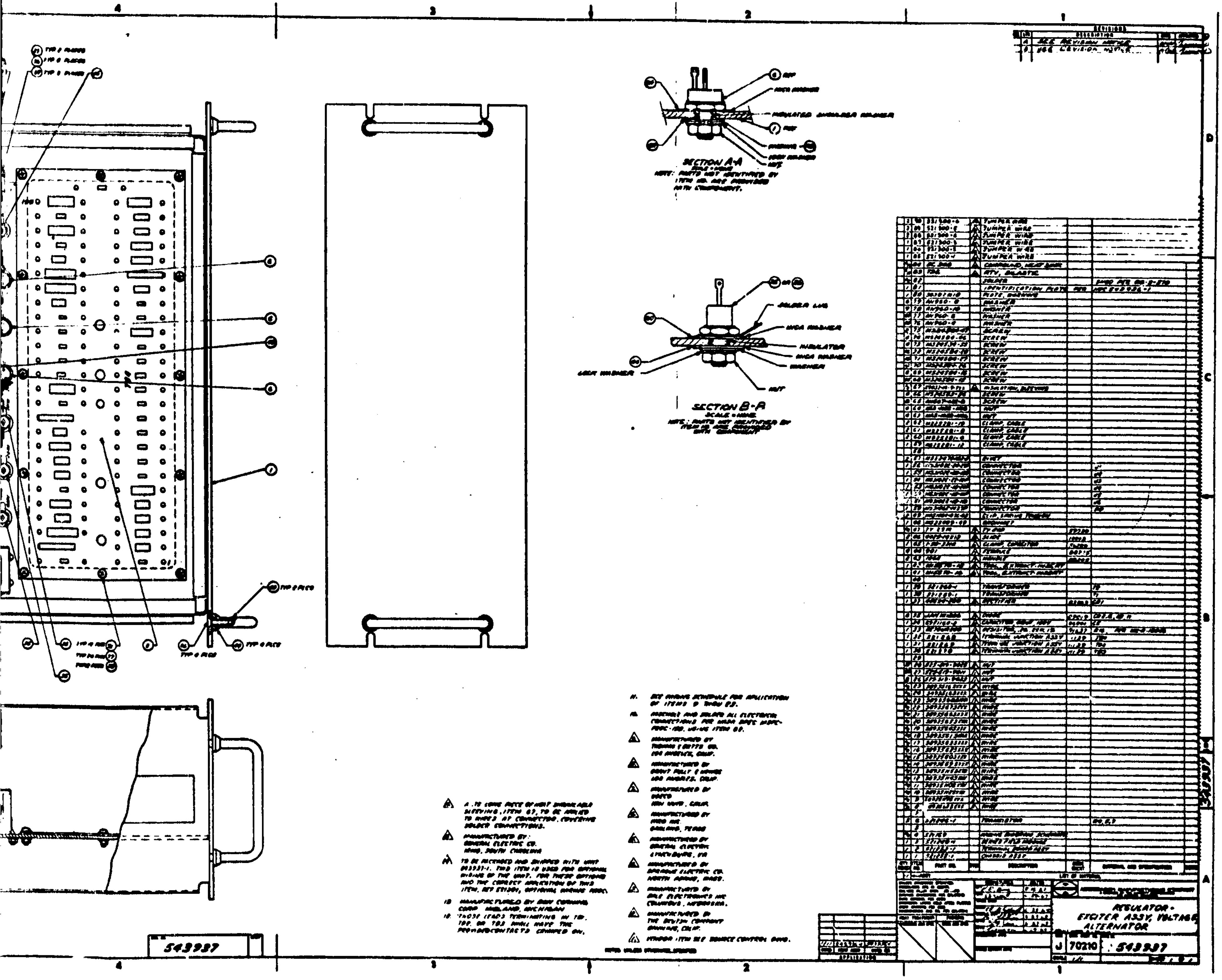

FIGURE 4-16

APS-5286-R
Page 4-55

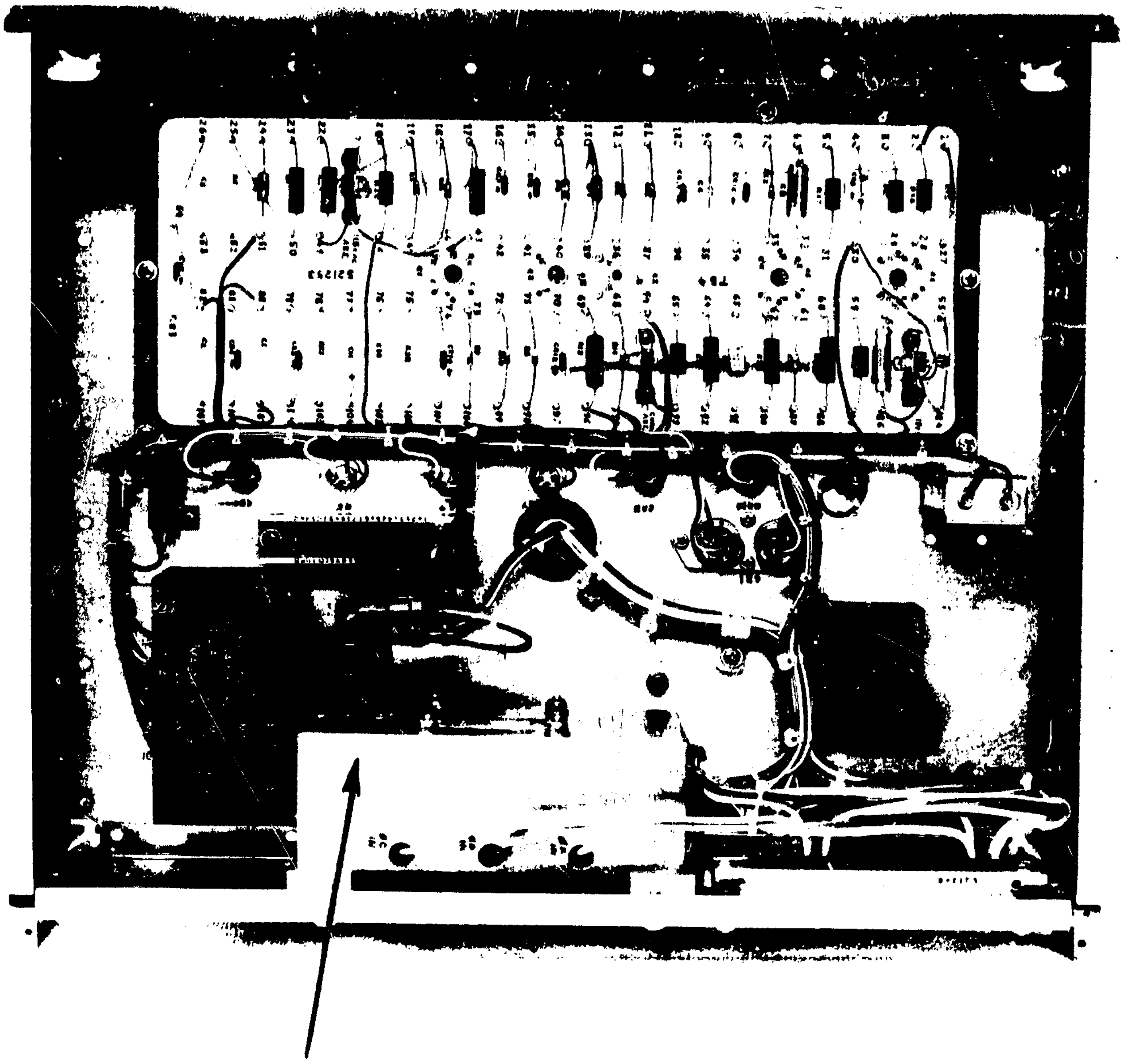

SERIES FIELD
MODULE

TOP VIEW

VOLTAGE REGULATOR/EXCITER ASSEMBLY

FIGURE 4-17

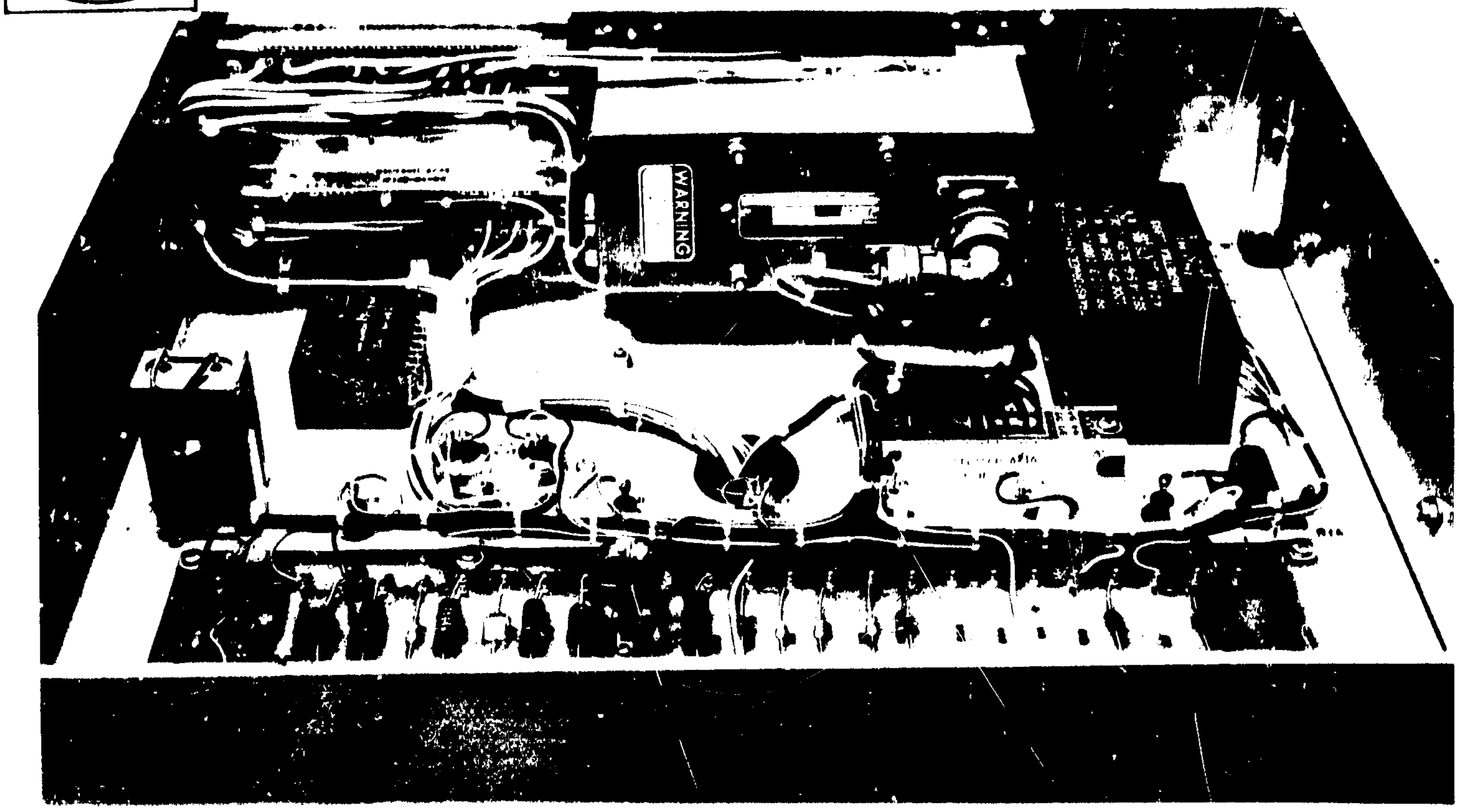

FRONT VIEW
WITH PANEL REMOVED

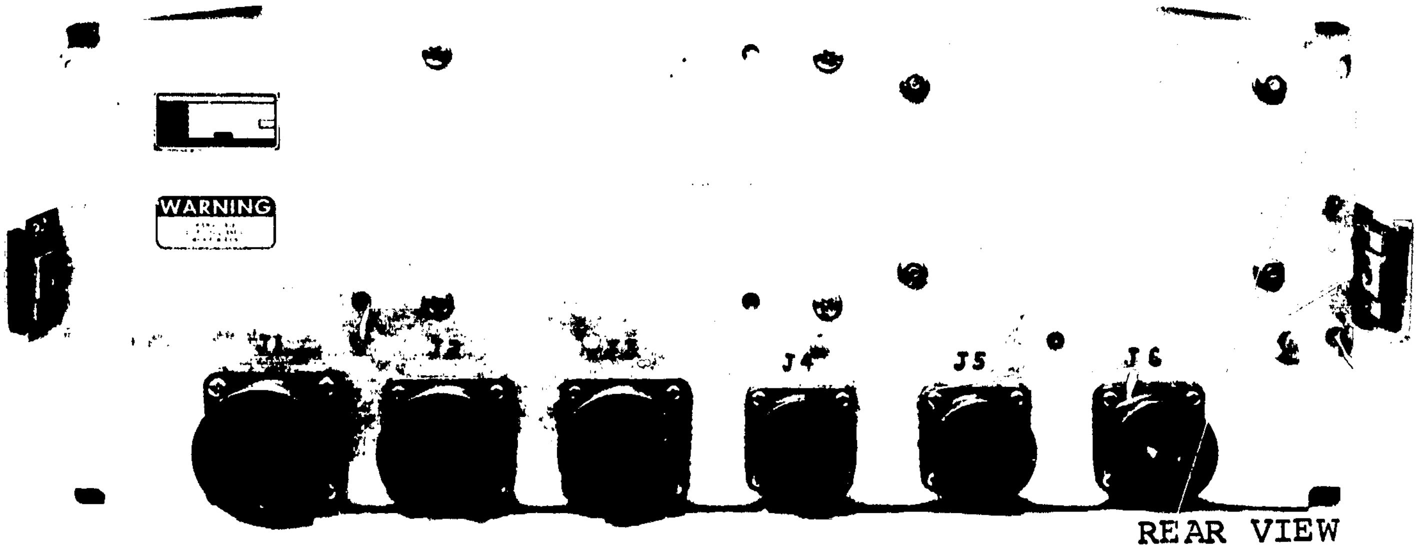

REAR VIEW

VOLTAGE REGULATOR/EXCITER ASSEMBLY

FIGURE 4-18

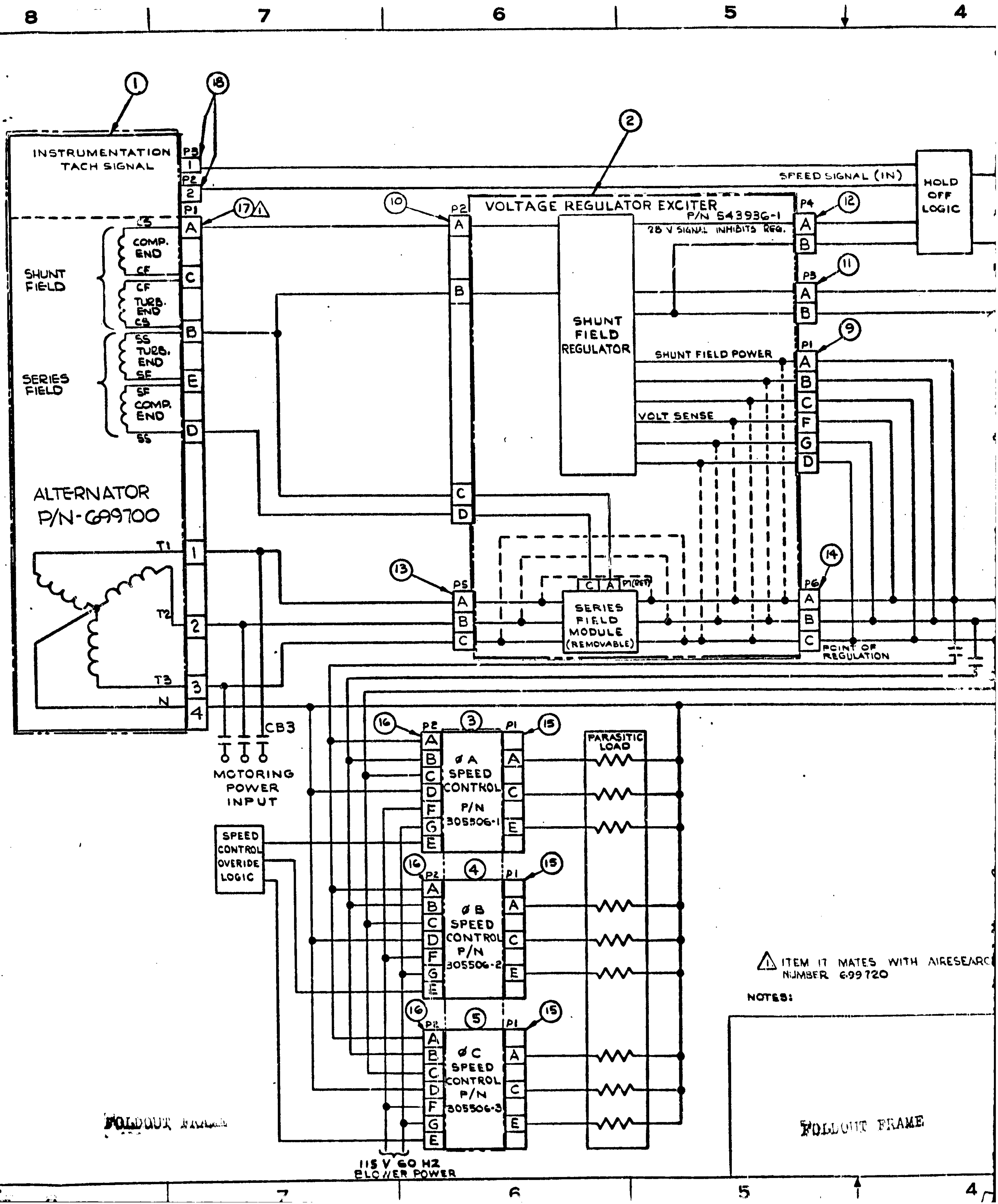

⚠1 ITEM 17 MATES WITH AIRESEARC
NUMBER 699720

NOTES:

REVISIONS

ZONE	LTR	DESCRIPTION	DATE	APPROVED
	A	ADDED DESIGNATORS (SEE E.O.)	2-7-68	
	B	REVISED CALLOUTS (SEE E.O.)	2-22-68	

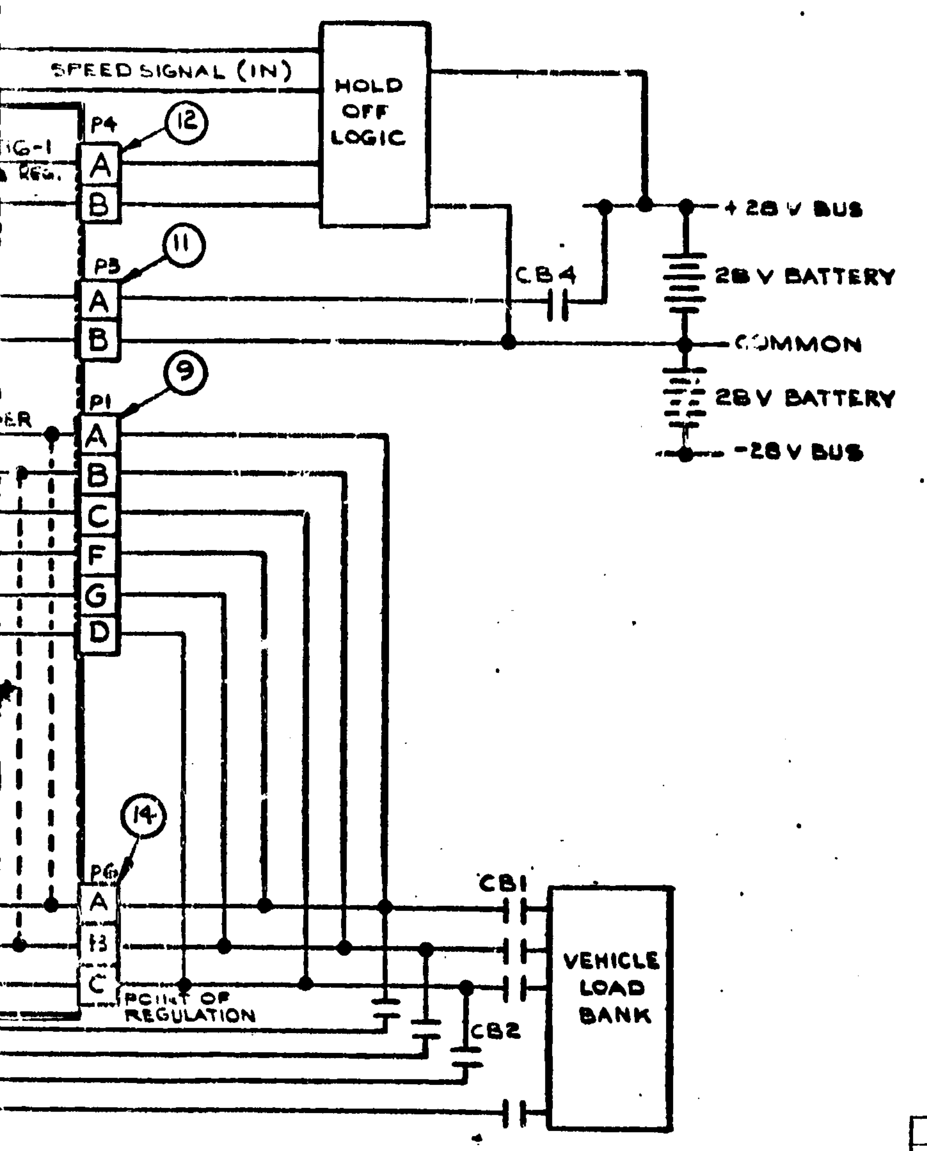

FIGURE 4-20

APS-5286-R
Page 4-59

ITEM NO.	PART NO.	SYM	DESCRIPTION	CODE IDENT	MATERIAL AND SPECIFICATION	ZONE
18	5255		CONNECTOR (P2, P3)			
17	699720		CONNECTOR (P1)			
16	MS3106R-20-15S		CONNECTOR (P2)			
15	MS3106R-20-15P		CONNECTOR (P1)			
14	MS3106E-10-11P		CONNECTOR (P6)			
13	MS3106E-18-11S		CONNECTOR (P5)			
12	MS3106E-18-20S		CONNECTOR (P4)			
11	MS3106E-22-8S		CONNECTOR (P3)			
10	MS3106E-22-18P		CONNECTOR (P2)			
9	MS3106E-24-2S		CONNECTOR (P1)			
5	305506-3		ØC SPEED CONTROL			
4	305506-2		ØB SPEED CONTROL			
3	305506-1		ØA SPEED CONTROL			
2	F42976-1		VOLTAGE REGULATOR EXCITER			
1	699700-1		ALTERNATOR			

QUANTITY REQD

← ASSY

LIST OF MATERIAL

1 ITEM 17 MATES WITH AIRESEARCH PART NUMBER 699720

TES:

SIGNATURES	DATES
DFT CANTRELL	10-6-67
CHK	
MFG	
MATL	
STRESS	
AERO	
APPD H Wilson	10-11-67
APPD	
DESIGN ACTIVITY APPD	10-12-67
OTHER ACTIVITY APPD	

REQD | NEXT ASSY | USED ON
HEAT TREATMENT | PROCESS
HARDNESS AND SPEC | NAME AND SPEC

UNLESS OTHERWISE SPECIFIED ON THIS DRAWING, FABRICATION OF THIS ITEM SHALL BE IN ACCORDANCE WITH AIRESEARCH SPECIFICATION SC-5535, STANDARD DRAWING INTERPRETATIONS.

GARRETT AIRESEARCH MANUFACTURING COMPANY OF ARIZONA
A DIVISION OF THE GARRETT CORPORATION
PHOENIX, ARIZONA

DWG TITLE
WIRING DIAGRAM (SCHEMATIC)
BRAYTON CYCLE
SYSTEM

SIZE D | CODE IDENT NO. 99193 | DWG NO. 43486

SCALE NONE | WT | SHEET 1 OF 1

FOLDOUT FRAME

5.0 DESCRIPTION OF THE SPEED CONTROLLER

The speed control system is a parasitic-load-type using dissipative resistive load to balance real load changes and/or variations in net turbine shaft power input to the alternator. The speed control requirements include the following:

(a) Capability of controlling speed using a frequency error signal.

(b) Capability of maintaining the alternator frequency at 1200 Hz to within the specified limits.

(c) Minimizing the effect of the control device on harmonic content of the alternator voltage and current.

(d) Minimizing the losses in the control device when the demand for parasitic load is zero.

(e) Provide capability for loading the alternator to 150 percent of design rating.

The speed-control system schematic is shown on Drawing 43534, Figure 5-1. This system utilizes three control circuits (one to sense each phase of the 1200-Hz, 120-V, 10.5-KW alternator) to apply or remove parasitic loading to maintain a constant frequency under varying vehicle load and alternator input conditions. Three control circuits are utilized to improve system reliability. Each control circuit loads all three phases simultaneously. The parasitic loads were established at 2 KW each to provide a total of 6 KW per control circuit. As the maximum parasitic load required is 10.5 KW, one control circuit may fail in the OFF-condition without affecting overall system performance.

Each control circuit consists of a frequency detector, an amplifier section, and a firing circuit. The frequency detector converts the frequency error to a d-c signal. This signal is amplified by two stages of push-pull magnetic amplifiers. The output from the magnetic

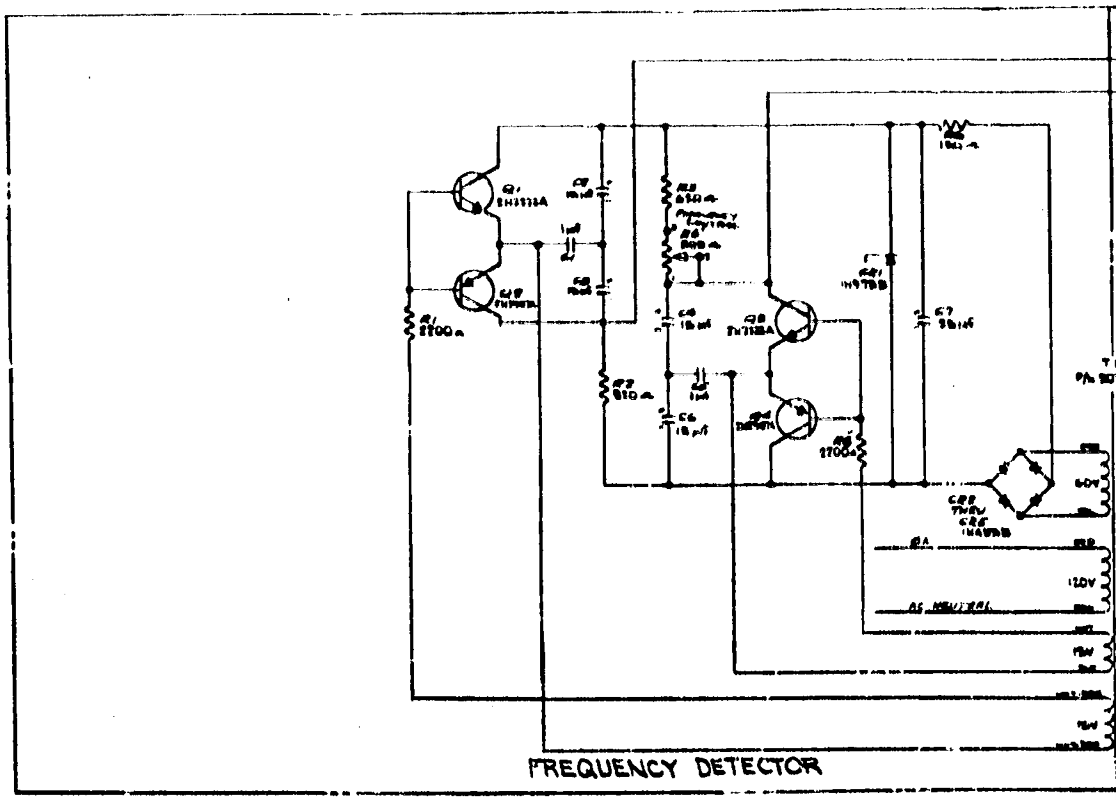

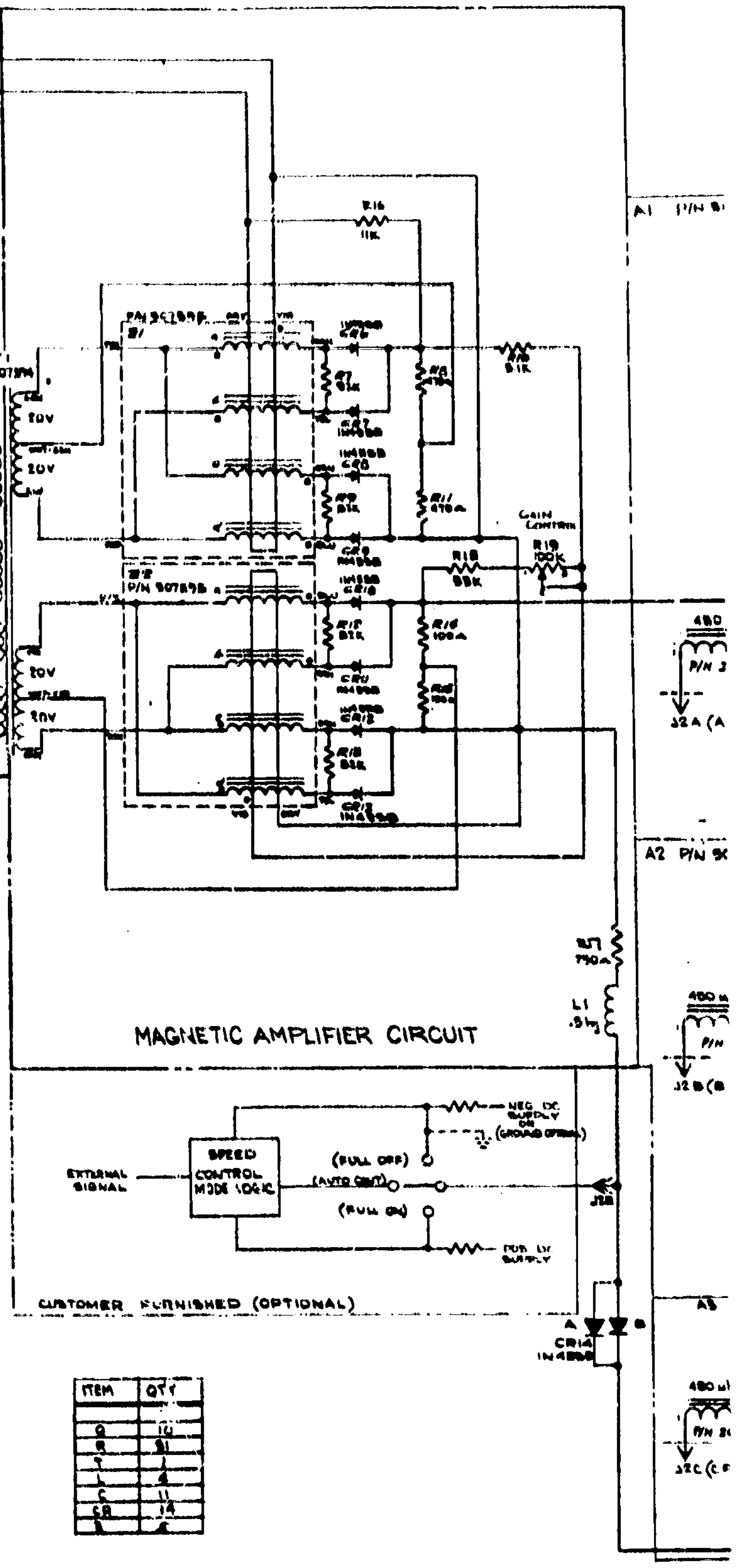

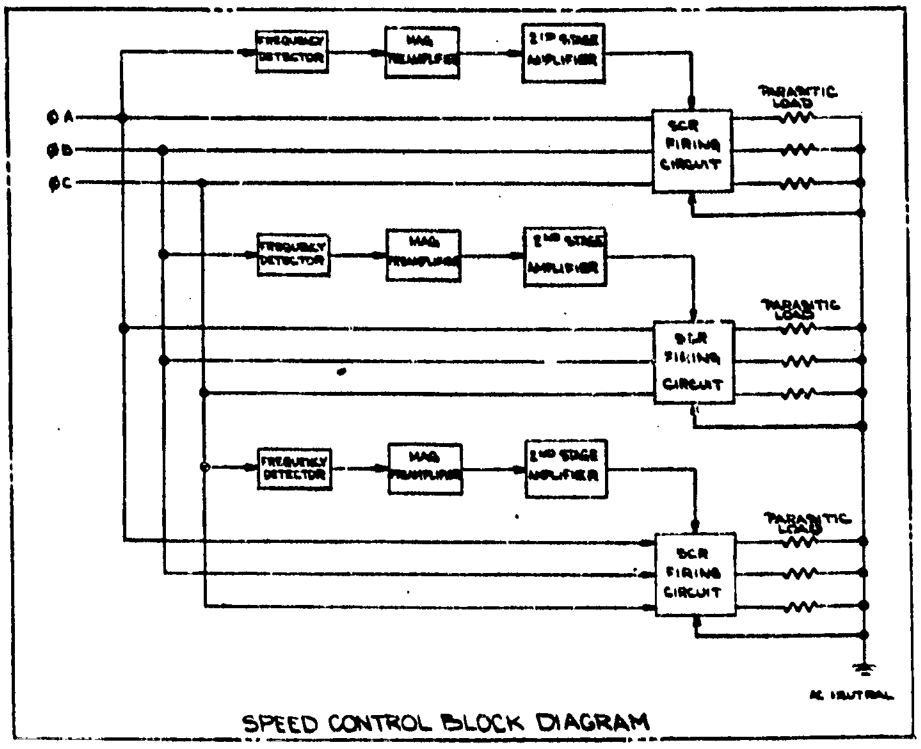

SPEED CONTROL BLOCK DIAGRAM

ITEM	QTY
Q	10
R	31
T	1
L	4
C	11
CR	14
[illegible]	[illegible]

NOTE: SCHEMATIC IS FOR PHASE A CONTROL CIRCUIT (TYPICAL FOR PHASES B AND C)

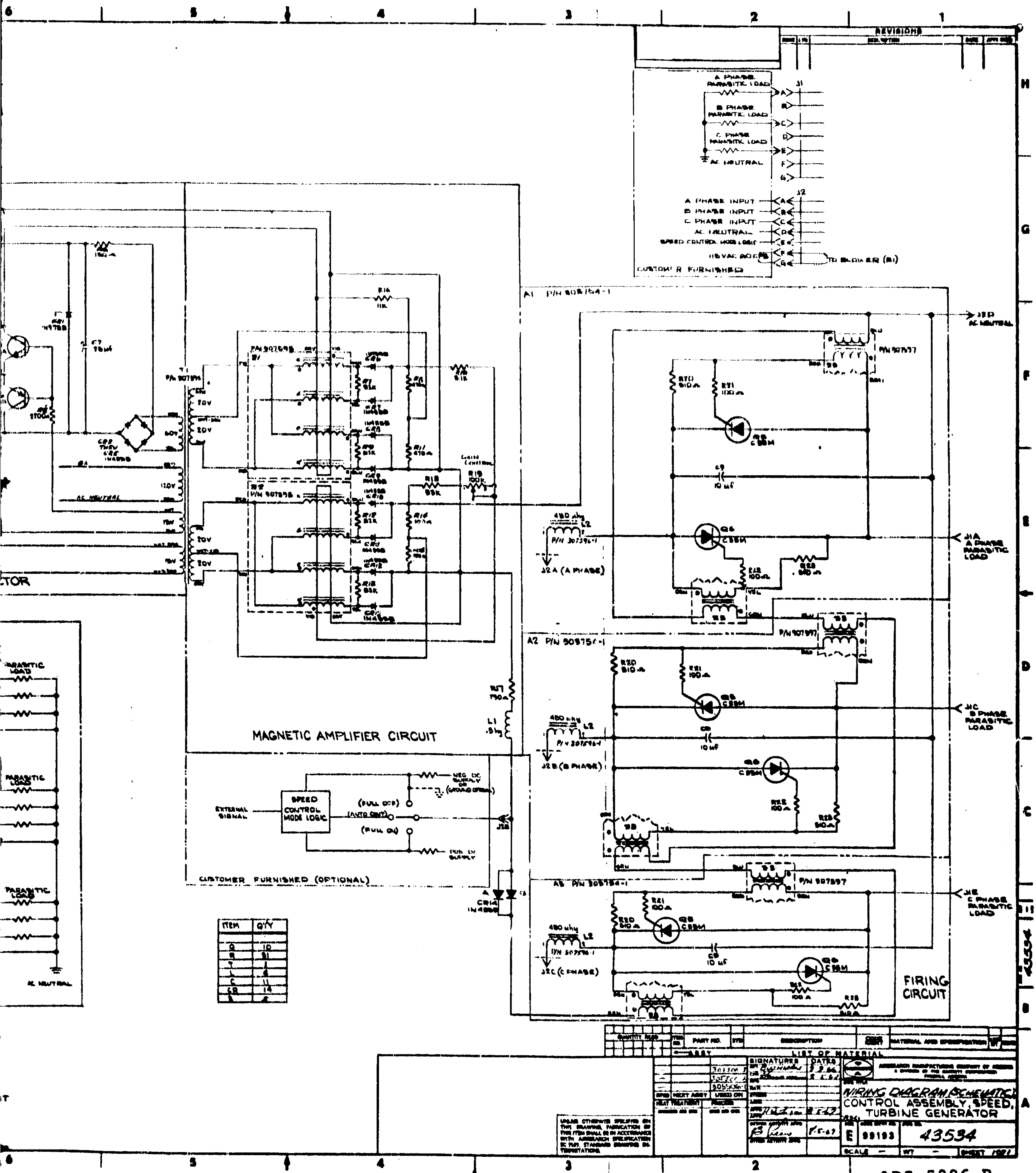

FIGURE 5-1

FOLDOUT FRAME

FOLDOUT FRAME

amplifiers is a monopolarity pulse that occurs at the center of each half-cycle. The duration of each pulse is proportional to the frequency error. (This signal could also be used for transistor control of the parasitic load at such time as a 600-V, 10-amp transistor of proven reliability is available.) For use with the SCR circuit shown, additional signal conditioning is required. This is accomplished with saturable reactors Z_3, Z_4, and Z_5.

Variable-frequency and variable-gain controls, located on the front panel, are incorporated in each control circuit.

A filter circuit has been incorporated in the design to reduce the effect of the speed control on the generator output.

NASA has requested incorporation of a scheme to allow manual or automatic full-on/full-off parasitic load control, Figure 5-2. This control system is not to be furnished by AiResearch. However, a tie-in point is provided as shown on the schematic, Wiring Diagram 43534, Figure 5-1. For the full-off mode, a negative bias was suggested. As discussed below, this would not be satisfactory for linear control. Grounding the tie-lead through a controlled impedance would satisfy the requirement. The circuit in the full-on mode serves to override the speed-control signal to the saturable reactors by providing sufficient current to saturate the saturable reactors for full-on, and grounding short-circuits the signal for full-off. For automatic control, the speed control normally is not affected by the manual control circuit. The control logic circuit is to be provided by NASA to turn the speed control on or off, based on other system requirements.

Table 5-1 lists the components shown on Schematic 43534, Figure 5-1, together with ratings, manufacturer, and reliability information.

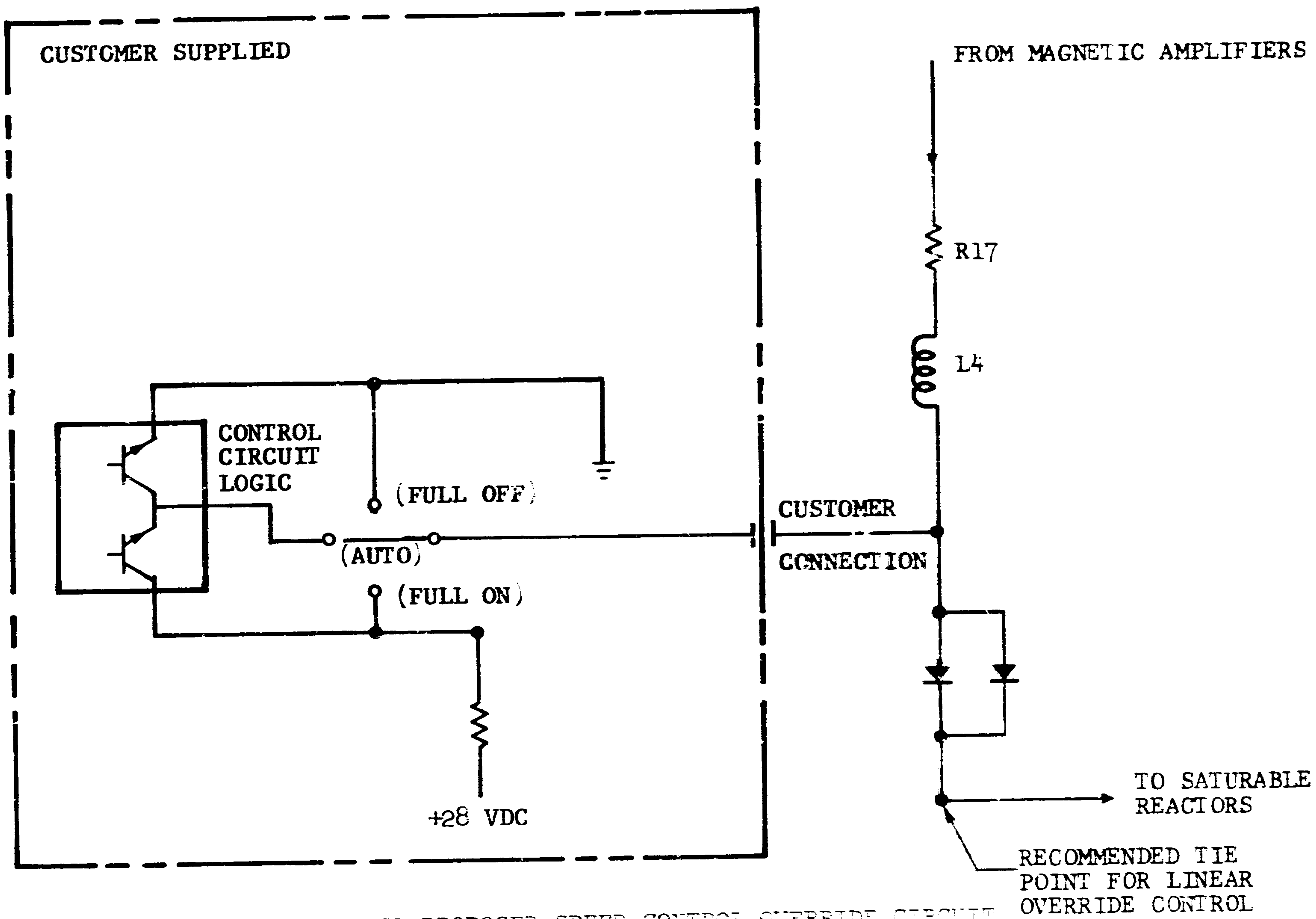

NASA PROPOSED SPEED-CONTROL OVERRIDE CIRCUIT

FIGURE 5-2

TABLE 5-1

COMPONENT DATA (Reference Dwg No. 43534)

Comp.	Manufacturer	Part No.	Rating[1]	Design Condition[1]	JPL Rating[2]	App. MIL-STD
Q5, 6	GE	C35M	Tjm/Td 125°C	Tj 75°C	V for 600 V	MIL-S-19500 108A
Q1, 3	TI	2N2222A	Tjm/Td 175°C/ 25°C	Tj 55°C	P	-
Q2, 4	TI	2N2907A	Tjm/Td 200°C/ 25°C	Tj 53°C	P	-
T1	AiResearch	307594	Insul Cl A	Top 66°C	No	MIL-T-27
L2	AiResearch	307596	Insul Cl A	Top 76°C	No	MIL-T-27
L1	UTC	MQA9	Insul Cl A	Top 56°C	V	MIL-T-27B
C1, 5	GE	74F01BA105	200 V	50 V	V	-
C2, 3, 4, 6	Sprague	350D156X9075S2	75 V	25 V	H for 6-50 volts	-
C7	Mallory	XTH256U180POC	180 V	50 V	V	MIL-C-39658B1
C9	GE	28F959	600 VDC/ 330 VAC	120 V	V	-
CR1	Motorola	IN978B	Tjm/Td 170°C/ 50°C	Tj 46°C	H and P	-
CR2-14	TRW	IN485B	Tjm/Td 200°C/ 25°C	Tj 46°C	H and P	-
Z1, 2	AiResearch	307595	Insul Cl A	56°C	No	MIL-T-27
Z3	AiResearch	307597	Insul Cl A	56°C	No	MIL-T-27
R1, 5	ABC/OHMITE	EB/RC20GF	2.2K, 1/2 W	0.125 W	P	MIL-R-38101
R2, 3	Dale	AGS-5	820/620/4 W	0.76 W	P	MIL-R-38101
R4	Bourns	3500-1	500Ω 2 W	0.460 W	V	-
R6	Dale	AGS-5	150Ω 4W	0.665 W	P	MIL-R-38101
R7, 9, 12, 13	Angstrom Prec. Inc.	RN60E	82K ±1/8 W	0.001 W	V	MIL-R-10509

TABLE 5-1 (CONT)

COMPONENT DATA (Reference Dwg No. 43534)

Comp.	Manufacturer	Part No.	Rating[1]	Design Condition[1]	JPL Rating[2]	App. MIL-STD
R8, 11	Dale	AGS-5	470 +1%	0.850 W	P	MIL-R-38101
R10	ABC/OHMITE	EB/RC20GF	5.1 K ±5% 1/2 W	0.0785 W	P	MIL-R-11
R14, 15	Dale	AGS-5	100Ω ±1% 4 W	1.50 W	P	MIL-R-38101
R16	Angstrom Prec. Inc.	RN60E	11K ±1/8 W	0.009 W	V	MIL-R-10509
R17	ABC/OHMITE	EB/RC20GF	750Ω ±5% 1/2 W	0.041 W	P	MIL-R-11
R20, 23	ABC/OHMITE	EB/RC20GF	510Ω ±5% 1/2 W	0.056 W	P	MIL-R-11
R21, 22	ABC/OHMITE	EB/RC20GF	100Ω ±5% 1/2 W	0.011 W	P	MIL-R-11
R18	ABC/OHMITE	EB/RC20GF	33K ±5% 1/2 W	0.01 W	P	MIL-R-11
R19	OHMITE	CLU 1041	100K 2 W	0.01 W	V(ABC)	MIL-R-94B

NOTES:

1. Operating temperatures assume a maximum ambient temperature of 46°C (115°F) per Specification P0055-2.
2. Refers to Jet Propulsion Laboratory Preferred Parts List, dated 1 July 1966. "H" indicates HiRel rating, "P" indicates spacecraft preferred rating, and "V" indicates qualified vendor.
3. Tjm = Max allowable junction temperature
   Td = Junction temperature at which component derating begins
   Tj = Junction temperature
4. L2 and C9 will be changed as the filter design is revised.

Speed Controller Transfer Function

The effects of transients such as those specified in 2.3b are dependent upon the total system. An analog study (included as Appendix V), investigating such system effects, has been completed. The transfer function of the speed control is as follows:

$$K = \frac{24\ \text{KW/percent of speed change}}{\underbrace{(1+0.00082\ S)^2}_{\text{Frequency detector}}\ \underbrace{(1+0.0157\ S)^2}_{\text{2 mag-amps}}\ \underbrace{(1+0.010\ S)}_{\text{Saturable reactor}}\ \underbrace{(S^2+3\text{x}10^4 S+2.25\text{x}10^8)}_{\text{Line filter}}}$$

The above relationship is based upon adding the phase-control sections sequentially. For example, the 6-KW load controlled by Phase A will be added as required for the first 1/4-percent error; the 6-KW load controlled by Phase B will be added as required for the next 1/4-percent error; and the 6-KW load controlled by Phase C will be added as required for the next 1/4-percent error should either Phase A or Phase B control section fail. The possibility of loading with all three control sections simultaneously (72 KW/percent of change in frequency) is being investigated. This would allow complete interchangeability of modules (refer to Drawing 43534, Figure 5-1).

5.1 Design of the Speed Controller

As shown on the block diagram section of AiResearch Drawing 43534, there are three basic sections to the speed control. These are

(a) The frequency detector
(b) Magnetic amplifier
(c) The firing circuit

The design of these sections was based upon considerable previous experience with the frequency detector and with similar magnetic amplifier arrangements. In the following paragraphs, details of the design are discussed. For component call-outs, refer to the wiring schematic, Drawing 43534, Figure 5-1.

The speed-control is designed for a parasitic load speed-control power loss of less than 24 W when no parasitic load is being applied. Large derating factors have been used for components that would cause loading if the component failed (see Paragraph 5.2, Reliability Study and Failure Analysis).

Frequency Detector

The circuit consists of a bridge with two active and two resistive legs. The active element consists of two charging capacitors in series, C's 2 and 3 and C's 4 and 6, around which there is a two-transistor switch (Q's 1 and 3 and Q's 2 and 4). The transistors are complementary NPN and PNP so that when one transistor is turned on, the other one is turned off. A timing capacitor (C's 1 and 5) is connected from the junction of the two series charging capacitors to the junction of the two emitters of the switching transistors. The collectors are tied to the extremes of the charging capacitors. With this arrangement the timing capacitor is switched, on alternate half cycles, from one end of the charging condensors to the opposite end. This action removes a charge from these charging condensors, with the result that there is continual charging current through the fixed resistive legs of the bridge. The bridge must be balanced at the reference frequency. With a bridge supply voltage V_s, the voltage drop across R_2 (or $R_3 + R_4$) is $V_s/2 = IR_2$, where

$$I = \frac{Q}{t} = Qf = \frac{V_s}{2} C_1 f$$

therefore

$$R_2 = \frac{V_s}{2I} = \frac{1}{C_1 f}$$

The change in the detector output, V_c, per percent frequency change or detector gain, by voltage loop equations is

$$\frac{5.2 \text{ millivolt} \times V_s}{\text{Percent frequency change}}$$

Before determining C_1 and V_s, it is necessary to determine the preamplifier input requirements. The gain of the frequency detector must be large enough to minimize the drift level of the first stage of amplification. This drift is difficult to accurately predict; however, from experience with similar magnetic amplifiers, it has been found that if the ambient temperature is kept below 130°C and the core material is well-matched Mo-Permalloy, a worst-case drift figure of 0.033-ma turn/°C/100 gate turns can be expected.

It is obvious that since all the drift is not the fault of the gate diodes, the drift level is not directly proportional to gate turns; however, for a number of turns between 200 and 1000, this figure will suffice. In the case in question, there are 670 gate turns; therefore, the worst-case drift will be 6.7 x 0.033 or 0.221 ma turns/°C. For a ±50°C change, this represents 11.1-ma turns drift. With 2000 turns on the control, this represents ±5.5 μa. Since the control range of this device will be approximately 1/4 percent, the gain should be much larger than 22 μa/percent of change in frequency. In addition to this, the impedance of the detector should be high with respect to the d-c resistance of the control winding. This will minimize the gain change as a function of ambient-temperature change. For 2000 turns control, the minimum resistance (R_c) will be approximately 100 ohms; therefore, the impedance of the frequency detector should be approximately 1000 ohms.

If R_2 must be approximately 1000 ohms,

$$C_1 = \frac{1}{R_2 f} = \frac{1}{(1.2) \times (10^6)} = 0.83\ \mu f$$

If $C_1 = 1\ \mu f$, R_2 adjusts to

$$\frac{1}{C_1 f} = 830 \text{ ohms}$$

For the gain to just equal the drift of 22 μa/percent of change in frequency, from Ohm's Law, the d-c voltage change must be current x ($R_2 + R_c$) or $22 \times 10^{-6} \times (830 + 100) = 20.5$ mv. From the gain relationship for the detector, the supply voltage required would be:

$$V_s = \frac{20.5 \text{ mv/\%f change}}{5.2 \text{ mv/\%f change}} = 3.9$$

By setting $V_s = 50$ V, the gain due to drift from temperature change is negligible, and medium voltage transistors ($V_s/2$ is seen by the transistor) may be used for switching. The 2N2222A and 2N2907A transistors listed in the JPL Preferred Parts List are adequate. The charging capacitors C_2, C_3, C_4, and C_6 must be large with respect to C_1 and C_5 and are set at 15 μf.

A V_s of 50 V results in a frequency detector gain of 260 mv/percent of frequency change or 65 mv/1/4 percent.

The only components that would cause drift due to temperature are C_1, C_5, R_2, and R_3 (Drawing 43534, Figure 5-1). Precision components have been selected for these requirements as shown in Table 5-1. At this time, it is assumed that R_4 will be eliminated from the flight package.

Magnetic Amplifiers

From the previous discussion, it can be seen that the magnetic preamplifier design must be tailored to the frequency detector characteristics. The gate voltage, which is an arbitrary value, was selected as 20 V RMS. Even though the value of this voltage is arbitrary, once it has been selected, it determines the number of gate turns and the gain of the amplifier per given number of control turns. It also has an effect on the time-constant of the amplifier. From the standard transformer equation, i.e.,

$$N_g = \frac{(E)(10^8)}{4.44\ f\ BA_c}$$

the gate turns are 670 turns for a standard core (Part 52002-2D, Magnetics Inc.). For control, 2000 turns were selected on an arbitrary basis; however, there are factors that limit this selection. The time constant of the amplifier is proportional to the number of control turns squared and is divided by the resistance of the control circuit. Gain is directly proportional to the number of turns, while the d-c resistance of the control winding is related to the number of turns squared. Of course, the number of windings establishes the minimum window area of the core.

Gain of this device can be calculated by using some of the fundamental equations that express the relationship between NI, gausses, Oersteds, and volts. These relationships must also include such things as ratio of ID to OD and the incremental permeability in the control region. However, from past experience, it has been found by empirical means that the gain of this device is approximately 0.003 V/ma control/control turn/volt gate. Therefore, with a gate voltage of 20 and 2000 control turns, the gain will be 0.003 x 20 x 2000 or 120 V/ma. This figure includes the degenerative action that results from self-bias.

Self-bias is the next consideration in the design and, as in the case of control, the following relationship expresses the bias current, $I_B = Hlc/0.4\pi N$, where H is the drive required to reset the core to the mid-point or the 90-deg firing point. The voltage available is 1.5 times the gate voltage. By using these relationships, the self-bias resistance is equal to 82,000 ohms. From the frequency-detector analysis, the current for 1/4-percent frequency error will be 80 μa; and the gain through the magnetic preamplifier is 9.6 V/0.25 percent change in frequency. Response time of the amplifier can be expressed as follows:

$$T = \frac{KN^2}{R}$$

where

N = number of control turns
R = bridge resistance
$K = (V/AT)/(2N_g f_g)$

and

V/AT = gain of the amplifier (volts per ampere turn)
N_g = number of turns on the gate
f_g = frequency of gate

Solving for K:

$$V/AT = 60, \quad N_g = 670, \quad f_g = 1{,}200$$

Therefore,

$$K = 3.73 \times 10^{-5}$$

$$T = \frac{(37.3)(4)}{950} \approx 0.1575$$

Since

$$T = \frac{1}{W} \text{ and } f = \frac{W}{2\pi}$$

$$W = 6.35 \text{ radian/sec.}$$

$$f = 1.10 \text{ Hz}$$

Where f is the high-frequency cutoff, it becomes obvious that the bandwidth must be expanded at least 10 times by negative feedback. With this much feedback, the 80 μa for 9.6-V output now becomes 800 μa, with all but 80 being cancelled by the feedback. Therefore,

$$R_{fb} = \frac{(8.0)(10^3)}{0.72} = 11{,}000 \text{ ohms}$$

A complete description of the transfer function for this amplifier is (12 V/ma)/(1 + 0.0157S). The second stage of magnetic amplification is identical with the first stage except that the coupling resistance is 10 times the impedance of the frequency detector, (12V/V)/(1+0.0157S).

By multiplying the gains of the three elements, for 1/4-percent change in frequency, the voltage out is 9.22 d-c. From a transfer-function standpoint, there is a double lag at 63 rad/sec.

Transformer

Transformer T-1 provides power to the frequency detector and the magnetic amplifiers. It is assumed that the saturated condition of the generator will supply full voltage at 60-percent speed (120 V RMS at 720 Hz). The primary current is found by summing the reflected secondary currents and the excitation current. Starting with the magnetic amplifiers, two will reflect a total of 13 ma to the primary while the frequency detector will reflect 35 ma, which will make a total of 48. The exciter current cannot be calculated until the magnetic core is selected. However, with the excitation of 10 percent or less, the primary wire size of 33 was chosen. This gives a circular area of 50 mills. It is assumed that the maximum flux density is 10,000 gauss.

From the standard transformer equation, an expression for the primary turns can be found, $N_p = 58/A_c$, where A_c is the cross-sectional area of the magnetic path, in inches. The number of primary turns can also be expressed as a function of window area and wire size. It can be assumed that half the window area will be filled with copper and that half of this area will be the primary. Therefore, the window area (W_a) = $(N \times 50 \times 10^{-6})/0.25$ or $N = 5 \times 10^3 W_a$. By equating the two relationships, $5 \times 10^3 W_a = 58/A_c$ or $W_a A_c = 0.0116$-in.^{4} From the manufacturer's catalog, a core can be selected (E127) that has a $W_a A_c$ of 0.0176. This is more than required, according to the previous calculation. A_c for this case is 0.141 in.^{2}, from which $N_p = 411$ turns and requires less than 0.25 of the available window area. Solving for the excitation, $I_c = Hc\ell c/0.4\pi N$. Let $Hc = 0.60$, then $I_c = 6.7$ ma. The resistance of this winding is found to be approximately 12 ohms; however, an arbitrary maximum limit of 18 ohms was chosen. This should allow for production tolerances and, from a regulation and heat-generation standpoint, should cause no problems. The secondaries were designed by using 1000 circular mils per ampere wire. Resistance values were calculated and all other design details were considered (see AiResearch Drawing 307594, Appendix II).

Firing Circuit - A magnetic amplifier was originally considered; however, from a reliability standpoint, a saturable reactor would be preferable. In the case of zero control signal, the parasitic load will go to zero if a saturable reactor is used. In the design of the gate windings, the volt-second integral should accommodate the saturation of the generator--that is, 120 V RMS at 720 Hz. With the use of a standard Magnetics Inc., Case 52106-2A, the

$$N_G = \frac{0.45E}{(f)(2B_m A_c)(10^{-8})} = 1,400 \text{ turns}$$

Solving for the excitation current gives $I_c = Hc\ell c/0.4N = 1.68$ ma. The gain of this device is expressed through the basic relationship of the ampere turns of the gates must equal the ampere turns of the control. When these devices are used in a parallel configuration, as in this case, the gates then carry twice the NI that the control does. The final design configuration and considerations are shown on AiResearch Drawing 307597, Appendix VII.

The SCRs (Q5 and Q6) must handle the current for half of the 2-KW loads or

$$\frac{2000}{(2)(120)} = 8.33 \text{ amp RMS}$$

and a peak voltage of 170. Initially, General Electric C35M SCRs were selected because they are included on the JPL Preferred Parts List. Consideration was given to the use of Type C135 SCRs because of a higher dv/dt* rating. However, the gate current requirement for the C135 is greater than that available from the control circuit. An analysis was made to determine the worst-case dv/dt that could occur with this design. It was calculated with the filter in the firing circuit, as

$$\frac{dv}{dt} = 2.15 \text{ V/sec.}$$

without the filter in the firing circuit,

$$\frac{dv}{dt} = 3.0 \text{ V/sec.}$$

C35M rating

$$\frac{dv}{dt} = 10 \text{ V/sec.}$$

From this it is seen that the C35M SCRs have adequate design margin, either with or without the filter. C35Ms rated at 600 V peak and 35 amp RMS are used in the breadboard controls. The thermal and reliability analysis shows the device to be satisfactory for this design. However, care is required when mounting the SCRs on a 150°F heat-sink.

The saturable reactor firing circuit for the SCRs should be carefully evaluated when operated at rated-load. Some additional development may be required to obtain balanced loading of the phases and to assure adequate gate current to the SCRs.

---

*dv/dt is the rate of rise of forward blocking voltage that will not turn on the SCR.

Filter Circuit

As indicated in 2.3c, the system is to be designed to control EMI to meet the requirements of MIL-STD-826 and to minimize harmonic distortion of the alternator output resulting from speed-control switching (Paragraph 2.3e).

Because the configuration of the controls supplied to NASA were of the open-breadboard type, not the configuration planned for the flight units, and because the controls would not be located in the system as finally proposed, the EMI analysis has been postponed until the system is flight-packaged.

Included in the speed control is a passive filter for harmonic distortion caused by the application of pulsed loads. However, it has been determined that the voltage regulator/exciter (VRE) will not function satisfactorily with a leading power factor such as produced by this filter.

NASA agreed to accept the speed-control to the approved design with the filters connected. Prior to operation with the VRE, NASA will disable the filters. This will be accomplished by lifting the ground on capacitor C9 and connecting a jumper around L2 as shown in the schematic section of Figure 5-3.

The modification below is required for all three phases in all three modules to render the filters inoperative.

Additional analysis and development will be performed by NASA to determine the optimum type and location of the filter.

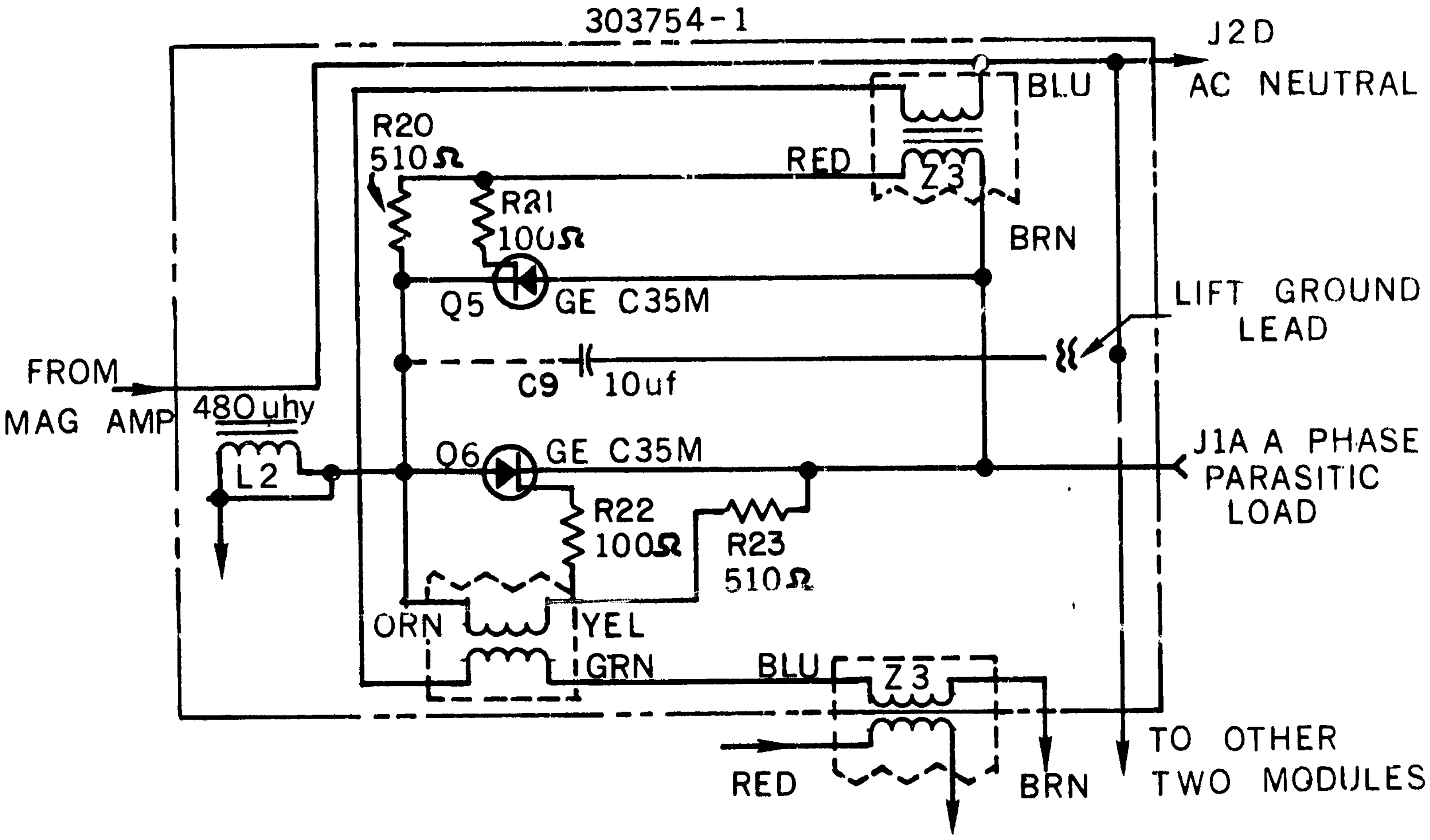

FIGURE 5-3

Because the generator output contains about 4-percent distortion, AiResearch has recommended that the filter be placed in the vehicle load-line and that an active filter be considered. (One is described in Appendix VI.) VRE regulation and interaction is improved by placing a filter between the speed-control and the VRE voltage-sense leads.

5.2 Reliability Study and Failure Analysis

For the reliability study performed on the speed-control, three sources of data were used:

(a) MIL-HDBK-217A, Reliability Stress and Failure Rate Data for Electronic Equipment, dated December 1965.

(b) BuWEPS Failure Rate Data Program.

(c) Reliability Application and Analysis Guide by D. R. Earles, The Martin Company, dated July 1961.

The results of this study were separately reported in Reliability Report, RC-5199-R, dated October 14, 1966.

Because the reliability data were for a class of components rather than for specific items, the results of this study did not appear to be particularly applicable to design improvement. In addition, the data were not applicable for the specific high-reliability components contemplated for use in the flight package. Further reduction in the usefulness of the analysis results from the fact that only limited rating characteristics were considered.

In view of the unsatisfactory study, the system requirements were reviewed to establish a better reliability approach.

Reliability was the primary consideration for establishing the speed-control philosophy. The control consists of three sections that apply up to 2 KW/phase/section. As the design power rating of the BRU is 10.5 KW_e maximum, only two sections (12-KW capacity) are required to fully load the BRU. Therefore, one section serves as a backup for failure of a section in the full-off condition. Also, a speed-control override is available to control the firing circuit.

From a system standpoint, a failure is the condition where the system fails "on". Table 5-2 lists those failures that will result in a failure in the "on" mode. Table 5-3 lists the critical components with their operating and rated parameters.

TABLE 5-2
SPEED-CONTROL CRITICAL COMPONENTS (FAIL-ON)

Component	Failure Mode	Effect on Circuit	Remarks
Q1, Q2, Q3, Q4	Shorted	Full on	
Q5, Q6	Shorted	Related Phase on	Note 1
C2, C3, C4, C6, C9	Shorted	Full on	
R7, R13	Open	Full on	
R16, R18, R19	Open	Full on or Full off	Note 2
R20, R23	Open	Related Phase 1/2 on	Note 1
CR8, CR9	Shorted or open	Full on	
Z1, Z2	Shorted or open	Full on	
Z3	Shorted	Related Phase on	

NOTES

1. Not corrected by customer-furnished speed control override circuit shown in Figure 5-2.
2. Full-on with any input signal from speed-detector (with speed above the set-point) section as negative feedback is removed.

TABLE 5-3

SPEED CONTROL CRITICAL COMPONENTS OPERATING CHARACTERISTICS

	Q1, Q3 2N2222A	Q2, Q4 2N2907A	Q5, Q6 C35M
V_{ce} rated, V	40	60	600
V_{ce} operating, V	25	25	170
P_D max at 46°C, mw	430	350	--
P_D operating, mw	20	20	--
I_c max	800 ma	600 ma	35 amp RMS
I_c operating	30 ma	30 ma	8.5 amp RMS
T_j max, °C	175	200	125
T_j operating, °C	52	55	75

Capacitors

	C2, C3, C4, C6	C9
Volts rated/operating	75/25	330/170 RMS
Current-rated, amp	--	43 at 50°C, 25 at 80°C
Current-operating, amp	--	15 at 46°C

Resistors

For power ratings, see Table 5-1.

Reactors

Z1, Z2, Z3 - See AiResearch Drawings 307595, 307596, and 307597, Appendix II.

Heat-transfer calculations for these devices follow:

Junction Temperatures

Q5 and Q6, G.E. C35M (2N690)
Selected from JPL list, 600 V, 35 amp RMS
Max OP = 125°C (derating temp 30°C) = T_j max
Average current for 2 KW and 120 V RMS

$$I = \frac{2{,}000}{120} = 16.7 \text{ amp RMS}$$

$$I_{avg} = 0.9 \times I_{RMS} = 0.9 \times 16.7 = 15 \text{ amp}$$

Each SCR conducts for 1/2-cycle

Therefore, I_{avg}/SCR = 7.5 amp for 180-deg conduction.

From the G.E. curve for forward dissipation, Pd = 11 W.
From the G.E. curve for maximum case temperature to 7-1/2 amp, T_c max = 100°C.
From the work statement, 150°F (66°C) is the heat-sink and 115°F (46°C) is the maximum ambient temperature.

Based upon Wakefield NC 303 dissipation data for natural convection (for research package):

$$T_s = 28°\text{C (11 watts)} + Ta = 28 + 46 = 74°\text{C}$$

$$T_j = T_s + P\ (\theta_{s\ \text{to}\ c} + \theta\ \text{to}\ j)$$

where

c = case
s = sink
j = junction
a = ambient

From the GE data,

$$\theta_c \text{ to } j = 1.7°\text{C/W max}$$

$$\Delta T_c \text{ to } j = 11 \times 1.7 = 18.7°\text{C}$$

ΔT_c to x is very low, when using joint compound, assume 2.2°C.

$$\therefore T_j = 74 + 18.7 + 2.2 = 95°\text{C}$$

Conclusion

$T_j < T_{j\ max}$ and was satisfactory, but for additional margin a fan was included in the rack. For 10-ft^3/min. flow, $\theta_{s-a} = 0.75°\text{C/W}$.

$$\Delta T_{s-a} = 11.\times 0.75 = 8.25°\text{C}$$

$$T_j = 8.25 + 46 + 18.7 + 2.2 = 75.2°\text{C}$$

For a heat-sink of 66°C,

$$\Delta T_c \text{ to } s = 11 \times 0.2 = 2.2°\text{C}$$

$$T_j = 66 + 2.2 + 18.7 = 86.9°\text{C}$$

Table 5-4 lists the estimated heat losses for the various components.

5.3 Mechanical Analysis

Packaging of the speed control is in accordance with the applicable specifications. Component size and arrangement is shown on Drawing L305444, Figure 5-4. Based upon NASA Specification P0055-2 (Figure 2), design calculations for the components assume an ambient temperature of 115°F and a heat-sink of 150°F. In this design, the SCRs are the only components requiring a heat-sink in a 115°F atmosphere. A blower is provided in each chassis for cooling the SCR under breadboard test conditions.

Weight - Each system weighs approximately 105 lb., or 35 lb./section. This weight includes filters C9 and L1,which are to be disabled as previously discussed.

AiResearch Drawing 305444 (Figure 5-4) is a layout of one of three identical sections comprising a speed control. Table 5-5 presents a list of AiResearch drawings pertaining to the speed control. Figure 5-5 shows the three modules comprising the complete control package. A view from the front of one of the three speed-control modules is shown in Figure 5-6. The components mounted on the circuit board, located in the right-front of the photo, form the detector or discriminator. The three small components, a transformer (T1), and two saturable reactors (Z1 and Z2), mounted on the left-front of the chassis, comprise the amplifier section. The remainder of the components at the rear of the package make up the firing circuit. The three large cans and the inductor immediately to the left of each can form the filter. More than half the size and weight of the control system is due to the filter components. Figure 5-7 shows a rear view of a speed-control module. The electrical connectors mounted on the rear of the chassis and the heat exchangers for the SCRs are seen in this view. Not shown are the front panel, the blower, and the SCRs.

TABLE 5-4
SPEED CONTROLLER HEAT LOAD ANALYSIS

		Full Load
Q5 and 6 - G.E. SCR C35B From G.E. data sheets for 7.5 amp average current 11 watts per SCR x 18		198 W
Q1 through 4 The current through each transistor will be that through Resistors R2 and R3 and R4 or		
	$\frac{25V}{820\Omega}$ 30 ma	
	P_D $\frac{1}{2}$ EI x duty cycle x $\frac{4}{\phi}$ x 3ϕ	[illegible] W
C9, 10, 11	15 amp x dissipation factor x 6	54
R1 and 5	0.125 W/res x 2 res/phase x 3 phases	0.75 W
2 and 3	0.75 W/res x 2 res/phase x 3 phases	4.5
4	0.5 W/res x 1 res/phase x 3 phases	1.5
6	1.0 W/res x 1 res/phase x 3 phases	3.0
7 and 9	neg	-
8 and 11	1.0 W/res x 2 res/phase x 3 phases	6.0
10	neg	-
12 and 13	neg	-
14 and 15	1.5 W/res x 2 res/phase x 3 phases	9.0
16 29	neg	-
	Res subtotal 279	
Magnetics		
T1	0.75 W/phase x 3 phases	2.25
L1, 2 and 3	7 W/ind x 9 ind	63
C1 and 5 C2, 3, 4 and 6 C7 and 8 CR-1 CR2-14	2 W/phase x 3 phases	6.00
Z1	0.25 W/phase x 3 phases	0.75
Z2	0.75 W/phase x 3 phases	2.25
Z3, 4 and 5	0.75 W/reactor x 9 reactors	6.75
	Subtotal 81	
	279	
	360 W	

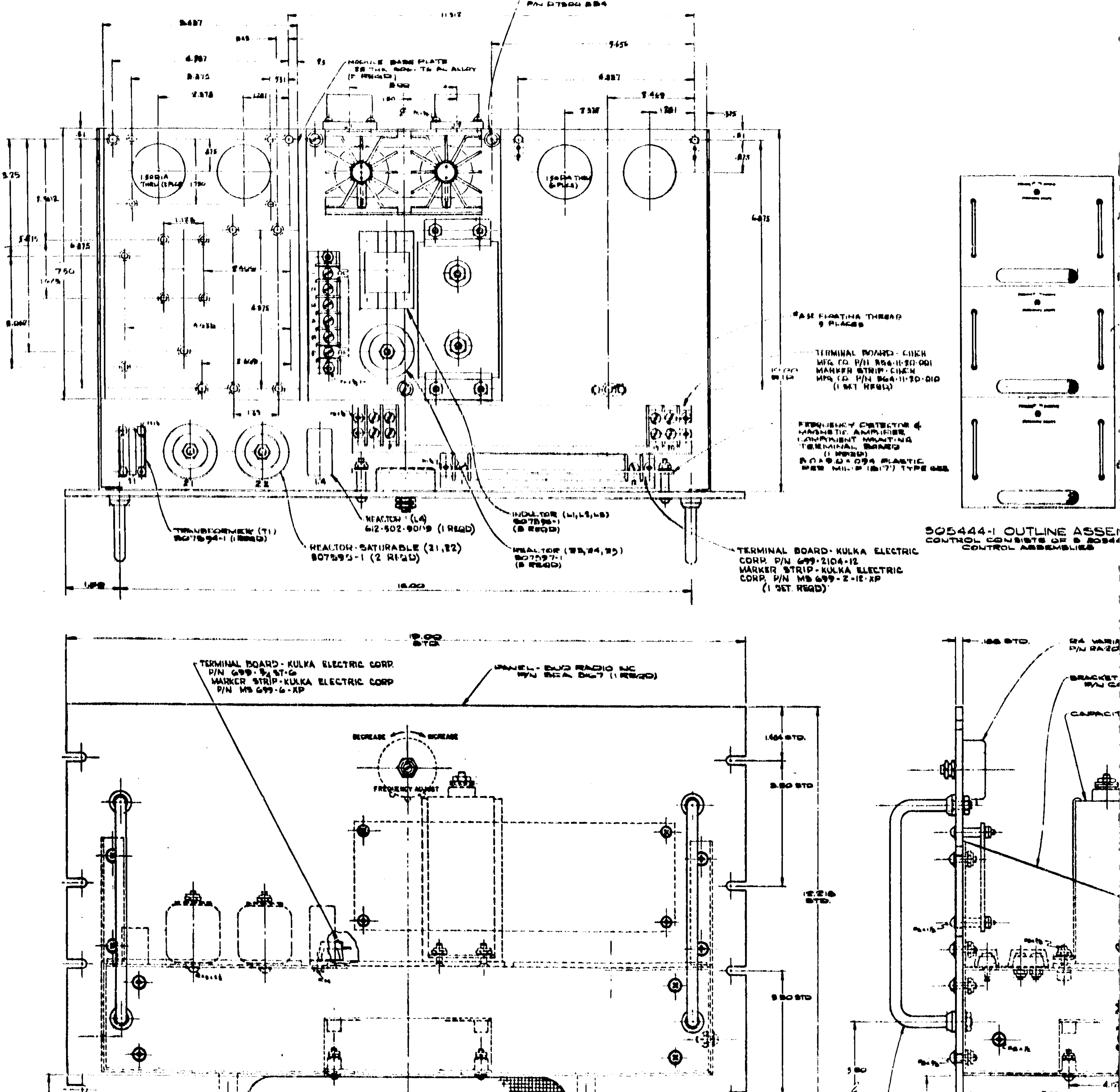

505444-1 OUTLINE ASSE
CONTROL CONSISTS OF 5 30544
CONTROL ASSEMBLIES

DETAIL 305445 ASSEMBLY

1. THIS LAYOUT IS INTENDED TO DEMONSTRATE FEASABILITY AND COMPONENT SIZE AND CONFIGURATION ONLY. COMPONENTS MAY BE REPOSITIONED SLIGHTLY TO FACILITATE INTERCONNECTION.
2. J1-MS3102R20-15S - J2-MS3102R20-15P
3. FOR SCHEMATIC DIAGRAM SEE DRAWING PA43534

FOLDOUT FRAME

FOLDOUT FRAME

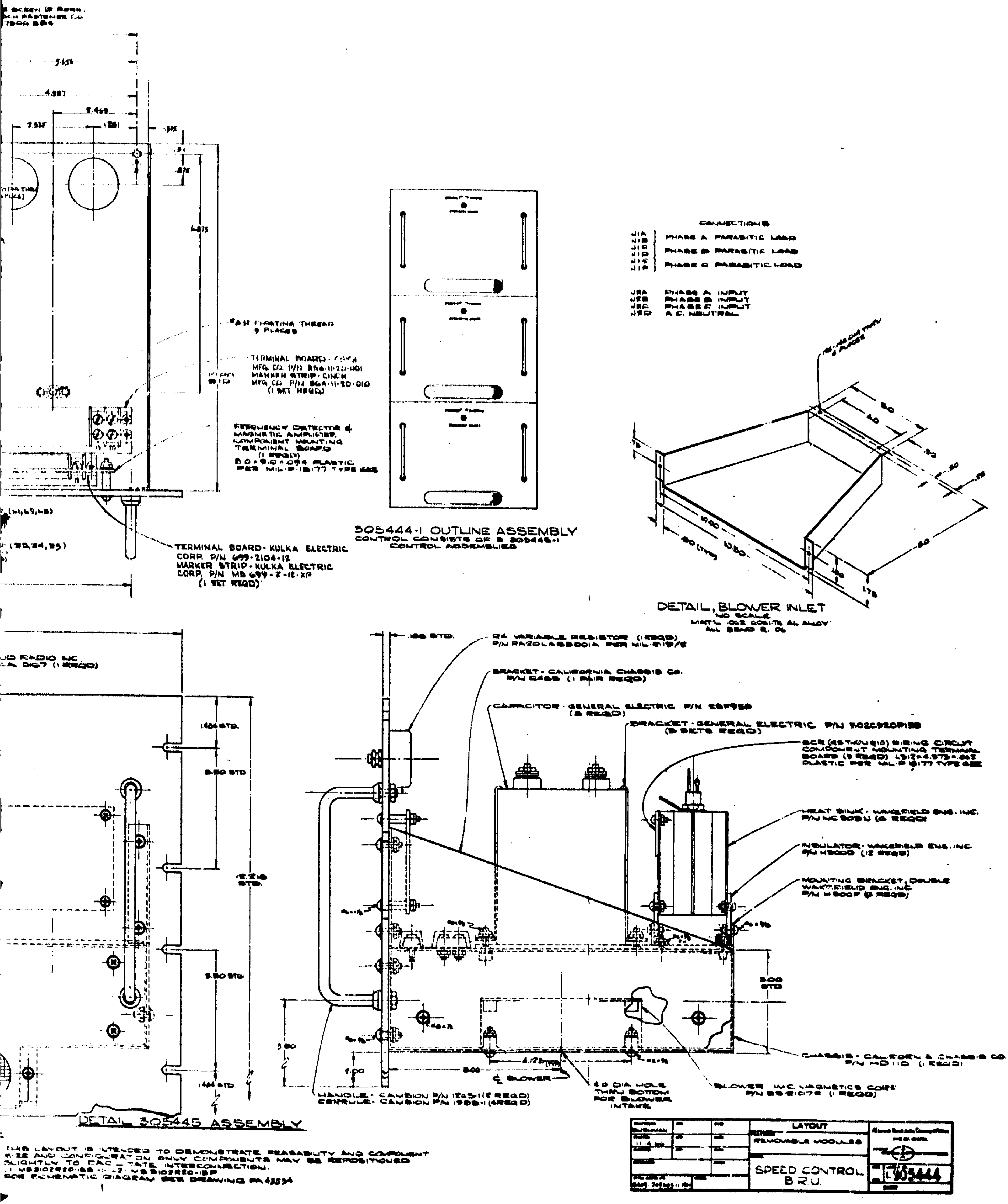

FIGURE 5-4

FOLDOUT FRAME

FOLDOUT FRAME

TABLE 5-5
SPEED CONTROL DRAWINGS (BREADBOARD UNIT)

Drawing No.	Title
303749	Terminal Board Assembly
303750	Terminal Board Assembly Electrical
303751	Terminal Board Assembly
303752	Terminal Board Assembly Electrical
303753	Electronic Component Mounting Plate
303754	Module Assembly (Firing Circuit)
303755	Instrument Panel Assembly
303756	Chassis Assembly
303757	Air Blower Inlet
303758	Instruction - Warning - Plate
305444	System Outline
305445	Control Assembly
305506	Control Outline
43534	Schematic Wiring Diagram
43574	Wiring Diagram (Pictorial)
43577	System Wiring Diagram

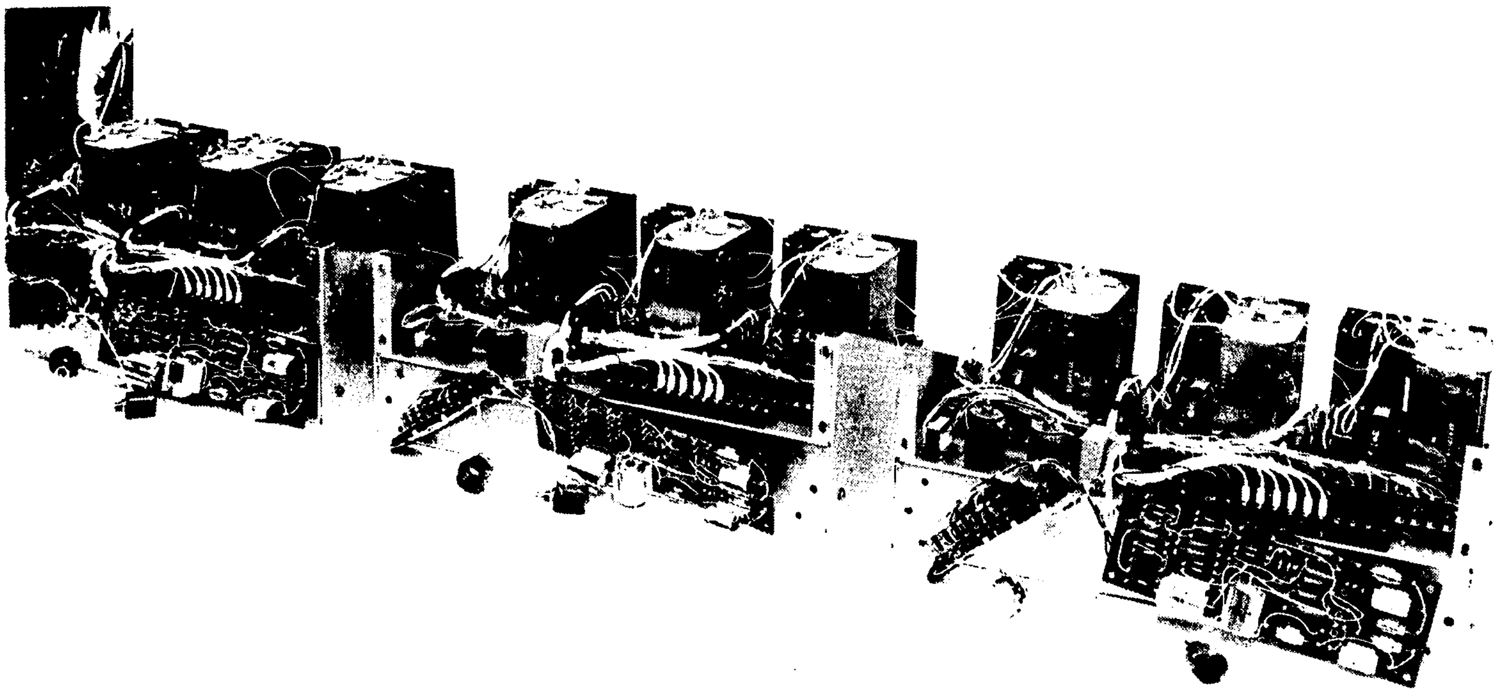

BRU SPEED-CONTROL ASSEMBLY
THREE SUBASSEMBLIES REQUIRED

FIGURE 5-5

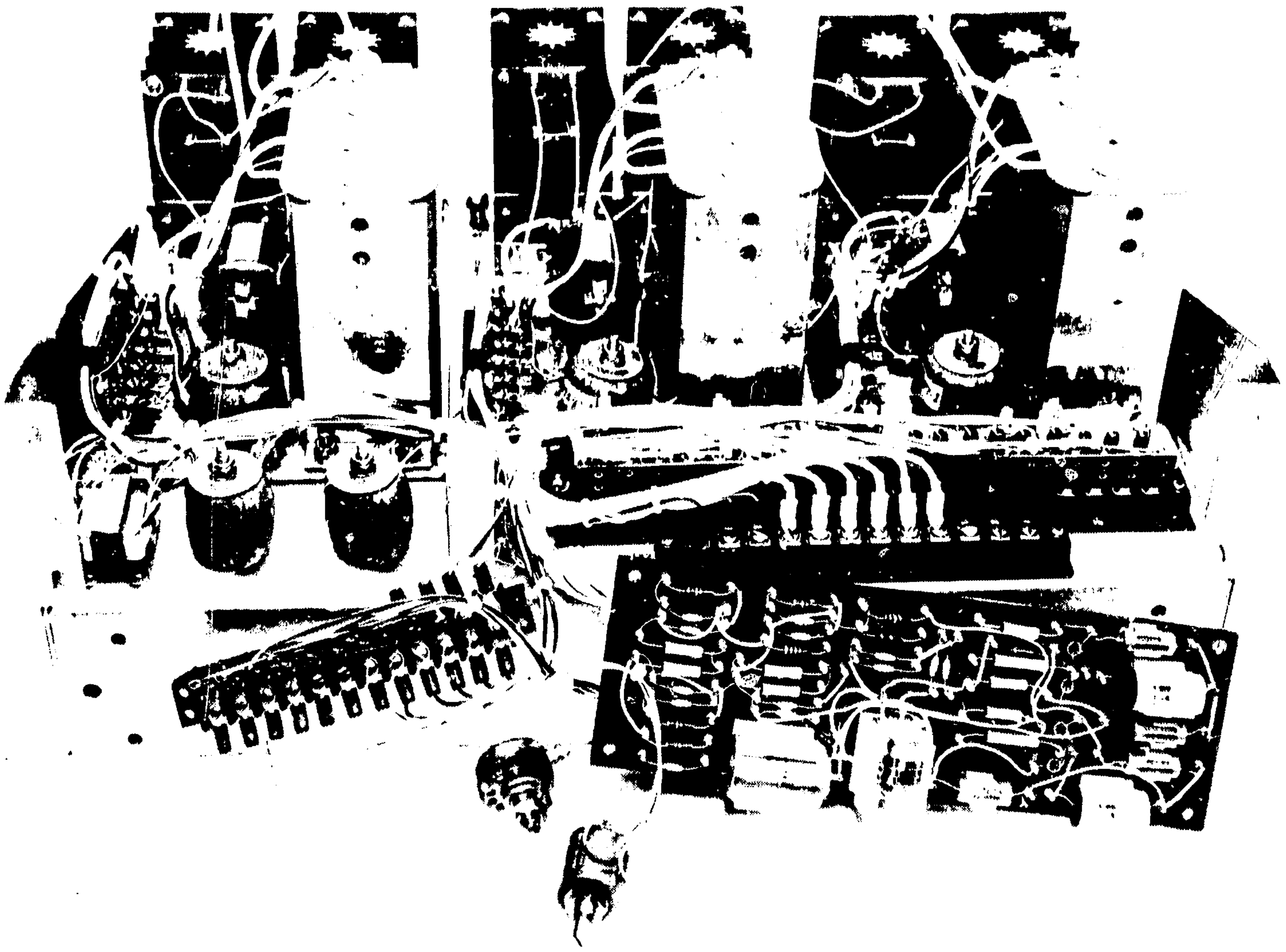

BRU SPEED-CONTROL SUBASSEMBLY
FRONT VIEW

FIGURE 5-6

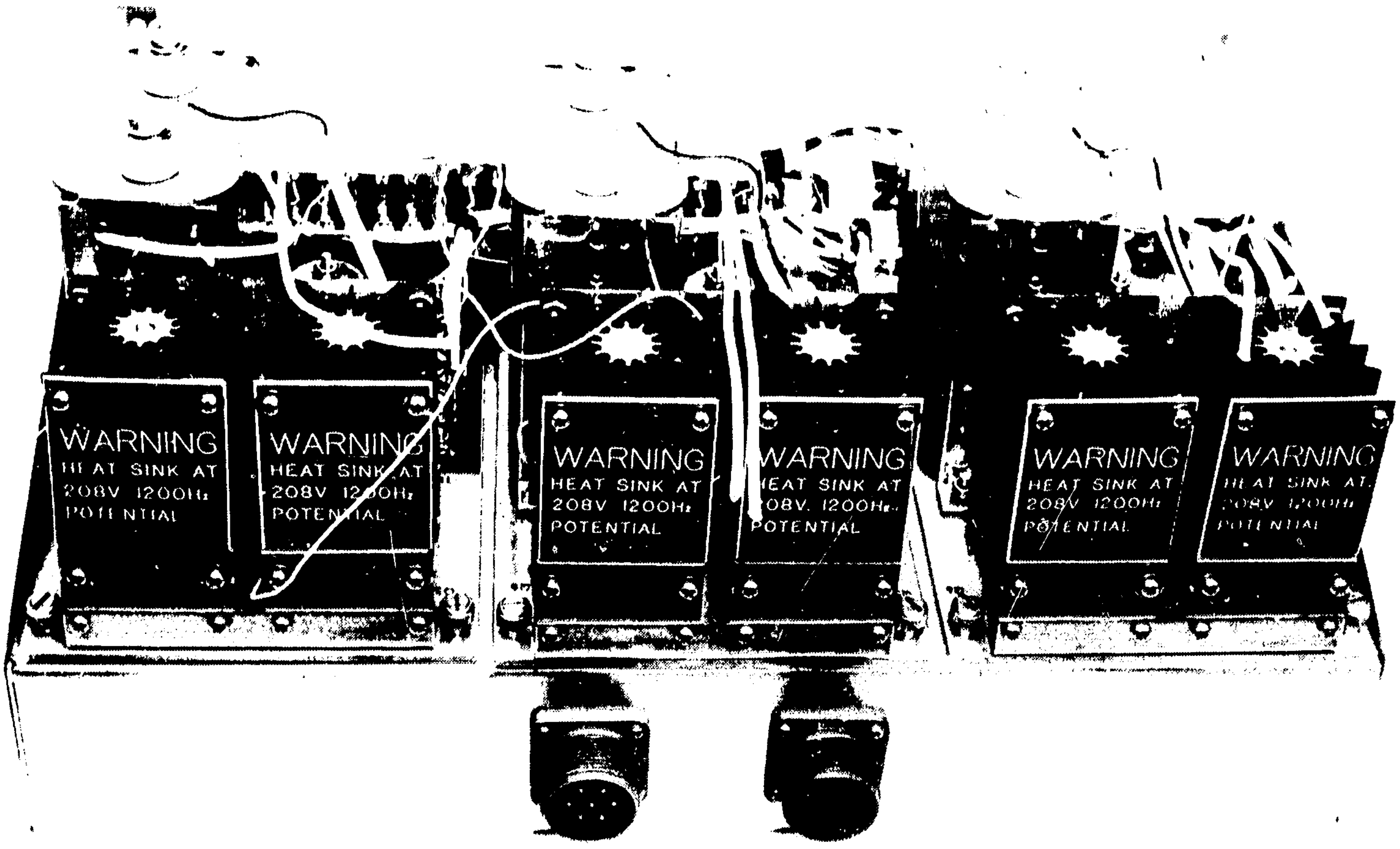

BRU SPEED-CONTROL SUBASSEMBLY
REAR VIEW

FIGURE 5-7

6.0 SYSTEMS ANALYSIS

An analog study was performed to determine the transient characteristics and stability margins for the NASA BRU components; namely, turbine, compressor, and alternator. The study included the VRE and speed controller performance characteristics.

The compressor and turbine maps which were incorporated in the analog simulation are also employed with the AiResearch, Phoenix system start-up analysis programmed for the digital computer. These maps represent the predicted aerodynamic performance of both components. The speed-control transfer functions were obtained by analytical and experimental methods. Transfer functions and constraints representing the alternator with VRE were derived, and equivalent circuits were generated which described the combined alternator and VRE dynamic response for this application. This analysis is included in Appendix VII.

7.0 CONCLUSION

The electrical components designed and fabricated by the AiResearch Manufacturing Company are satisfactory for use in a 1200-Hz Brayton energy conversion system. The alternator delivers design output for all specified operating conditions by 1-p.u. load, 2-p.u. load, and 3-p.u. short circuit. The alternator is suitable for application in a gas bearing system. The electrical control packages enable the system output to remain within the design tolerances regarding voltage regulation, speed regulation, voltage and speed recovery times, and short-circuit operation.

The operating mode of the speed controller generates additional voltage harmonics on the system and will require further analysis. The voltage regulator and speed controllers interact when operating in a system; this will be analyzed further.

AIRESEARCH MANUFACTURING COMPANY OF ARIZONA
A DIVISION OF THE GARRETT CORPORATION

APPENDIX I

GLOSSARY OF TERMS AND SYMBOLS

(7 pages)

GLOSSARY OF TERMS AND SYMBOLS

A_c	Core area
a-c	Alternating current
AG	Auxiliary flux gap
ARP	Alternator Research Package
BA_c	Flux density in the core area
B_M	Flux density - kilogauss
BRU	Brayton rotating unit
B_S	Flux saturation
C	Capacitance
c.g.	Center of gravity
cm	centimeters
C.T.	Current transformer
d-c	Direct current
E	Electromagnetic force - volts
e	Incremental voltage
E_B	Feedback d-c level
e_B	Feedback signal
E_{FF}	Field forcing voltage
E.M.	Electromagnetic
EMI	Electromagnetic interference
(ET)	Transformer voltage
$(ET)_c$	Core volt seconds

GLOSSARY OF TERMS AND SYMBOLS (Contd.)

F	Magnetic force
°F	Degrees Fahrenheit
f	Frequency-hertz
Fg	Main flux gap
f_g	Gate frequency
FH	Shunt field
FR	Series field
$F_{(s)}$	Feedback signal - see e_B
F_{ss}	Magnetic force - no rotation
ft.	foot
H	HiRel rating
H_c	Coercive force - oersteds
H_{FE}	d-c base input voltage; common emitter
hr.	Hour
Hz	Hertz
I	Current-amperes
i	Incremental current
I_B	Base current
I_C	Collector current
in.	Inch
I_L	Load current
I_p	Polar moment of inertia
i_s	Pulse current from power supply
$I_{sh.c}$	Short circuit current

GLOSSARY OF TERMS AND SYMBOLS (Contd.)

j	Vector
K	Gain or proportionality constant
ksi	Thousand pounds per square inch
KVA	Thousand volt amperes
KW	Kilowatts
L	Inductance
ℓ	Mean magnetic length of core-centimeters
lbs.	Pounds
m	Mass
ma	Milliamps
min.	Minutes
mm	Millimeter
MMF	Magnetomotive force
MTBF	Mean time between failure
MTU	Electromagnetic test unit
mv	Millivolt
mW	Milliwatts
n	Speed perturbations
N	Number of turns
Ng	Number of gate turns
NI	Number of ampere turns
Np	Number of primary turns
$N\sqrt{\theta}$	Corrected speed

GLOSSARY OF TERMS AND SYMBOLS (Contd.)

P	Spacecraft preferred components
P_a	Actual operating power
P_D	Power dissipation
pf	Power factor
pF	Picofarad
P_J	Junction power rating
pk	Peak
P_p	Parasitic load (KW)
P-P	Peak-to-peak
ppi	Pounds per inch
P_r	Rated power
psi	Pounds per square inch
psia	Pounds per square inch absolute
p.u.	Per unit
Q	Charge in coulombs
Qc	Corrected torque
R	Resistance - ohms
r	ripple
RMS	Root mean square
rpm	Revolutions per minute
°R	Degrees Rankine

GLOSSARY OF TERMS AND SYMBOLS (Contd.)

S	Laplace Operator (sec^{-1})
sat.	Saturation
SCR	Silicon controlled rectifier
sec.	Second
sq. in.	Square inch
T	Turns (Page 4-2)
T	Time
T	Total
t	Incremental time
T_A	Ambient temperature
T_C	Case temperature
T_c	Capacitor time constant
T_d	Junction temperature at which component derating begins
T_J	Junction temperature
Tjm	Maximum allowable junction temperature
T_R	Rated temperature rise
T_s	Sink temperature
V	Qualified vendor rating (Table 5-1)
V	Volts
VA	Volt amps
V_a	Actual operating voltage
VAC	Volts alternating current (RMS)
V_{BB}	Base-to-base voltage

TABLE 5-5

SPEED CONTROL DRAWINGS (BREADBOARD UNIT)

Drawing No.	Title
303749	Terminal Board Assembly
303750	Terminal Board Assembly Electrical
303751	Terminal Board Assembly
303752	Terminal Board Assembly Electrical
303753	Electronic Component Mounting Plate
303754	Module Assembly (Firing Circuit)
303755	Instrument Panel Assembly
303756	Chassis Assembly
303757	Air Blower Inlet
303758	Instruction - Warning - Plate
305444	System Outline
305445	Control Assembly
305506	Control Outline
43534	Schematic Wiring Diagram
43574	Wiring Diagram (Pictorial)
43577	System Wiring Diagram

GLOSSARY OF TERMS AND SYMBOLS (Contd.)

V_{BE}	Base-to-emitter voltage
V_{CE}	Collector-to-emitter voltage
V_{L-L}	Volts line-to-line (RMS)
VRE	Voltage regulator exciter
V_r	Rated voltage
V_S	Bridge supply voltage
V_Z	Zener reference voltage
W	Watts
W_a	Window area
$W\sqrt{\theta}/\delta$	Corrected weight flow
X_C	Capacitive reactance
X_L	Inductive reactance
X_1	Armature winding leakage reactance
X_2	Negative sequence reactance
Z	Impedance
Z_a	Armature impedance
α	Proportional
β	Transfer function
Δr	Radial displacement of "rotor" - inches
ϵ	Error
Ω	Ohms
ω	3,768 radians per second
ϕ	Flux

GLOSSARY OF TERMS AND SYMBOLS (Contd.)

θ	Angle
μf	Microfarad
ν	Specific heat ratio

AIRESEARCH MANUFACTURING COMPANY OF ARIZONA
A DIVISION OF THE GARRETT CORPORATION

APPENDIX II

DRAWINGS

307594
307595
307596
307597
358498

521246
521247
521258
521259
521260

699650
699651
699652
699667

PART Nº
307594-1

REVISIONS

LTR	DESCRIPTION	DATE	APPROVED
A	ADDED C.T. TO L3 & L4 SEE E.O.	[illegible]	
B	CHANGED DIM. ON BASE PLATE (SEE E.O.)	1-31-67	
C	ADDED POLARITY ON FIG. 2 & (SEE E.O.) CHANGED PAR. 4.10	[illegible]	
D	CHANGED 4.7, L1 (SEE E.O.)	[illegible]	
E	CHANGED 4.7, L1 + 4.20 (SEE E.O.	11/22/67	

D
D
D

See tab block (upper left corner) for PART NUMBER

SHEET INDEX	REVISION LTR	
	SHEET NO.	

SHEET INDEX	REVISION LTR	E	—	—	—	—	E	D	C	A
	SHEET NO.	1	2	3	4	5	6	7	8	9

UNLESS OTHERWISE SPECIFIED ON THIS DRAWING, FABRICATION OF THIS ITEM SHALL BE IN ACCORDANCE WITH AIRESEARCH SPECIFICATION SC-5535, STANDARD DRAWING INTERPRETATIONS

SIGNATURES	DATES
DFT BUSHMAN	11-2-66
CHK	[illegible]
APPD	
APPD	11/21/66
DSGN ACTIVITY	
OTHER ACTIVITY	

AIRESEARCH MANUFACTURING COMPANY
A DIVISION OF THE GARRETT CORPORATION
PHOENIX, ARIZONA

DWG TITLE
TRANSFORMER, POWER

SIZE	CODE IDENT NO.	DWG NO	REV
A	99193	307594	E

SCALE — | WT — | SHEET 1 OF 9

FORM P1807A

BRJ

AFFECTS SHEETS 1 + 6　　　　　ATTACH TO SHEET 1 ONLY

AiResearch Manufacturing Company of Arizona

FORM F25320-2

ENGINEERING ORDER

REVISION　　SHEET 1 OF 1

DRAWING TITLE	TRANSFORMER POWER	DWG NO	307594	CHG LET.	E

TO BE INCORP. IN DRAWING	YES	NO	INCORP. BY	/		DATE	INCORP CHK'D BY				DATE		ADV. CHG. LET.	
MANDATORY		1	DRAWING CHG.	✓	VARIATION		VOID AFTER	DATE			DISTRIBUTION		L.A.	PHX.
PRIORITY		2	ADV. DWG. CHG.		SUBSTITUTION		VOID AFTER	NO. OF PARTS			NORMAL			✓
ROUTINE		3	EMERGENCY DWG.		REWORK		S.I.L.		YES	NO	RUSH			
MINOR		4	E.C.P. NO.		MATL. REV. ACT.		SERVICE BULLETIN		YES	NO	TELETYPE			

ZONE	LET. SUB	TYPE CHG.	DESCRIPTION	SPARE PARTS CODE	AUTHORITY	DISPOSITION OF AFFECTED PART
			SHEET 6		ENG	
			PARA. 4.7　WAS 800 HZ			
			PARA 4.20　WAS 120 RMS VOLTS 500 HZ ---			
			--- EXCITATION CURRENT SHALL			
			BE 8 MA RMS MAX			

NEXT ASSY.	MODEL NO.	M.E.O.	OUTLINE
			305506-1

EFFECTIVITY INSTRUCTIONS

UNDELIVERED ITEMS

DELIVERED ITEMS

PARTS LIST CHANGE ONLY　NO EFFECT ON MODEL NO

COORDINATED BY [illegible]　DATE 11/2/67

REASON FOR CHANGE FACILITATE MANUFACTURE BY VENDOR

REQUESTED BY	DATE	PREPARED BY	DATE	CHECKED BY	DATE	APPROVED BY	DATE
WORCESTER	11/2/67	Heiseman	11/2/67	Heiseman	11/2/67	[illegible]	11-2-67

NOTE: A LINE DRAWN THROUGH ANY REQUIREMENT SHOWN ON THIS DRAWING INDICATES NO REQUIREMENT

1. GENERAL NOTES

1.1 PROCUREMENT SOURCE(S) PER ASL 307594 .

1.2 PART TO BE PERMANENTLY MARKED WITH AIRESEARCH PART NO. 307594-1 .

1.3 ALL DESIGN AND PART NO. CHANGES REQUIRE PRIOR AIRESEARCH APPROVAL.

1.4 ONLY THE ITEMS LISTED ON THIS DRAWING AND IDENTIFIED BY VENDORS NAMES, ADDRESSES, AND PART NO. ON ASL 307594 HAVE BEEN TESTED AND APPROVED FOR USE IN THE END UNIT. A SUBSTITUTE PART SHALL NOT BE USED WITHOUT PRIOR TESTING AND APPROVAL BY AIRESEARCH.

1.5 IDENTIFY PACKAGING WITH AIRESEARCH PART NO. 307594-1 .

1.6 PARTS PROCURED BY VENDOR PART NO. SHALL BE PROCURED IN ACCORDANCE WITH THIS AIRESEARCH SOURCE CONTROL DRAWING AND ASL 307594 .

1.7 MARKING REQUIREMENTS.

1.7.1 MARKINGS TO BE PER MIL-T-27 PARA. 3.20 AS APPLICABLE.

1.7.2 MARKING TO BE LOCATED AS SHOWN IN FIGURE 1.

1.7.3 MARKINGS TO BE A MINIMUM OF .031 INCH FROM ANY CORNER, TERMINAL OR EDGE UNLESS OTHERWISE SPECIFIED.

1.7.4 HEIGHT OF MARKINGS SHALL BE A MINIMUM OF .12 INCH UNLESS OTHERWISE NOTED.

1.7.5 (1) MARKINGS TO BE PER MIL-STD-130 EXCEPT ACID ETCHING AND BRANDING NOT PERMITTED.
(2) OTHER

1.7.6 MARKINGS TO BE OF A CONTRASTING COLOR.

1.7.7 INK TO BE PER TT-I-558 AS APPLICABLE.

1.7.8 MARKINGS TO BE COVERED WITH ONE COAT OF CLEAR EPOXY AS APPLICABLE.

1.8 DETAILS OF DESIGN AND CONSTRUCTION OTHER THAN SHOWN SHALL BE AT THE OPTION OF THE VENDOR.

SEE SHEET 1 FOR CONTROLLING REV LTR

SIZE	CODE IDENT NO	DWG NO.	REV LTR
A	99193	307594	–
SCALE –		WT –	SHEET 2

1.9 (1) VACUUM IMPREGNATE WOUND BOBBIN WITH EPOXY CL F - DIP
COAT ENTIRE ASSEMBLY WITH EPOXY
(2) OTHER

1.10 SOLDER PER MIL-S-6872 USING QQ-S-571 COMP SN60 SOLDER.

1.11 ________ AS SHOWN WITH ________. IF CUP OR BOX IS USED MATERIAL TO BE PER ________.

1.12 TOP ________ OF TERMINALS TO BE FREE AND CLEAR OF POTTING COMPOUND FOR EXTERNAL WIRES.

1.13 DUTY CYCLE: (1) CONTINUOUS ~~(2) OTHER~~

1.14 OTHER

2. PHYSICAL CONSTRUCTION REQUIREMENTS

2.1 CORE: NO. REQ'D 1 SEE PARA. ________
(1) PART NO. EI-27-6H MFG. BY MAGNETICS INC
BUTLER PA.
(2) PART NO. ________ MFG. BY ________
(3) PART NO. ________ MFG. BY ________

2.2 * WRAP CORE(S) WITH ________

2.3 * WIND EACH CORE WITH GATE WINDING. SECTOR ________°.

2.4 ** PLACE WOUND CORES TOGETHER AND WIND ON CONTROL WINDINGS.

2.5 WINDING SEQUENCE L1, L2, L3, L4, L5 & L6

* DEVICES WITH WINDINGS WRAPPED DIRECTLY ON CORE ONLY
** SATURABLE MULTICORE DEVICES ONLY

SEE SHEET 1 FOR CONTROLLING REV LTR

SIZE	CODE IDENT NO.	DWG NO.	REV LTR
A	99193	307594	–
SCALE –		WT –	SHEET 3

2.6 WIRE INSULATION SHALL BE IN ACCORDANCE WITH MIL-T-27 AND BE SUFFICIENT TO WITHSTAND VOLTAGES LISTED IN PARAGRAPH 4.

2.7 UNLESS OTHERWISE SPECIFIED ON THIS DRAWING, FABRICATION OF THIS ITEM SHALL BE IN ACCORDANCE WITH AIRESEARCH SPECIFICATION SC-5535, STANDARD DRAWING INTERPRETATIONS.

3. SPECIFICATIONS

3.1 CLASSIFICATION: TYPE TF5SX03ZZ PER MIL-T-27 EXCEPT AS NOTED IN PARAGRAPH 3.1.1.

3.1.1

3.2 INSULATION RESISTANCE PER MIL-T-27, PARA. 3.10. MEASURE USING A D-C SOURCE OF 1000 VOLTS, WINDING TO NORMAL MOUNTING MEANS 1000 MEGOHMS, WINDING TO WINDING 1000 MEGOHMS.

3.3 MAXIMUM WORKING VOLTAGE 120 V RMS.

3.3.1 DIELECTRIC STRENGTH PER MIL-T-27 PARA. 4.7.5. TEST BY APPLYING 500 RMS VOLTS AT 60 Hz ~~CPS~~ FOR 5 SECONDS BETWEEN WINDINGS AND BETWEEN EACH WINDING AND THE BASE OR NORMAL MOUNTING MEANS.

3.4 TEMPERATURE RISE PER MIL-T-27 PARA. 4.7.10. MAX TEMPERATURE RISE 30°C OPERATING AT AN AMBIENT TEMPERATURE OF 85 °C.

3.5 MAXIMUM OPERATING ALTITUDE 80,000 FEET.

3.6 ENVIRONMENTAL REQUIREMENTS:

~~3.6.1~~ MOISTURE RESISTANCE:
(1) MIL-T-27 PARA. 4.7.11.4
(2) OTHER

~~3.6.2~~ SALT SPRAY:
(1) MIL-E-5272 PROCEDURE__________
(2) OTHER

~~3.6.3~~ VIBRATION REQUIREMENTS:
(1) MIL-T-27 PARA. 4.7.12
(2) OTHER

SEE SHEET 1 FOR CONTROLLING REV LTR

SIZE A	CODE IDENT NO. 99193	DWG NO. 307594	REV — LTR
SCALE —	WT —	SHEET 4	

3.6.4 SHOCK REQUIREMENTS:
(1) MIL-T-27 PARA. 4.7.13
(2) OTHER

3.6.5 AMBIENT TEMPERATURE RANGE:
(1) OPERATING -55 °C MIN, 70 °C MAX.
(2) NON OPERATING -55 °C MIN, 70 °C MAX.
(3) OTHER

3.7 LIFE:

3.7.1 OPERATING: 1000 HOURS AT 85 °C WITH POWER APPLIED PER PARA. 4.6.

3.7.2 STORAGE: 5 YEARS AT 50 °C AND 50 % RELATIVE HUMIDITY.

3.8 ALLOW UNIT TO STABILIZE TO ROOM TEMPERATURE BEFORE EXPOSING TO OPPOSITE TEMPERATURE EXTREME.

3.9 OTHER

SEE SHEET 1 FOR CONTROLLING REV LTR

SIZE	CODE IDENT NO.	DWG NO.	REV
A	99193	307594	– LTR
SCALE –		WT –	SHEET 5

4. ELECTRICAL REQUIREMENTS (SEE FIGURE 2)

	WINDINGS	L1	L2	L3	L4	L5	L6	L7	L8	L9	L10	L11	L12	L13
4.1	WIRE GAGE NO. (AWG)	33	32	34	34	38	38							
4.2	NO. OF TURNS (SEE 4.12)	411	206	140	140	52	52							
4.3	WINDING TOLERANCE (TURNS)	±2	±2	±1	±1	±1	±1							
4.4	MAX D.C. RESISTANCE (OHMS)	18	7	10	10	9	9							
4.5	WORKING VOLTAGE TO GROUND	120	60	20	20	15	15							
4.6	RATED VOLTAGE (RMS)	120	60	40	40	15	15							
4.7	FREQUENCY ~~(CPS)~~ Hz.	1200	-	-	-	-	-							
4.8	FREQUENCY TOLERANCE (CPS)	-	-	-	-	-	-							
4.9	OPERATING POWER LEVEL (WATTS)	6	3.9	.80	.80	.15	.15							
*4.10	MAX CONTROL CURRENT (AMPS)													
4.11	RATED CURRENT (AMPS)	.05	.065	.04	.04	.01	.01							
4.12	CENTER TAP @ TURNS			70	70									
4.13														
4.14														
4.15														
4.16														
4.17														
4.18														
4.19														

4.20 SELF INDUCTION: WITH 120 RMS VOLTS/200 ~~CPS~~ APPLIED ACROSS L1, THE RESULTING EXCITATION CURRENT SHALL BE 10 MA RMS MAX.

~~*4.21~~ CORES TO BE MATCHED TO ____% FOR BIAS AND ____% FOR GAIN USING AIEE TEST PROCEDURE FOR TOROIDAL MAGNETIC AMPLIFIER CORES NO.________.

4.22 ALL ELECTRICAL REQUIREMENTS ARE TO BE MET AT AN AMBIENT OF 25 °C.

*SATURABLE MULTICORE DEVICES ONLY

SEE SHEET 1 FOR CONTROLLING REV LTR

SIZE	CODE IDENT NO.	DWG NO.	REV LTR
A	99193	307594	E
SCALE –		WT –	SHEET 6

PHYSICAL SIZE
FIGURE 1

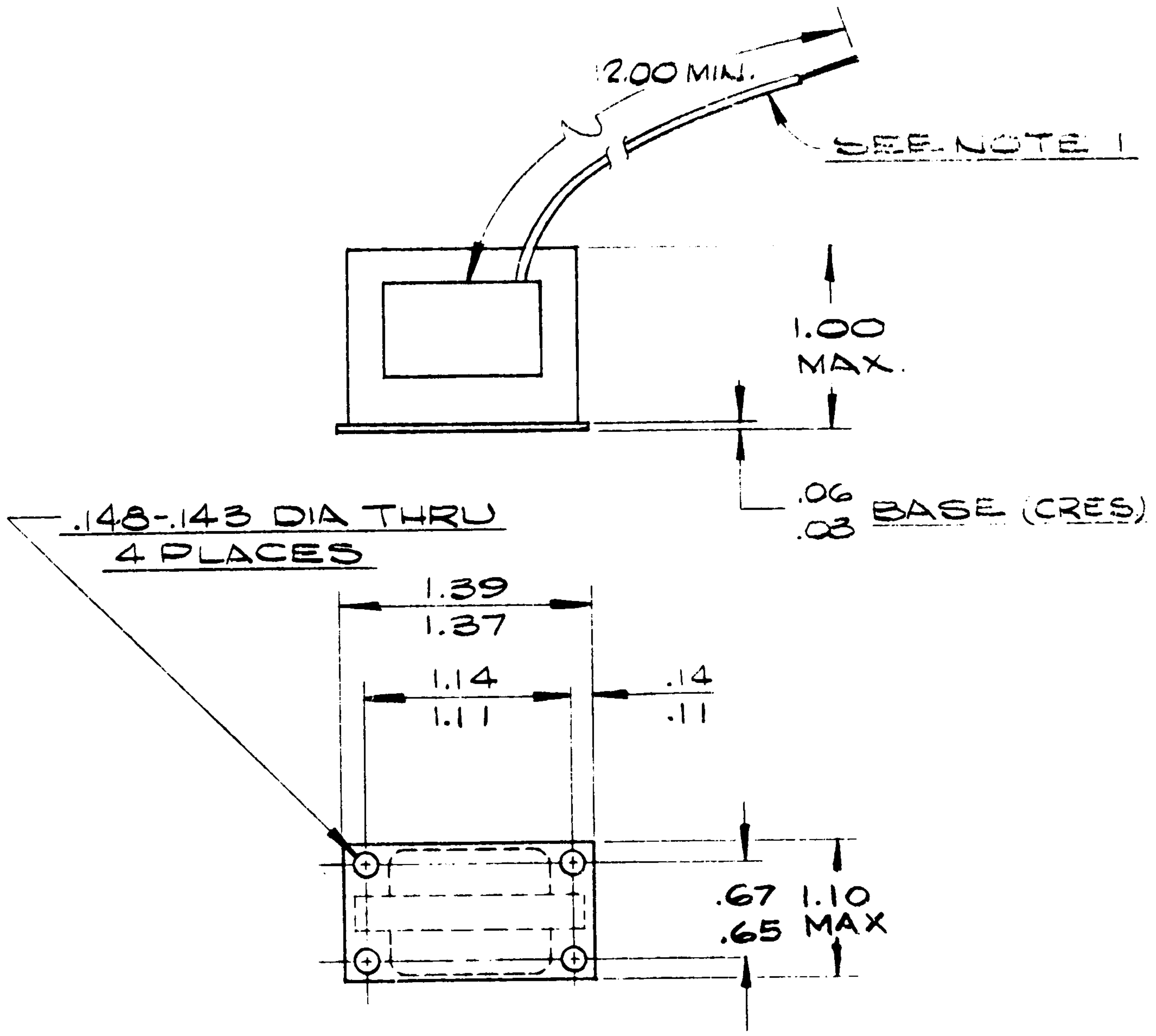

2. MOUNTING HOLE LOCATIONS ARE TO BE AS SHOWN. OTHER DIMENSIONS AND OUTLINE CONFIGURATION ARE MAXIMUM ALLOWABLE AND ARE NOT INTENDED TO DEFINE ACTUAL PHYSICAL SHAPE. PHYSICAL PACKAGE IS TO BE AS SMALL AS PRACTICAL WITHIN LIMITS SPECIFIED.

1. LEAD WIRE TO BE Nº 24 AWG PER MIL-W-16878 TYPE E EXCEPT 19 STRAND. LEAD COLOR CODING PER SCHEMATIC (FIG 2). LEAD ENDS TO BE STRIPPED 3/8 INCH AND TINNED.

SEE SHEET 1 FOR CONTROLLING REV LTR

NOTES:

SIZE A	CODE IDENT NO. 99193	DWG NO. 307594	REV D LTR
SCALE FULL		WT -	SHEET 7

FORM P1807-1A

SCHEMATIC DIAGRAM

FIGURE 2

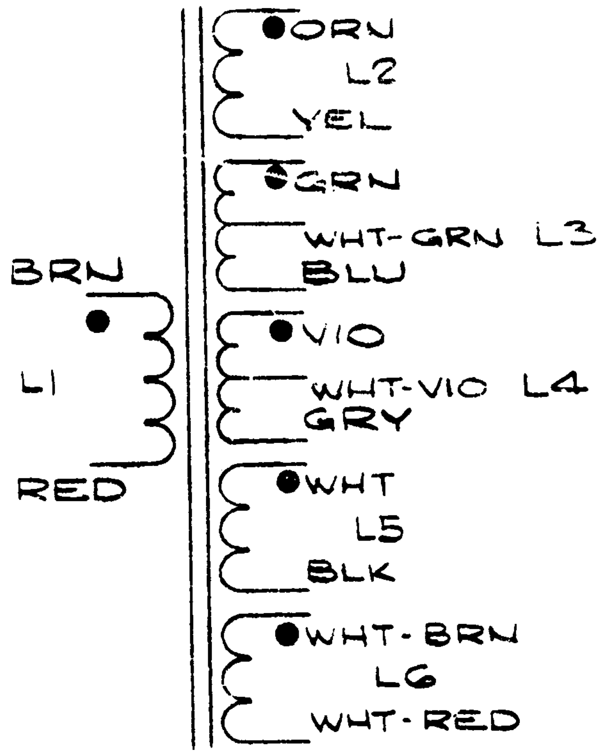

● TERMINALS TO BE OF SAME POLARITY

WINDINGS		TERMINAL FROM	TERMINAL TO
411 TURNS	L1	BRN	RED
206 TURNS	L2	ORN	YEL
140 TURN C.T.@70	L3	GRN C.T. WHT-GRN	BLU
140 TURN C.T.@70	L4	VIO C.T. WHT-VIO	GRY
52 TURNS	L5	WHT	BLK
52 TURNS	L6	WHT-BRN	WHT/RED
	L7		
	L8		
	L9		
	L10		
	L11		
	L12		
	L13		

TEST CIRCUIT & INSPECTION INFORMATION

FIGURE 3

SEE SHEET 1 FOR CONTROLLING REV LTR

SIZE	CODE IDENT NO.	DWG NO.	REV LTR
A	99193	307594	[illegible]
SCALE —		WT —	SHEET 8

TEST CIRCUIT & INSPECTION INFORMATION
FIGURE 3

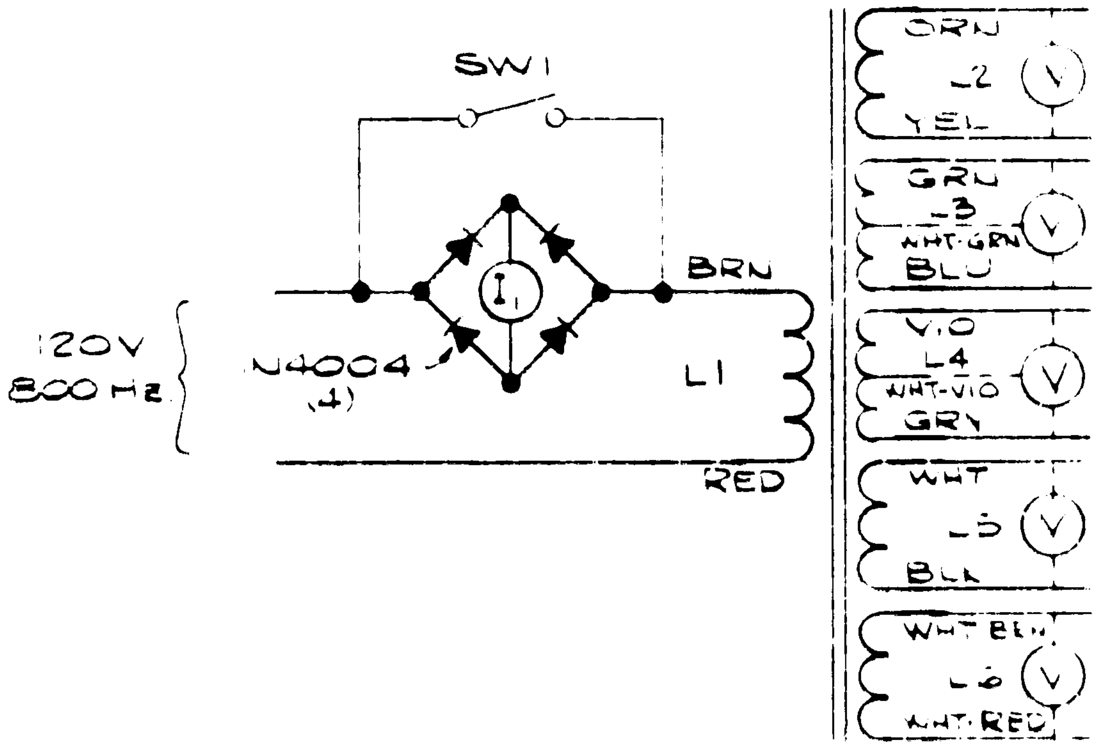

EXCITATION:

WITH ALL SECONDARY WINDINGS OPEN, 120VRMS 800 HZ CONNECTED AS SHOWN AND

A: SW1 OPEN; I1 WILL READ LESS THAN 8 MADC.

B: SW1 CLOSED; THE FOLLOWING VOLTAGES SHALL BE MEASURED:

WINDING	VRMS
L2	60 ± 3
L3	40 ± 3 WITH 20 ± 2 TO CT
L4	40 ± 3 WITH 20 ± 2 TO CT
L5	15 ± 2
L6	15 ± 2

SEE SHEET 1 FOR CONTROLLING REV LTR

SIZE	CODE IDENT NO	DWG NO.	REV LTR
A	99193	307394	L
SCALE –		WT –	SHEET 9

PART NO
307595-1

REVISIONS

LTR	DESCRIPTION	DATE	APPROVED
A	REVISED TEST CKT SEE	[illegible]	[illegible]
B	REVISED TEST CKT SEE EO	[illegible]	[illegible]

See tab block (upper left corner) for PART NUMBER

SHEET INDEX										
	REVISION LTR									
	SHEET NO									

SHEET INDEX										
	REVISION LTR	B	-	-	-	-	-	-	B	-
	SHEET NO	1	2	3	4	5	6	7	8	9

UNLESS OTHERWISE SPECIFIED ON THIS DRAWING, FABRICATION OF THIS ITEM SHALL BE IN ACCORDANCE WITH AIRESEARCH SPECIFICATION SC-5535, STANDARD DRAWING INTERPRETATIONS

SIGNATURES	DATES
DFT BUSHMAN	11 21 66
CHK	[illegible]
APPD	
APPD	[illegible]
DSGN ACTIVITY	
OTHER ACTIVITY	

AIRESEARCH MANUFACTURING COMPANY
A DIVISION OF THE GARRETT CORPORATION
PHOENIX ARIZONA

DWG TITLE
REACTOR, SATURABLE

SIZE	CODE IDENT NO	DWG NO.	REV LTR
A	99193	**307595**	B

SCALE — WT — SHEET 1 OF 9

FORM P1807A

BRU

NOTE: A LINE DRAWN THROUGH ANY REQUIREMENT SHOWN ON THIS DRAWING INDICATES NO REQUIREMENT

1. GENERAL NOTES

1.1 PROCUREMENT SOURCE(S) PER ASL 307595.

1.2 PART TO BE PERMANENTLY MARKED WITH AIRESEARCH PART NO. 307595-.

1.3 ALL DESIGN AND PART NO. CHANGES REQUIRE PRIOR AIRESEARCH APPROVAL.

1.4 ONLY THE ITEMS LISTED ON THIS DRAWING AND IDENTIFIED BY VENDORS NAMES, ADDRESSES, AND PART NO. ON ASL 307595 HAVE BEEN TESTED AND APPROVED FOR USE IN THE END UNIT. A SUBSTITUTE PART SHALL NOT BE USED WITHOUT PRIOR TESTING AND APPROVAL BY AIRESEARCH.

1.5 IDENTIFY PACKAGING WITH AIRESEARCH PART NO. 307595-1.

1.6 PARTS PROCURED BY VENDOR PART NO. SHALL BE PROCURED IN ACCORDANCE WITH THIS AIRESEARCH SOURCE CONTROL DRAWING AND ASL 307595.

1.7 MARKING REQUIREMENTS.

1.7.1 MARKINGS TO BE PER MIL-T-27 PARA. 3.20 AS APPLICABLE.

1.7.2 MARKING TO BE LOCATED AS SHOWN IN FIGURE 1.

1.7.3 MARKINGS TO BE A MINIMUM OF .031 INCH FROM ANY CORNER, TERMINAL OR EDGE UNLESS OTHERWISE SPECIFIED.

1.7.4 HEIGHT OF MARKINGS SHALL BE A MINIMUM OF .12 INCH UNLESS OTHERWISE NOTED.

1.7.5 (1) MARKINGS TO BE PER MIL-STD-130 EXCEPT ACID ETCHING AND BRANDING NOT PERMITTED.
(2) OTHER

1.7.6 MARKINGS TO BE OF A CONTRASTING COLOR.

1.7.7 INK TO BE PER TT-I-558 AS APPLICABLE.

1.7.8 MARKINGS TO BE COVERED WITH ONE COAT OF CLEAR EPOXY AS APPLICABLE.

1.8 DETAILS OF DESIGN AND CONSTRUCTION OTHER THAN SHOWN SHALL BE AT THE OPTION OF THE VENDOR.

SEE SHEET 1 FOR CONTROLLING REV LTR

SIZE	CODE IDENT NO	DWG NO.	REV LTR
A	99193	307595	—
SCALE —		WT —	SHEET 2

~~1.9~~ ~~(1) VACUUM IMPREGNATE~~ ______ ~~WITH~~ ______
DIP COAT COMPLETE UNIT WITH EPOXY
(2) OTHER

1.10 SOLDER PER MIL-S-6872 USING COMP SN60 PER QQ S 571 SOLDER.

~~1.11~~ ______ AS SHOWN WITH ______. IF CUP OR BOX IS USED MATERIAL TO BE PER ______.

~~1.12~~ TOP ______ OF TERMINALS TO BE FREE AND CLEAR OF POTTING COMPOUND FOR EXTERNAL WIRES.

1.13 DUTY CYCLE: (1) CONTINUOUS ~~(2) OTHER~~

~~1.14~~ OTHER

2. PHYSICAL CONSTRUCTION REQUIREMENTS

2.1 CORE: NO. REQ'D 4 SEE PARA. 4.21
(1) PART NO. 52002-2D MFG. BY MAGNETICS INC.
BUTLER PA.
(2) PART NO. ______ MFG. BY ______
(3) PART NO. ______ MFG. BY ______

~~2.2 * WRAP CORE(S) WITH~~ ______

2.3 * WIND EACH CORE WITH GATE WINDING. SECTOR 360°.

2.4 ** PLACE WOUND CORES TOGETHER AND WIND ON CONTROL WINDINGS.

2.5 WINDING SEQUENCE L1, L2, L3, L4, L5

* DEVICES WITH WINDINGS WRAPPED DIRECTLY ON CORE ONLY
** SATURABLE MULTICORE DEVICES ONLY

SEE SHEET 1 FOR CONTROLLING REV LTR

SIZE	CODE IDENT NO.	DWG NO.	REV
A	99193	307595	— LTR
SCALE —	WT —	SHEET 3	

FORM P18C7-3A

2.6 WIRE INSULATION SHALL BE IN ACCORDANCE WITH MIL-T-27 AND BE SUFFICIENT TO WITHSTAND VOLTAGES LISTED IN PARAGRAPH 4.

2.7 UNLESS OTHERWISE SPECIFIED ON THIS DRAWING, FABRICATION OF THIS ITEM SHALL BE IN ACCORDANCE WITH AIRESEARCH SPECIFICATION SC-5535, STANDARD DRAWING INTERPRETATIONS.

3. SPECIFICATIONS

3.1 CLASSIFICATION: TYPE TF5SX40ZZ PER MIL-T-27 EXCEPT AS NOTED IN PARAGRAPH 3.1.1.

3.1.1

3.2 INSULATION RESISTANCE PER MIL-T-27, PARA. 3.10. MEASURE USING A D-C SOURCE OF 1000 VOLTS. ~~WINDING TO NORMAL MOUNTING MEANS ________ MEGOHMS~~, WINDING TO WINDING 1000 MEGOHMS.

3.3 MAXIMUM WORKING VOLTAGE 10 VRMS.

3.3.1 DIELECTRIC STRENGTH PER MIL-T-27 PARA. 4.7.5. TEST BY APPLYING 500 RMS VOLTS AT 60 Hz ~~CPS~~ FOR 5 SECONDS BETWEEN WINDINGS AND BETWEEN EACH WINDING AND THE BASE OR NORMAL MOUNTING MEANS.

3.4 TEMPERATURE RISE PER MIL-T-27 PARA. 4.7.10. MAX TEMPERATURE RISE 30° OPERATING AT AN AMBIENT TEMPERATURE OF 85°.

3.5 MAXIMUM OPERATING ALTITUDE 80000 FEET.

3.6 ENVIRONMENTAL REQUIREMENTS:

~~3.6.1~~ MOISTURE RESISTANCE:
(1) MIL-T-27 PARA. 4.7.11.4
(2) OTHER

~~3.6.2~~ SALT SPRAY:
(1) MIL-E-5272 PROCEDURE ________
(2) OTHER

~~3.6.3~~ VIBRATION REQUIREMENTS:
(1) MIL-T-27 PARA. 4.7.12
(2) OTHER

SEE SHEET 1 FOR CONTROLLING REV LTR

SIZE	CODE IDENT NO.	DWG NO.	REV
A	99193	307595	– LTR
SCALE –		WT –	SHEET 4

3.6.4 SHOCK REQUIREMENTS:
(1) MIL-T-27 PARA. 4.7.13
~~(2) OTHER~~

3.6.5 AMBIENT TEMPERATURE RANGE:
(1) OPERATING -55 °C MIN, 70 °C MAX.
(2) NON OPERATING -55 °C MIN, 70 °C MAX.
(3) OTHER

3.7 LIFE:

3.7.1 OPERATING: 10,000 HOURS AT 85 °C WITH POWER APPLIED PER PARA. 4.6.

3.7.2 STORAGE: 5 YEARS AT 50 °C AND 50 % RELATIVE HUMIDITY.

3.8 ALLOW UNIT TO STABILIZE TO ROOM TEMPERATURE BEFORE EXPOSING TO OPPOSITE TEMPERATURE EXTREME.

3.9 OTHER

SEE SHEET 1 FOR CONTROLLING REV LTR

SIZE A	CODE IDENT NO. 99193	DWG NO. 307595	REV — LTR
SCALE —		WT —	SHEET 5

FORM P1807-5A

4. ELECTRICAL REQUIREMENTS (SEE FIGURE 2)

	WINDINGS	L1	L2	L3	L4	L5	L6	L7	L8	L9	L10	L11	L12	L13
4.1	WIRE GAGE NO. (AWG)	34	34	34	34	36								
4.2	NO. OF TURNS	670	670	670	670	2000								
4.3	WINDING TOLERANCE (TURNS)	±1	±1	±1	±1	±5								
4.4	MAX D.C. RESISTANCE (OHMS)	22	22	22	22	250								
4.5	WORKING VOLTAGE TO GROUND	20	20	20	20	30								
4.6	RATED VOLTAGE (RMS)	22	20	20	20	—								
4.7	FREQUENCY ~~(CPS)~~ Hz	1200	1200	1200	1200	—								
4.8	FREQUENCY TOLERANCE ~~(CPS)~~ Hz	—	—	—	—	—								
4.9	OPERATING POWER LEVEL (WATTS)	.5	.5	.5	.5	—								
*4.10	MAX CONTROL CURRENT (AMPS)	.015	.015	.015	.015	.015								
4.11	RATED CURRENT (AMPS)	.040	.040	.040	.040	.040								
4.12														
4.13														
4.14														
4.15														
4.16														
4.17														
4.18														
4.19														

4.20 SELF INDUCTION: WITH ______ RMS VOLTS ______ CPS APPLIED ACROSS __________, THE RESULTING EXCITATION CURRENT SHALL BE ______ MA RMS MAX.

*4.21 CORES TO BE MATCHED TO 5 % FOR BIAS AND 10 % FOR GAIN USING AIEE TEST PROCEDURE FOR TOROIDAL MAGNETIC AMPLIFIER CORES NO. 432.

4.22 ALL ELECTRICAL REQUIREMENTS ARE TO BE MET AT AN AMBIENT OF 25°C.

*SATURABLE MULTICORE DEVICES ONLY

SEE SHEET 1 FOR CONTROLLING REV LTR

SIZE	CODE IDENT NO.	DWG NO.	REV LTR
A	99193	307595	-
SCALE -		WT -	SHEET 6

SCHEMATIC DIAGRAM

FIGURE 2

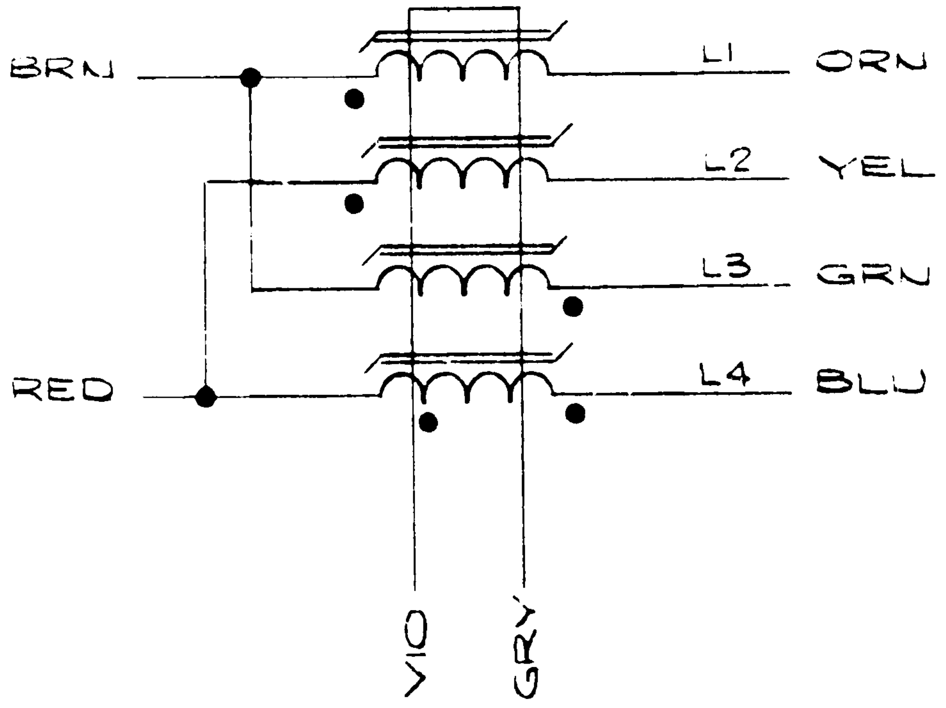

● TERMINALS TO BE OF SAME POLARITY

WINDINGS		TERMINAL	
		FROM	TO
670 T	L1	ORN	BRN
670T	L2	YEL	RED
670T	L3	GRN	BRN
670T	L4	BLU	RED
2000T	L5	VIO	GRY
	L6		
	L7		
	L8		
	L9		
	L10		
	L11		
	L12		
	L13		

~~TEST CIRCUIT & INSPECTION INFORMATION~~

~~FIGURE 3~~

SEE SHEET 1 FOR CONTROLLING REV LTR

SIZE A	CODE IDENT NO. 99193	DWG NO. 307595	REV – LTR
SCALE –		WT –	SHEET 7

TEST CIRCUIT & INSPECTION INFORMATION
FIGURE 3

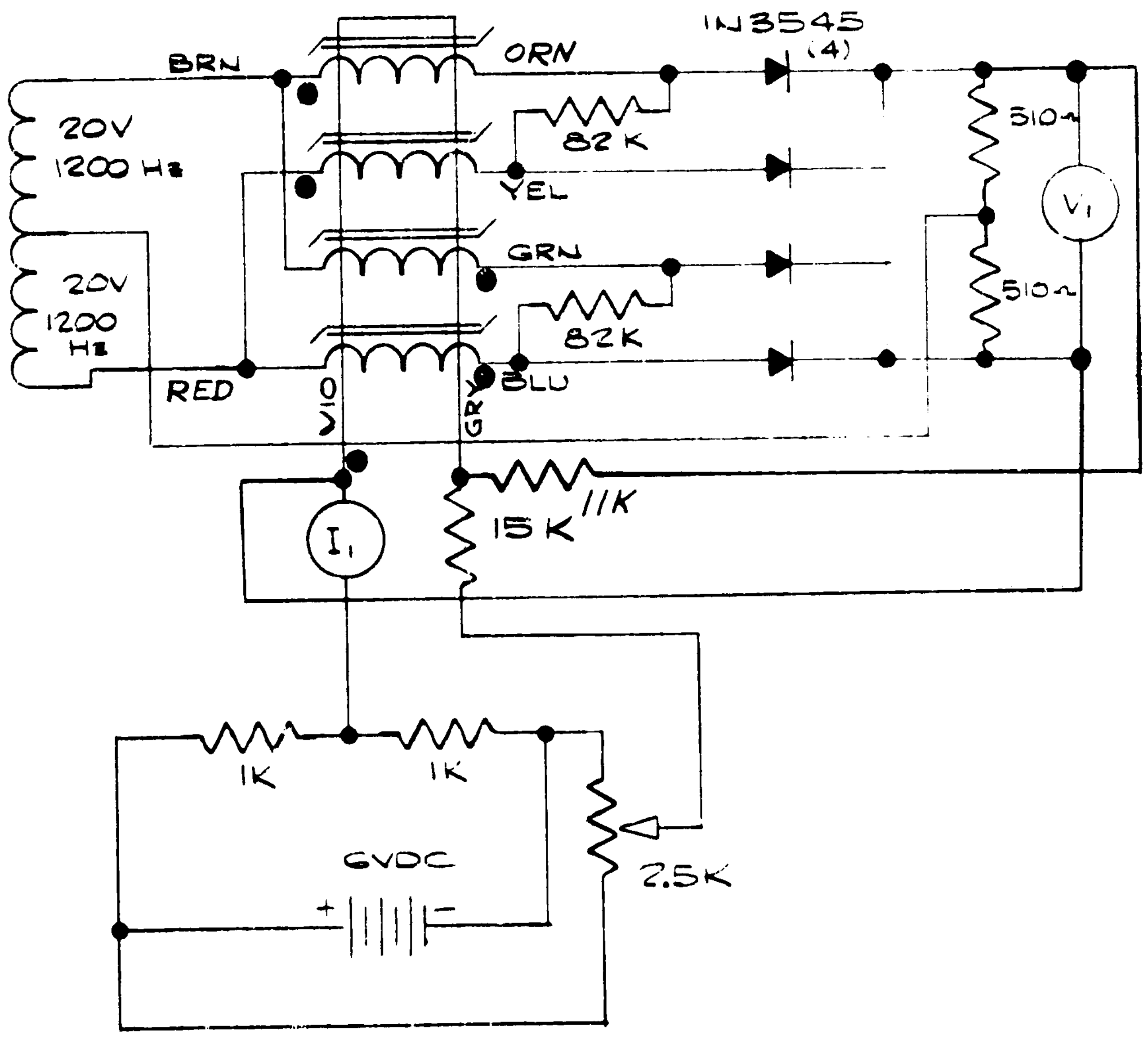

± I_1 MICRO AMP	± V_1 DC. VOLTS
0	0 ±.75
450	5 ±.75
900	10 ±1.0

SEE SHEET 1 FOR CONTROLLING REV LTR

SIZE	CODE IDENT NO.	DWG NO.	REV LTR
A	99193	307595	B
SCALE –		WT –	SHEET 8

A- ADDED 11K, I_1 :54[illegible] -300 WAS 45 [illegible] B REVERSED V_1 LEADS TO CONTROL WINDING

FORM P1807-1A

PHYSICAL SIZE

FIGURE 1

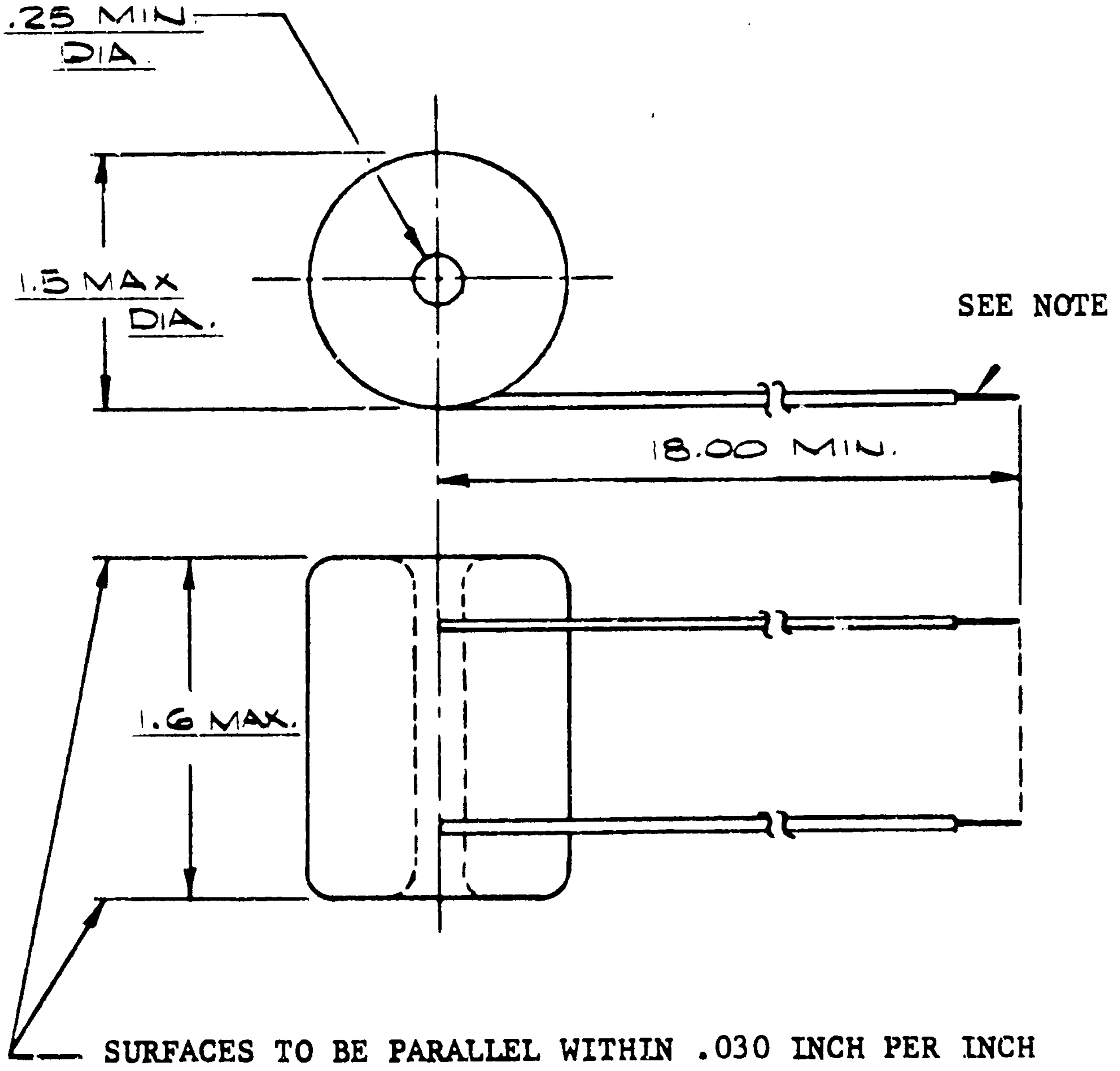

NOTE:

LEAD WIRE TO BE #22 AWG PER MIL-W-16878 TYPE 'E'
EXCEPT 19 STRAND

LEAD COLOR CODING TO BE AS SHOWN IN SCHEMATIC. LEAD ENDS TO BE STRIPPED 3/8 INCH AND TINNED.

SEE SHEET 1 FOR CONTROLLING REV LTR

SIZE	CODE IDENT NO.	DWG NO.		REV LTR
A	99193	307595		—
SCALE NONE		WT —	SHEET 9	

FORM F1807-8A

D

PART NO
307596-1

REVISIONS

LTR	DESCRIPTION	DATE	APPROVED
A	REV. PG.6 PARA 4.2,4.4,4.23 SEE E.O.	1-13-67	
B	REV. PG. 6 PARA 4.2 ,4.23 SEE E.O.	[illegible]	

D

D

See tab block (upper left corner) for PART NUMBER

SOURCE CONTROL DRAWING

SHEET INDEX	REVISION LTR								
	SHEET NO.								

SHEET INDEX	REVISION LTR	B	–	–	–	–	B	–	–
	SHEET NO.	1	2	3	4	5	6	7	8

UNLESS OTHERWISE SPECIFIED ON THIS DRAWING, FABRICATION OF THIS ITEM SHALL BE IN ACCORDANCE WITH AIRESEARCH SPECIFICATION SC-5535, STANDARD DRAWING INTERPRETATIONS

SIGNATURES	DATES
DFT BUSHMAN	11-21-66
CHK	11-29-66
APPD	
APPD	11/23/66
DSGN ACTIVITY	
OTHER ACTIVITY	

AIRESEARCH MANUFACTURING COMPANY
A DIVISION OF THE GARRETT CORPORATION
PHOENIX, ARIZONA

DWG TITLE
REACTOR-AUDIO,
INDUCTOR

SIZE	CODE IDENT NO.	DWG NO.	REV LTR
A	99193	307596	B

SCALE –	WT –	SHEET 1 OF 8

BRU

FORM P1807A

AFFECTS SHEETS 1-6 ATTACH TO SHEET 1 ONLY

AiResearch Manufacturing Company of Arizona
ENGINEERING ORDER

FORM F2532-8 REVISION SHEET 1 OF 1

DRAWING TITLE REACTOR - AUDIO, INDUCTOR				DWG NO 307596		CHG LET. B	
TO BE INCORP. IN DRAWING	YES	NO	INCORP. BY	DATE	INCORP CHK'D BY	DATE	ADV. CHG. LET. —
MANDATORY		1	DRAWING CHG. ☒	VARIATION	VOID AFTER DATE	DISTRIBUTION	L.A. / PHR.
PRIORITY		2	ADV. DWG. CHG.	SUBSTITUTION	VOID AFTER NO OF PARTS	NORMAL	PHR. ☒
ROUTINE		[✓ 3]	EMERGENCY DWG.	REWORK	S.I.L. YES NO	RUSH	
MINOR		4	E.C.P. NO.	MATL. REV. ACT.	SERVICE BULLETIN YES NO	TELETYPE	

ZONE	LET. SUB	TYPE CHG.	DESCRIPTION	SPARE PARTS CODE	AUTHORITY	DISPOSITION OF AFFECTED PART
			REVISED PAGE 6		DRN	
			PARA. 4.2 27 TURNS WAS 34		15699	
			PARA. 4.23 .002 AIRGAP, TOTAL OF .004 WAS			
			.006 AIRGAP, TOTAL OF .012			

NEXT ASSY	MODEL NO.	M.E.O.	OUTLINE
			305506

PARTS LIST CHANGE ONLY — NO EFFECT ON MODEL NO 10/13

EFFECTIVITY INSTRUCTIONS

UNDELIVERED ITEMS

N/A

DELIVERED ITEMS

COORDINATED BY DATE

REASON FOR CHANGE VENDOR REQUEST TO MEET TEST REQUIREMENTS

REQUESTED BY	DATE	PREPARED BY	DATE	CHECKED BY	DATE	APPROVED BY	DATE
HAUSMAN	10-11-67	M. ZIMMERMAN	10-12-67				10-12-67

NOTE: A LINE DRAWN THROUGH ANY REQUIREMENT SHOWN ON THIS DRAWING INDICATES NO REQUIREMENT

1. GENERAL NOTES

1.1 PROCUREMENT SOURCE(S) PER ASL 307596 .

1.2 PART TO BE PERMANENTLY MARKED WITH AIRESEARCH PART NO. 307596-1 .

1.3 ALL DESIGN AND PART NO. CHANGES REQUIRE PRIOR AIRESEARCH APPROVAL.

1.4 ONLY THE ITEMS LISTED ON THIS DRAWING AND IDENTIFIED BY VENDORS NAMES, ADDRESSES, AND PART NO. ON ASL 307596 HAVE BEEN TESTED AND APPROVED FOR USE IN THE END UNIT. A SUBSTITUTE PART SHALL NOT BE USED WITHOUT PRIOR TESTING AND APPROVAL BY AIRESEARCH.

1.5 IDENTIFY PACKAGING WITH AIRESEARCH PART NO. 307596-1 .

1.6 PARTS PROCURED BY VENDOR PART NO. SHALL BE PROCURED IN ACCORDANCE WITH THIS AIRESEARCH SOURCE CONTROL DRAWING AND ASL 307596 .

1.7 MARKING REQUIREMENTS.

1.7.1 MARKINGS TO BE PER MIL-T-27 PARA. 3.20 AS APPLICABLE.

1.7.2 MARKING TO BE LOCATED AS SHOWN IN FIGURE 1.

1.7.3 MARKINGS TO BE A MINIMUM OF .031 INCH FROM ANY CORNER, TERMINAL OR EDGE UNLESS OTHERWISE SPECIFIED.

1.7.4 HEIGHT OF MARKINGS SHALL BE A MINIMUM OF .12 INCH UNLESS OTHERWISE NOTED.

1.7.5 (1) MARKINGS TO BE PER MIL-STD-130 EXCEPT ACID ETCHING AND BRANDING NOT PERMITTED.
(2) OTHER

1.7.6 MARKINGS TO BE OF A CONTRASTING COLOR.

1.7.7 INK TO BE PER TT-I-558 AS APPLICABLE.

1.7.8 MARKINGS TO BE COVERED WITH ONE COAT OF CLEAR EPOXY AS APPLICABLE.

1.8 DETAILS OF DESIGN AND CONSTRUCTION OTHER THAN SHOWN SHALL BE AT THE OPTION OF THE VENDOR.

SEE SHEET 1 FOR CONTROLLING REV LTR

SIZE	CODE IDENT NO.	DWG NO.	REV LTR
A	99193	307596	—
SCALE -		WT -	SHEET 2

FORM F1807-2A

1.9 (1) VACUUM IMPREGNATE WOUND BOBBIN WITH CLASS'F' RESIN.
DIP COAT ASSY WITH EPOXY
(2) OTHER

1.10 SOLDER PER MIL-S-6872 USING QQ-S-571, COMP SN60 SOLDER.

1.11 ______ AS SHOWN WITH ______. IF CUP OR BOX IS USED MATERIAL TO BE PER ______.

1.12 TOP .40 OF TERMINALS TO BE FREE AND CLEAR OF POTTING COMPOUND FOR EXTERNAL WIRES.

1.13 DUTY CYCLE: (1) CONTINUOUS ~~(2) OTHER~~

1.14 OTHER

2. PHYSICAL CONSTRUCTION REQUIREMENTS

2.1 CORE: NO. REQ'D 1 SEE PARA. ______
(1) PART NO. AL-12 MFG. BY ARNOLD ENG CO
MARENGO ILL.
(2) PART NO. ______ MFG. BY ______
(3) PART NO. ______ MFG. BY ______

2.2 * ~~WRAP CORE(S) WITH~~ USE A BOBBIN

~~2.3 *~~ WIND EACH CORE WITH GATE WINDING. SECTOR ______°.

~~2.4 **~~ PLACE WOUND CORES TOGETHER AND WIND ON CONTROL WINDINGS.

2.5 WINDING SEQUENCE L1

* DEVICES WITH WINDINGS WRAPPED DIRECTLY ON CORE ONLY
** SATURABLE MULTICORE DEVICES ONLY

SEE SHEET 1 FOR CONTROLLING REV LTR

SIZE	CODE IDENT NO.	DWG NO.	REV LTR
A	99193	307596	-
SCALE -		WT -	SHEET 3

2.6 WIRE INSULATION SHALL BE IN ACCORDANCE WITH MIL-T-27 AND BE SUFFICIENT TO WITHSTAND VOLTAGES LISTED IN PARAGRAPH 4.

2.7 UNLESS OTHERWISE SPECIFIED ON THIS DRAWING, FABRICATION OF THIS ITEM SHALL BE IN ACCORDANCE WITH AIRESEARCH SPECIFICATION SC-5535, STANDARD DRAWING INTERPRETATIONS.

3. SPECIFICATIONS

3.1 CLASSIFICATION: TYPE TF5SX04ZZ PER MIL-T-27 EXCEPT AS NOTED IN PARAGRAPH 3.1.1.

3.1.1

3.2 INSULATION RESISTANCE PER MIL-T-27, PARA. 3.10. MEASURE USING A D-C SOURCE OF 1000 VOLTS, WINDING TO NORMAL MOUNTING MEANS 1000 MEGOHMS, ~~WINDING TO WINDING~~ ________ ~~MEGOHMS~~.

3.3 MAXIMUM WORKING VOLTAGE 120 VRMS.

3.3.1 DIELECTRIC STRENGTH PER MIL-T-27 PARA. 4.7.5. TEST BY APPLYING 500 RMS VOLTS AT 60 Hz ~~CPS~~ FOR 5 SECONDS BETWEEN WINDINGS AND BETWEEN EACH WINDING AND THE BASE OR NORMAL MOUNTING MEANS.

3.4 TEMPERATURE RISE PER MIL-T-27 PARA. 4.7.10. MAX TEMPERATURE RISE 30 OPERATING AT AN AMBIENT TEMPERATURE OF 85°C.

3.5 MAXIMUM OPERATING ALTITUDE 80,000 FEET.

3.6 ENVIRONMENTAL REQUIREMENTS:

~~3.6.1~~ MOISTURE RESISTANCE:
(1) MIL-T-27 PARA. 4.7.11.4
(2) OTHER

~~3.6.2~~ SALT SPRAY:
(1) MIL-E-5272 PROCEDURE________
(2) OTHER

~~3.6.3~~ VIBRATION REQUIREMENTS:
(1) MIL-T-27 PARA. 4.7.12
(2) OTHER

SEE SHEET 1 FOR CONTROLLING REV LTR

SIZE	CODE IDENT NO.	DWG NO.	REV LTR
A	99193	307596	—
SCALE		WT —	SHEET 4

3.6.4 SHOCK REQUIREMENTS:
(1) MIL-T-27 PARA. 4.7.13
(2) OTHER

3.6.5 AMBIENT TEMPERATURE RANGE:
(1) OPERATING -55 °C MIN, 70 °C MAX.
(2) NON OPERATING -55 °C MIN, 70 °C MAX.
(3) OTHER

3.7 LIFE:

3.7.1 OPERATING: 10,000 HOURS AT 85 °C WITH POWER APPLIED PER PARA. 4.6.

3.7.2 STORAGE: 5 YEARS AT 50 °C AND 50 % RELATIVE HUMIDITY.

3.8 ALLOW UNIT TO STABILIZE TO ROOM TEMPERATURE BEFORE EXPOSING TO OPPOSITE TEMPERATURE EXTREME.

3.9 OTHER

SEE SHEET 1 FOR CONTROLLING REV LTR

SIZE A	CODE IDENT NO. 99193	DWG NO. 307596	REV — LTR
SCALE —		WT —	SHEET 5

4. ELECTRICAL REQUIREMENTS (SEE FIGURE 2)

	WINDINGS	L1	L2	L3	L4	L5	L6	L7	L8	L9	L10	L11	L12	L13
4.1	WIRE GAGE NO. (AWG)	10												
4.2	NO. OF TURNS	27												
4.3	WINDING TOLERANCE (TURNS)	±0												
4.4	MAX D.C. RESISTANCE (OHMS)	.015												
4.5	WORKING VOLTAGE TO GROUND	120												
4.6	RATED VOLTAGE (RMS)	120												
4.7	FREQUENCY ~~(CPS)~~ Hz	1200												
4.8	FREQUENCY TOLERANCE (CPS)	—												
4.9	OPERATING POWER LEVEL (WATTS)	10												
*4.10	MAX CONTROL CURRENT (AMPS)	—												
4.11	RATED CURRENT (AMPS)	16												
4.12														
4.13														
4.14														
4.15														
4.16														
4.17														
4.18														
4.19														

4.20 SELF INDUCTION: WITH ______ RMS VOLTS ______ CPS APPLIED ACROSS __________, THE RESULTING EXCITATION CURRENT SHALL BE ______ MA RMS MAX.

*4.21 CORES TO BE MATCHED TO ______ % FOR BIAS AND ______ % FOR GAIN USING AIEE TEST PROCEDURE FOR TOROIDAL MAGNETIC AMPLIFIER CORES NO. ______________.

4.22 ALL ELECTRICAL REQUIREMENTS ARE TO BE MET AT AN AMBIENT OF 25°C.

4.23 AIRGAP- EACH LEG OF THE MAGNETIC PATH SHALL HAVE A 0.002 INCH GAP - MAKING A TOTAL OF 0.004 (4 MILS) FOR THE TOTAL PATH.

*SATURABLE MULTICORE DEVICES ONLY

SEE SHEET 1 FOR CONTROLLING REV LTR

SIZE	CODE IDENT NO.	DWG NO.	REV LTR
A	99193	307596	B
SCALE –		WT –	SHEET 6

FORM P1807-6A

SCHEMATIC DIAGRAM

FIGURE 2

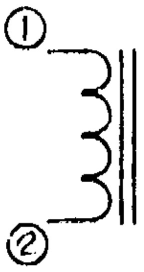

● ~~TERMINALS TO BE OF SAME POLARITY~~

WINDINGS		TERMINAL FROM	TERMINAL TO
25 T	L1	1	2
	L2		
	L3		
	L4		
	L5		
	L6		
	L7		
	L8		
	L9		
	L10		
	L11		
	L12		
	L13		

TEST CIRCUIT & INSPECTION INFORMATION

FIGURE 3

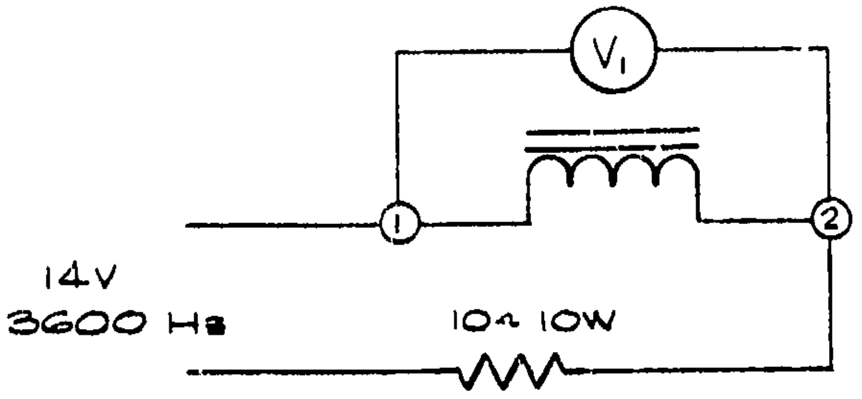

V_1 SHALL READ 10V ± 2V

SEE SHEET 1 FOR CONTROLLING REV LTR

SIZE	CODE IDENT NO.	DWG NO.		REV LTR
A	99193	307596		–
SCALE --		WT -	SHEET 7	

PHYSICAL SIZE

FIGURE 1

TERMINALS, 2 REQ'D, TO BE IN APPROXIMATE LOCATION SHOWN. MIN. SPACING BETWEEN TERMINALS TO BE .81 INCH MIN. EDGE DISTANCE TO BE .06 INCH MIN. ~~TERMINAL PART NO.~~ ________ ~~OR EQUIV.~~ ~~MFG. BY~~ TERMINAL TO BE FORMED FROM WINDING WIRE (AWG 10) SEE DETAIL

SCHEMATIC DIAGRAM & PART NO. TO APPEAR ON THIS SURFACE PER MIL-T-27. (SHALL SHOW PICTORIAL DIAGRAM TERMINAL NO. AND POLARITY.) LETTERING MAY BE REDUCED IN SIZE BUT MUST BE CLEAR AND LEGIBLE.

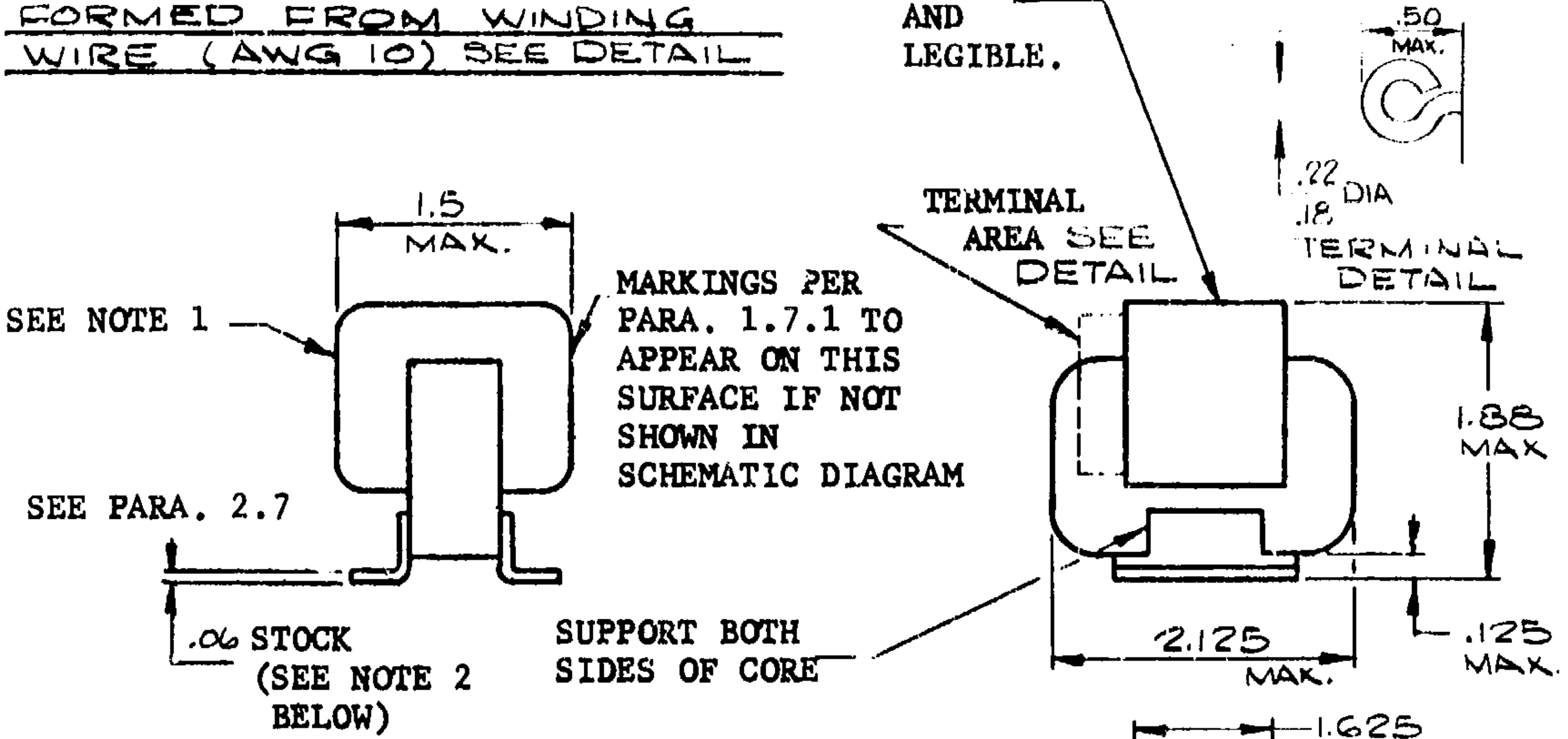

.148-.143 DIA THRU 4 PLACES

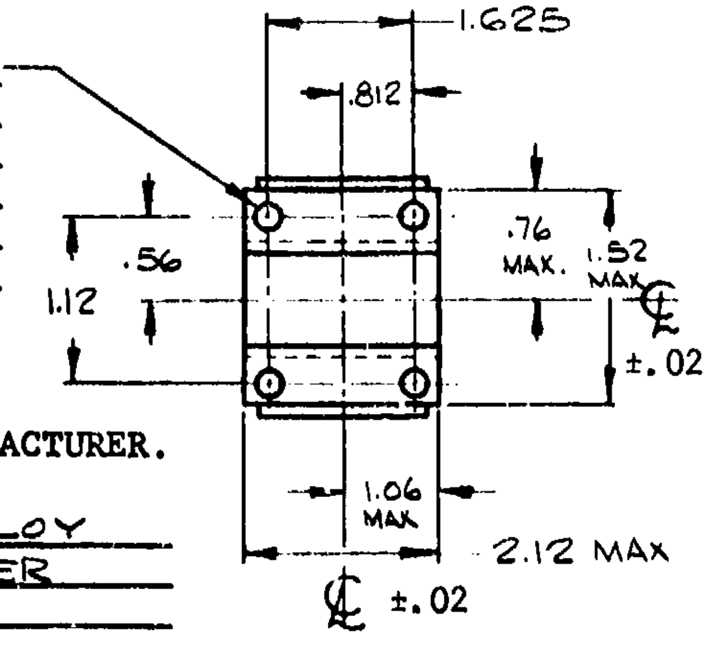

NOTES:

1. BOBBIN & WINDING ASSY PROVIDED BY MANUFACTURER.
2. MOUNTING BASE MAT'L & FINISH: AL ALLOY TURCOAT 4178-6 OR IRIDITE PER MIL-C-5541

SEE SHEET 1 FOR CONTROLLING REV LTR

SIZE	CODE IDENT NO.	DWG NO.	REV
A	99193	307596	– LTR
SCALE NONE		WT –	SHEET 8

PART №
307597-1

REVISIONS			
LTR	DESCRIPTION	DATE	APPROVED

See tab block (upper left corner) for PART NUMBER

SHEET INDEX	REVISION LTR									
	SHEET NO.									

SHEET INDEX	REVISION LTR									
	SHEET NO.	1	2	3	4	5	6	7	8	9

UNLESS OTHERWISE SPECIFIED ON THIS DRAWING, FABRICATION OF THIS ITEM SHALL BE IN ACCORDANCE WITH AIRESEARCH SPECIFICATION SC-5535, STANDARD DRAWING INTERPRETATIONS

SIGNATURES	DATES
DFT BUSHMAN	11·30·66
CHK	12·1·66
APPD	11·30·66
APPD	
DSGN ACTIVITY	12/1/66
OTHER ACTIVITY	

AIRESEARCH MANUFACTURING COMPANY
A DIVISION OF THE GARRETT CORPORATION
PHOENIX, ARIZONA

DWG TITLE
REACTOR, SATURABLE

SIZE	CODE IDENT NO.	DWG NO.	REV
A	99193	307597	— LTR

SCALE —	WT —	SHEET 1 OF 9

FORM P1807A

NOTE: A LINE DRAWN THROUGH ANY REQUIREMENT SHOWN ON THIS DRAWING INDICATES NO REQUIREMENT

1. GENERAL NOTES

1.1 PROCUREMENT SOURCE(S) PER ASL 307597.

1.2 PART TO BE PERMANENTLY MARKED WITH AIRESEARCH PART NO. 307597-1.

1.3 ALL DESIGN AND PART NO. CHANGES REQUIRE PRIOR AIRESEARCH APPROVAL.

1.4 ONLY THE ITEMS LISTED ON THIS DRAWING AND IDENTIFIED BY VENDORS NAMES, ADDRESSES, AND PART NO. ON ASL 307597 HAVE BEEN TESTED AND APPROVED FOR USE IN THE END UNIT. A SUBSTITUTE PART SHALL NOT BE USED WITHOUT PRIOR TESTING AND APPROVAL BY AIRESEARCH.

1.5 IDENTIFY PACKAGING WITH AIRESEARCH PART NO. 307597-1.

1.6 PARTS PROCURED BY VENDOR PART NO. SHALL BE PROCURED IN ACCORDANCE WITH THIS AIRESEARCH SOURCE CONTROL DRAWING AND ASL 307597.

1.7 MARKING REQUIREMENTS.

1.7.1 MARKINGS TO BE PER MIL-T-27 PARA. 3.20 AS APPLICABLE.

1.7.2 MARKING TO BE LOCATED AS SHOWN IN FIGURE 1.

1.7.3 MARKINGS TO BE A MINIMUM OF .031 INCH FROM ANY CORNER, TERMINAL OR EDGE UNLESS OTHERWISE SPECIFIED.

1.7.4 HEIGHT OF MARKINGS SHALL BE A MINIMUM OF .12 INCH UNLESS OTHERWISE NOTED.

1.7.5 (1) MARKINGS TO BE PER MIL-STD-130 EXCEPT ACID ETCHING AND BRANDING NOT PERMITTED.
(2) OTHER

1.7.6 MARKINGS TO BE OF A CONTRASTING COLOR.

1.7.7 INK TO BE PER TT·1·558 AS APPLICABLE.

1.7.8 MARKINGS TO BE COVERED WITH ONE COAT OF CLEAR EPOXY AS APPLICABLE.

1.8 DETAILS OF DESIGN AND CONSTRUCTION OTHER THAN SHOWN SHALL BE AT THE OPTION OF THE VENDOR.

SEE SHEET 1 FOR CONTROLLING REV LTR

SIZE A	CODE IDENT NO. 99193	DWG NO. 307597	REV – LTR
SCALE –		WT –	SHEET 2

1.9 (1) ~~VACUUM IMPREGNATE~~ ______ WITH ______

(2) OTHER DIP COAT COMPLETED UNIT WITH EPOXY.

1.10 SOLDER PER MIL-S-6872 USING COMP. SN60 PER QQ-S-571 SOLDER.

~~1.11~~ ______ AS SHOWN WITH ______. IF CUP OR BOX IS USED MATERIAL TO BE PER ______.

1.12 TOP ______ OF TERMINALS TO BE FREE AND CLEAR OF POTTING COMPOUND FOR EXTERNAL WIRES.

1.13 DUTY CYCLE: (1) CONTINUOUS ~~(2) OTHER~~

1.14 OTHER

2. **PHYSICAL CONSTRUCTION REQUIREMENTS**

2.1 CORE: NO. REQ'D 2 SEE PARA. 4.21

(1) PART NO. 52106-2A MFG. BY MAGNETICS INC. BUTLER PA.

(2) PART NO. ______ MFG. BY ______

(3) PART NO. ______ MFG. BY ______

2.2 * WRAP CORE(S) WITH ______

2.3 * WIND EACH CORE WITH GATE WINDING. SECTOR 360 °.

2.4 ** PLACE WOUND CORES TOGETHER AND WIND ON CONTROL WINDINGS.

2.5 WINDING SEQUENCE L1, L2, L3

* DEVICES WITH WINDINGS WRAPPED DIRECTLY ON CORE ONLY

** SATURABLE MULTICORE DEVICES ONLY

SEE SHEET 1 FOR CONTROLLING REV LTR

SIZE	CODE IDENT NO.	DWG NO.	REV LTR
A	99193	307597	--
SCALE -		WT -	SHEET 3

FORM P1807-3A

2.6 WIRE INSULATION SHALL BE IN ACCORDANCE WITH MIL-T-27 AND BE SUFFICIENT TO WITHSTAND VOLTAGES LISTED IN PARAGRAPH 4.

2.7 UNLESS OTHERWISE SPECIFIED ON THIS DRAWING, FABRICATION OF THIS ITEM SHALL BE IN ACCORDANCE WITH AIRESEARCH SPECIFICATION SC-5535, STANDARD DRAWING INTERPRETATIONS.

3. SPECIFICATIONS

3.1 CLASSIFICATION: TYPE TF5SX40ZZ PER MIL-T-27 EXCEPT AS NOTED IN PARAGRAPH 3.1.1.

3.1.1

3.2 INSULATION RESISTANCE PER MIL-T-27, PARA. 3.10. MEASURE USING A D-C SOURCE OF 500 VOLTS, ~~WINDING TO NORMAL MOUNTING MEANS~~ ______ ~~MEGOHMS~~, WINDING TO WINDING 1000 MEGOHMS.

3.3 MAXIMUM WORKING VOLTAGE 120 VRMS.

3.3.1 DIELECTRIC STRENGTH PER MIL-T-27 PARA. 4.7.5. TEST BY APPLYING 500 RMS VOLTS AT 60 Hz ~~CPS~~ FOR 5 SECONDS BETWEEN WINDINGS AND BETWEEN EACH WINDING AND THE BASE OR NORMAL MOUNTING MEANS.

3.4 TEMPERATURE RISE PER MIL-T-27 PARA. 4.7.10. MAX TEMPERATURE RISE 30°C OPERATING AT AN AMBIENT TEMPERATURE OF 85°C.

3.5 MAXIMUM OPERATING ALTITUDE 80,000 FEET.

3.6 ENVIRONMENTAL REQUIREMENTS:

~~3.6.1~~ MOISTURE RESISTANCE:
(1) MIL-T-27 PARA. 4.7.11.4
(2) OTHER

~~3.6.2~~ SALT SPRAY:
(1) MIL-E-5272 PROCEDURE ______
(2) OTHER

~~3.6.3~~ VIBRATION REQUIREMENTS:
(1) MIL-T-27 PARA. 4.7.12
(2) OTHER

SEE SHEET 1 FOR CONTROLLING REV LTR

SIZE	CODE IDENT NO.	DWG NO.	REV LTR
A	99193	307597	—
SCALE —		WT —	SHEET 4

3.6.4 SHOCK REQUIREMENTS:
(1) MIL-T-27 PARA. 4.7.13
(2) OTHER

3.6.5 AMBIENT TEMPERATURE RANGE:
(1) OPERATING -55 °C MIN, 70 °C MAX.
(2) NON OPERATING -55 °C MIN, 70 °C MAX.
(3) OTHER

3.7 LIFE:

3.7.1 OPERATING: 10000 HOURS AT 85 °C WITH POWER APPLIED PER PARA. 4.6.

3.7.2 STORAGE: 5 YEARS AT 50 °C AND 50 % RELATIVE HUMIDITY.

3.8 ALLOW UNIT TO STABILIZE TO ROOM TEMPERATURE BEFORE EXPOSING TO OPPOSITE TEMPERATURE EXTREME.

3.9 OTHER

SEE SHEET 1 FOR CONTROLLING REV LTR

SIZE	CODE IDENT NO.	DWG NO.	REV LTR
A	99193	307597	–
SCALE –		WT –	SHEET 5

FORM P1807-5A

4. ELECTRICAL REQUIREMENTS (SEE FIGURE 2)

	WINDINGS	L1	L2	L3	L4	L5	L6	L7	L8	L9	L10	L11	L12	L13
4.1	WIRE GAGE NO. (AWG)	32	32	37										
4.2	NO. OF TURNS	1400	1400	1000										
4.3	WINDING TOLERANCE (TURNS)	±1	±1	±2										
4.4	MAX D.C. RESISTANCE (OHMS)	35	35	150										
4.5	WORKING VOLTAGE TO GROUND	120	120	10										
4.6	RATED VOLTAGE (RMS)	120	120	-										
4.7	FREQUENCY ~~(CPS)~~ Hz	1200	1200	-										
4.8	FREQUENCY TOLERANCE ~~(CPS)~~ Hz	-	-	-										
4.9	OPERATING POWER LEVEL (WATTS)	9	9	-										
*4.10	MAX CONTROL CURRENT (AMPS)	-	-	-										
4.11	RATED CURRENT (AMPS)	.08	.08	.04										
4.12														
4.13														
4.14														
4.15														
4.16														
4.17														
4.18														
4.19														

~~4.20~~ SELF INDUCTION: WITH ______ RMS VOLTS ______ CPS APPLIED ACROSS ________, THE RESULTING EXCITATION CURRENT SHALL BE ______ MA RMS MAX.

*4.21 CORES TO BE MATCHED TO 5 % FOR BIAS AND 10 % FOR GAIN USING AIEE TEST PROCEDURE FOR TOROIDAL MAGNETIC AMPLIFIER CORES NO. 432.

4.22 ALL ELECTRICAL REQUIREMENTS ARE TO BE MET AT AN AMBIENT OF 25°C.

*SATURABLE MULTICORE DEVICES ONLY

SEE SHEET 1 FOR CONTROLLING REV LTR

SIZE	CODE IDENT NO.	DWG NO.	REV
A	99193	307597	-

SCALE - WT - SHEET 6

FORM P1807-6A

SCHEMATIC DIAGRAM

FIGURE 2

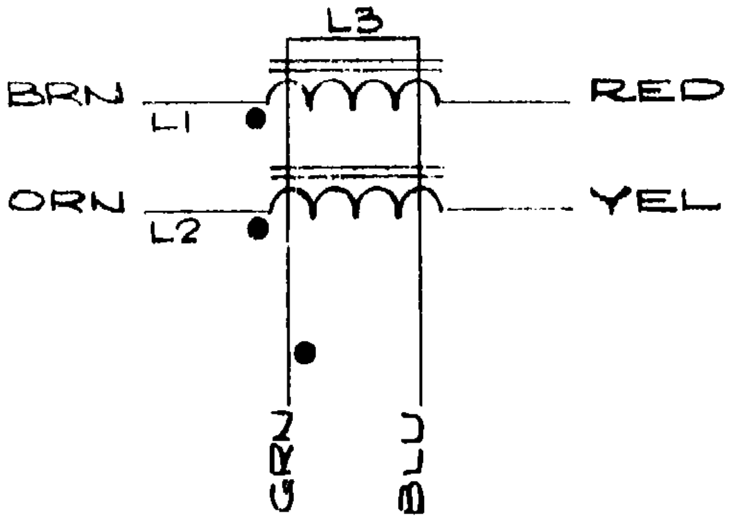

● TERMINALS TO BE OF SAME POLARITY

WINDINGS		TERMINAL	
		FROM	TO
1400 TURNS	L1	BRN	RED
1400 TURNS	L2	ORN	YEL
1000 TURNS	L3	GRN	BLU
	L4		
	L5		
	L6		
	L7		
	L8		
	L9		
	L10		
	L11		
	L12		
	L13		

~~TEST CIRCUIT & INSPECTION INFORMATION~~

~~FIGURE 3~~

FOR TEST CIRCUIT & INSPECTION INFORMATION SEE SHEET 8

SEE SHEET 1 FOR CONTROLLING REV LTR

SIZE	CODE IDENT NO.	DWG NO.	REV LTR
A	99193	307597	—
SCALE —		WT --	SHEET 7

FORM F1807-7A

TEST CIRCUIT & INSPECTION INFORMATION
FIGURE 8

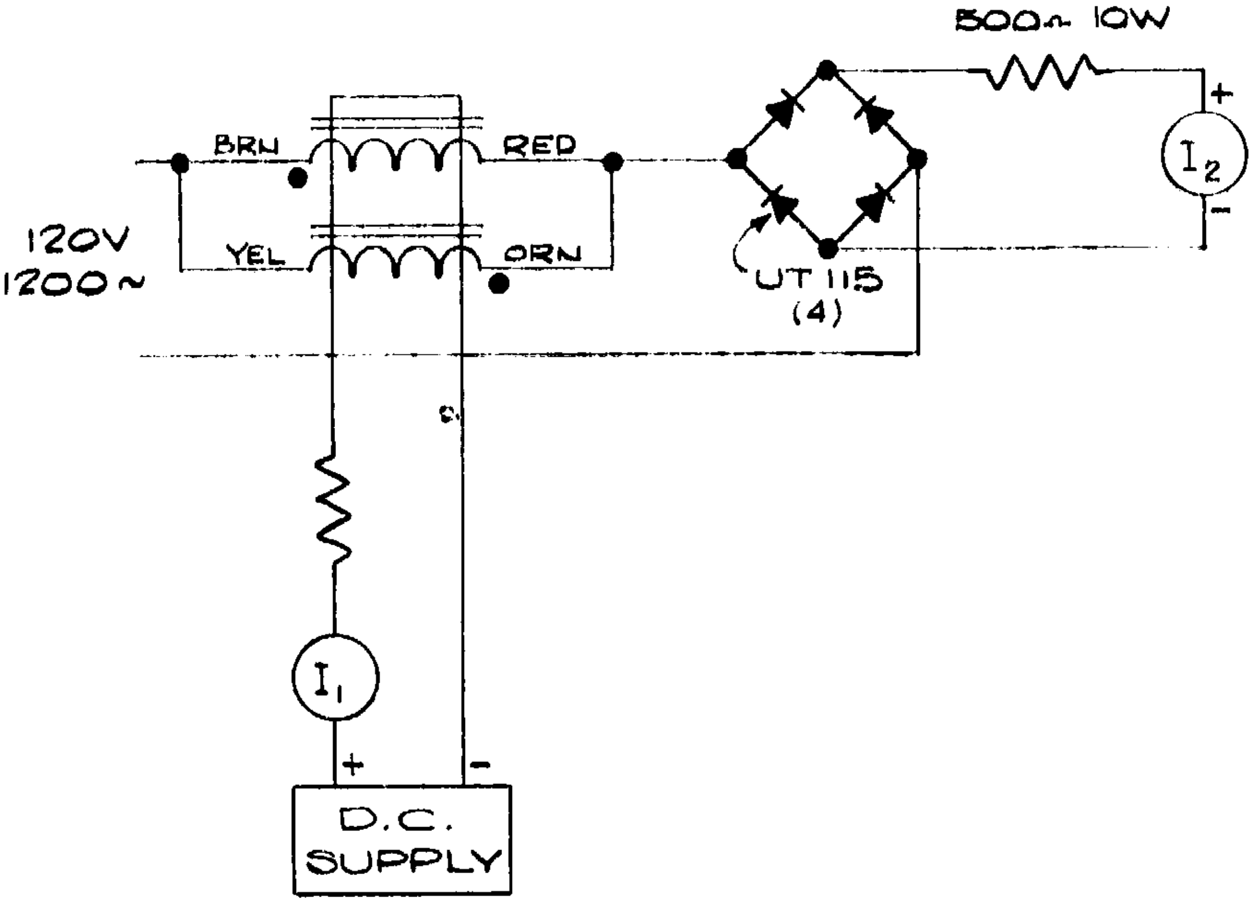

WITH THE REACTOR CONNECTED AS SHOWN
THE GAIN FIGURES OF TABLE SHALL APPLY

I1 MA	I2 MA
0	LESS THAN 4
20	31 ± 4
40	62 ± 4

SEE SHEET 1 FOR CONTROLLING REV LTR

SIZE	CODE IDENT NO.	DWG NO.	REV
A	99193	307597	— LTR

SCALE	WT	SHEET
—	—	8

FORM P1807-1A

PHYSICAL SIZE

FIGURE 1

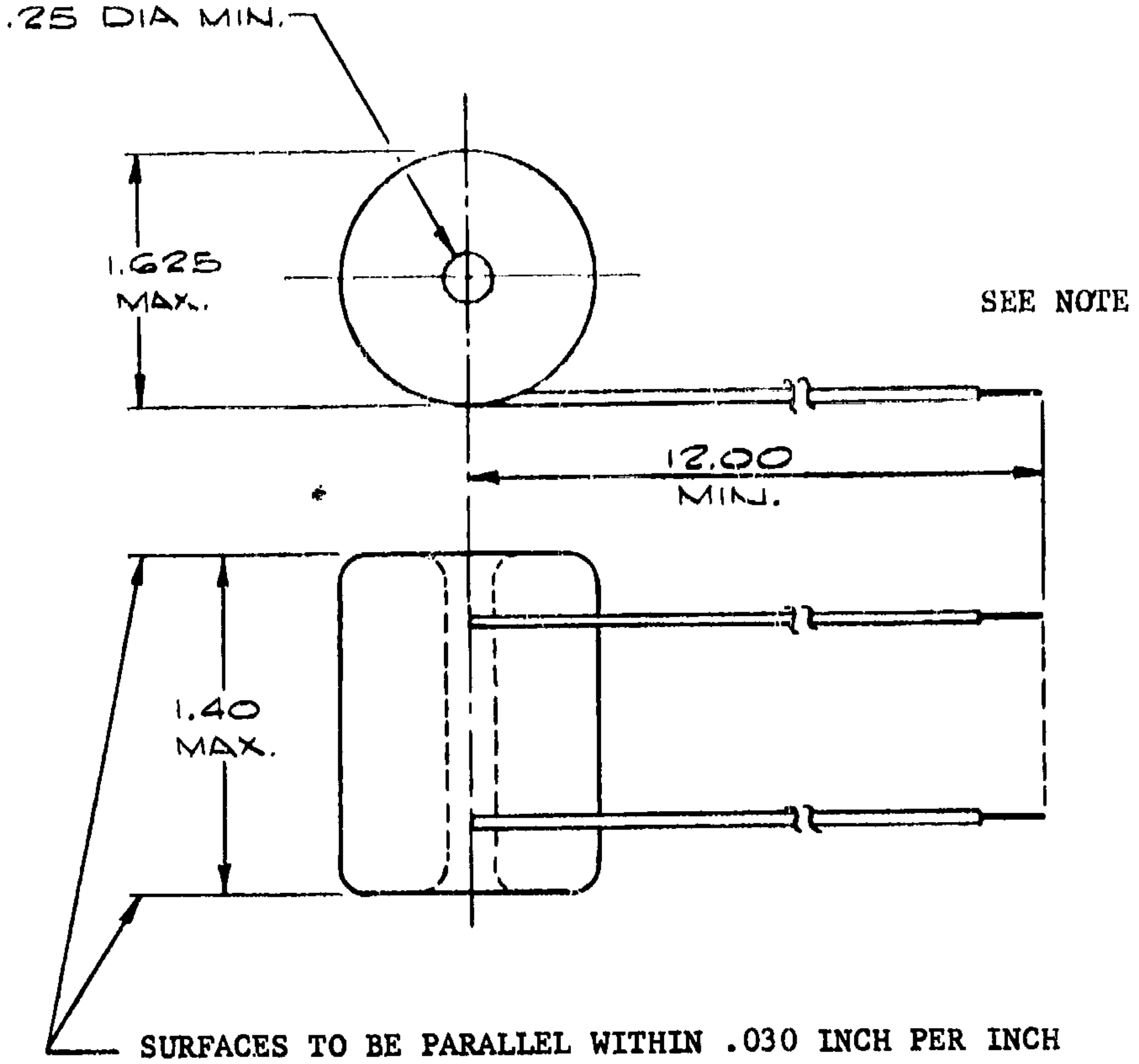

SURFACES TO BE PARALLEL WITHIN .030 INCH PER INCH

NOTE:

LEAD WIRE TO BE #22 AWG PER MIL-W-16878 TYPE 'E' (EXCEPT 19 STRAND)

LEAD COLOR CODING TO BE AS SHOWN IN SCHEMATIC. LEAD ENDS TO BE STRIPPED 3/8 INCH AND TINNED.

SEE SHEET 1 FOR CONTROLLING REV LTR

SIZE	CODE IDENT NO.	DWG NO.	REV LTR
A	99193	307597	—
SCALE NONE		WT -	SHEET 9

FORM P1807-8A

PART NUMBER
358498 -1

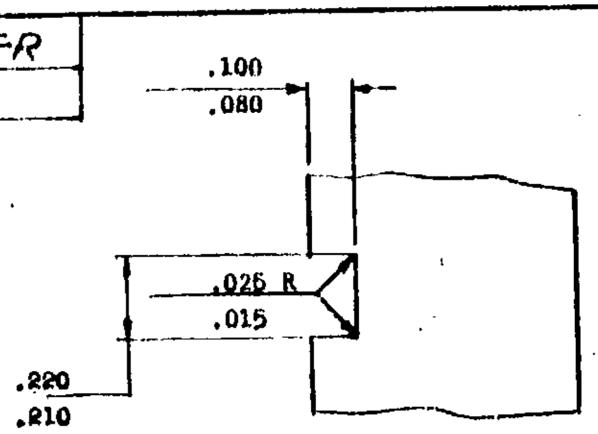

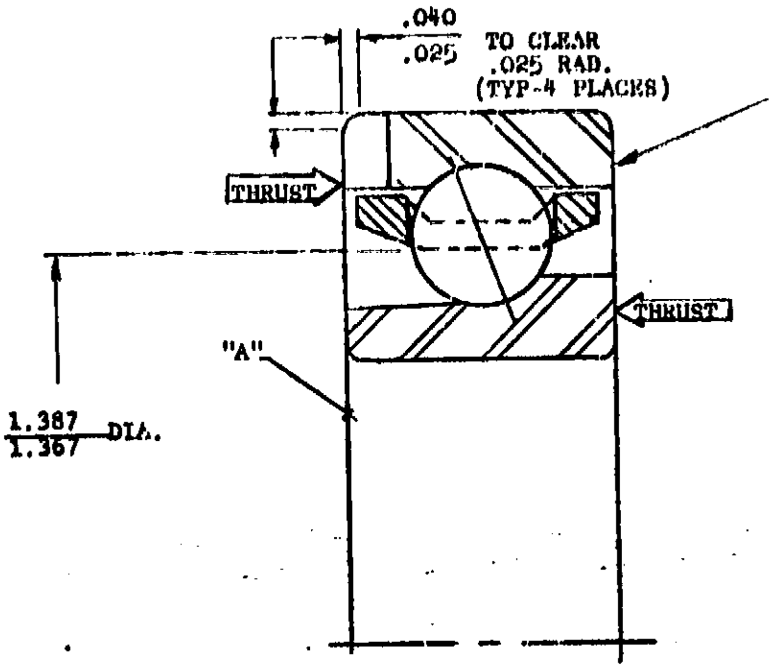

MARK PART NUMBER AND SERIAL NUMBER HERE PER AIRESEARCH SPEC. MO-5014 CLASS II

BEARING DESCRIPTION	BALL, ANGU
INNER RING	
MATERIAL:	CEVM M-50 PER AMS 649 Rc 60-64
BORE: Ⓜ	.9843-.9841 (25MM) TAPER/
WIDTH:	.4724-.4624 (12MM) Ⓜ
RACE DEPTH:	20 MIN %
RACE CURVATURE:	52-53 %
SEPARATOR PILOT LAND TO GROOVE RUNOUT:	
SEPARATOR	
MATERIALS:	FORGED SILICON IRON PER AMS 4616
CONSTRUCTION:	MACHINED
ASSEMBLY:	ONE-PIECE
PILOTING SURFACE:	OUTER RING LAN
PILOT CLEARANCE:	.008-.016
OPERATIONAL LUBRICANT	
NAME:	OIL, SYNTHETIC, AIRCRA GAS TURBINE, LUBRICAT
MILITARY SPEC NO.:	MIL-L-7808
BEARING PRELUBRICATION:	DIP and D
PACKAGING PER AIR. SPEC CP-14	
PRESERVATIVE:	
AIRESEARCH PART NUMBER:	
PROCUREMENT PER ASL	358498

9. ⟨C⟩ DESIGNATES CRITICAL CHARACTERISTIC
⟨M⟩ DESIGNATES MAJOR CHARACTERISTIC
8. PARTS SHALL CONFORM TO AIRESEARCH SPEC SC 5354
7. PARTS PROCURED BY VENDOR PART NUMBER SHALL BE PROCURED IN ACCORDANCE WITH THIS AIRESEARCH SOURCE CONTROL DRAWING.
6. IDENTIFY PACKAGING WITH AIRESEARCH PART NUMBER.
5. ALL DESIGN AND PART NUMBER CHANGES SHALL RECEIVE PRIOR AIRESEARCH APPROVAL.
4. ONLY THE ITEMS LISTED ON THE ASL AND IDENTIFIED BY VENDOR'S NAMES, ADDRESSES AND PART NUMBERS HAVE BEEN TESTED AND APPROVED FOR USE IN THE END UNIT. A SUBSTITUTE ITEM SHALL NOT BE USED WITHOUT PRIOR TESTING AND APPROVAL BY AIRESEARCH.
3. MILITARY SPARES PACK BEARINGS ARE INTENDED TO FILL MILITARY SPARES ORDERS. BEFORE INSTALLATION, WASH OUT THE PRESERVATIVE AND REPLACE WITH OPERATING LUBRICANT. AFTER THIS OPERATION THE -4 IDENTIFICATION IS CHANGED TO -1 AND THE BEARINGS BECOME INTERCHANGEABLE WITH THE PRODUCTION BULK AND COMMERCIAL SPARES PACK BEARINGS. THEY SHOULD NOT BE USED IN FACTORY INSTALLATIONS BECAUSE OF THEIR RELATIVELY HIGH COST.
2. FOR ECONOMY, PRODUCTION BULK PACK BEARINGS ARE PREFERRED FOR ALL FACTORY INSTALLATIONS. COMMERCIAL SPARES PACK BEARINGS ARE INTENDED TO FILL COMMERCIAL SPARES ORDERS.
1. PRODUCTION BULK AND COMMERCIAL SPARES PACK BEARINGS ARE INTERCHANGEABLE.

UNLESS OTHERWISE SPECIFIED:

SO
DFT
CHK
APP
APP
APP
DES
OTH

CRITICAL ITEM

SATISFACTORY PERFORMANCE OF THE END PRODUCT DEPENDS ON THE INTEGRITY AND RELIABILITY OF THIS SELECTED CRITICAL ITEM. THE GARRETT CORPORATION RECOMMENDS PROCUREMENT FROM THE ORIGINAL SUPPLIER AS SET FORTH IN ASPR 1-313.

REVISIONS			
LTR	DESCRIPTION	DATE	APPROVED
A	17° WAS 24° SEE E.O.	3-9-67	

D
D

PART NUMBER AND SERIAL NUMBER
PER AIRESEARCH SPEC. MO-5014 CLASS II

See tab block (upper left corner) for PART NUMBER

BEARING DESCRIPTION B.LL, ANGULAR CONTACT, 7105	GRADE AIRESEARCH 5

INNER RING	
MATERIAL:	CEVM M-50 PER AMS 6490 Rc 60-64
BORE:	Ⓜ .9843-.9841 (25MM)
TAPER/FT:	
WIDTH:	.4724-.4624 (12MM) Ⓜ
RACE DEPTH:	20 MIN % BALL DIA
RACE CURVATURE:	52-53 % BALL DIA
SEPARATOR PILOT LAND TO GROOVE RUNOUT:	TIR
SEPARATOR	
MATERIALS:	FORGED SILICON IRON BRONZE PER AMS 4616
CONSTRUCTION:	MACHINED
ASSEMBLY:	ONE-PIECE
PILOTING SURFACE:	OUTER RING LANDS
PILOT CLEARANCE:	.008-.016
OPERATIONAL LUBRICANT	
NAME:	OIL, SYNTHETIC, AIRCRAFT GAS TURBINE, LUBRICATING
MILITARY SPEC NO.	MIL-L-7808
BEARING PRELUBRICATION:	DIP and DRAIN

OUTER RING	
MATERIAL:	CEVM M-50 PER AMS 6490 Rc 60-64
OD:	1.8504-1.8502 (47MM) Ⓜ
FLANGE OD:	
WIDTH:	.4724-.4674 (12MM)
FLANGE WIDTH:	
RACE DEPTH:	16 MIN % BALL DIA
RACE CURVATURE:	52-53 % BALL DIA
SEPARATOR PILOT LAND TO GROOVE RUNOUT:	.0005 TIR
ROLLING ELEMENTS	
MATERIAL:	CEVM M-50 PER AMS 6490 Rc 60-64
COMPLEMENT PER ROW:	13-1/4" DIA.
CLOSURES	
NUMBER:	NONE
TYPE: (SHIELDS, SEALS)	
MATERIAL:	
CONSTRUCTION:	

ASSEMBLED BEARING CHARACTERISTICS

TOTAL DIAMETRAL Ⓜ (DIAMETRAL, AXIAL) CLEARANCE OF .0009 - .0013 UNDER 2 LBS GAGE LOAD

SPECIAL FEATURES

1. PARTS MUST NOT CHANGE IN DIMENSION IN EXCESS OF .000050 in/in WHEN SUBJECTED TO 750°F FOR 10 HOURS.
2. FACES "A" TO BE FLUSH WITHIN ±.0001 WITH 30 LBS. THRUST LOAD APPLIED AS SHOWN.
3. SEPARATOR POCKET SURFACES CIRCUMFERENTIALLY FORE AND AFT TO BE AT BEARING P.D.
4. SEPARATOR TO BE SILVER PLATED .0005-.0020 THICK PER AMS2412.
5. CONTACT ANGLE 17° (REF).
6. SIMILAR TO AIRESEARCH ~~P/N 358313.~~
7. HEAT TREATMENT OF M 50 TO BE PER AIRESEARCH PROCESS SPEC. H-55.

PACKAGING PER AIR. SPEC CP-14	PRODUCTION BULK PACK	COMMERCIAL SPARES PACK	MILITARY SPARES PACK
PRESERVATIVE:	MIL-L-6085	MIL-L-6085	MIL-P-197
AIRESEARCH PART NUMBER:	358498 -1	358498 -1	358498 -4

PROCUREMENT PER ASL 358498

REV A

DWG NO. 358498

:RITICAL CHARACTERISTIC
IAJOR CHARACTERISTIC

AIRESEARCH SPEC. SC 5354

)R PART NUMBER SHALL BE PROCURED
HIS AIRESEARCH SOURCE CONTROL

I AIRESEARCH PART NUMBER.

MBER CHANGES SHALL RECEIVE PRIOR AIRESEARCH APPROVAL.

I THE ASL AND IDENTIFIED BY VENDOR'S NAMES, ADDRESSES AND PART
TD AND APPROVED FOR USE IN THE END UNIT. A SUBSTITUTE ITEM
OUT PRIOR TESTING AND APPROVAL BY AIRESEARCH.

ARINGS ARE INTENDED TO FILL MILITARY SPARES ORDERS. BEFORE IN-
HE PRESERVATIVE AND REPLACE WITH OPERATING LUBRICANT. AFTER
ENTIFICATION IS CHANGED TO -1 AND THE BEARINGS BECOME INTER-
RODUCTION BULK AND COMMERCIAL SPARES PACK BEARINGS. THEY
ACTORY INSTALLATIONS BECAUSE OF THEIR RELATIVELY HIGH COST.

ON BULK PACK BEARINGS ARE PREFERRED FOR ALL FACTORY INSTALLA-
S PACK BEARINGS ARE INTENDED TO FILL COMMERCIAL SPARES ORDERS.

OMMERCIAL SPARES PACK BEARINGS ARE INTERCHANGEABLE.

UNLESS OTHERWISE SPECIFIED:

SOURCE CONTROL DRAWING	
SIGNATURES	DATES
DFT	1/12/67
CHK	1/13/67
APPD	1/13/67
APPD	
APPD	1/13/67
DESIGN ACTIVITY APPD Bob Elliott	2-16-67
OTHER ACTIVITY APPD	

AIRESEARCH MANUFACTURING COMPANY
A DIVISION OF THE GARRETT CORPORATION
PHOENIX, ARIZONA

DWG TITLE
BEARING, BALL, THRUST

3-2-67

SIZE	CODE IDENT NO.	DWG NO.	
C	99193	358498	
SCALE NONE		WT —	SHEET 1 OF 1

FOLDOUT FRAME FOLDOUT FRAME

REVISIONS

SYM	DESCRIPTION	DATE	APPROVAL

SOURCE CONTROL DRAWING

PROCUREMENT PER AVL 521246-1

SHEET INDEX																						
	REVISION SYM																					
	SHEET NO.	1	2	3	4	5	6	7	8	9												

SIGNATURES	DATES
DFT K. R. King	3-10-67
CHK	3-10-67
MFG	
MATL	
~~CHKD~~ RELIABILITY	3-17-67
APP	3-16-67
APP	
DSGN ACTIVITY APP	
OTHER ACTIVITY APP	

AiResearch Manufacturing Company
LOS ANGELES, CALIFORNIA
A Division of THE GARRETT CORPORATION

DWG TITLE
TRANSISTOR, POWER, NPN, SILICON

CODE IDENT NO.	SIZE	DWG NO.	REVISION
70210	A	X521246	SYM

SCALE NONE

SHEET 1 OF 9

1. SCOPE

1.1 SCOPE. THIS SPECIFICATION COVERS THE DETAIL REQUIREMENTS FOR A SILICON NPN POWER TRANSISTOR. IT IS A REPACKAGED VERSION OF COMMERCIALLY AVAILABLE MHT 7604 AND IS INTENDED FOR HIGH RELIABILITY APPLICATIONS.

1.2 PHYSICAL DIMENSIONS. PHYSICAL DIMENSIONS SHALL BE PER FIGURE 1.

1.3 ABSOLUTE MAXIMUM RATINGS. THE VALUES SPECIFIED IN TABLE I (WITH EXCEPTION OF THE THERMAL TIME CONSTANT) ARE LIMITING VALUES ABOVE WHICH THE SERVICEABILITY OF THE DEVICE MAY BE IMPAIRED.

1.4 PRECAUTIONS. DURING HANDLING, INSTALLATION, OR OPERATION, THE APPLICABLE RATINGS OF TABLE II MAY NOT BE EXCEEDED.

2. APPLICABLE DOCUMENTS

2.1 THE FOLLOWING DOCUMENTS FORM A PART OF THIS SPECIFICATION TO THE EXTENT SPECIFIED HEREIN:

MIL-S-19500D - SEMICONDUCTOR DEVICES, GENERAL SPECIFICATION FOR

MIL-STD-750A - TEST METHODS FOR SEMICONDUCTOR DEVICES

3. REQUIREMENTS

3.1 MANUFACTURER'S PROCESSING. THE MANUFACTURER'S FACTORY PROCESSING FOR DEVICES FURNISHED TO THIS SPECIFICATION SHALL INCLUDE BUT NOT BE LIMITED TO THE FOLLOWING PROCEDURES UNLESS OTHERWISE SPECIFIED ON THE PURCHASE ORDER:

3.1.1 HIGH TEMPERATURE STABILIZATION BAKE FOR A MINIMUM OF 60 HOURS AT A MINIMUM TEMPERATURE OF 200°C.

3.1.2 HIGH TEMPERATURE REVERSE BIAS TEST FOR A MINIMUM OF 12 HOURS AT A MINIMUM TEMPERATURE OF 150°C.

3.1.3 APPLICATION OF AT LEAST 5 (FIVE) POWER PULSES AT A 60 Hz REPETITION RATE:

I_c = 7.5 AMPS V_{ce} = 75 VOLTS PW = 100 MICROSECONDS

AT START OF TEST THE CASE TEMPERATURE SHALL BE 25°C

3.1.4 X-RAY INSPECTION IN THREE ORTHOGONAL AXES. THE X-RAY FILMS SHALL BE SHIPPED TO AIRESEARCH AND SHALL BE TRACEABLE TO EACH DEVICE.

3.2 DESIGN CHANGES. ALL DESIGN CHANGES SUBSEQUENT TO SHIPMENT OF THE FIRST LOT FURNISHED TO THIS SPECIFICATION REQUIRE AIRESEARCH ENGINEERING APPROVAL.

3.3 MARKING. EACH PART SHALL BE PERMANENTLY MARKED WITH THE FOLLOWING:

3.3.1 THE AIRESEARCH PART NUMBER AS SHOWN: 521246-1

3.3.2 THE MANUFACTURER'S LOT CODE. THE SUPPLIER SHALL PROVIDE TRACEABILITY FROM THE LOT CODE TO ALL MATERIALS AND PROCESSES USED DURING DEVICE FABRICATION.

3.3.3 SERIAL NUMBER. THE SERIAL NUMBER SHALL BE OMITTED WHEN THE PURCHASE ORDER DELETES THE REQUIREMENTS FOR X-RAY EXAMINATION AND VARIABLES DATA.

3.3.4 THE MANUFACTURER'S IDENTIFICATION.

3.4 PERFORMANCE. THE PERFORMANCE OF THE TRANSISTOR SHALL BE AS SPECIFIED IN TABLES I, II, III, IV AND IN FIGURE 2.

3.4.1 DEFINITIONS, SYMBOLS AND ABBREVIATIONS ARE PER MIL-S-19500.

3.5 RELIABILITY CONDITIONING. UNLESS OTHERWISE SPECIFIED ON THE PURCHASE ORDER, EACH DEVICE PROCURED TO THIS SPECIFICATION SHALL BE PROCESSED AS FOLLOWS AND IN THE ORDER SHOWN.

3.5.1 TEMPERATURE CYCLING. A MINIMUM OF 5 (FIVE) CYCLES T(HIGH) = 200 ±20°C T(LOW) = -65 ±10°C HOLD AT EXTREMES FOR AT LEAST 20 MINUTES AND AT ROOM AMBIENT (DURING TRANSFER) FOR NOT LONGER THAN 5 MINUTES. SPECIFIED AMBIENT TEMPERATURE SHALL BE REACHED WITHIN 2 MINUTES OF TRANSFER.

3.5.2 SHOCK. 1 (ONE) BLOW, 1500 G MINIMUM 0.3 MILLISECOND DURATION, Y_1 AXIS ONLY.

3.5.3 VIBRATION. VARIABLE FREQUENCY PER MIL-STD-750, METHOD 2056, EXCEPT THAT 1 (ONE) CYCLE IS REQUIRED IN EACH OF THREE ORTHOGONAL AXES.

3.5.4 ACCELERATION. 15000 G MINIMUM FOR AT LEAST 1 MINUTE, Y_1 ORIENTATION ONLY.

3.5.5 HERMETIC SEAL

3.5.5.1 FINE LEAK (VEECO). MIL-STD-202C. METHOD 112, TEST CONDITION C, PROCEDURE IIIa. MAXIMUM LEAK RATE 1×10^{-8} ATM CC/SEC. PROCEDURE IV IS ACCEPTABLE

3.5.5.2 GROSS LEAK (BUBBLE TEST). MIL-STD-202C, METHOD 112, TEST CONDITION A. FLUID TO BE POLYETHYLENE GLYCOL AT A MINIMUM TEMPERATURE OF 125°C.

3.5.6 BURN-IN. ALL DEVICES ARE TO BE OPERATED FOR AT LEAST 168 HOURS BUT NOT MORE THAN 240 HOURS UNDER THE FOLLOWING CONDITIONS:

V_{ce} = 10 VDC MIN I_c = 1.0 ADC MIN

T_c = 95°C MIN P_T = 40 W MIN

3.5.6.1 VARIABLES DATA. THE DATA INDICATED IN TABLE V SHALL BE RECORDED BEFORE AND AFTER THE BURN-IN TEST. THIS INFORMATION SHALL BE SHIPPED TO AIRESEARCH TOGETHER WITH THE DEVICES AND SHALL BE TRACEABLE TO EACH DEVICE.

3.5.7 END POINTS. AT THE CONCLUSION OF THE RELIABILITY CONDITIONING THE DEVICES SHALL MEET THE REQUIREMENTS OF TABLE III AND TABLE V.

4. QUALITY ASSURANCE PROVISIONS

4.1 QUALIFICATION TESTING. NOT APPLICABLE

4.2 ACCEPTANCE INSPECTION

4.2.1 ACCEPTANCE INSPECTION SHALL BE IN ACCORDANCE WITH PARAGRAPHS 3.1.4, 3.5.5, 3.5.6 AND 3.5.7.

4.2.2 LOT REJECTION. WHEN MORE THAN 10% OF THE DEVICES IN A LOT SHOW PARAMETER CHANGES IN EXCESS OF THE VALUES SPECIFIED IN TABLE V, THE ENTIRE LOT SHALL BE REJECTED.

4.3 DEVIATIONS. WHEN THE REQUIREMENTS FOR BURN-IN (3.5.5) AND/OR FOR X-RAY INSPECTION (3.1.4) ARE DELETED THE MARKING SHALL BE IN ACCORDANCE WITH PARAGRAPH 3.3.3.

4.3.1 NO OTHER DEVIATIONS ARE PERMITTED. WHEN THE PURCHASE ORDER CALLS FOR THE DELIVERY OF ELECTRICALLY EQUIVALENT DEVICES SUCH DEVICES SHALL BE IDENTIFIED BY THEIR COMMERCIAL PART NUMBER ONLY.

5. GENERAL NOTES

5.1 PROCUREMENT PER AVL 521246-1. ONLY THE ITEMS LISTED ON THE AVL AND IDENTIFIED BY VENDORS NAME, ADDRESS AND PART NUMBERS HAVE BEEN TESTED AND APPROVED FOR USE IN THE END UNIT. SUBSTITUTE ITEM SHALL NOT BE USED PRIOR TO TESTING AND APPROVAL BY AIRESEARCH ENGINEERING.

5.2 PART TO BE PERMANENTLY MARKED WITH THE FOLLOWING: "AIRESEARCH PART NUMBER 521246".

5.3 ALL DESIGN AND PART NUMBER CHANGES REQUIRE AIRESEARCH ENGINEERING APPROVAL.

5.4 IDENTIFY PACKAGING WITH AIRESEARCH PART NUMBER.

5.5 PARTS PROCURED BY VENDOR PART NUMBER SHALL BE PROCURED IN ACCORDANCE WITH THIS SOURCE CONTROL DRAWING.

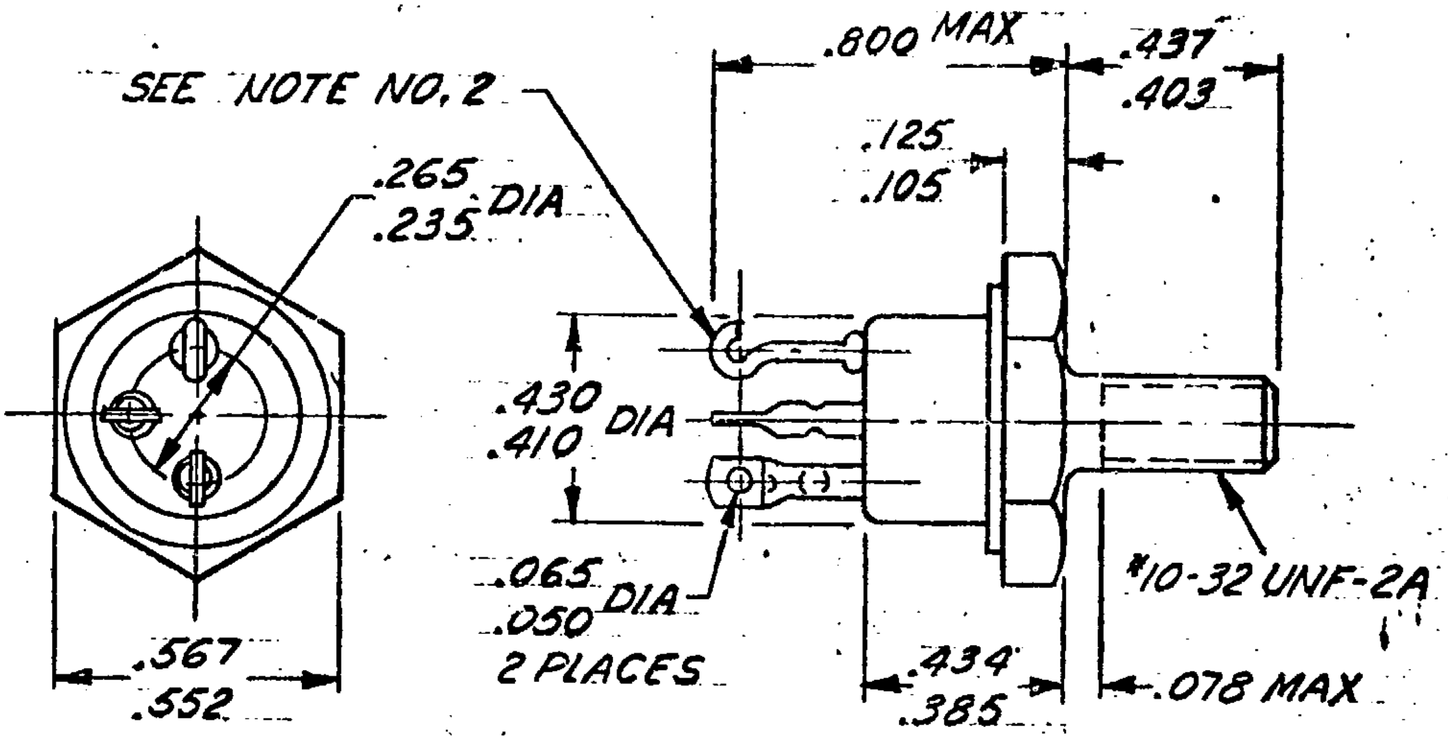

DIMENSIONS IN INCHES.

NOTES:

1. COMPLETE THREADS EXTEND TO WITHIN $2\frac{1}{2}$ THDS OF SEATING PLAN.
2. THIS TERMINAL MAY BE HOOK TYPE OR FLATTENED AND PIERCED.
3. POSITION OF TERMINALS WITH RESPECT TO HEXAGON IS NOT CONTROLLED.
4. COLLECTOR IS ELECTRICALLY COMMON TO CASE.
5. NOMINAL WEIGHT IS 8.4 GM.

SIZE	CODE IDENT NO.	DWG NO.	REV LTR
A	70210	521246	
SCALE NONE		SHEET 5 OF 9	

TABLE I

RATINGS, ELECTRICAL

V_{CBO}	Collector to Base Voltage, Emitter Open	140 vdc max
V_{CEO}	Collector to Emitter Voltage, Base Open	120 vdc max
V_{BEO}	Reverse Base to Emitter Voltage	8.0 vdc max
I_c	Continuous Collector Current	10 A dc max
I_b	Continuous Base Current	2.0 A dc max
P_t	Total Power Dissipation at 100°C Case	40 Watts max
T_j	Junction to Case Thermal Time Constant	.014 Sec. Typ
T_{stg}	Storage Temperature	-65°C to +200°C
T_j	Operating Junction Temperature	-65°C to +200°C

TABLE II

RATINGS, MECHANICAL

Stud Torque	240 Inch-ounces max
Terminal Strength	Torque - 15 Inch-ounces max Tension - 5 pounds max
Soldering Heat	260°C max for 10 seconds max, 1/16' from case
Solderability	MIL-STD-202, Method 208
Shock	1500 G, 0.5 Milliseconds, all orientation
Vibration	20 G, 100 to 2000 cps
Acceleration	15000 G, all orientations
Temperature Cycling	MIL-STD-202, Method 107, Condition C
Glass Strain	MIL-STD-750, Method 1056.1, Condition B
Corrosion	MIL-STD-750, Method 1041.1
Moisture Resistance	MIL-STD-202, Method 106 Followed by MIL-STD-750, Method 1066

TABLE III

ELECTRICAL INSPECTION (1)

PARAMETER	METHOD MIL-STD-750	CONDITIONS	NOTES	LIMITS MIN	LIMITS MAX	UNITS
$BV_{CEO}(SUS)$	3011.1	I_c = 100 ma I_b = 0	2	120		Vdc
I_{CES}	3041.1	V_{EB} = 0 V_{CE} = 120V			1.0	µAdc
I_{CEO1}	3041.1	I_b = 0 V_{CE} = 120V			100	µAdc
I_{CEO2}	3041.1	I_b = 0 V_{CE} = 120V T_c = 150 ±3°C			500	µAdc
I_{EBO}	3061.1	V_{EB} = 5 Vdc I_c = 0			0.50	µAdc
H_{FE1}	3076.1	I_c = 5A V_{CE} = 2 V	2	40	120	
H_{FE2}	3076.1	I_c = 50 mA V_{CE} = 2 V		60	240	
H_{FE3}	3076.1	I_c = 50 mA V_{CE} = 2 V T_c = -55 ±3°C		30		
H_{fe}		I_c = 1A V_{CE} = 10 V f = 10m Hz		$\|2\|$	$\|12\|$	
$V_{CE}(SAT)$	3071	I_c = 5A I_b = 0.5A	2		0.50	Vdc
$V_{BE}(SAT)$	3066.1	I_c = 5A I_b = 0.5A	2		1.50	Vdc
θ_{J-C}	3151				2.5	°C/W

NOTES: 1. Unless otherwise specified all test are to be performed at a case temperature of 25 ±3°C.

2. Pulse Test. Pulse Width 300 ±100 microseconds, nominal duty cycle 2%.

TABLE IV

PULSE RESPONSE

PARAMETER	SYMBOL	METHOD AND CONDITIONS	LIMITS
Turn-on Time	td + tr	MIL-STD-750, Method 3251 Vcc = 30 vdc I_c = 5A (nominal) I_{b1} = 0.5A (nominal) I_{b2} = -0.5A (max)	0.5 µsec max
Storage Time	ts		1.5 µsec max
Fall Time	t_f		0.5 µsec max

TABLE V

PARAMETER VARIATIONS (1)

PARAMETER	CONDITIONS	PRE BURN-IN VALUE	POST BURN-IN VALUE	REJECTION LEVEL	UNITS
I_{CES}	V_{CE} = 120 Vdc V_{BE} = 0			Δ > ±0.5 µAdc	µAdc
H_{FE}	V_{CE} = 2.0 Vdc I_c = 5.0A			Δ > -20%, +30%	-

(1) Measurements at T_c = 25°C nominal

SIZE	CODE IDENT NO.	DWG NO.	REV LTR
A	70210	521246	
SCALE NONE		SHEET 8 OF 9	

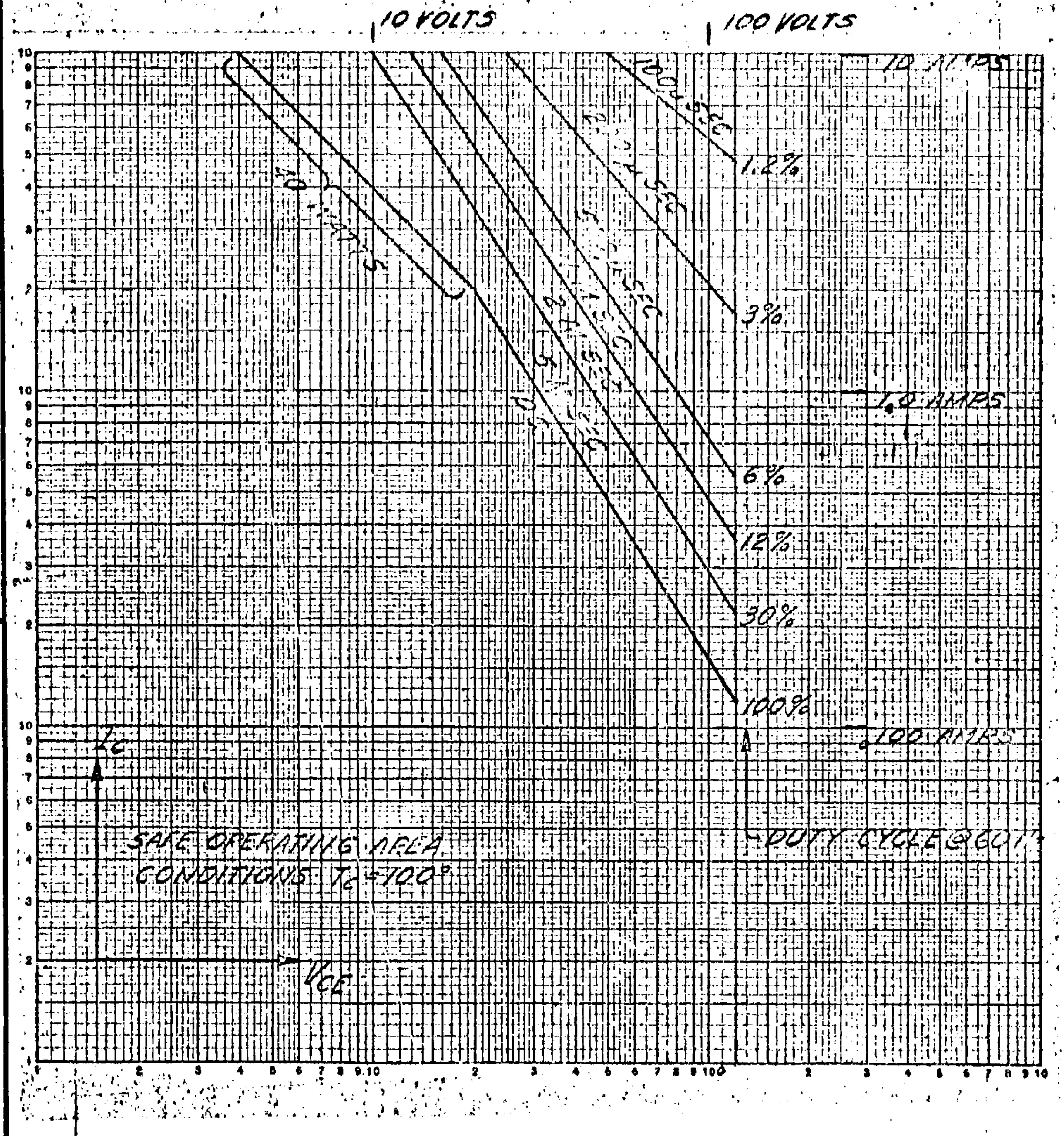

FIGURE 2

SIZE	CODE IDENT NO.	DWG NO.	REV
A	70210	X521246	LTR
SCALE NONE		SHEET 9 OF 9	

AIRESEARCH MANUFACTURING COMPANY
A DIVISION OF THE GARRETT CORPORATION
LOS ANGELES, CALIFORNIA

FORM [illegible] D

AVL 521246-1

APPROVED VENDOR LIST

VENDOR			ENGINEERING APPROVAL	QUALITY CONTROL & PURCHASING CONCURRENCE
NAME AND ADDRESS	PART NUMBER OR DESCRIPTION	CODE IDENT NO.		
SOLITRON DEVICES INC RIVIERA BEACH, FLA.	TRANSISTOR, POWER-SILICON NPN	21845	3-10-67	3/14/67 E. Phillips

REVISIONS	
LET	DATE
A	
B	
C	
D	
E	
F	
G	
H	
J	
K	
L	
M	
N	
P	
R	
S	
T	
U	
V	
W	
Y	
Z	

PREPARED BY K. R. King DATE 3-10-67

AVL 521246-1

CODE M

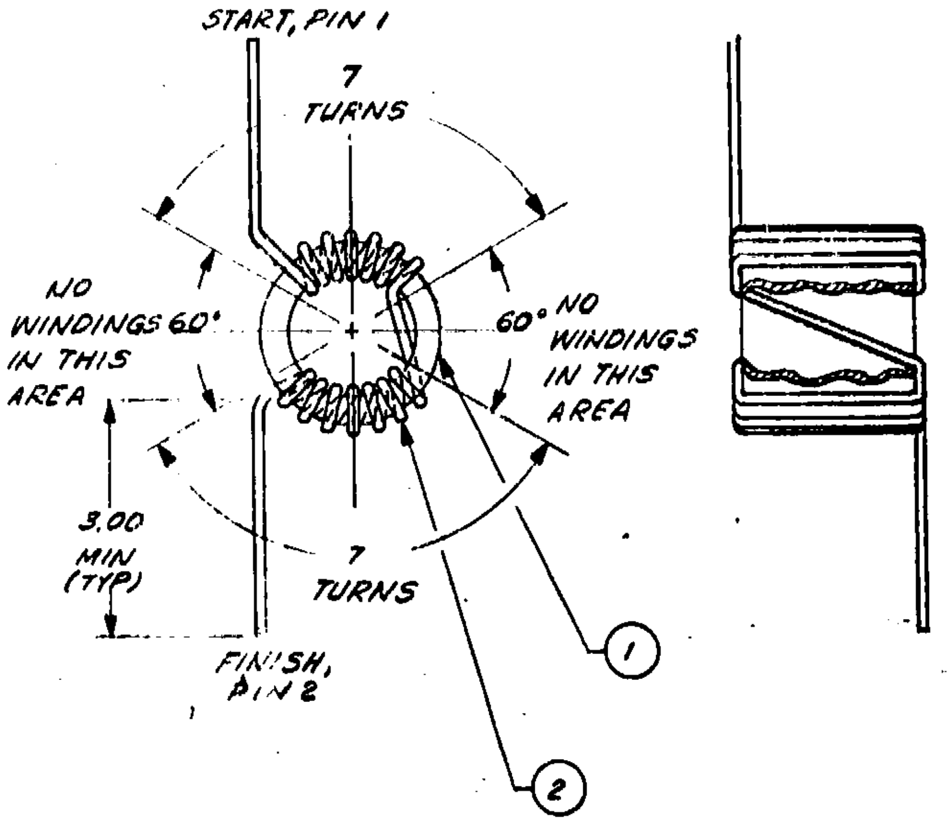

			AR	3	71643	TSPX 1/2
			AR	2		HML
			1	1		521258-1
QTY REQD				ITEM NO.	CODE IDENT NO.	PART OR IDENTIFYING NO
			-1	← ASSY		

3. VENDOR ITEM SEE SOURCE OR SPEC CONTROL DWG.

2. MANUFACTURED BY:
CONNECTICUT HARD RUBBER CO.
NEW HAVEN, CONN.

1. AFTER WINDING AS SHOWN, TRANSFORMERS SHALL BE WRAPPED WITH 2 LAYERS OF TAPE (ITEM 3), VACUUM IMPREGNATE AND CURE PER RS Co.

NOTES: UNLESS OTHERWISE SPECIFIED.

(-1)	521243-1	543936
REQD	NEXT ASSY	USED ON
APPLICATION		

UNLESS OTHERWISE SPECIFIED:
DIMENSIONS ARE IN INCHES.
MACHINE FILLET RADII .015 — .030
SURFACE ROUGHNESS PER MIL-STD-10
BURR CONTROL PER SC653
DIMENSION LIMITS HELD AFTER PLATING
IDENT MARKING PER MC16
DIMENSIONING AND TOL PER MIL-STD-8

HEAT TREATMENT	PROCESS
HARDNESS AND SPEC	NAME AND SPEC

DFT K. R. K
CHK
VALUE ENGR
APPD
APPD
AIRESEARCH APPD
OTHER ACTIVITY AP

FOLDOUT FRAME

FOLDOUT FRAME

REVISIONS			
LTR	DESCRIPTION	DATE	APPROVED
A	SEE REVISION NOTICE	8-14-67	[illegible]

AR	3	71643	TSPX 1/8	TAPE, GLASS			A
AR	2		HML	WIRE, 20GA, PER MIL-W-583, CL 220, TYPE M2			
1	1		521258-1	CORE			
QTY REQD	ITEM NO.	CODE IDENT NO.	PART OR IDENTIFYING NO.	NOMENCLATURE OR DESCRIPTION			SYM
-1	← ASSY			PARTS LIST			

(1)	521243-1	543936
REQD	NEXT ASSY	USED ON
APPLICATION		

UNLESS OTHERWISE SPECIFIED:
DIMENSIONS ARE IN INCHES.
MACHINE FILLET RADII .015 — .030
SURFACE ROUGHNESS PER MIL-STD-10
BURR CONTROL PER SC653
DIMENSION LIMITS HELD AFTER PLATING
IDENT MARKING PER MC16
DIMENSIONING AND TOL PER MIL-STD-8

HEAT TREATMENT	PROCESS
HARDNESS AND SPEC	NAME AND SPEC

CONTRACT NO.

DFT K. R. King	6-28-67
CHK	6-21-67
VALUE ENGR	
	6-21-67
	6-29-67
APPD	6-29-67
APPD	6-29-67
AIRESEARCH APPD	
OTHER ACTIVITY APPD	

GARRETT AIRESEARCH MANUFACTURING COMPANY
A DIVISION OF THE GARRETT CORPORATION
LOS ANGELES, CALIFORNIA

TRANSFORMER ASSY,
SERIES FIELD MODULE

SIZE	CODE IDENT NO.	DWG NO.
C	70210	521247
SCALE 1/1		SHEET 1 OF 1

521247 REV LETTER A

FOLDOUT FRAME FOLDOUT FRAME

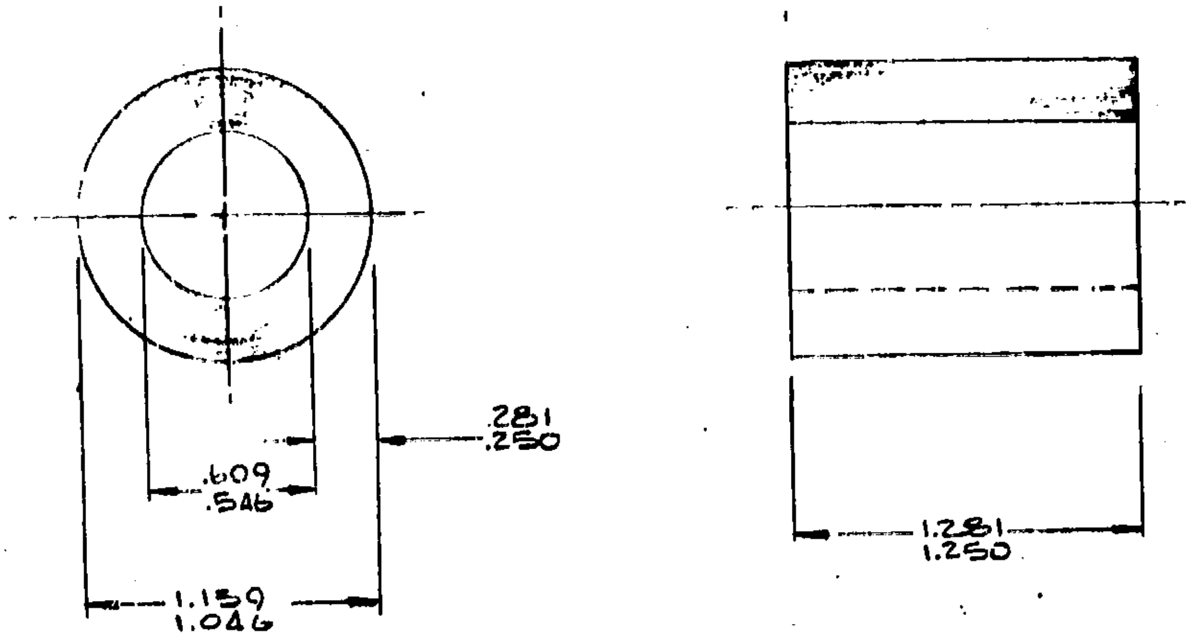

6. PARTS PROCURED BY VENDOR PART NUMBER SHALL BE PROCURED IN ACCORDANCE WITH THIS SOURCE CONTROL DRAWING.

5. IDENTIFY PACKAGING WITH AIRESEARCH PART NUMBER.

4. ALL DESIGN AND PART NUMBER CHANGES REQUIRE AIRESEARCH ENGINEERING APPROVAL.

3. PARTS TO BE PERMANENTLY MARKED WITH THE FOLLOWING: "AIRESEARCH PART NUMBER 521258-1"

2. PROCUREMENT PER AVL 521258-1. ONLY THE ITEMS LISTED ON THE AVL AND IDENTIFIED BY VENDORS NAME, ADDRESS AND PART NUMBER HAVE BEEN TESTED AND APPROVED FOR USE IN THE END UNIT. SUBSTITUTE ITEMS SHALL NOT BE USED PRIOR TO TESTING AND APPROVAL BY AIRESEARCH ENGINEERING.

1. PART TO RECEIVE A COAT OF VENDOR PROPRIETARY "SUPER SEAL", OVER CERAMIC BOND IMPREGNATION, .015 NOMINAL BUILD UP OVER DIMS SHOWN.

NOTES: UNLESS OTHERWISE SPECIFIED

SOURCE

					521258-1		.0
QTY REQD				ITEM NO.	PART NO.	SYM	
				←ASSY			

UNLESS OTHERWISE SPECIFIED:
DIMENSIONS ARE IN INCHES.
MACHINE FILLET RADII .015—.030
SURFACE ROUGHNESS PER MIL-STD-10
BURR CONTROL PER BC653
DIMENSION LIMITS HELD AFTER PLATING
IDENT MARKING PER MC16
DIMENSIONING AND TOL PER MIL-STD-8

(-1)	521247-1	52124C-
REQD	NEXT ASSY	USED ON
APPLICATION		

HEAT TREATMENT	PROCESS
HARDNESS AND SPEC	NAME AND SPEC

SIGNA
DFT J.W.
CHK
VALUE ENGR
MATL
STRESS
APPD
APPD
AIRESEARCH
OTHER ACTIV

FOLDOUT FRAME

FOLDOUT FRAME

REVISIONS			
LTR	DESCRIPTION	DATE	APPROVED
A	SEE REVISION NOTICE	6.16.67	

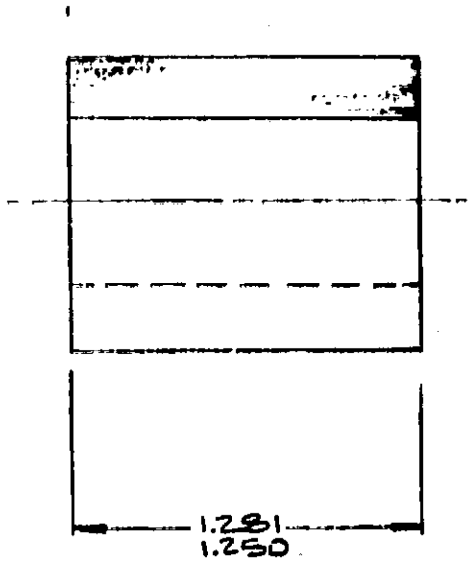

BER.

SOURCE CONTROL DRAWING

EMS

ARCH

REV A LETTER

521258

QTY REQD	ITEM NO.	PART NO.	SYM	DESCRIPTION	CODE IDENT	MATERIAL AND SPECIFICATION
		521258-1		.004 SHEET X LENGTH A/R		TYPE Z, SILECTRON, COMML
←ASSY		LIST OF MATERIAL				

UNLESS OTHERWISE SPECIFIED:
DIMENSIONS ARE IN INCHES.
MACHINE FILLET RADII .015—.030
SURFACE ROUGHNESS PER MIL-STD-10
BURR CONTROL PER SC653
DIMENSION LIMITS HELD AFTER PLATING
IDENT MARKING PER MC18
DIMENSIONING AND TOL PER MIL-STD-8

HEAT TREATMENT	PROCESS
HARDNESS AND SPEC	NAME AND SPEC

SIGNATURES	DATES
DFT	5/26/67
CHK	
VALUE ENGR	6-12-67
MATL	
STRESS	
APPD	
APPD	
AIRESEARCH APPD	
OTHER ACTIVITY APPD	

AIRESEARCH MANUFACTURING COMPANY
A DIVISION OF THE GARRETT CORPORATION
LOS ANGELES, CALIFORNIA

CORE, TOROID

SIZE	CODE IDENT NO.	DWG NO.
C	70210	X521258

SCALE 2:1 SHEET 1 OF 1

REQD	NEXT ASSY	USED ON
1(-1)	521241-1	521240-1

APPLICATION

FOLDOUT FRAME

FOLDOUT FRAME

AIRESEARCH MANUFACTURING COMPANY
A DIVISION OF THE GARRETT CORPORATION
LOS ANGELES, CALIFORNIA

FORM 2986 D

AVL 521258-1

APPROVED VENDOR LIST

VENDOR			ENGINEERING APPROVAL	QUALITY CONTROL & PURCHASING CONCURRENCE	REVISIONS	
NAME AND ADDRESS	PART NUMBER OR DESCRIPTION	CODE IDENT NO.			LET	DATE
CARSTEDT RESEARCH 2501 E. 68th ST LONG BEACH, CALIF	CORE, TOROID CRZ-10-TM	09797	93-7	QC 6/6/67 H. [illegible] 6/6/67	A	
					B	
					C	
					D	
					E	
					F	
					G	
					H	
					J	
					K	
					L	
					M	
					N	
					P	
					R	
					S	
					T	
					U	
					V	
					W	
					Y	
					Z	

PREPARED BY Kenneth R. King DATE 6-6-67

AVL 521258-1

REVISIONS

LTR	DESCRIPTION	DATE	APPROVAL
A	SEE DRAWING REVISION NOTICE	9.29.67	Bauk
B	SEE DRN	12-7-67	

SOURCE CONTROL DRAWING
FOR PROCUREMENT SEE AVL 521259-1

SHEET INDEX								
REVISION LTR	B		A	B		A	
SHEET NO.	1	2	3	4	5	6	7

SIGNATURES	DATES
DFT K. R. King	6-14-67
CHK L Spencer	6-19-67
APP'D RE/IAB/KEY	6-27-67
APP'D QC	6-19-67
DSGN ACTIVITY KK	6-28-67
OTHER ACTIVITY	

AIRESEARCH MANUFACTURING COMPANY
A DIVISION OF THE GARRETT CORPORATION
LOS ANGELES, CALIFORNIA

POWER TRANSFORMER,
3 PHASE

SIZE A
CODE IDENT NO. 70210
DWG NO. 521259
REV B
SCALE NONE
SHEET 1 OF 7

SPECIFICATION

1. SCOPE

1.1 SCOPE. THIS SPECIFICATION COVERS THE DETAIL REQUIREMENTS FOR A 3-PHASE POWER TRANSFORMER.

1.2 RATING.

1.2.1 PRIMARY: 208 VRMS LINE-TO-LINE

1.2.2 SECONDARY: 32 VRMS LINE-TO-LINE, NO-LOAD

1.2.3 POWER: 220 VA

1.2.4 FREQUENCY: 1200 HZ

1.3 SCHEMATIC, TERMINATIONS, AND DIMENSIONS SHALL BE PER FIGURES (1) AND (2).

2. REQUIREMENTS

2.1 CONSTRUCTION. CONSTRUCTION SHALL BE PER MIL-T-27B GRADE 5, CLASS T, FAMILY 02.

2.2 LIFE EXPECTANCY. DESIGN LIFE SHALL BE 20 YEARS MINIMUM.

2.3 ENVIRONMENT. THE UNIT SHALL BE DESIGNED TO OPERATE IN A VACUUM WITH ALL HEAT TRANSFER TAKING PLACE AT THE MOUNTING PLATE. THE MOUNTING BASE TEMPERATURE WILL BE MAINTAINED AT 70°C MAXIMUM.

2.4 VIBRATION, HIGH FREQUENCY. THE TRANSFORMER SHALL BE DESIGNED TO MEET THE HIGH FREQUENCY VIBRATION REQUIREMENTS OF MIL-T-27B.

2.5 DESIGN INFORMATION.

2.5.1 CORE: CTL-22 MANUFACTURED BY CARSTEDT RESEARCH INC., LONG BEACH, CALIFORNIA, OR EQUIVALENT.

CORE SHALL BE LAPPED TO MINIMIZE AIR GAPS.

2.5.2 PRIMARIES: 350 ±2 TURNS HEAVY ML OR AI 220 WIRE.

2.5.3 SECONDARIES: 54 ±1 TURNS HEAVY ML OR AI 220 WIRE.

2.5.4 FLUX DENSITY (REF): 7400 GAUSS.

2.5.5 COILS USED IN ANY ONE TRANSFORMER SHALL HAVE MATCHED TURNS RATIOS IN ORDER TO AVOID FUNDAMENTAL FREQUENCY CIRCULATING CURRENTS.

2.6 MATERIALS.

2.6.1 INSULATION: ISOMICA

2.6.2 ENCAPSULANT: STYCAST 1090 WITH CATALYST NO. 9, MANUFACTURED BY EMERSON AND CUMMINGS, GARDENA, CALIFORNIA.

2.6.3 MOUNTING BASE: BLACK ANODIZED ALUMINUM.

2.6.4 PAINT WITH CORLAR EPOXY ENAMEL 585 BLACK E. I. DU PONT DE NEMOURS AND COMPANY, WILMINGTON, DELAWARE.

2.7 TERMINATIONS.

2.7.1 TERMINATIONS SHALL BE BY MEANS OF DOUBLE TURRET SOLDER TERMINALS, LERCO TYPE 4045 OR EQUIVALENT.

2.7.2 INTERNAL TERMINATIONS SHALL NOT BE DAMAGEABLE BY NORMAL SOLDERING OPERATIONS AS ASSOCIATED WITH THE INSTALLATION OF THE TRANSFORMER.

2.8 MARKING.

2.8.1 THE MARKING INK SHALL BE TYPE MFR-73X, WHITE OR ORANGE, MANUFACTURED BY INDEPENDENT INK COMPANY.

2.8.2 THE MARKING SHALL INCLUDE AS A MINIMUM THE FOLLOWING:

2.8.2.1 THE AIRESEARCH PART NUMBER (SEE GENERAL NOTES)

2.8.2.2 TERMINAL IDENTIFICATION (SEE DRAWING)

2.8.2.3 THE MANUFACTURER'S IDENTIFICATION

2.8.2.4 THE DATE CODE AND SERIAL NUMBER CONSISTING OF A NINE DIGIT NUMBER AS FOLLOWS:

FIRST TWO DIGITS:	YEAR
SECOND TWO DIGITS:	MONTH
THIRD TWO DIGITS:	DAY
LAST THREE DIGITS:	SERIAL NUMBER

3. RELIABILITY CONDITIONING

EACH TRANSFORMER SHIPPED TO THIS SPECIFICATION SHALL BE SUBJECTED TO THE PROCEDURE DEFINED BY MIL-STD-202, METHOD 107B, TEST CONDITION A, EXCEPT LOW TEMPERATURE LIMIT SHALL BE -55 ±5°C, HIGH TEMPERATURE LIMIT SHALL BE +120 ±5°C. AFTER THIS PROCEDURE EACH TRANSFORMER SHALL BE INSPECTED TO THE REQUIREMENT OF PARAGRAPH 4 OF THIS SPECIFICATION.

4. ACCEPTANCE INSPECTION

4.1 ACCEPTANCE INSPECTION SHALL INCLUDE AS A MINIMUM THE FOLLOWING TEST AND MEASUREMENTS PERFORMED TO THE APPLICABLE REQUIREMENTS AND METHODS OF MIL-T-27B EXCEPT AS NOTED HEREIN.

4.1.1 VISUAL AND MECHANICAL INSPECTION.

4.1.2 DIELECTRIC WITHSTANDING VOLTAGE AT ATMOSPHERIC PRESSURE ONLY.

4.1.3 INSULATION RESISTANCE FOLLOWING PROCEDURE OF PARAGRAPH 4.1.2. MINIMUM RESISTANCE 10,000 MEGOHMS.

4.1.4 TURNS RATIO AND POLARITY.

4.1.5 <u>DC RESISTANCE</u>. DC RESISTANCE SHALL BE MEASURED BETWEEN THE FOLLOWING TERMINAL PAIRS AT AMBIENT ROOM TEMPERATURE.

1 AND 2	2 AND 3	3 AND 1	LIMIT: 2.5 ± .5 ohms
4 AND 5	5 AND 6	6 AND 4	LIMIT: .08 ± .03 ohms

4.1.6 <u>EXCITING CURRENT</u>. THE EXCITING CURRENT SHALL BE MEASURED BY MEANS OF THE TEST SETUP SHOWN BETWEEN TERMINALS 1 AND 2, 2 AND 3, 3 AND 1.

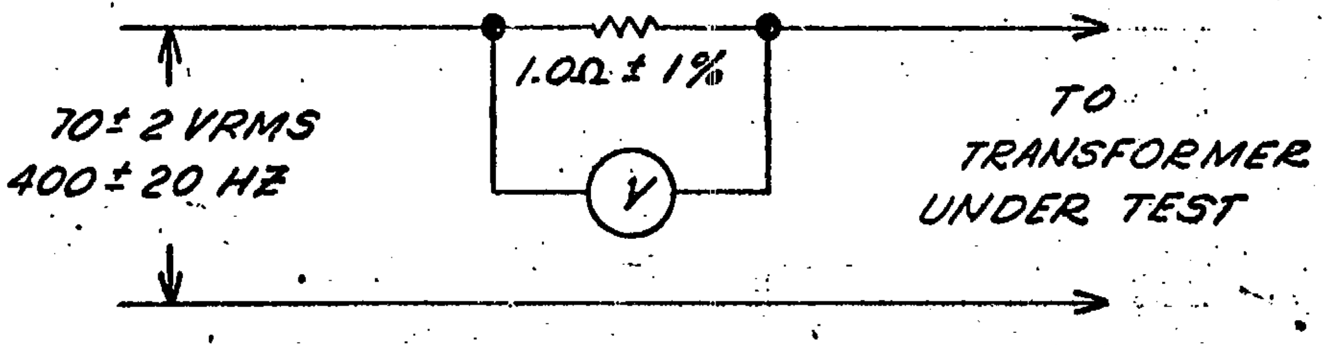

THE VOLT METER SHALL BE HEWLETT PACKARD MODEL 400H OR EQUIVALENT. LIMIT: 50.0 MILLIVOLTS RMS MAXIMUM.

4.2 <u>DATA</u>. THE DATA OBTAINED FROM THE TEST OF PARAGRAPH 4.1 SHALL BE RECORDED ON A SUITABLE FORM AND SHIPPED TO AIRESEARCH TOGETHER WITH THE PARTS. THE DATA FORM SHALL IDENTIFY ALL INSTRUMENTS INCLUDING SERIAL NUMBERS AND THE NEXT CALIBRATION DUE DATE.

SIZE	CODE IDENT NO.	DWG NO.	REV LTR
A	70210	521259	B
SCALE NONE		SHEET 4 OF 7	

5. GENERAL NOTES

5.1 PROCUREMENT PER AVL 521259-1. ONLY THE ITEMS LISTED ON THE AVL AND IDENTIFIED BY VENDOR'S NAME, ADDRESS, AND PART NUMBER HAVE BEEN TESTED AND APPROVED FOR USE IN THE END ITEM. SUBSTITUTE ITEMS SHALL NOT BE USED PRIOR TO TESTING AND APPROVAL BY AIRESEARCH ENGINEERING.

5.2 ALL DESIGN AND PART NUMBER CHANGES REQUIRE AIRESEARCH ENGINEERING APPROVAL.

5.3 IDENTIFY PACKAGING WITH AIRESEARCH PART NUMBER 521259-1.

5.4 PARTS PROCURED BY VENDOR PART NUMBER SHALL BE PROCURED IN ACCORDANCE WITH THIS SOURCE CONTROL DRAWING.

SIZE	CODE IDENT NO.	DWG NO.	REV
A	70210	521259	LTR
SCALE NONE		SHEET 5 OF 7	

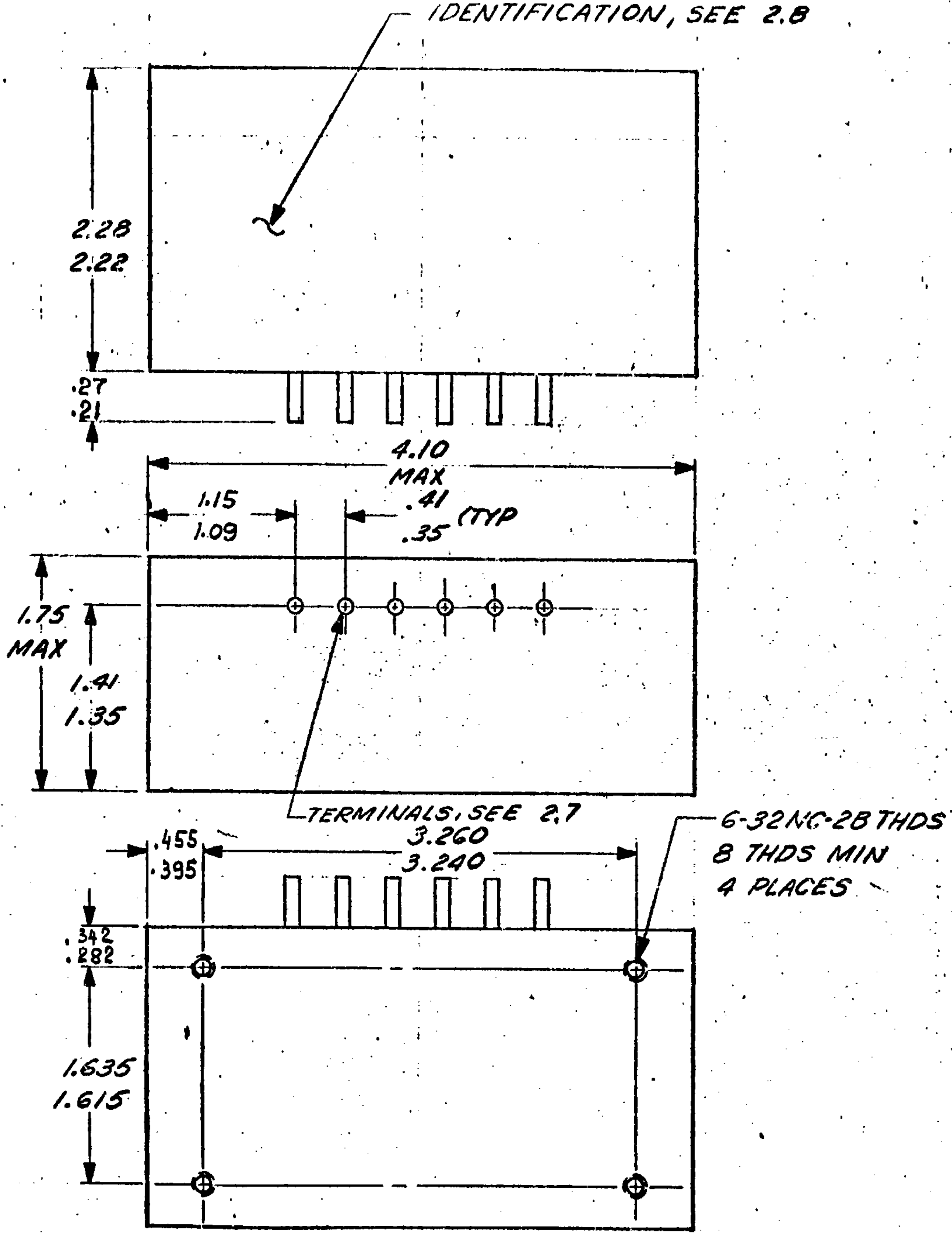

SIZE A	CODE IDENT NO. 70210	DWG NO. 521259	REV A LTR
SCALE 1/1		SHEET 6 OF 7	

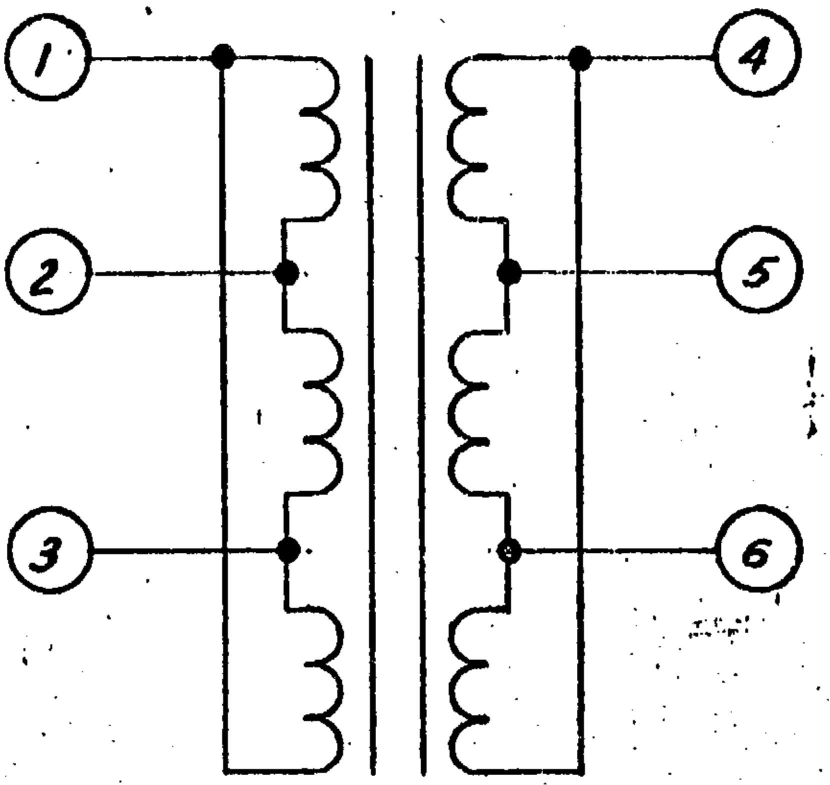

SCHEMATIC DIAGRAM

SIZE	CODE IDENT NO.	DWG NO.	REV LTR
A	70210	521259	
SCALE NONE		SHEET 7 OF 7	

AIRESEARCH MANUFACTURING COMPANY
A DIVISION OF THE GARRETT CORPORATION
LOS ANGELES, CALIFORNIA

FORM 3956 D

AVL 5212[illegible]-1

APPROVED VENDOR LIST

VENDOR				
NAME AND ADDRESS	PART NUMBER OR DESCRIPTION	CODE IDENT NO.	ENGINEERING APPROVAL	QUALITY CONTROL & PURCHASING CONCURRENCE
MAGNETIKA INC SANTA MONICA, CALIF.	3 PHASE POWER XMFR 01993	15634	Rudick	[illegible] Q.C. 6/19/67 [illegible] 6/20/67

REVISIONS	
LET	DATE
A	
B	
C	
D	
E	
F	
G	
H	
J	
K	
L	
M	
N	
P	
R	
S	
T	
U	
V	
W	
Y	
Z	

PREPARED BY K. R. King DATE 6-14-67

AVL 5[illegible]

CODE

REVISIONS

LTR	DESCRIPTION	DATE	APPROVAL
A	SEE DRAWING REVISION NOTICE	9.29.67	

SOURCE CONTROL DRAWING
FOR PROCUREMENT SEE AVL521260-1

SHEET INDEX								
	REVISION LTR	A		A	A		A	
	SHEET NO.	1	2	3	4	5	6	7

SIGNATURES	DATES
DFT K. King	6-19-67
CHK L. Spellman	6-19-67
APPD RELIABILITY Carl Phillips	6-21-67
APP D	6-14-67
DSGN ACTIVITY	6-22-67
OTHER ACTIVITY	

AIRESEARCH MANUFACTURING COMPANY
A DIVISION OF THE GARRETT CORPORATION
LOS ANGELES, CALIFORNIA

TRANSFORMER, SENSING - 3 ∅
PHASE

SIZE	CODE IDENT NO.	DWG NO	REV LTR
A	70210	521260	A

SCALE NONE

SHEET 1 OF 7

SPECIFICATION

1. SCOPE

1.1 SCOPE. THIS SPECIFICATION COVERS THE DETAIL REQUIREMENTS FOR A 3-PHASE SENSING TRANSFORMER.

1.2 RATING.

1.2.1 PRIMARY: 208 VRMS LINE-TO-LINE

1.2.1 SECONDARY: 25 VRMS LINE-TO-NEUTRAL, NO-LOAD

1.2.3 POWER: 4.4 VA

1.2.4 FREQUENCY: 1200 HZ

1.3 SCHEMATIC, TERMINATIONS, AND DIMENSIONS SHALL BE PER FIGURES (1) AND (2).

2. REQUIREMENTS

2.1 CONSTRUCTION. CONSTRUCTION SHALL BE PER MIL-T-27B GRADE 5, CLASS T, FAMILY 02.

2.2 LIFE EXPECTANCY. DESIGN LIFE SHALL BE 20 YEARS MINIMUM.

2.3 ENVIRONMENT. THE UNIT SHALL BE DESIGNED TO OPERATE IN A VACUUM WITH ALL HEAT TRANSFER TAKING PLACE AT THE MOUNTING PLATE. THE MOUNTING BASE TEMPERATURE WILL BE MAINTAINED AT 70°C MAXIMUM.

2.4 VIBRATION, HIGH FREQUENCY. THE TRANSFORMER SHALL BE DESIGNED TO MEET THE HIGH FREQUENCY VIBRATION REQUIREMENTS OF MIL-T-27B.

2.5 DESIGN INFORMATION.

2.5.1 CORE: CTL-8 MANUFACTURED BY CARSTEDT RESEARCH INC., LONG BEACH, CALIFORNIA, OR EQUIVALENT.

CORE SHALL BE LAPPED TO MINIMIZE AIR GAPS.

2.5.2 PRIMARIES: 1900 ±20 TURNS HEAVY ML OR AI 220 WIRE.

2.5.3 SECONDARIES: 229 ±2 TURNS HEAVY ML OR AI 220 WIRE.

2.5.4 FLUX DENSITY (REF): 7400 GAUSS.

2.6 MATERIALS.

2.6.1 INSULATION: ISOMICA.

2.6.2 ENCAPSULANT: STYCAST 1090 WITH CATALYST NO. 9, MANUFACTURED BY EMERSON AND CUMMINGS, GARDENA, CALIFORNIA.

2.6.3 MOUNTING BASE: BLACK ANODIZED ALUMINUM.

2.6.4 PAINT WITH CORLAR EPOXY ENAMEL 585 BLACK E. I. DU PONT DE NEMOURS AND COMPANY, WILMINGTON, DELAWARE.

2.7 TERMINATIONS.

2.7.1 TERMINATIONS SHALL BE BY MEANS OF DOUBLE TURRET SOLDER TERMINALS, LERCO TYPE 5010 OR EQUIVALENT.

2.7.2 INTERNAL TERMINATIONS SHALL NOT BE DAMAGEABLE BY NORMAL SOLDERING OPERATIONS AS ASSOCIATED WITH THE INSTALLATION OF THE TRANSFORMER.

2.8 MARKING.

2.8.1 THE MARKING INK SHALL BE TYPE MFR-73X, WHITE OR ORANGE, MANUFACTURED BY INDEPENDENT INK COMPANY.

2.8.2 THE MARKING SHALL INCLUDE AS A MINIMUM THE FOLLOWING:

2.8.2.1 THE AIRESEARCH PART NUMBER (SEE GENERAL NOTES)

2.8.2.2 TERMINAL IDENTIFICATION (SEE DRAWING)

2.8.2.3 THE MANUFACTURER'S IDENTIFICATION

2.8.2.4 THE DATE CODE AND SERIAL NUMBER CONSISTING OF A NINE DIGIT NUMBER AS FOLLOWS:

FIRST TWO DIGITS:	YEAR
SECOND TWO DIGITS:	MONTH
THIRD TWO DIGITS:	DAY
LAST THREE DIGITS:	SERIAL NUMBER

3. RELIABILITY CONDITIONING

EACH TRANSFORMER SHIPPED TO THIS SPECIFICATION SHALL BE SUBJECTED TO THE PROCEDURE DEFINED BY MIL-STD-202, METHOD 107B, TEST CONDITION A, EXCEPT LOW TEMPERATURE LIMIT SHALL BE -55 ±5°C, HIGH TEMPERATURE LIMIT SHALL BE +120 ±5°C. AFTER THIS PROCEDURE EACH TRANSFORMER SHALL BE INSPECTED TO THE REQUIREMENT OF PARAGRAPH 4 OF THIS SPECIFICATION.

4. ACCEPTANCE INSPECTION

4.1 ACCEPTANCE INSPECTION SHALL INCLUDE AS A MINIMUM THE FOLLOWING TESTS AND MEASUREMENTS PERFORMED TO THE APPLICABLE REQUIREMENTS AND METHODS OF MIL-T-27B EXCEPT AS NOTED HEREIN.

4.1.1 VISUAL AND MECHANICAL INSPECTION.

4.1.2 DIELECTRIC WITHSTANDING VOLTAGE AT ATMOSPHERIC PRESSURE ONLY.

4.1.3 INSULATION RESISTANCE FOLLOWING PROCEDURE OF PARAGRAPH 4.1.2. MINIMUM RESISTANCE 10,000 MEGOHMS.

4.1.4 TURNS RATIO AND POLARITY.

4.1.5 DC RESISTANCE. DC RESISTANCE SHALL BE MEASURED BETWEEN THE FOLLOWING TERMINAL PAIRS AT AMBIENT ROOM TEMPERATURE.

1 AND 2	2 AND 3	3 AND 1	LIMIT: 180 ± 30 ohms
4 AND 5	5 AND 6	6 AND 4	LIMIT: 18 ±3 OHMS

4.1.6 EXCITING CURRENT. THE EXCITING CURRENT SHALL BE MEASURED BY MEANS OF THE TEST SETUP SHOWN BETWEEN TERMINALS 1 AND 2, 2 AND 3, 3 AND 1.

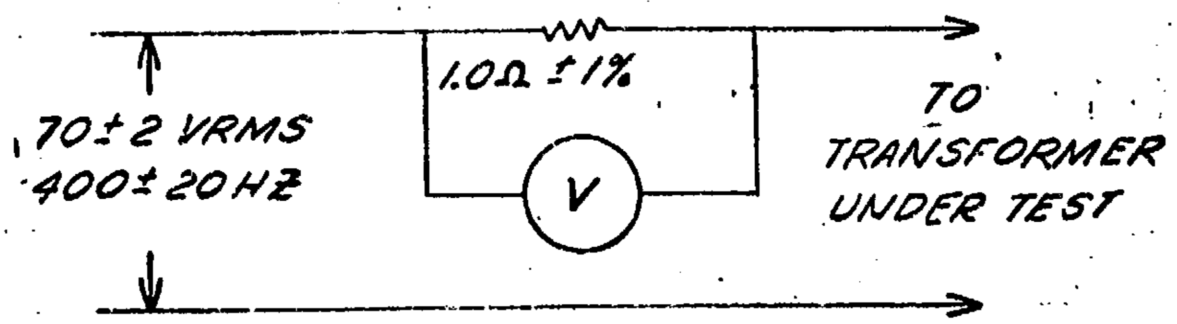

THE VOLT METER SHALL BE HEWLETT PACKARD MODEL 400 H OR EQUIVALENT. LIMIT: 10 MILLIVOLTS RMS MAXIMUM.

4.2 DATA. THE DATA OBTAINED FROM THE TEST OF PARAGRAPH 4.1 SHALL BE RECORDED ON A SUITABLE FORM AND SHIPPED TO AIRESEARCH TOGETHER WITH THE PARTS. THE DATA FORM SHALL IDENTIFY ALL INSTRUMENTS INCLUDING SERIAL NUMBERS AND THE NEXT CALIBRATION DUE DATE.

5. GENERAL NOTES

5.1 PROCUREMENT PER AVL 521260-1. ONLY THE ITEMS LISTED ON THE AVL AND IDENTIFIED BY VENDOR'S NAME, ADDRESS, AND PART NUMBER HAVE BEEN TESTED AND APPROVED FOR USE IN THE END ITEM. SUBSTITUTE ITEMS SHALL NOT BE USED PRIOR TO TESTING AND APPROVAL BY AIRESEARCH ENGINEERING.

5.2 ALL DESIGN AND PART NUMBER CHANGES REQUIRE AIRESEARCH ENGINEERING APPROVAL.

5.3 IDENTIFY PACKAGING WITH AIRESEARCH PART NUMBER 521260-1.

5.4 PARTS PROCURED BY VENDOR PART NUMBER SHALL BE PROCURED IN ACCORDANCE WITH THIS SOURCE CONTROL DRAWING.

SIZE A	CODE IDENT NO. 70210	DWG NO. 521260	REV LTR
SCALE NONE		SHEET 5 OF 7	

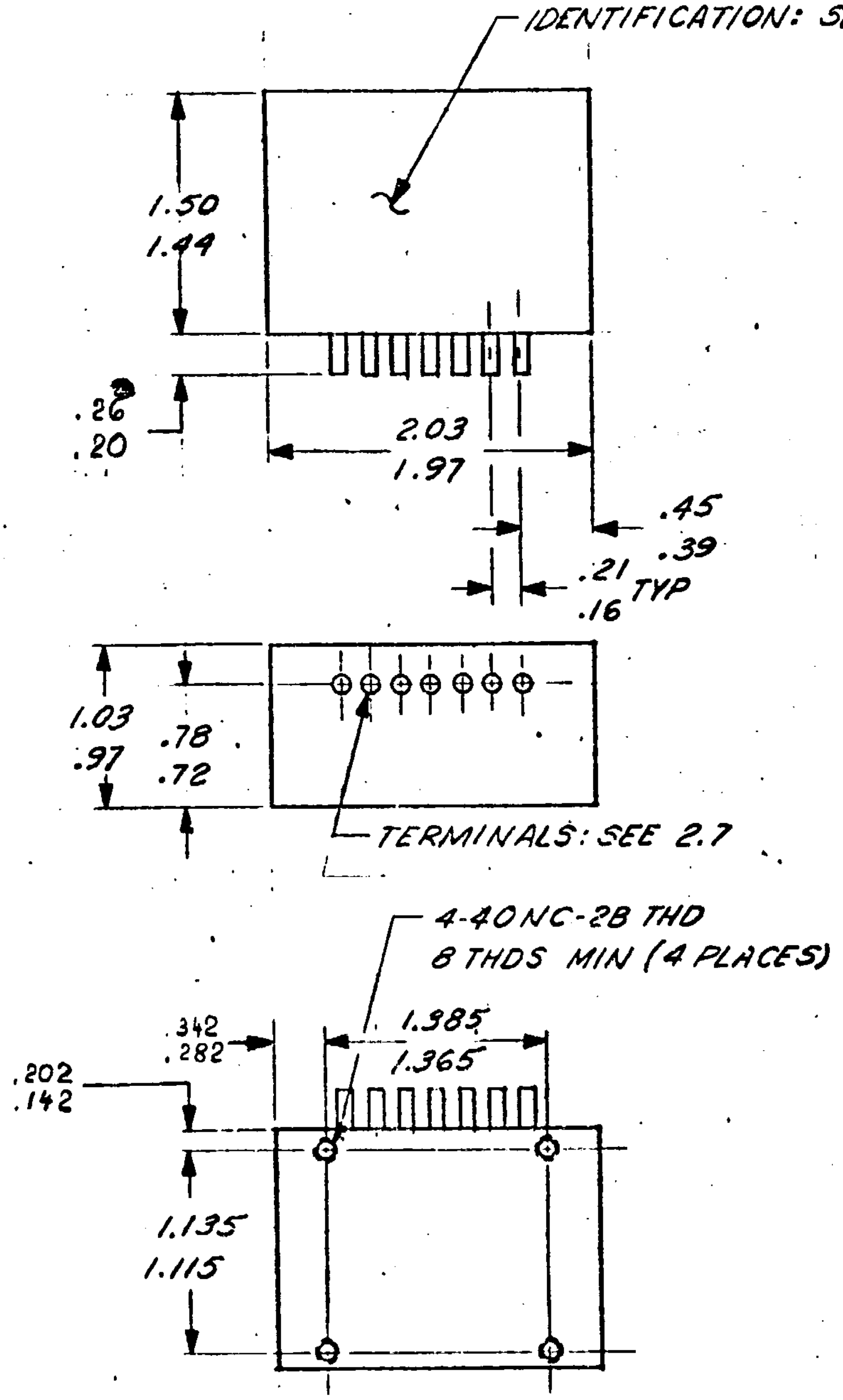

SIZE	CODE IDENT NO.	DWG NO.	REV
A	70210	521260	A LTR
SCALE NONE		SHEET 6 OF 7	

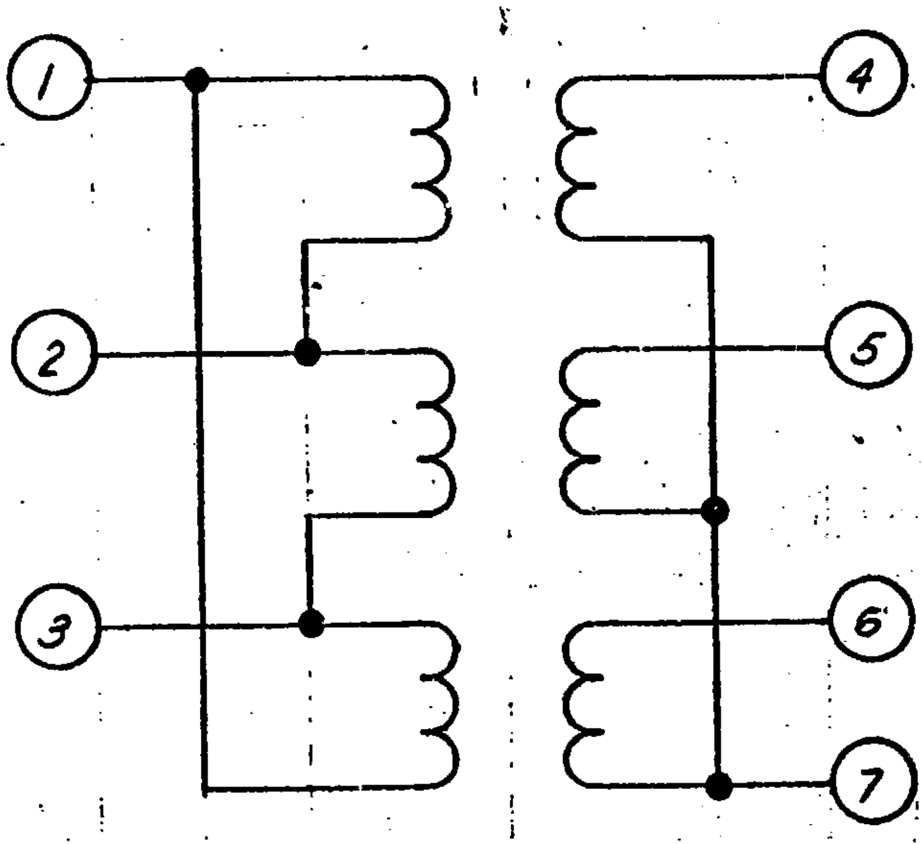

SCHEMATIC DIAGRAM

SIZE	CODE IDENT NO.	DWG NO.	REV LTR
A	70210	521260	
SCALE NONE		SHEET 7 OF 7	

AIRESEARCH MANUFACTURING COMPANY
A DIVISION OF THE GARRETT CORPORATION
LOS ANGELES, CALIFORNIA

FORM 2866D

AVL 521260-1

APPROVED VENDOR LIST

VENDOR			ENGINEERING APPROVAL	QUALITY CONTROL & PURCHASING CONCURRENCE
NAME AND ADDRESS	PART NUMBER OR DESCRIPTION	CODE IDENT NO.		
MAGNETIKA INC SANTA MONICA, CALIF.	3 PHASE SENSING XMFR 01999	15634	Rudich	Q.C. 6/19/67 6/30/67

REVISIONS	
LET	DATE
A	
B	
C	
D	
E	
F	
G	
H	
J	
K	
L	
M	
N	
P	
R	
S	
T	
U	
V	
W	
Y	
Z	

PREPARED BY K. King DATE 6-19-67

AVL [illegible]

OUTLINE NUMBER	END UNIT IDENTIFICATION NO	ASSEMBLY NUMBER
699650-1	NOC 699650-1	699651-1

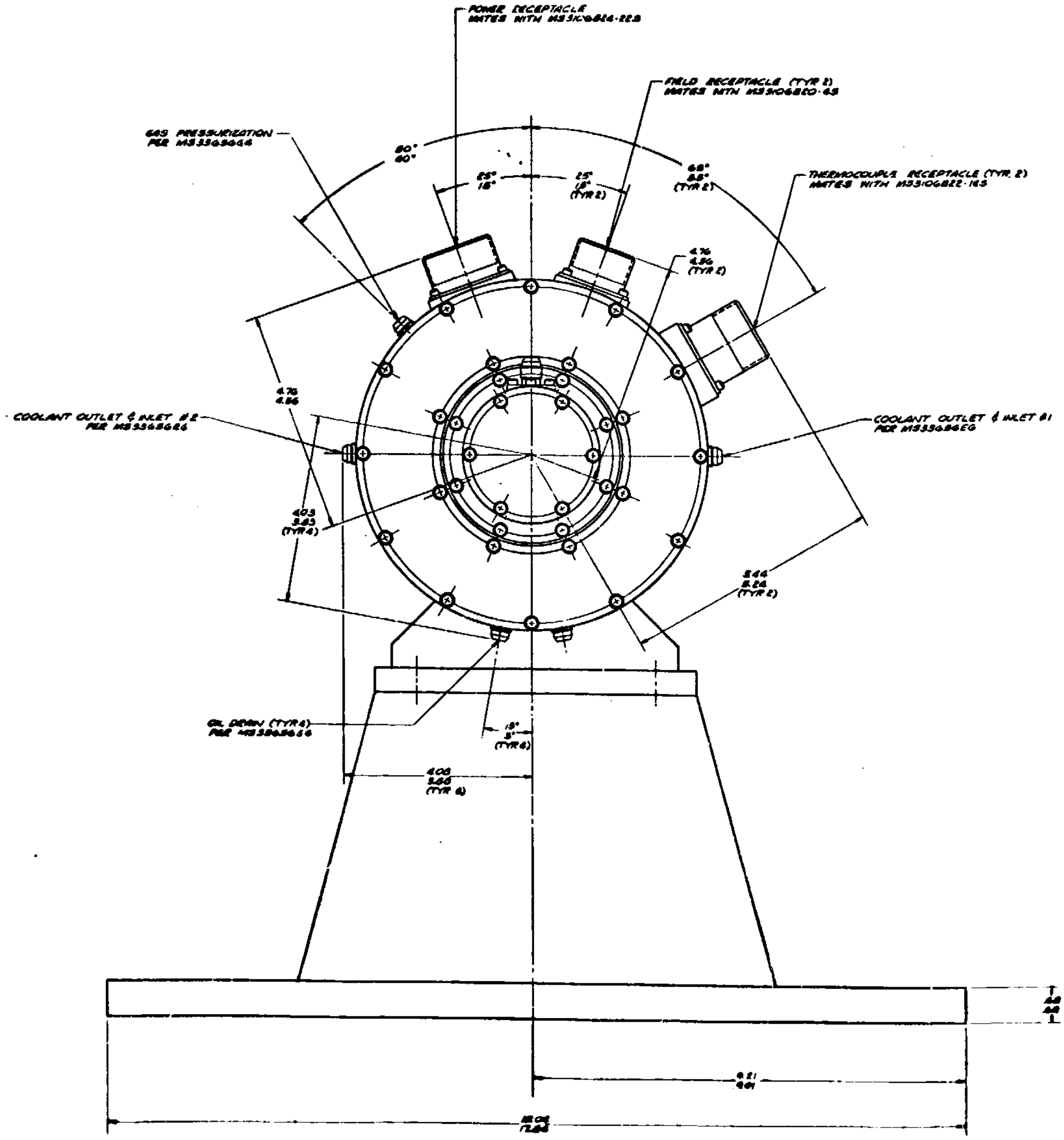

FOLDOUT FRAME

FOLDOUT FRAME

10
9
8
7
6
5

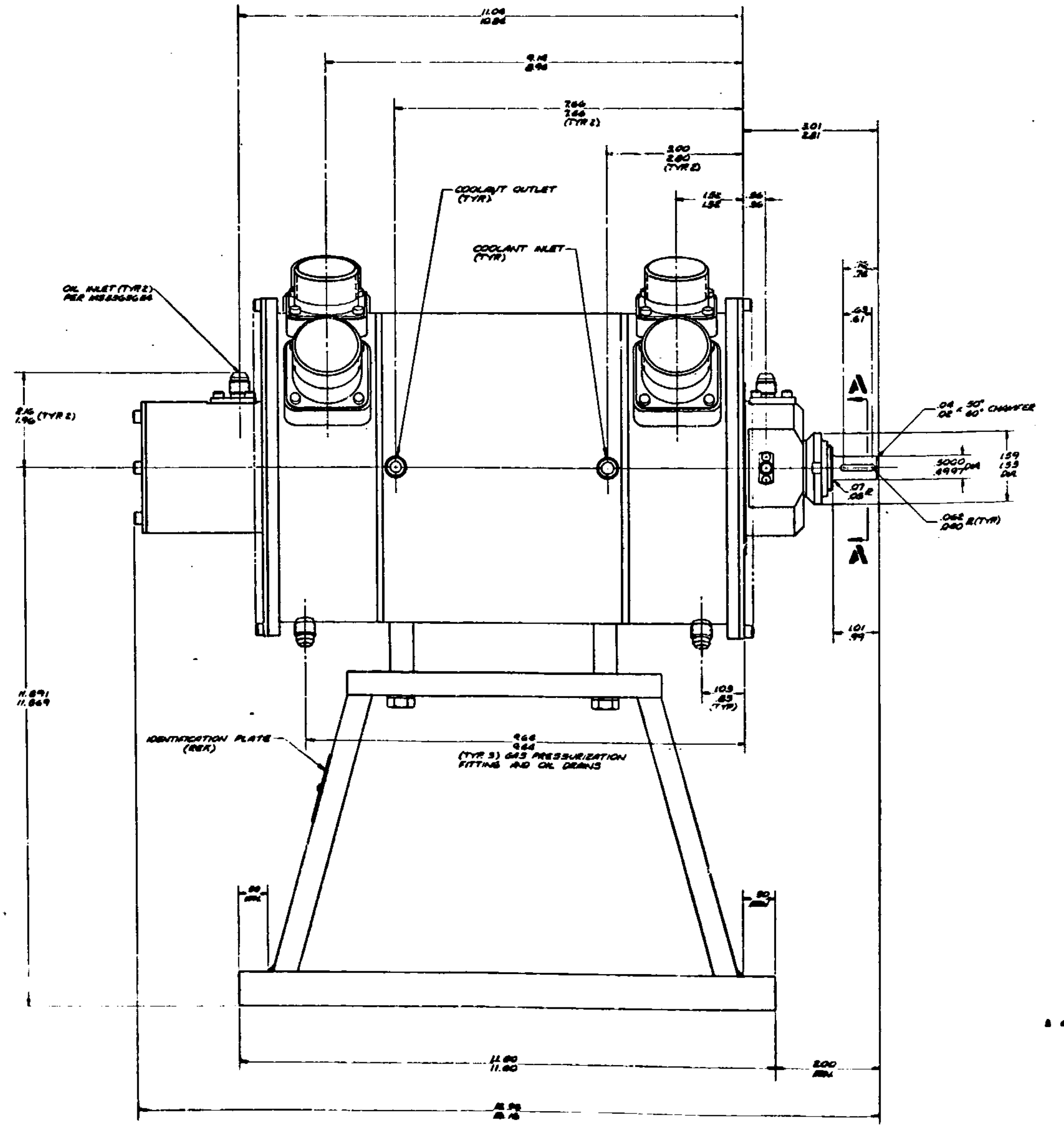

11.06
10.86
9.16
8.96
7.64
7.66
(TYP 2)
3.01
2.81
3.00
2.80
(TYP 2)
1.56
1.56
.86
.86
COOLANT OUTLET
(TYP)
COOLANT INLET
(TYP)
OIL INLET (TYP 2)
PER
2.16
1.96 (TYP 2)
A
.04 × 50°
.02 × 60° CHAMFER
.5000
.4997 DIA
1.59
1.53
DIA
.07
.05 R
.062
.060 R(TYP)
.63
.61
1.01
.99
11.891
11.869
1.09
.83
(TYP)
IDENTIFICATION PLATE
(REF)
9.64
9.64
(TYP 3) GAS PRESSURIZATION
FITTING AND OIL DRAINS
.50
MIN
11.80
11.60
2.00
MIN

EPTACLE (TYP 2)
6322-145
OUTLET & INLET #1
6896EG

699650

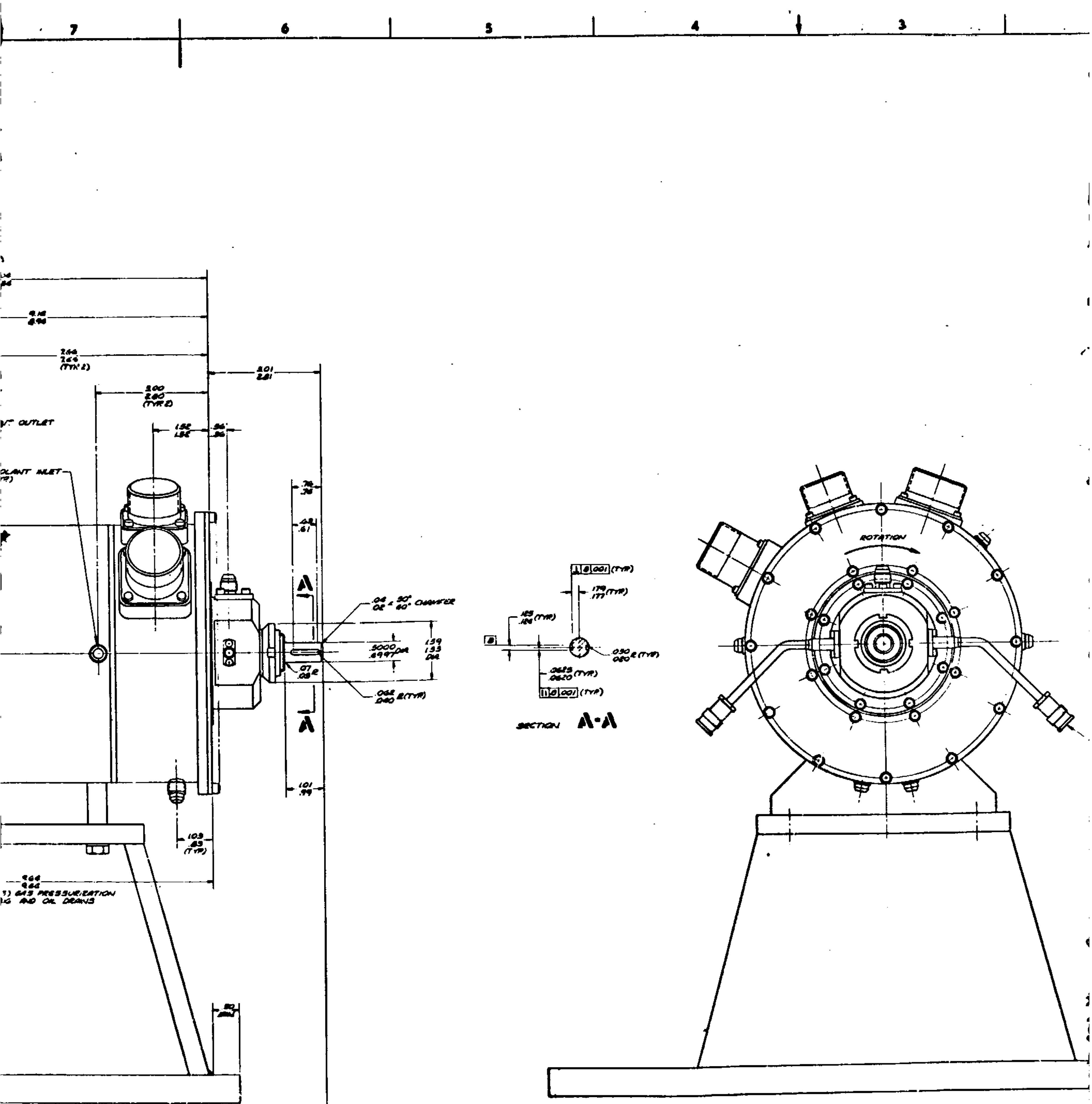

3. OPERATING CONDITIONS
COOLANT DOW CORNING 200 20 CENTISTOKE BLEND
COOLANT INLET TEMPERATURE 70°F
COOLANT INLET FLOW 12 LB/SEC
OIL INLET PRESSURE (MIST LUBRICATION)
SPEED: 0 - 43200 RPM
1ST CRITICAL - 9700 RPM
2ND CRITICAL - 19700 RPM

2. POSITIONAL AND GEOMETRIC TOLERANCE SYMBOLS PER MIL STD-8

1. ALL DIMENSIONS SHOWN ARE FOR INSTALLATION AND ASSEMBLY [illegible]

699650

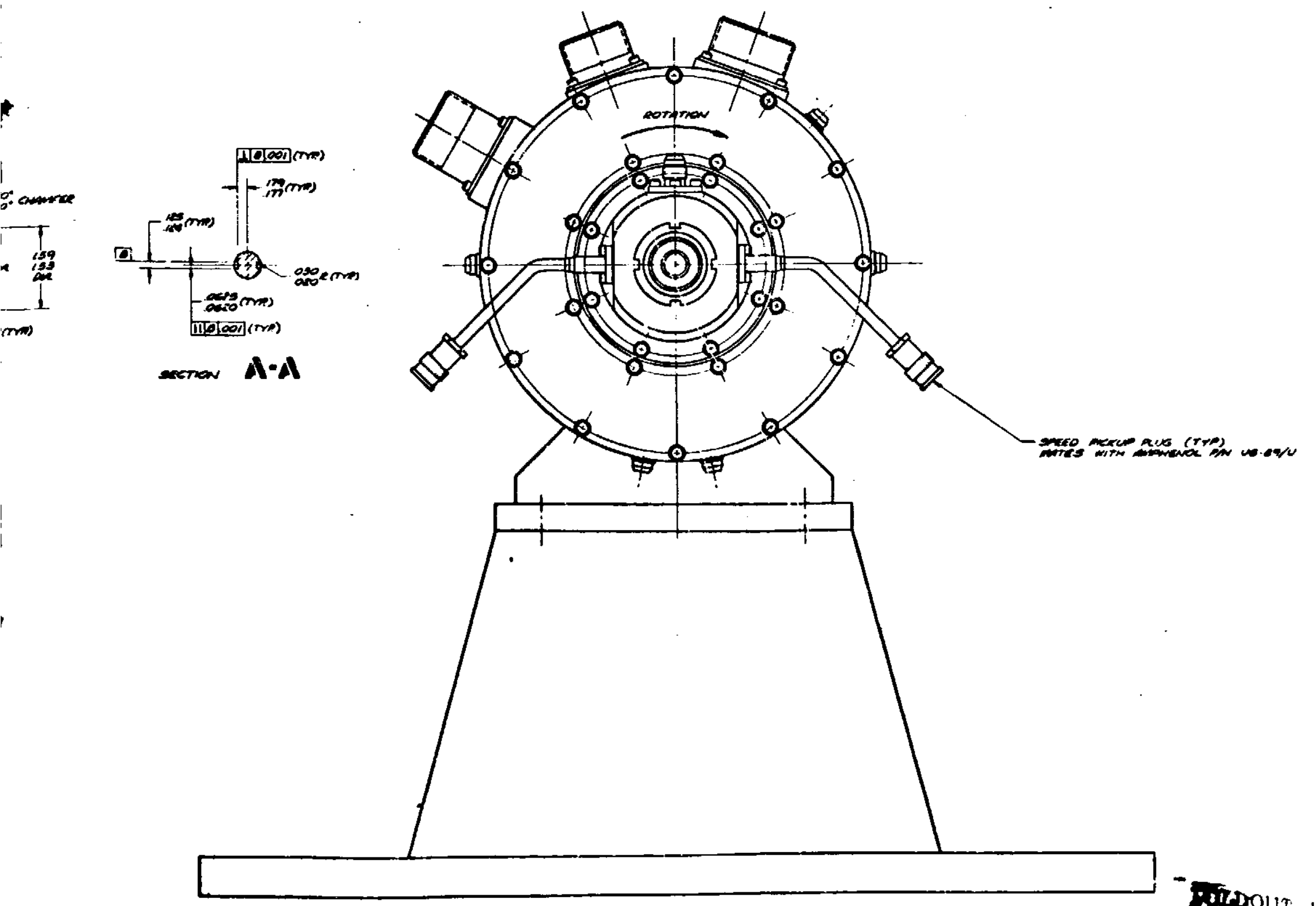

SECTION A-A

SEE TAG (UPPER LEFT HAND CORNER) FOR OUTLINE AND IDENTIFICATION NUMBER

FOLDOUT FRAME

3 OPERATING CONDITIONS
COOLANT DOW CORNING 200 20 CENTISTOKE BLEND
COOLANT INLET TEMPERATURE 70°F
COOLANT INLET FLOW 2 LB/SEC
OIL INLET PRESSURE (MIST LUBRICATION)
SPEED: 0 - 63200 RPM
1ST CRITICAL - 9700 RPM
2ND CRITICAL - 19700 RPM

2 POSITIONAL AND GEOMETRIC TOLERANCE SYMBOLS PER MIL-STD-8

1 ALL DIMENSIONS SHOWN ARE FOR INSTALLATION AND [illegible]

QUANTITY REQD	FIND NO.	PART NO.	SYM	DESCRIPTION	CODE IDENT	MATERIAL AND SPECIFICATION	UNIT WT	ZONE

—ASSY LIST OF MATERIAL

NEXT ASSY | USED ON

SIGNATURES | DATES

AIRESEARCH MANUFACTURING COMPANY OF ARIZONA
A DIVISION OF THE GARRETT CORPORATION
PHOENIX, ARIZONA

RESEARCH PACKAGE
OUTLINE, ALTERNATOR

J | 99193 | 699650

SCALE | WT | SHEET OF

13 12 11 10

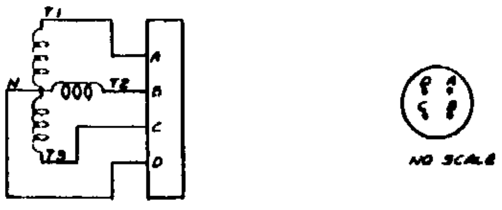

WIRING SCHEMATIC AND PIN LOCATIONS
FOR POWER CONNECTOR
(REF. ITEM 39)

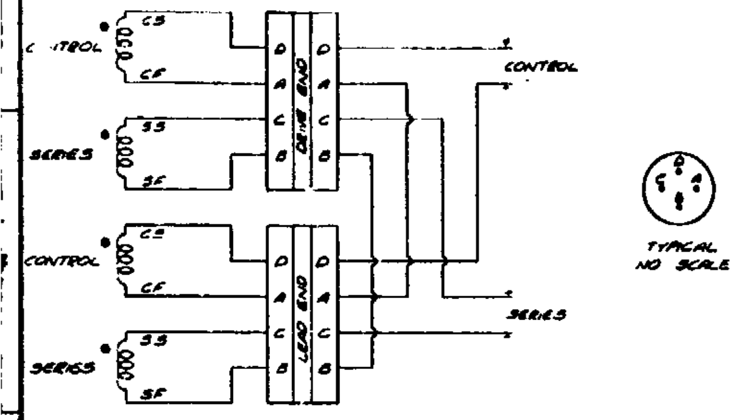

WIRING SCHEMATIC AND PIN LOCATIONS
FOR FIELD CONNECTORS
(REF ITEM 41)

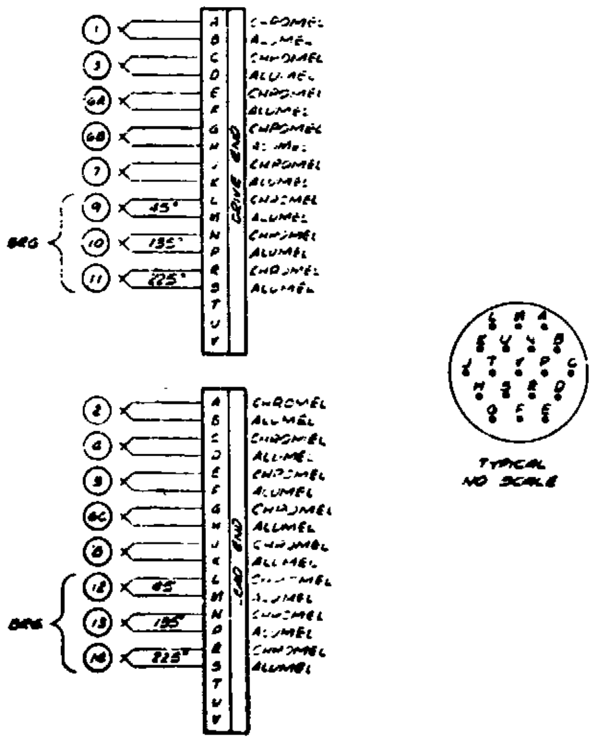

WIRING SCHEMATIC AND PIN LOCATIONS
FOR THERMOCOUPLE CONNECTORS
(REF ITEM 44)

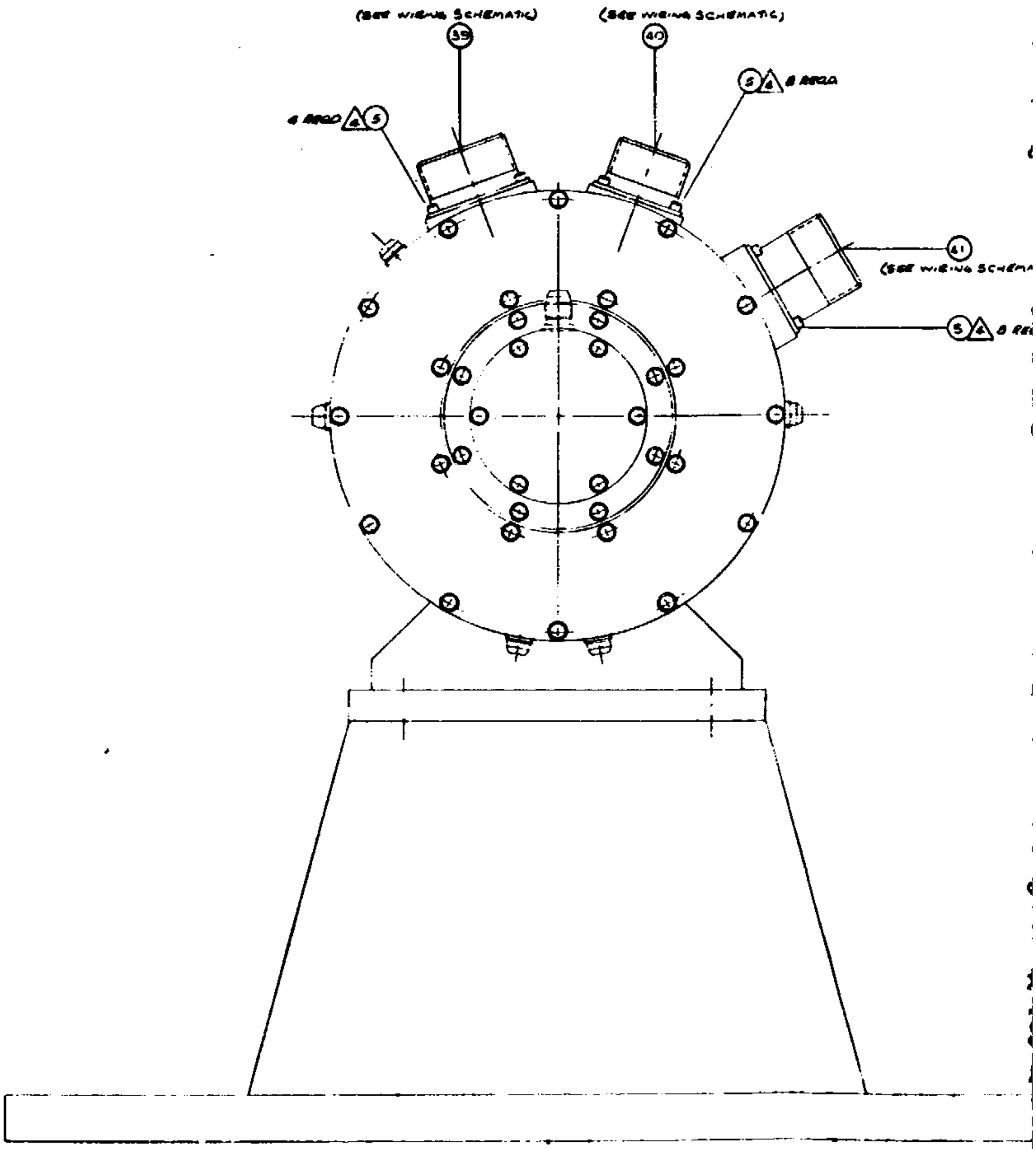

FOLDOUT FRAME

FOLDOUT FRAME

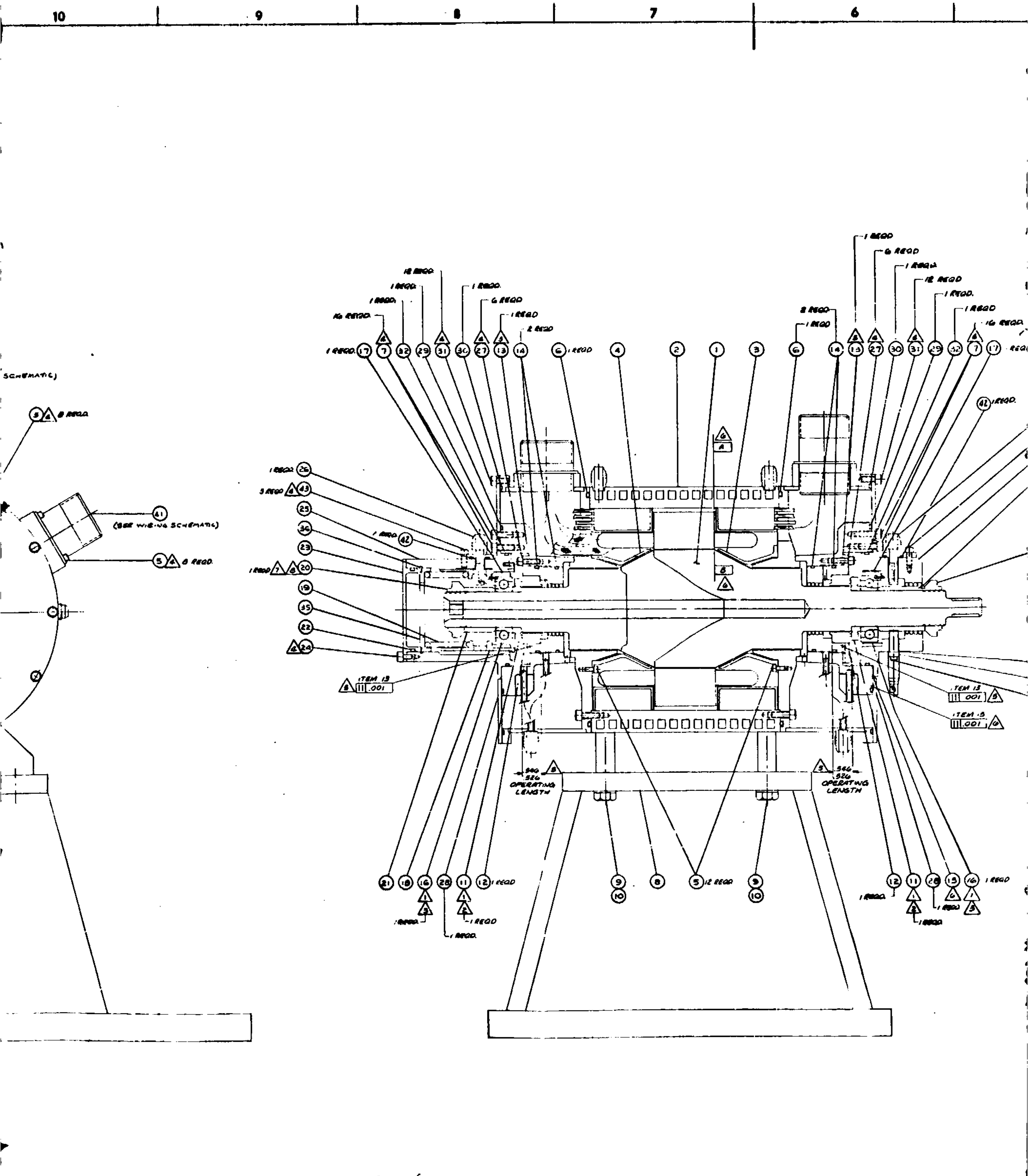

ME

FOLDOUT FRAME

699651

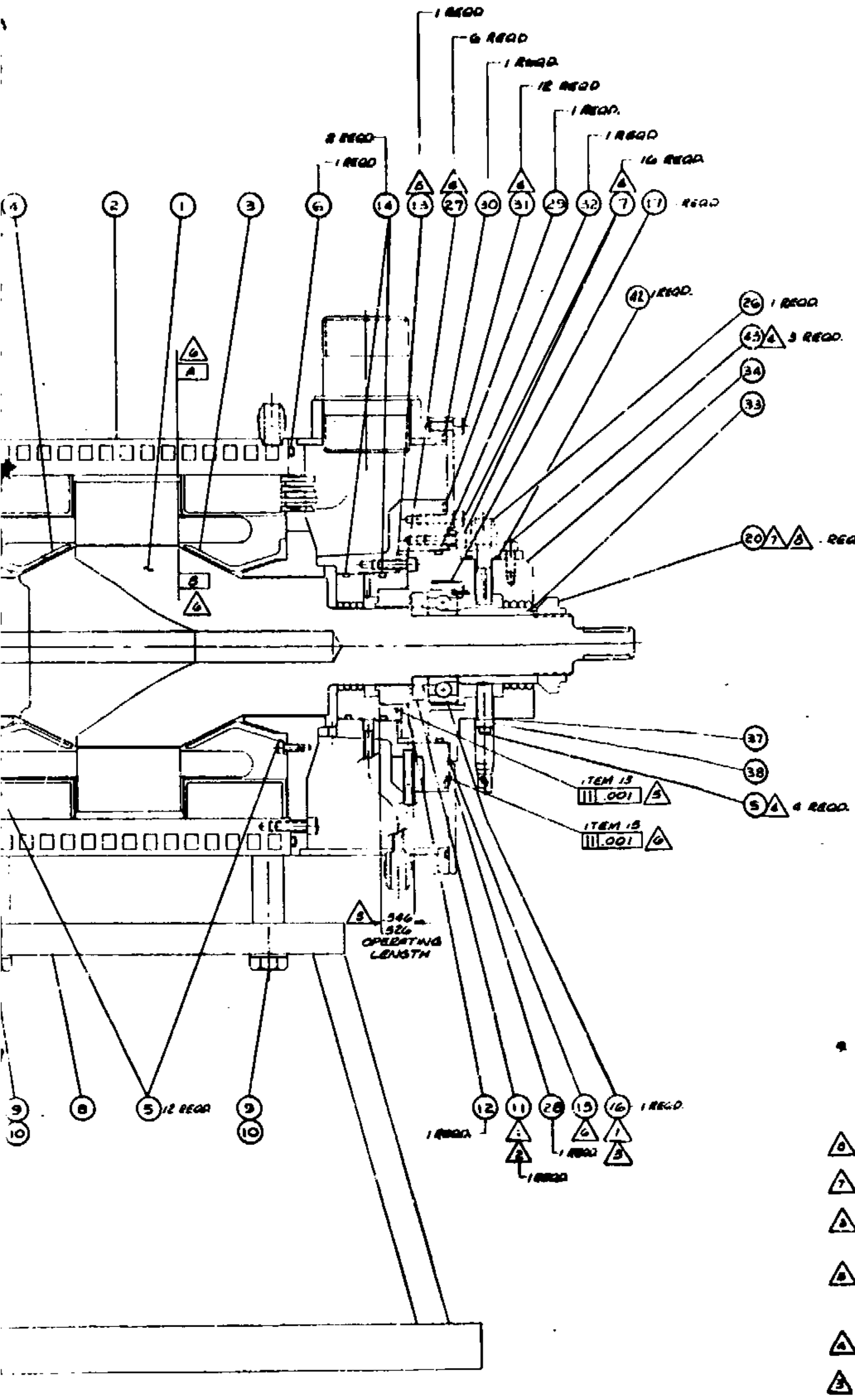

9. FOR TORQUE REQUIREMENTS ON THREADED FASTENERS SEE AIRESEARCH SPEC AF-349. THE FRICTION TORQUE DEVELOPED FROM SELF LOCKING DEVICES IS TO BE ADDED TO FASTENER LOADING TORQUE AND MUST BE DETERMINED FOR EACH FASTENER.

△8 APPLY 473-010-9001 △1 LUBE TO THREADS OF NOTED ITEMS PRIOR TO ASSEMBLY.

△7 TIGHTEN NUT ITEM 20 ON ROTOR ITEM 1 TO 300-360 IN. LBS. TORQUE.

△6 GRIND ITEM 18 AT ASSEMBLY SO THAT DATUM B IS WITHIN .005 OF DATUM A. REMOVE MATERIAL FROM SIDE OPPOSITE PART NUMBER ONLY.

△5 GRIND ITEM 13 AT ASSEMBLY TO OBTAIN .536 REF OPERATING LENGTH OF SEAL. REMOVE MATERIAL FROM SIDE OPPOSITE PART NUMBER ONLY PERFORM AFTER ESTABLISHING △6.

△4 ALL SCREWS TO BE SAFETY WIRED PER MS33540.

△3 SEE DRAWING 358498 FOR SPECIAL INSTRUCTIONS

△2 SEE DRAWING 699652 FOR SPECIAL INSTRUCTIONS

△1 VENDOR ITEM - SEE APPLICABLE SPECIFICATION OR SOURCE CONTROL DRAWING

QUANTITY REQD	ITEM NO	PART NO
[illegible]	45	[illegible]-419-9208
2	42	MS9593-019
2	41	223-549-9101
2	40	223-048-9112
1	39	223-048-9264
2	38	699746-1
2	37	699733-1
1	36	MS6625 4238
1	35	699656-1
1	34	699689-1
1	33	699688-1
2	32	NAS1593-041
24	31	MS24674-7
2	30	NAS1593-166
2	29	NAS1593-047
2	28	699687-1
12	27	MS24674-2
2	26	699699-1
1	25	699698-1
6	24	MS24674-6
1	23	699697-1
1	22	NAS1593-130
1	21	699696-1
2	20	329-577-9006
1	19	699823-1
1	18	699695-1
2	17	699656-1
2	16	358498-1
1	15	699655-1
4	14	NAS1593-095
2	13	699694-1
2	12	699693-1
2	11	699652-1
4	10	AN960C616
4	9	AN6CH10A
1	8	699659-1
28	7	MS24674-8
2	6	NAS1593-64
16	5	NAS1352C4H4
1	4	699778-2
1	3	699778-1
1	2	519266-1
1	1	699653-1

←ASSY

	NEXT ASSY	USED ON
1	[illegible]	699650

HEAT TREATMENT

FOLDOUT FRAME

REVISIONS				
ZONE	LTR	DESCRIPTION	DATE	APPROVED
	A	ADDED ITEM 42-43 (SEE E.O.)	11-6-67	[illegible]

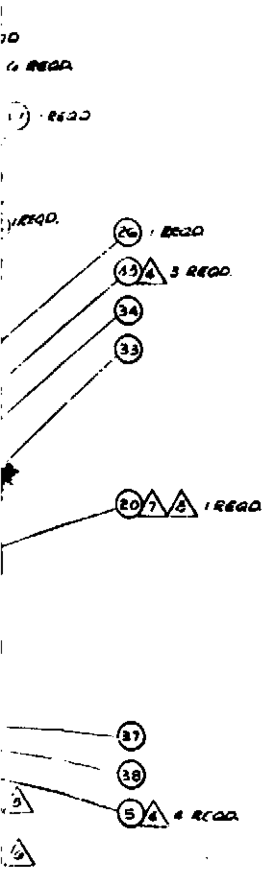

9. FOR TORQUE REQUIREMENTS ON THREADED FASTENERS SEE AIRESEARCH SPEC AF-949. THE FRICTION TORQUE DEVELOPED FROM SELF LOCKING DEVICES IS TO BE ADDED TO FASTENER LOADING TORQUE AND MUST BE DETERMINED FOR EACH FASTENER.

8. APPLY 475-010-9001 1 LUBE TO THREADS OF NOTED ITEMS PRIOR TO ASSEMBLY.

7. TIGHTEN NUT ITEM 20 ON ROTOR ITEM 1 TO 300-350 IN LBS TORQUE.

6. GRIND ITEM 16 AT ASSEMBLY SO THAT DATUM B IS WITHIN .005 OF DATUM A. REMOVE MATERIAL FROM SIDE OPPOSITE PART NUMBER ONLY

5. GRIND ITEM 13 AT ASSEMBLY TO OBTAIN .556 REF OPERATING LENGTH OF SEAL. REMOVE MATERIAL FROM SIDE OPPOSITE PART NUMBER ONLY PERFORM AFTER ESTABLISHING 6.

4. ALL SCREWS TO BE SAFETY WIRED PER MS33540.

3. SEE DRAWING 358498 FOR SPECIAL INSTRUCTIONS

2. SEE DRAWING 699652 FOR SPECIAL INSTRUCTIONS

1. VENDOR ITEM - SEE APPLICABLE SPECIFICATION OR SOURCE CONTROL DRAWING

QUANTITY REQD	ITEM NO	PART NO	STK	DESCRIPTION	CODE IDENT	MATERIAL AND SPECIFICATION	UNIT WT	ZONE
[illegible]	43	[illegible]-419-9006		SCREW, CAP, SOCKET HEAD				4/.
2	42	NAS1593-013		PACKING O RING				1/.
2	41	223-587-9101		CONNECTOR, ELECTRICAL				2
2	40	223-045-9112		CONNECTOR, ELECTRICAL				2
1	39	223-045-9064		CONNECTOR, ELECTRICAL				1
2	38	699746-1		PROBE, CAPACITANCE				5
2	37	699735-1		SHIM, PROBE				5
1	36	MS16625-4251		RING, RETAINING, INTERNAL				4
1	35	699656-1		RETAINER, SPRING				4
1	34	699689-1		CARRIER, LABYRINTH				5
1	33	699688-1		SPACER, SHAFT				5
2	32	NAS1593-041		PACKING "O" RING				2/5
24	31	MS24674-7		SCREW, CAP, SOCKET HEAD				2/4
2	30	NAS1593-46		PACKING "O" RING				3/4
2	29	NAS1593-047		PACKING "O" RING				2/4
2	28	699687-1		PLATE, ACCESS				15/4
12	27	MS24674-2		SCREW, CAP, SOCKET HEAD				[illegible]
2	26	699699-1		NOZZLE ASSEMBLY				5
1	25	699698-1		HOUSING, BEARING SUPPORT				4
6	24	MS24674-6		SCREW, CAP, SOCKET HEAD				4
1	23	699697-1		CAP, END				4
1	22	NAS1593-130		PACKING "O" RING				4
1	21	699696-1		SPACER, BEARING				8
2	20	525-577-9006		NUT, SELF LOCKING, ROUND				9/8
1	19	699823-1		SPRING, HELICAL, COMPRESSION				4
1	18	699695-1		CARRIER, BEARING				3
2	17	699686-1		MOUNT BEARING, RESILIENT				9/5
2	16	358498-1		BEARING, BALL, THRUST				2/6
1	15	699685-1		SPACER, CARRIER				[illegible]
4	14	NAS1593-035		PACKING "O" RING				8/5
2	13	699694-1		SPACER, SEAL				[illegible]
2	12	699693-1		ADAPTER, SEAL				4/6
2	11	699652-1		SEAL & ROTOR SET, MATCHED				4/6
4	10	AN960C616		WASHER, FLAT				[illegible]
4	9	AN6CH10A		BOLT, MACHINE, AIRCRAFT				7
1	8	699659-1		STAND ASSEMBLY, MOUNTING				[illegible]
32	7	MS24674-8		SCREW, CAP, SOCKET HEAD				8/5
2	6	NAS1593-164		PACKING "O" RING				1/6
36	5	MS1352C0448		SCREW, CAP, SOCKET HEAD				[illegible]
1	4	699770-2		SHROUD, ROTOR				7
1	3	699738-1		SHROUD, ROTOR				[illegible]
1	2	519246-1		[illegible], ASSEMBLY				[illegible]
1	1	699653-1		ROTOR ASSEMBLY, GENERATOR				[illegible]

←ASSY LIST OF MATERIAL

1(-1)	FINAL	699650
	NEXT ASSY	USED ON
HEAT TREATMENT		PROCESS

UNLESS OTHERWISE SPECIFIED ON THIS DRAWING, FABRICATION OF THIS ITEM SHALL BE IN ACCORDANCE WITH AIRESEARCH SPECIFICATION SC 9111 STANDARD DRAWING INTERPRETATIONS

SIGNATURES	DATES
[illegible]	4-4-67
	6-16-67
[illegible]	7-?-67
[illegible]	5-18-67
[illegible]	7-26-67
[illegible]	7-?-67

AIRESEARCH MANUFACTURING COMPANY OF ARIZONA
A DIVISION OF THE GARRETT CORPORATION
PHOENIX, ARIZONA

RESEARCH PACKAGE
ASSEMBLY, ALTERNATOR

SIZE	CODE IDENT NO	DWG NO
J	99193	699651

SCALE ½ WT — SHEET OF

699651 A

FOLDOUT FRAME

PART NO.	OPERATING CONDITIONS		
699652-1		P_1	P_2
	MEDIUM	AIR-OIL MIST (MIL-L-7808)	HELIUM-XENON MIXTURE (60%-40%)
		14.7 PSIA	42.6 PSIA
		14.7 PSIA	25.1 PSIA
		14.7 PSIA	12.6 PSIA

NORMAL OPERATING SPEED — 36,000 RPM
OVERSPEED — 43,200 RPM FOR 5 MIN.
LIFE — 300 HRS. MIN.
TEMPERATURE — 250°F MAX.

12. Ⓒ DESIGNATES CRITICAL CHARACTERISTIC
Ⓜ DESIGNATES MAJOR CHARACTERISTIC

11. THESE PARTS TO BE MANUFACTURED, INSPECTED, STOCKED AND SOLD AS REPLACEMENT PARTS IN MATCHED SETS ONLY.

10. SHAFT MATERIAL: 4340

9. SEAL HSG. MATERIAL: 300 SERIES STAINLESS

8. PROCUREMENT SOURCE(S) PER ASL 699652

7. AIRESEARCH PART NUMBER & SERIAL NUMBER OF MATCHED SET HERE PER AIRESEARCH SPEC. MC-5014, CLASS II

6. ALL DESIGN AND PART NUMBER CHANGES REQUIRE PRIOR AIRESEARCH APPROVAL.

5. ONLY THE ITEM DESCRIBED ON THIS DRAWING WHEN PROCURED FROM THE VENDOR(S) LISTED HEREON IS APPROVED BY AIRESEARCH MANUFACTURING COMPANY, PHOENIX, ARIZONA FOR USE IN THE APPLICATION(S) SPECIFIED HEREON. A SUBSTITUTE ITEM SHALL NOT BE USED WITHOUT PRIOR TESTING AND APPROVAL BY AIRESEARCH MANUFACTURING COMPANY OR BY THE GOVERNMENT PROCURING ACTIVITY.

4. DRAWING REVISIONS FOR SUBSTITUTE ITEMS SHALL NOT BE MADE WITHOUT PRIOR APPROVAL BY AIRESEARCH MANUFACTURING COMPANY.

3. IDENTIFY PACKAGING WITH AIRESEARCH PART NUMBER.

2. PARTS PROCURED BY VENDOR PART NUMBER SHALL BE PROCURED IN ACCORDANCE WITH THIS AIRESEARCH SOURCE CONTROL DRAWING.

1. DETAILS OF DESIGN AND CONSTRUCTION OTHER THAN SHOWN SHALL BE AT OPTION OF VENDOR.

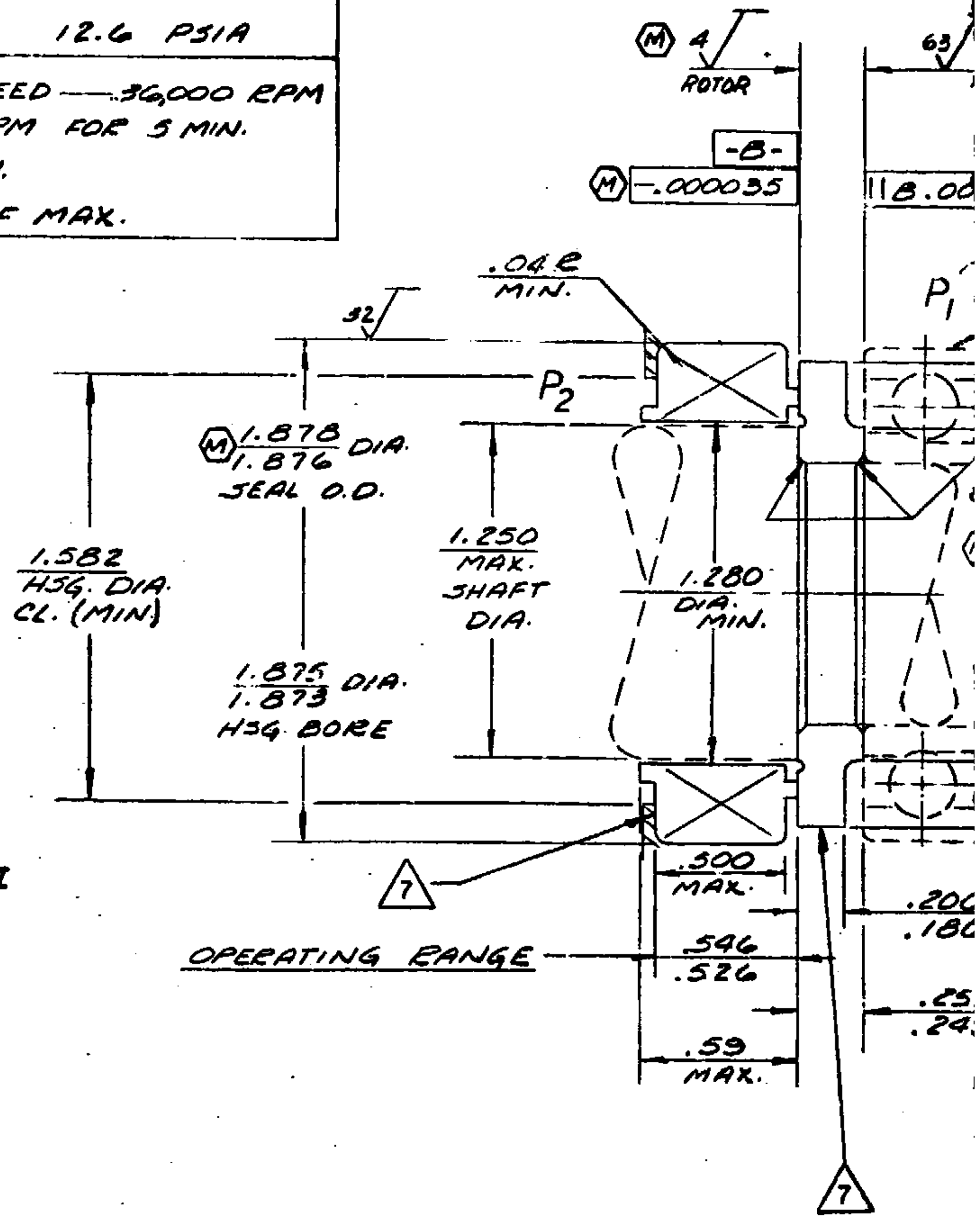

QUANTITY REQD	ITEM NO.	PART NO.	SYM
	←ASSY		

REQD	NEXT ASSY	USED ON
2(-1)	699651-1	699650-1

HEAT TREATMENT	PROCESS
HARDNESS AND SPEC	NAME AND SPEC

SIGN
DFT
CHK
MFG
MATL
STRESS
AERO
A-PD
APPD
DESIGN A
OTHER A

UNLESS OTHERWISE SPECIFIED ON THIS DRAWING, FABRICATION OF THIS ITEM SHALL BE IN ACCORDANCE WITH AIRESEARCH SPECIFICATION SC-5535, STANDARD DRAWING INTERPRETATIONS.

CRITICAL ITEM
SATISFACTORY PERFORMANCE OF THE END PRODUCT DEPENDS ON THE INTEGRITY AND RELIABILITY OF THIS SELECTED CRITICAL ITEM. THE GARRETT CORPORATION RECOMMENDS PROCUREMENT FROM THE ORIGINAL SUPPLIER AS SET FORTH IN ASPR 1-313.

FOLDOUT FRAME

FOLDOUT FRAME

REVISIONS				
ZONE	LTR	DESCRIPTION	DATE	APPROVED

N
%-40%)
IA
IA
IA
0 RPM
IN.

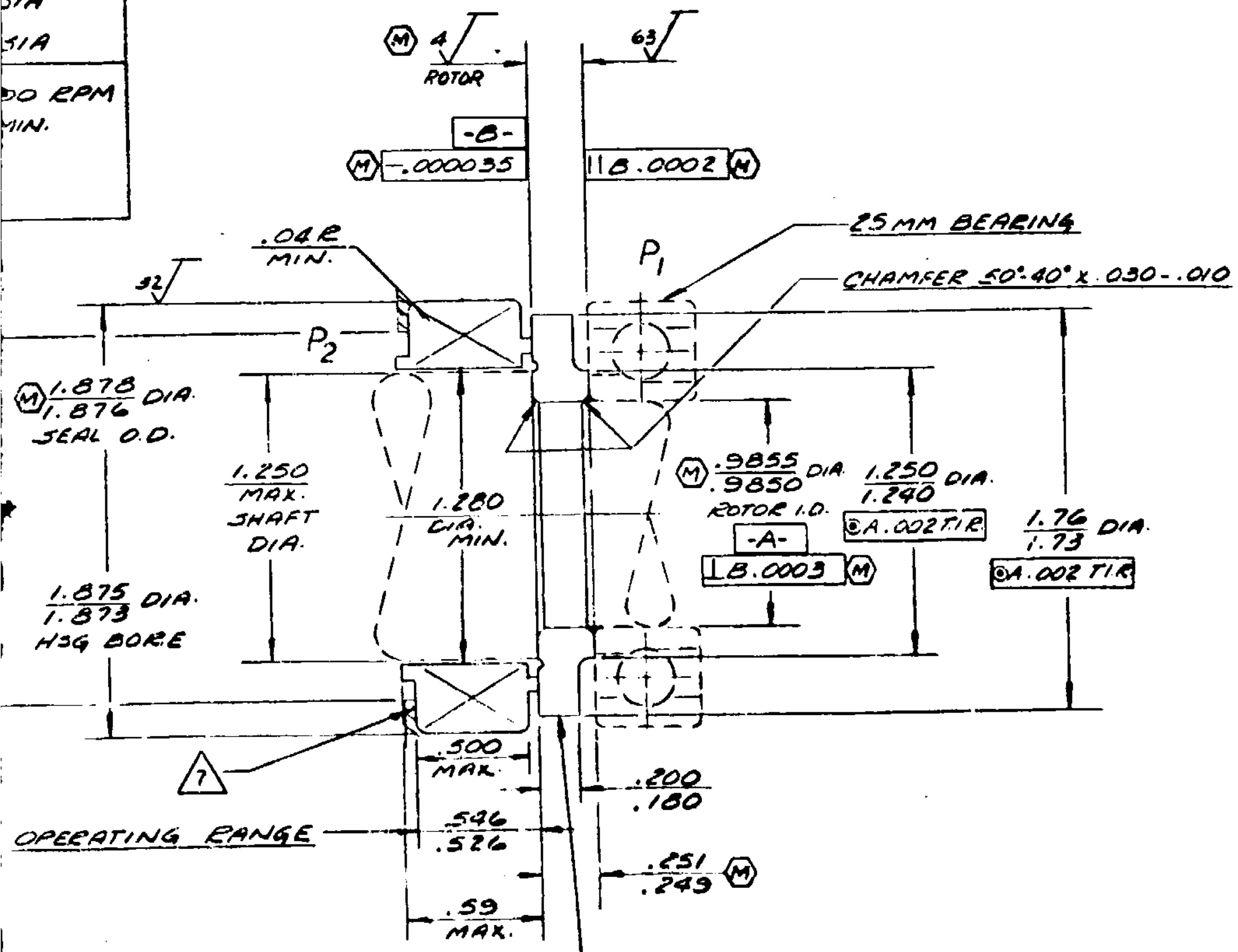

SOURCE CONTROL DRAWING

See tab block (upper left corner) for PART NUMBER

QUANTITY REQD	ITEM NO.	PART NO.	SYM	DESCRIPTION	CODE IDENT	MATERIAL AND SPECIFICATION	ZONE
←—ASSY							

LIST OF MATERIAL

REQD	NEXT ASSY	USED ON
2(-1)	699651-1	699650-1

HEAT TREATMENT	PROCESS
HARDNESS AND SPEC	NAME AND SPEC

SIGNATURES		DATES
DFT		1-11-67
CHK		2-16-67
MFG		
MATL		
STRESS		
AERO		
APPD		1-4-67
APPD		
DESIGN ACTIVITY APPD	S. J. Elliott	2-16-67
OTHER ACTIVITY APPD		

AIRESEARCH MANUFACTURING COMPANY OF ARIZONA
A DIVISION OF THE GARRETT CORPORATION
PHOENIX, ARIZONA

DWG TITLE
SEAL & ROTOR SET, MATCHED

SIZE	CODE IDENT NO.	DWG NO.
C	99193	699652
SCALE 2/1	WT —	SHEET 1 OF 1

NLESS OTHERWISE SPECIFIED ON
HIS DRAWING, FABRICATION OF
HIS ITEM SHALL BE IN ACCORDANCE
ITH AIRESEARCH SPECIFICATION
C5535, STANDARD DRAWING IN-
ERPRETATIONS.

699652

PART NO
699667-1

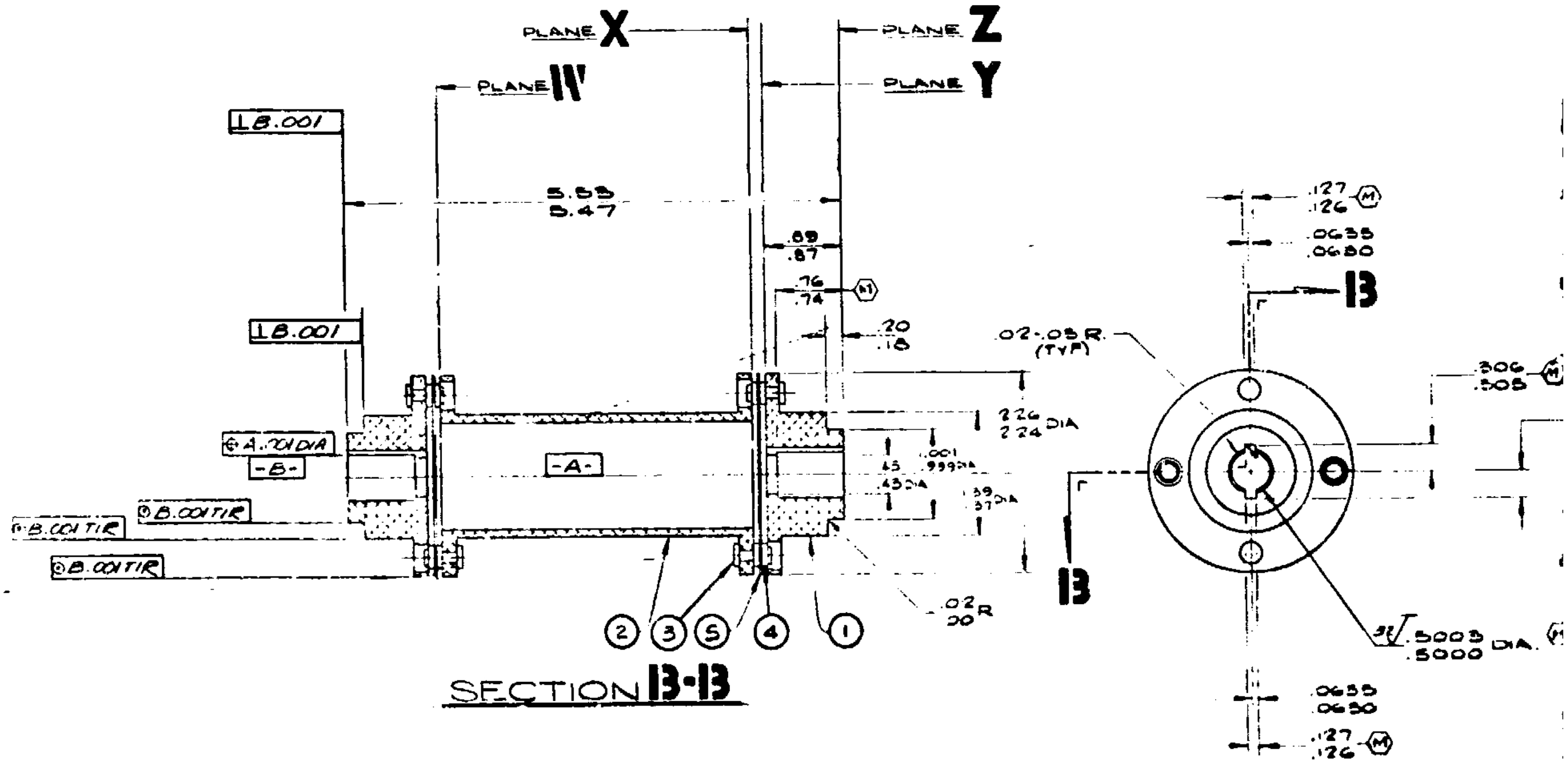

13. POSIONAL AND GEOMETRIC TOLERANCE SYMBOLS PER MIL-STD-8.

12. ⓒ DESIGNATES CRITICAL CHARACTERISTIC
Ⓜ DESIGNATES MAJOR CHARACTERISTIC

11. DYNAMIC BALANCE REQUIREMENTS:

11.1 BALANCING SPEED 2500 RPM MIN

11.2 A SINGLE ARBOR PRE BALANCED TO WITHIN [illegible] AND HAVING DATUM 'B' LOCATING [illegible] CONCENTRIC TO ITS ROTATING AXIS [illegible] T.I.R. SHALL BE UTILIZED THROUGHOUT BALANCING PROCEDURE

11.3 DYNAMICALLY BALANCE ITEMS INDIVIDUALLY [illegible] TO WITHIN .0002 OZ-IN [illegible] METAL FROM PLANES [illegible] IF NECESSARY

11.4 [illegible] ASSEMBLY COUPLING & DYNAMICALLY [illegible] ASSEMBLY ABOUT PLANES W & X TO WITHIN [illegible] OZ-IN, REMOVE METAL FROM PLANES W & X IF NECESSARY

[illegible] ACCESS HOLES OR ANODIZE

[illegible] EXCEPT NOTED

[illegible] CONSTRUCTION [illegible]

[illegible] ACCORDANCE

[illegible] CONTROL [illegible]

[illegible] PART NUMBER

[illegible]

[illegible] PART NUMBER, CHANGES REQUIRE [illegible] APPROVAL.

[illegible] PER [illegible]

[illegible] SOURCES PER ASL 699667.

NOTES:

FOLDOUT FRAME

CRITICAL ITEM

REVISIONS				
ZONE	LTR	DESCRIPTION	DATE	APPROVED

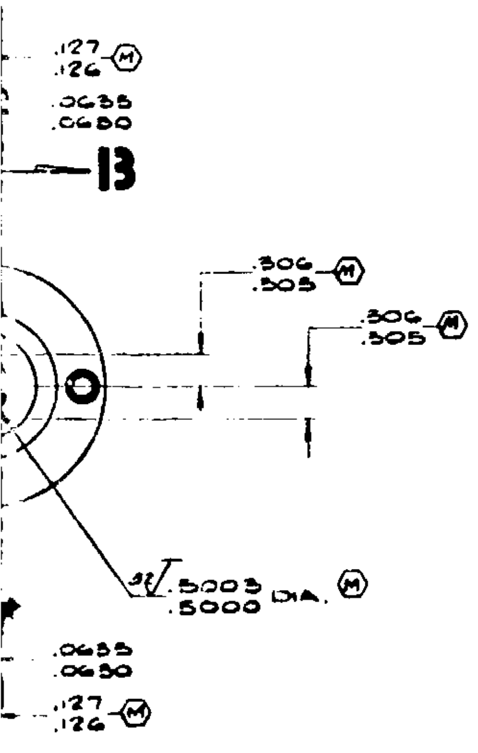

SEE TAB. BLOCK (UPPER LEFT CORNER) FOR PART NUMBER.

SOURCE CONTROL DRAWING

5		-19	DISC		BERYLLIUM COPPER [illegible]	
4		-17	WASHER		BRASS QQ-B-626	
		-15	RIVET		BRASS QQ-B-626	
		-?	FILTER MEMBER		[illegible] AMS 4122 / 7075-T6	
			FLANGE		[illegible] AMS 4122 / 7075-T6	
ITEM NO	PART NO			REQ	MATERIAL AND SPECIFICATION	ZONE

LIST OF MATERIAL

COMPANY OF ARIZONA

[illegible] ASSEMBLY, DRIVE

SIZE	CODE IDENT NO	DWG NO
D	99193	699667
SCALE 1/1	WT	SHEET 1 OF 1

CRITICAL ITEM

UNLESS OTHERWISE SPECIFIED ON THIS DRAWING, FABRICATION OF THIS ITEM SHALL BE IN ACCORDANCE WITH AIRESEARCH SPECIFICATION SC 5535, STANDARD DRAWING INTERPRETATIONS

FOLDOUT FRAME

FOLDOUT FRAME

AIRESEARCH MANUFACTURING COMPANY OF ARIZONA
A DIVISION OF THE GARRETT CORPORATION

APPENDIX III

UNBALANCED MAGNETIC FORCES

(6 pages)

UNBALANCED MAGNETIC FORCES

The two auxiliary and main flux gaps in the alternator are defined as 0.020 in. The maximum electromagnetic unbalance force occurs the instant that the displacement of the rotor relative to the stator is unidirectional and maximum. Table I presents the most recent calculations of the electromagnetic forces. An assumed radial displacement of 0.002 in. (10 percent of the gap) in each gap was used in the calculation for the various operating conditions. Speed effects were neglected that would substantially reduce the forces described herein. A survey of these conditions indicates that the no-load, 1.3 p.u.V condition can be chosen as the "worst-case" for evaluation purposes, as the 21.3-KVA overload, 1.0-p.u.V condition neglects to consider saturation, which tends to diminish the load.

TABLE I

Load Condition (rotor at standstill)	F_{ss}, lbs. Each Auxiliary Gap	Main Gap
No-load, 1.3 p.u.V	13.4	8.93
No-load, 1.0 p.u.V	7.0	5.06
12.6 KVA, full-load, 1.0 p.u.V	12.1	2.94
21.3 KVA, overload, 1.0 p.u.V	19.8	2.88

With the rotational effect of the alternator rotor on the flux distribution taken into account, the magnetic force at either of the auxiliary gaps or the main gap, for small displacements of the magnetic or shaft centers, can be defined by the following equation:

$$F = \left[\frac{1}{1 + j\omega t}\right] \frac{F_{ss}\Delta g}{0.002} \text{ lbs.}$$

where

$\omega = \frac{2\pi N}{60} = 3.768$ rad/sec.

t = time constant of the magnetic circuit, sec.

Δg = radial displacement of "center," in.

F_{ss} = the standstill maximum unbalance force with 0.002-in. radial displacement, lbs.

Since the time-constant of the yoke iron-flux change is believed to be typically in the range of 1 to 10 msec, the calculated forces for a stationary rotor, as in Table II, are thus modified by rotation, and Table II defines the results of varying the time constant for the chosen worst-case condition of a radial displacement of 0.002 in.

TABLE II

EFFECT OF TIME CONSTANT ON ELECTROMAGNETIC FORCES

t, sec.	$\left[\frac{1}{1 + j\omega t}\right]$	ΔF*, lbs.
0.010	0.0258	0.923
0.005	0.0507	1.810
0.002	0.1170	4.170
0.001	0.2100	7.480

*Base value for ΔF (standstill) = 35.73 lbs. total.

Therefore, ΔF represents the total unbalanced electromagnetic forces on the rotor assembly to be shared by the bearings. These forces are effective in both the unidirectional displacement case and in the rotating case where the rotor appears to have a lobing action with respect to the stator.

With reference to Figure 1, the conditions creating the overall worst-case electromagnetic forces may be established for machine operation at full speed (36,000 rpm). Both fixed and synchronous displacements of the rotor with respect to the stator must be considered, as follows:

(a) Fixed displacement of the rotor Z-axis in the Y-axis direction can be represented by two conditions if it is assumed that a "perfect" rotor is available--i.e., the mass center and magnetic center coincide with the geometric center.
   (1) A physical displacement of the perfect rotor axis to create a magnetic eccentricity Δg between the rotor magnetic center, A, and the stator magnetic center, 0, as shown in Figure 1(b).
   (2) A construction of the stator assembly such that its magnetic center, 0, is eccentric Δg from the rotor magnetic center, A, of a perfect rotor, as shown in Figure 1(c).

(b) Synchronous displacement of the rotor in an orbit about its Z-axis can also be represented by two conditions in the rotor:
   (1) A rotor having both mass and geometric centers coincident but a displaced magnetic center.
   (2) A rotor having coincident magnetic and geometric centers but with a displaced mass center.

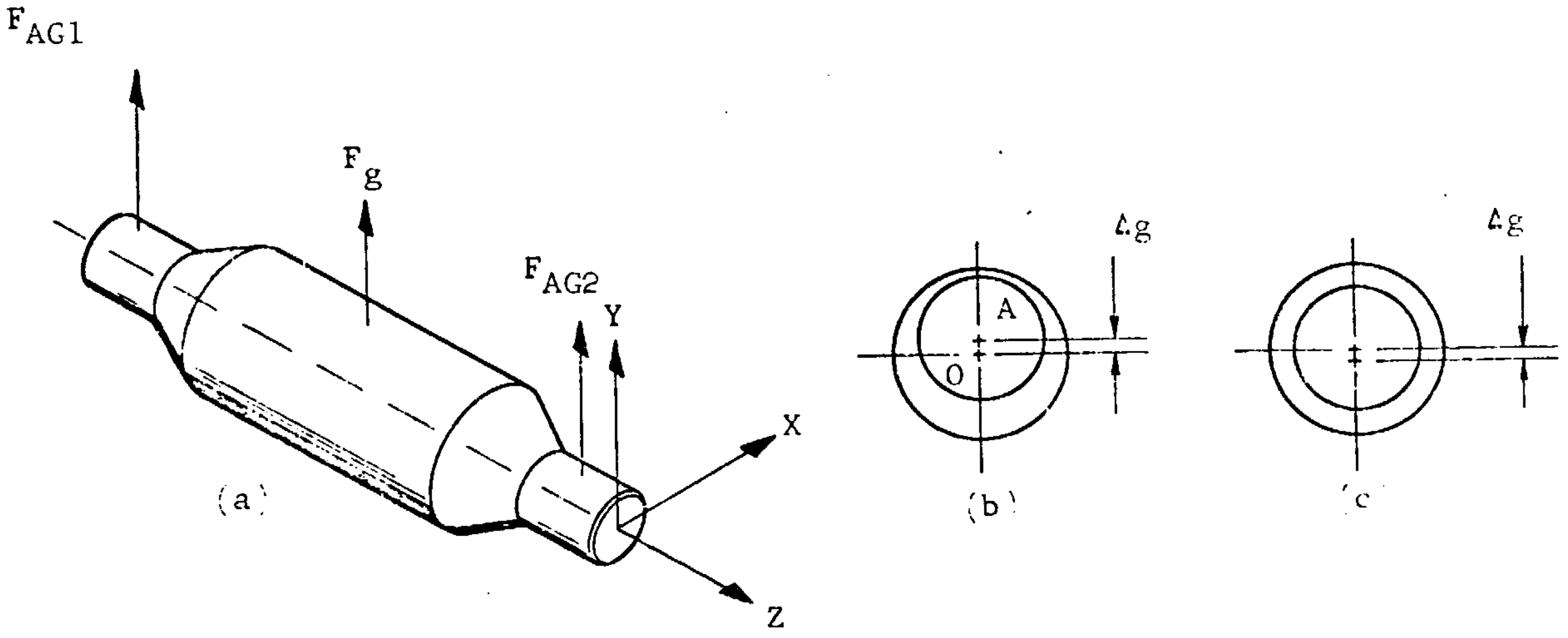

FIGURE 1

LOCATION OF ELECTROMAGNETIC CENTERS
AND DIRECTION OF FORCES

A review of these four conditions shows that (a)(1) is of particular importance in the machine where translation of the rotor is to be expected due to the bearing mounting system. Condition (a)(2) was discounted as having an effect due to the general accuracy of construction of the stator. Both Conditions (b)(1) and (2) should be presented. Thus, for the worst-case condition, the following displacements or eccentricities were presented:

Condition (a)(1)	-	0.002 in.
Condition (b)(1)	-	0.0002 in.
Condition (b)(2)	-	0.000[illegible] in.

Since 0.005-sec. is considered to more nearly represent the time-constant for flux change in solid iron, the forces for the two types of air gaps were obtained for various radial displacements, Δg, as

shown in Figure 2. Utilization of this data, with the application of a factor of 2 for a possible step-change in flux (an extremely transient condition), was defined for each journal bearing:

(a) A unidirectional load of 3.62 lbs. must be supported.

(b) A rotational load due to a total eccentricity of 0.0003 in. at a constant value of 0.27 lb. must also be supported.

An angular displacement between the direction of displacement and direction of application of these forces is a function of the location of the eddy currents being generated in the alternator components. The force shifts ahead of the member containing the eddy currents-- i.e., in the direction of the relative motion, or that of the moving member. The following describes the angular displacements:

Condition	Location of Eddy Currents	Force Action
Fixed displacement	Rotor	Leads the rotor
Synchronous displacement	Stator	Lags the rotor

The angular displacement depends upon the impedance of the conductor where, in the extreme, the superconductor tends toward 0 deg, and as damping is added, it approaches 90 deg.

For the purposes of the bearing study, experience indicates that an estimated value of 15 deg would be representative and was thus applied to the force for the fixed-displacement case. However, 0 deg was applied to the synchronous displacement case since any force lagging the rotor would tend to improve the bearing stability and thus reduce the worst-case condition.

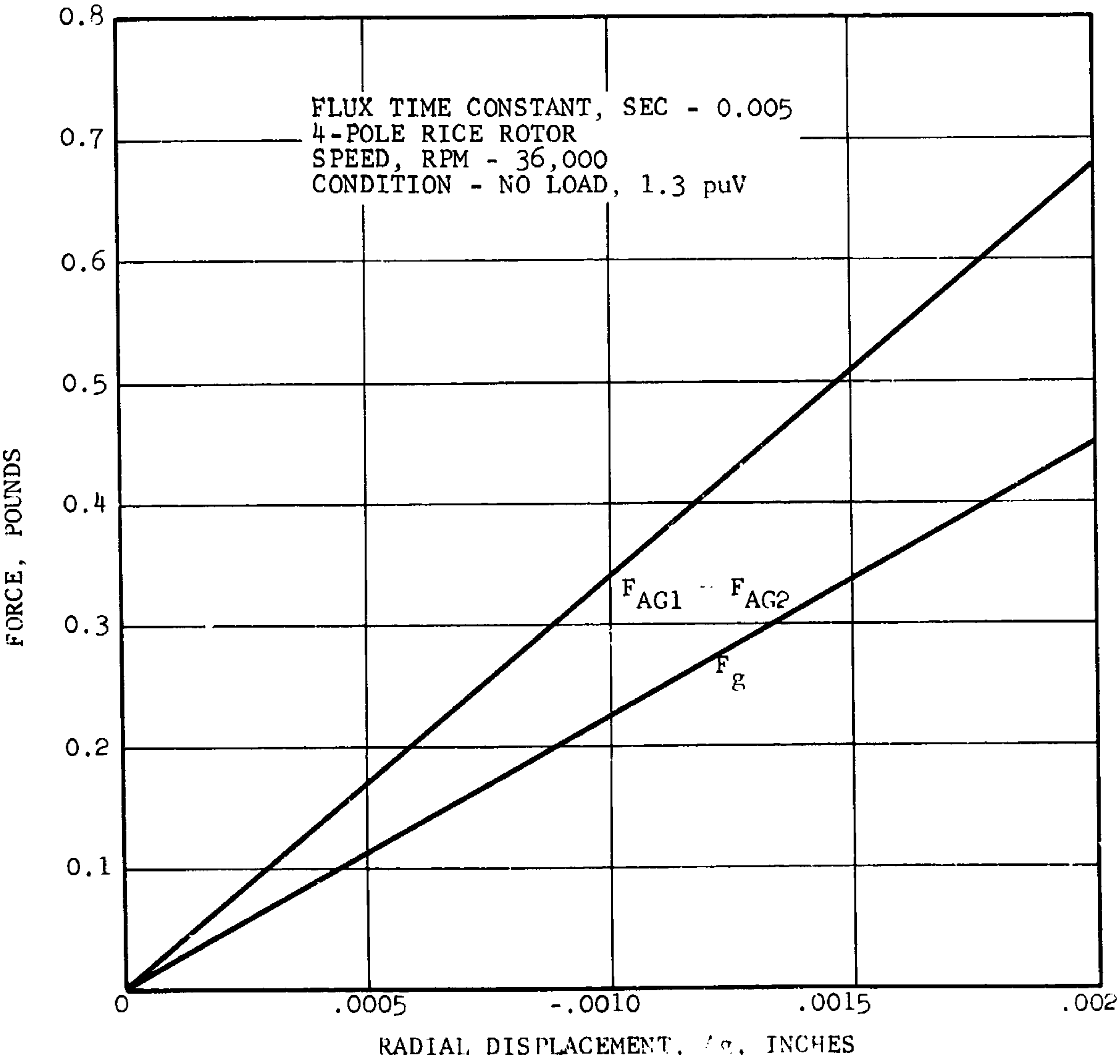

VARIATION IN MAIN AND AUXILIARY GAP FORCES
AT SYNCHRONOUS SPEED

FIGURE 2

AIRESEARCH MANUFACTURING COMPANY OF ARIZONA
A DIVISION OF THE GARRETT CORPORATION

APPENDIX IV

VOLTAGE REGULATOR/EXCITER OPTIONAL WIRING PROCEDURE

REVISIONS			
LTR	DESCRIPTION	DATE	APPROVAL

NAS 3-9427

SHEET INDEX																						
REVISION LTR																						
SHEET NO.																						

CONTRACT NO.

DFT	K. R. King	10/12/67
CHK	L C Lyxider	10/12/67
[redacted]		10/13
APPD		10-13-67

AIRESEARCH APPD 12-2-67

OTHER ACTIVITY APPD

AIRESEARCH MANUFACTURING COMPANY
A DIVISION OF THE GARRETT CORPORATION
LOS ANGELES, CALIFORNIA

OPTIONAL WIRING PROCEDURE, VOLTAGE REGULATOR-EXCITER

SIZE	CODE IDENT NO.	DWG NO.	REV LTR
A	70210	521301	

SCALE NONE

SHEET 1 OF 4

OPTIONAL WIRING ARRANGEMENT FOR VARIOUS FUNCTIONS MAY BE ACCOMPLISHED BY JUMPER WIRING THE EQUIPMENT IN THE FOLLOWING MANNER. THE JUMPER WIRES SPECIFIED IN THE FOLLOWING CONFIGURATIONS ARE FOUND IN THE PARTS LIST OF DRAWING NUMBER 543937, REGULATOR-EXCITOR ASSY.

1. SERIES FIELD MODULE BYPASSED CONFIGURATION. THIS CONFIGURATION IS USED WHEN THE SERIES FIELD MODULE IS REMOVED FROM THE VRE CHASSIS AND LOCATED ELSEWHERE, SAY AT THE ALTERNATOR.

1.1 REMOVE SERIES FIELD MODULE CONNECTION BUT NOT J7.

1.2 INSTALL JUMPER WIRING PER FOLLOWING TABULATION.

WIRE NUMBER	FROM	TO
521300-1	TBI-E3	TBI-F3
521300-2	TBI-Ej	TBI-Fj
521300-3	TBI-E16	TBI-F16

1.3 REVERSE PROCEDURE TO RECONNECT SERIES FIELD MODULE.

1.4 IN CASES WHERE JUMPER WIRES ARE NOT AVAILABLE, THE ALTERNATE METHOD MAY BE USED.

1.4.1 REMOVE WIRE FROM TBI-Fa AND RECONNECT TO TBI-E3.

1.4.2 REMOVE WIRE FROM TBI-F8 AND RECONNECT TO TBI-Fj.

1.4.3 REMOVE WIRE FROM TBI-Fr AND RECONNECT TO TBI-E16.

1.4.4 REVERSE PROCEDURE TO RECONNECT SERIES FIELD MODULE.

2. VOLTAGE SENSE CIRCUIT CONNECTED FOR EXTERNAL SENSE. THIS CONFIGURATION IS USEFUL IF THE VRE IS LOCATED REMOTELY FROM THE DESIRED POINT OF

REGULATION IN THE POWER SYSTEM.

2.1 DISCONNECT THE LEADS SPECIFIED IN THE FOLLOWING TABULATION.

FROM	TO	SIZE	COLOR
TB2-Eb	TB1-Fd	16	GRN
TB2-Ed	TB1-F11	16	BLUE
TB2-Eg	TB1-Fw	16	ORG

2.2 USING THE JUMPER WIRES SHOWN IN THE PARTS LIST OF DRWG. NO. 543937. MAKE THE CONNECTIONS PER THE FOLLOWING TABULATION.

WIRE NUMBER	FROM	TO
521300-4	TB2-Eb	TB2-Fb
521300-5	TB2-Ed	TB2-Fd
521300-6	TB2-Eg	TB2-Fg

2.3 NO ALTERNATE WIRING PLAN IS SUPPLIED OR ADVISED.

2.4 TO DISCONNECT EXTERNAL SENSE REVERSE THIS PROCEDURE.

3. CONTROL FIELD POWER CIRCUIT CONNECTED FOR EXTERNAL POWER. THIS CONFIGURATION IS NECESSARY IF THE MAIN POWER LINES ARE NOT FED THROUGH THE VRE. PARTICULARLY USEFUL IN COMBINATION WITH OPTION NUMBER 1.

3.1 DISCONNECT THE LEADS SPECIFIED IN THE FOLLOWING TABULATION.

AIRESEARCH MANUFACTURING CO.
LOS ANGELES. CALIFORNIA

SIZE	CODE IDENT NO.	DWG NO.	REV
A	70210	521301	LTR

SCALE NONE

FROM	TO	SIZE	COLOR
TB2-Ej	TB1-F6	16	GRN
TB2-En	TB1-Fn	16	BLUE
TB2-Er	TB1-F19	16	ORG

3.2 USING THE JUMPER WIRES SHOWN IN THE PARTS LIST OF DRWG. NO. 543937. MAKE THE CONNECTIONS PER THE FOLLOWING TABULATION.

WIRE NUMBER	FROM	TO
521300-4	TB2-Ej	TB2-Fj
521300-5	TB2-En	TB2-Fn
521300-6	TB2-Er	TB2-Fr

3.3 NO ALTERNATE WIRING PLAN IS SUPPLIED OR ADVISED.

3.4 TO DISCONNECT EXTERNAL POWER REVERSE THIS PROCEDURE.

AIRESEARCH MANUFACTURING CO.
LOS ANGELES, CALIFORNIA

SIZE	CODE IDENT NO.	DWG NO.	REV
A	70210	521301	LTR

SCALE NONE

SHEET 4 OF 4

AIRESEARCH MANUFACTURING COMPANY OF ARIZONA
A DIVISION OF THE GARRETT CORPORATION

APPENDIX V

TRANSIENT ANALYSIS AND VOLTAGE REGULATION OF A SYNCHRONOUS GENERATOR

AIRESEARCH REPORT 66-1300

(38 pages)

1. Introduction

This report attempts to outline a method to analyze the transient behaviour of a synchronous generator.

The two-reactance method is used in this analysis. The armature voltage, current and flux equations are first derived. A separate set of equations is given for each of the two axes - direct and quadrature.

The damper circuit at the rotor is next taken into consideration. The current equations for the damper and field circuits are then obtained. This completes the set of equations, the solutions of which describe the steady-state as well as the transient behaviour of a synchronous generator.

This set of equations is then applied to a voltage regulating system. Due to the presence of two fields (series and shunt), the field equation is modified to take the effect of both fields into consideration. The final result is presented in a block diagram which is readily programmed for an analog computer.

2. Machine Equations Relating Rotor and Stator Circuits

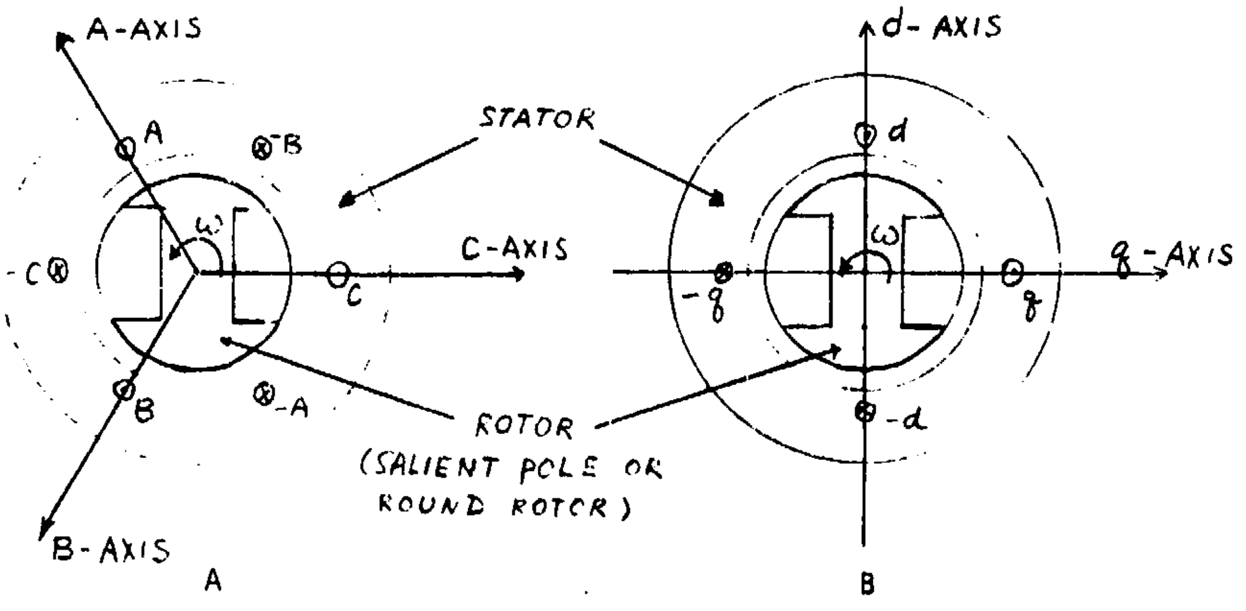

Figure 1

The essential features of a three-phase synchronous machine from the analytical viewpoint are shown in Figure 1A. On the stator are three distributed windings A, B, and C, one for each phase. They are symbolized by the correspondingly labeled concentrated coils, the magnetic axes of the phase windings coinciding with the coil axes.

The rotor, shown in the center, has two axes of symmetry, the polar, or direct, axis d and the interpolar, or quadrature axis q. However, the stator has three axes of symmetry, one for each phase. The analysis is greatly simplified if the three-phase current, voltage and flux linkage of the stator can be transformed into the d and q-axis components. This technique is sometimes referred to as the Blondel Two-reactance method and is given in Appendix A. The two-axes equivalence of Figure 1A is shown in Figure 1B.

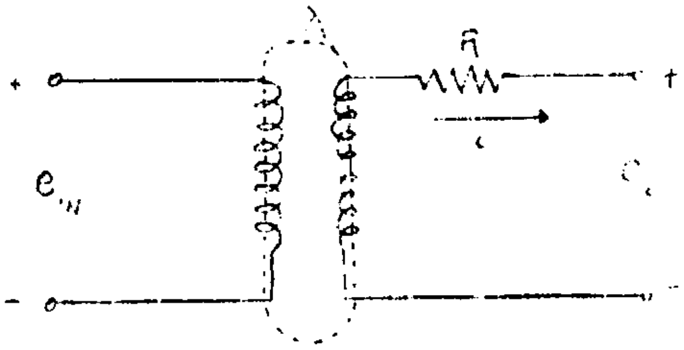

Figure 2

For any one winding as shown in Figure 2, the relationship of the induced voltage e_i and current i is:

$$e_i = -iR + p\lambda \qquad (1)$$

where

R = winding resistance
λ = flux linkages with the winding
p = differential operator = d/dt

Applying Equation 1 to the three phases A, B and C, we have

$$E_A = -I_A R_a + p\lambda_A \tag{2}$$

$$E_B = -I_B R_a + p\lambda_B \tag{3}$$

$$E_C = -I_C R_a + p\lambda_C \tag{4}$$

The generator condition is applied to Equations 2, 3 and 4, i.e., armature voltage is the generated voltage and armature current is out of the winding and produces negative armature and field linkages.

From Appendix I using transformation matrix (T), we obtain

$$E_{ad} = 2/3 \left[E_A \operatorname{Cos}\theta + E_B \operatorname{Cos}(\theta - 2\pi/3) + E_C \operatorname{Cos}(\theta - 4\pi/3)\right] \tag{5}$$

Substituting Equations 2, 3 and 4 into Equation 5 and rearranging, we have

$$\begin{aligned} E_{ad} &= -R_a \frac{2}{3}\left[I_a \operatorname{Cos}\theta + I_B \operatorname{Cos}(\theta - 2\pi/3) + I_C \operatorname{Cos}(\theta - 4\pi/3)\right] \\ &\quad + \frac{2}{3}\left[p\lambda_A \operatorname{Cos}\theta + p\lambda_B \operatorname{Cos}(\theta - 2\pi/3) + p\lambda_C \operatorname{Cos}(\theta - 4\pi/3)\right] \qquad (6) \\ &= -I_{ad} R_a + f(p\lambda) \qquad (6a) \end{aligned}$$

where f (pλ) is the second part of Equation 6.

By the same transformation matrix (T),

$$\lambda_{ad} = \frac{2}{3}\left[\lambda_A \text{Cos}\theta + \lambda_B \text{Cos}(\theta - 2\pi/3) + \lambda_C \text{Cos}(\theta - 4\pi/3)\right]$$

$$\lambda_{aq} = -\frac{2}{3}\left[\lambda_A \text{Sin}\theta + \lambda_B \text{Sin}(\theta - 2\pi/3) + \lambda_C \text{Sin}(\theta - 4\pi/3)\right] \qquad (7)$$

The time derivative of λ_{ad} is

$$p\lambda_{ad} = \frac{2}{3}\left[p\lambda_A \text{Cos}\theta + p\lambda_B \text{Cos}(\theta - 2\pi/3) + p\lambda_C \text{Cos}(\theta - 4\pi/3)\right]$$

$$-p\theta\left(\frac{2}{3}\right)\left[\lambda_A \text{Sin}\theta + \lambda_B \text{Sin}(\theta - 2\pi/3) + \lambda_C \text{Sin}(\theta - 4\pi/3)\right] \qquad (8)$$

$$= f(p\lambda) + \omega\lambda_{aq} \qquad (8a)$$

where

$\omega = p\theta =$ speed of generator.

From Equation 8a we can solve for $f(p\lambda)$ and putting it into Equation 6a we have

$$E_{ad} = -I_{ad}R_a + p\lambda_{ad} - \omega\lambda_{aq} \qquad (9)$$

Proceeding in the same manner with E_{aq}, we have

$$E_{aq} = -I_{aq}R_a + p\lambda_{aq} + \omega\lambda_{ad} \qquad (10)$$

To complete the set, we have

$$E_o = -I_o R_a + p\lambda_o \qquad (11)$$

where

E_{ad}, E_{aq} = Direct and quad axis armature voltage

I_{ad}, I_{aq} = Direct and quad axis armature current

λ_{ad}, λ_{aq} = Direct and quad axis stator and rotor mutual flux linkage

R_a = Armature resistance

ω = Speed of generator

Equations 10 and 11 are illustrated by Figure 3 below.

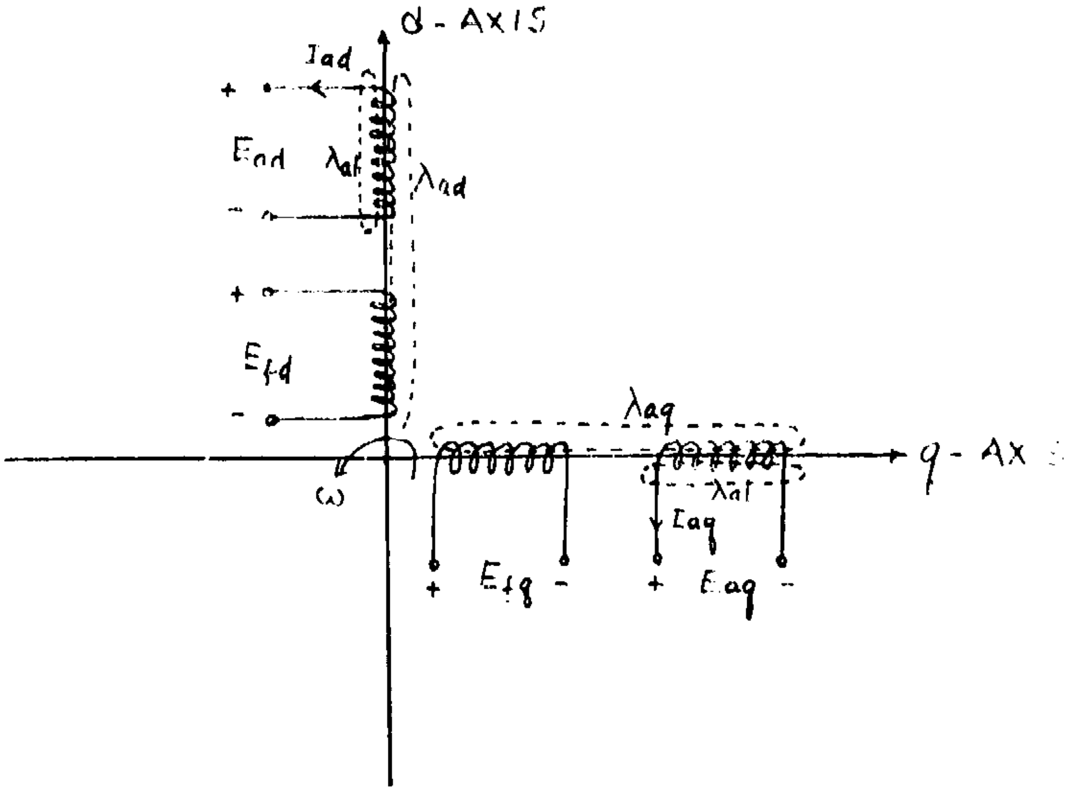

λ_{al} = Leakage flux linkage (assumed the same magnitude in both axis)

Figure 3

The terms $p\lambda_{ad}$ and $p\lambda_{aq}$ are transformer voltages and are generally small compared with speed voltages $\omega\lambda_{aq}$ and $\omega\lambda_{ad}$. (For a better understanding of the speed voltage, see page 62 of "Power System Stability, Vol. III," by Edward Kimbark, John Wiley & Sons, Inc.) Thus Equations 9 and 10 can be approximated as

$$E_{ad} \cong -I_{ad}R_a - \omega\lambda_{aq} \tag{12}$$

$$E_{aq} \simeq -I_{aq}R_a + \omega\lambda_{ad} \tag{13}$$

If the speed is constant, [illegible] 1 p.u. (per unit).

By the two-reactance theory,

$$E_a = E_{aq} - jE_{ad} = \sqrt{E_{aq}^2 + E_{ad}^2} \tag{14}$$

$$I_a = I_{aq} - jI_{ad} = \sqrt{I_{aq}^2 + I_{ad}^2} \tag{15}$$

where

E_a = Generator armature (terminal) voltage

I_a = Generator armature current

j = $\sqrt{-1}$ = imaginary axis unity vector

Equations 14 and 15 are so written to be consistent with the convention used in Figure 1B where the two axes are rotated through 90 deg.

From Equations 12, 13 and Figure 3 the total induced voltage E_i is

E_i = Terminal voltage + $I_a R_a$ voltage drop + armature reaction voltage + voltage due to armature leakage.

then

$$E_{id} = E_{ad} + I_{ad}R_a + I_{aq}X_{aq} + I_{aq}X_{al} \tag{16}$$

$$E_{iq} = E_{aq} + I_{aq}R_a + I_{ad}X_{ad} + I_{ad}X_{al} \tag{17}$$

where

X_{al} = Armature leakage reactance due to λ_{al}

X_{ad}, X_{aq} = Direct and quad-axis mutual reactance between stator and rotor

E_{id}, X_{iq} = Direct and quad axis induced voltage

From Appendix II,

$$X_d = X_{al} + X_{ad} \tag{18}$$

$$X_q = X_{al} + X_{aq} \tag{19}$$

where

X_d, X_q = Direct and quad axis synchronous reactance.

Since there is no applied voltage in the q-axis of the field, $E_{id} = 0$. Utilizing Equations 18 and 19, Equations 16 and 17 can be expressed as

$$E_{id} = E_{ad} + I_{ad}R_a + I_{aq}X_q = 0 \tag{20}$$

$$E_{iq} = E_{aq} + I_{aq}R_a + I_{ad}X_d \tag{21}$$

The phasor diagram of Equations 20 and 21 is shown in Figure 4.

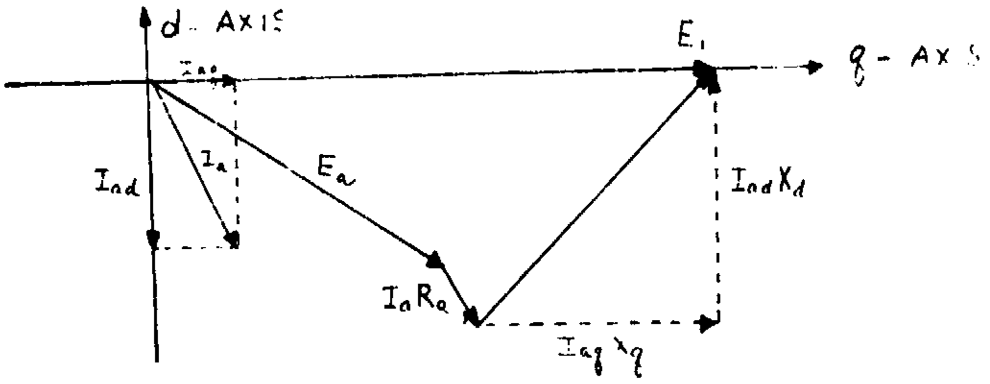

Figure 4

3. Machine Equations Relating Field, Armature and Damper Circuits

In a salient pole synchronous machine, generally there is a damper, or amortisseur, circuit on rotor to produce torque which helps to damp out oscillations of the rotor about its equilibrium position. It is formed by bars or cage windings embedded in the pole faces and connected at their ends by short-circuiting end rings.

The damper circuit has its own resistance, self and mutual inductance and should be treated as one unit when we consider its effect on the current-voltage performance of the machine following a disturbance.

In the machine transient period, since the damper circuit has a higher resistance to inductance ratio, the damper current has a smaller decay time constant; hence its effect on the induced voltage is shorter. The short time effect of the damper current is called the subtransient period and the longer time effect of the field current is called the transient period. Hence the transient variables that include the effect of the damper circuit have the subscript D and are called the subtransient variables.

In a round rotor synchronous machine, which is the type described in this report, there is no damper circuit. However, the transient envelope of the induced voltage is not in a pure exponential decay form due to the multiple flux paths between the N-S poles in the solid rotor. But this envelope can be approximated to have two time constants, T_1 and T_2.

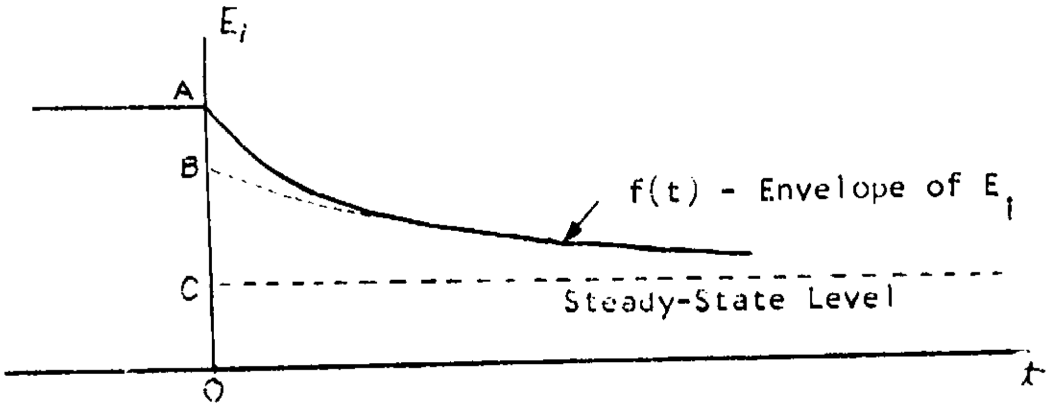

(assume a load is applied)

Figure 5

$$f(t) \cong (B - C)^{-t/T_1} + (A - B)e^{-t/T_2} + C \qquad (22)$$

We can see that $T_2 > T_1$. Like the salient pole machine, we can refer the first term of equation 22 to the effect of the transient circuit and refer the second term equivalent to the effect of a damper circuit. Thus T_1 is called the transient time constant and T_2 the subtransient time constants. Figure 3 is then modified to Figure 6 to include the damper circuit.

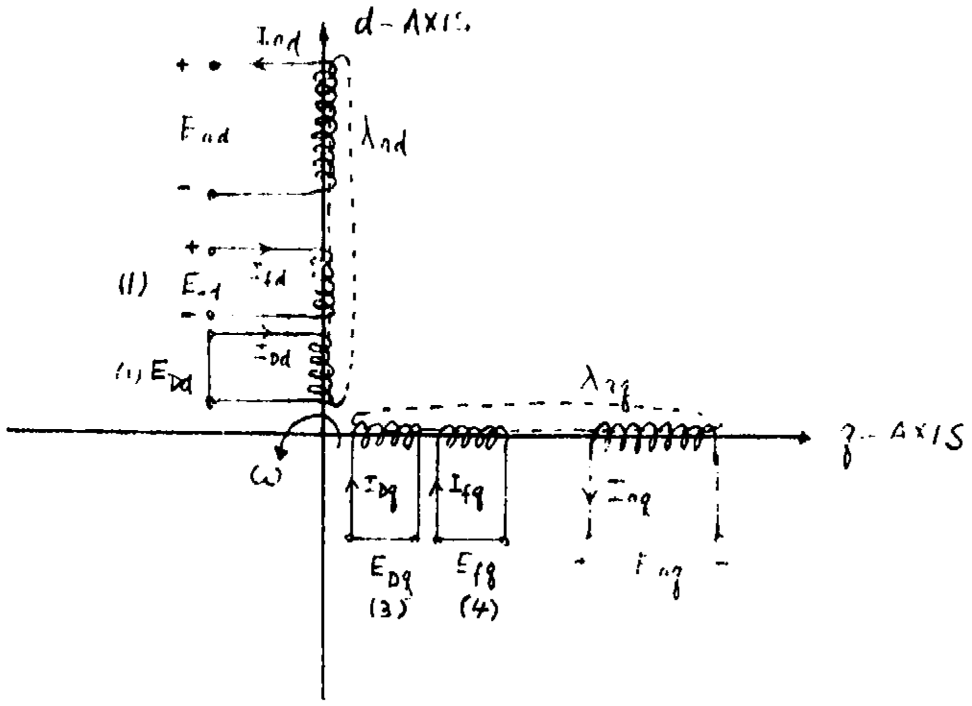

Figure 6

Let us first consider the field circuit by itself. The equivalent circuit is shown below in Figure 7.

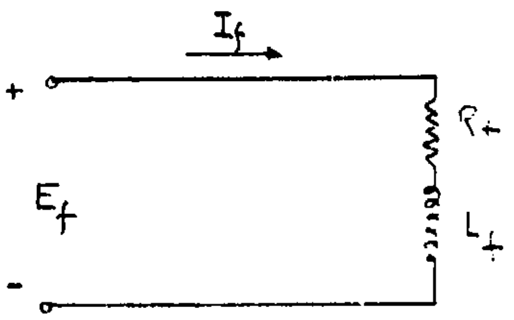

Figure 7

The field current, I_f, is given by

$$I_f = \frac{E_f}{R_f + pL_f} \tag{23}$$

where

E_f = Field applied voltage

R_f = Field resistance

L_f = Field inductance

Equation 23 can be re-arranged as

$$I_f = \frac{1}{R_f} \frac{E_f}{(1 + p\ L_f/R_f)}$$

$$= \frac{E_f}{1 + pT} \qquad (24)*$$

where

$T = L_f/R_f$

$R_f = 1$ p.u.

Applying equation 24 to the d and q-axis, we have

$$I_{fd} = \frac{E_{fd}}{1 + pT'_{do}} \qquad (25)*$$

---

*The asterisk denotes the equation is valid only in the per unit system

$$I_{fq} = \frac{E_{fq}}{1 + pT'_{qo}} \qquad (26)*$$

where

T'_{do}, T'_{qo} = Direct and quad-axis open circuit transient time constant

The induced voltage in the d and q-axis due to the field and damper current is

$$E_{fd} = I_{Dd}R_D + I_{fq}R_f \qquad (27)$$

$$E_{fq} = I_{Dq}R_D - I_{fd}R_f \qquad (28)$$

where

I_{Dd}, I_{Dq} = Direct and quad-axis subtransient current

I_{fd}, I_{fq} = Direct and quad-axis field current

R_D = Damper circuit resistance

The negative sign in equation 28 is chosen to comply with the concept that positive field current induces negative voltage.

Since R_D and r_f are 1 p.u. and equating with equations 20 and 21, we have:

$$E_{ad} + I_{ad}R_a + I_{aq}X_q = I_{Dq} + I_{fq} \qquad (29)*$$

---

*The asterisk denotes the equation is valid only in the per unit system

$$E_{aq} + I_{aq}R_a + I_{ad}X_d = I_{Dd} - I_{fd} \tag{30)*$$

From equations 12 and 13

$$\omega\lambda_{ad} = E_{aq} + I_{aq}R_a \tag{31}$$

$$-\omega\lambda_{aq} = E_{ad} + I_{ad}R_a \tag{32}$$

Since the field quadrature path has a very high impedance I_{fq} is small. Thus

$$I_{fq} \cong 0 \tag{33}$$

To simplify the analysis, the field quadrature circuit is completely eliminated.

Substituting equations 31 and 32 into equations 29 and 30 and assuming equation 33 is valid, we have

$$-\omega\lambda_{aq} + I_{aq}X_q \cong I_{Dq} \tag{34)*$$

$$\omega\lambda_{ad} + I_{ad}X_d = I_{Dd} - I_{fd} \tag{35)*$$

Equations 34 and 35 relate the damper, field and armature currents with the armature mutual flux linkage.

Equation 24 can be written as

$$E_{fd} = I_{fd}\,(1 + pT'_{do}) \tag{36)*$$

---

*The asterisk denotes the equation is valid only in the per unit system

If the effects of the armature and damper circuits are included, equation 36 is then

$$E_{fd} - M_{af}pI_{ad} - M_{Df}pI_{Dd} = I_{fd}\ (1 + pT'_{do}) \qquad (37)*$$

where

M_{af} = Mutual inductance between armature and field

M_{Df} = Mutual inductance between damper and field

Equation 37 can be re-arranged as:

$$\frac{E_{fd} - I_{fd}}{pT'_{do}} = I_{fd} + \left(\frac{M_{af}}{T'_{do}}\right) I_{ad} + \left(\frac{M_{Df}}{T'_{do}}\right) I_{Dd} \qquad (38)*$$

The coefficients of I_{ad} and I_{Dd} are evaluated by a separate method given in the next section. Equation 38 simply demonstrates the form of field current equation to be expected.

4. Evaluation of Field, Damper and Armature Currents

Since there is no applied voltage in the field quadrature, damper direct and quadrature circuits,

$$E_{fq} = E_{Dd} = E_{Dq} = 0 \qquad (39)$$

The set of equations describing the four circuits (1) to (4) in Figure 6 is then

$$E_{fd} = I_{fd} + p\lambda_{fd} \qquad (40)*$$

---

*The asterisk denotes the equation is valid only in the per unit system

$$0 = I_{fq} + p\lambda_{fq} \qquad (41)*$$

$$0 = I_{Dd} + p\lambda_{Dd} \qquad (42)*$$

$$0 = I_{Dq} + p\lambda_{Dq} \qquad (43)*$$

Equation 40 gives

$$\lambda_{fd} = \frac{E_{fd} - I_{fd}}{p} \qquad (44)*$$

The relationship between field, damper and armature currents and their induced flux linkages is given by:

$$\begin{vmatrix} \lambda_{fd} \\ \lambda_{Dd} \\ \lambda_{ad} \end{vmatrix} = \begin{vmatrix} T'_{do} & T'_{do}\dfrac{X_{ad}}{X_{ad} + X_{fd}} & -T'_{do}\dfrac{X_{ad}^2}{X_{ad} + X_{fd}} \\ T_{Ddo}\dfrac{X_{ad}}{X_{ad} + X_{Dd}} & T_{Ddo} & T_{dDo}\dfrac{X_{ad}^2}{X_{ad} + X_{Dd}} \\ -1 & 1 & -X_d \end{vmatrix} \begin{vmatrix} I_{fd} \\ I_{Dd} \\ I_{ad} \end{vmatrix} \qquad (45)*$$

$$\begin{vmatrix} \lambda_{fq} \\ \lambda_{dq} \\ \lambda_{aq} \end{vmatrix} = \begin{vmatrix} T'_{qo} & T'_{qo}\dfrac{X_{aq}}{X_{aq} + X_{fq}} & -T'_{qo}\dfrac{X_{aq}^2}{X_{aq} + X_{fq}} \\ T_{Dqo}\dfrac{X_{aq}}{X_{aq} + X_{Dq}} & T_{Dqo} & -T_{Dqo}\dfrac{X_{aq}^2}{X_{aq} + X_{Dq}} \\ 1 & 1 & -X_q \end{vmatrix} \begin{vmatrix} I_{fq} \\ I_{Dq} \\ I_{aq} \end{vmatrix} \qquad (46)*$$

---

*The asterisk denotes the equation is valid only in the per unit system

The derivation of Equations 45 and 46 is quite tedious and is not given in this report.

From Equation 45, we obtain

$$\lambda_{fd} = T'_{do}\left(I_{fd} + \frac{X_{ad}}{X_{ad} + X_{fd}} I_{Dd} - \frac{X_{ad}^{2}}{X_{ad} + X_{fd}} I_{ad}\right) \qquad (47)$$

since

$$X_{d} - X'_{d} = \frac{X_{ad}^{2}}{X_{ad} + X_{fd}} \qquad (48)$$

(See Appendix B for derivation)

after substituting λ_{fd} in Equation 47 into Equation 44 and dividing by T'_{d0} we have

$$\frac{E_{fd} - I_{fd}}{pT'_{do}} = I_{fd} - (X_{d} - X'_{d})\, I_{ad} + \frac{X_{ad}}{X_{ad} + X_{fd}} I_{Dd} \qquad (49)^{*}$$

Equation 49 is in the same form as Equation 38 given in Section 3. Similarly solving Equations 41 to 43, we have

$$-\frac{I_{fq}}{pT'_{qo}} = I_{fq} - (X_{q} - X'_{q})\, I_{aq} + \frac{X_{aq}}{X_{aq} + X_{fq}} I_{Dq} = 0 \qquad (50)^{*}$$

$$-\frac{I_{Dd}}{pT_{Ddo}} = I_{Dd} - \frac{X_{ad}^{2}}{X_{ad} + X_{Dd}} I_{ad} + \frac{X_{ad}}{X_{ad} + X_{Dd}} I_{fd} \qquad (51)^{*}$$

---

*The asterisk denotes the equation is valid only in the per unit system

$$-\frac{I_{Dq}}{pT_{Dqo}} = I_{Dq} - \frac{X_{aq}^2}{X_{aq} + X_{Dq}} I_{aq} + \frac{X_{aq}}{X_{aq} + X_{Dq}} I_{fq} \qquad (52)^*$$

where

X_{fd}, X_{fq} = Direct and quad axis field circuit leakage reactance

X_{Dd}, X_{Dq} = Direct and quad axis damper circuit leakage reactance

and

$$T_{Ddo} = T''_{do} \frac{(X_{ad} + X_{fd})(X_{ad} + X_{Dd})}{X_{ad}X_{fd} + X_{fd}X_{Dd} + X_{Dd}X_{ad}} \qquad (53)$$

$$T_{Dqo} = T''_{qo} \frac{(X_{aq} + X_{fq})(X_{aq} + X_{Dq})}{X_{aq}X_{fq} + X_{fq}X_{Dq} + X_{Dq}X_{aq}} \qquad (54)$$

Since X_{fq} is very large, (to give a very small I_{fq})

$$T_{Dqo} \cong T''_{qo} \frac{X_{fq}(X_{aq} + X_{Dq})}{X_{aq}X_{fq} + X_{fq}X_{Dq}}$$

$$\cong T''_{qo}$$

where

T''_{do}, T''_{qo} = Direct and quad axis open circuit subtransient time constant.

---

*The asterisk denotes the equation is valid only in the per unit system

T'_{do} and T'_{qo} are related to the short circuit parameters by the following

$$T'_d = \frac{X'_d}{X_d} T'_{do} \qquad (55)$$

$$T'_q = \frac{X'_q}{X_q} T'_{qo} \qquad (56)$$

where

T'_d, T'_q = Direct and quad-axis short circuit transient time constant.

5. Voltage Regulation

If a load is suddenly applied or removed from the generator, its terminal voltage will gradually decay or increase to another steady state level and will never return to its initial value. However, in almost all applications of synchronous generators, it is desirable that the terminal voltage remains substantially constant regardless of load. This can be accomplished by a voltage regulating system (with negative feedback) to change the field excitation whenever there is a change in terminal voltage.

A typical regulated response of a generator terminal voltage envelope when the load is completely or partially removed is shown in Figure 8. In the case of load application, the same characteristic response occurs except it is turned upside down with respect to the 1 p.u. line.

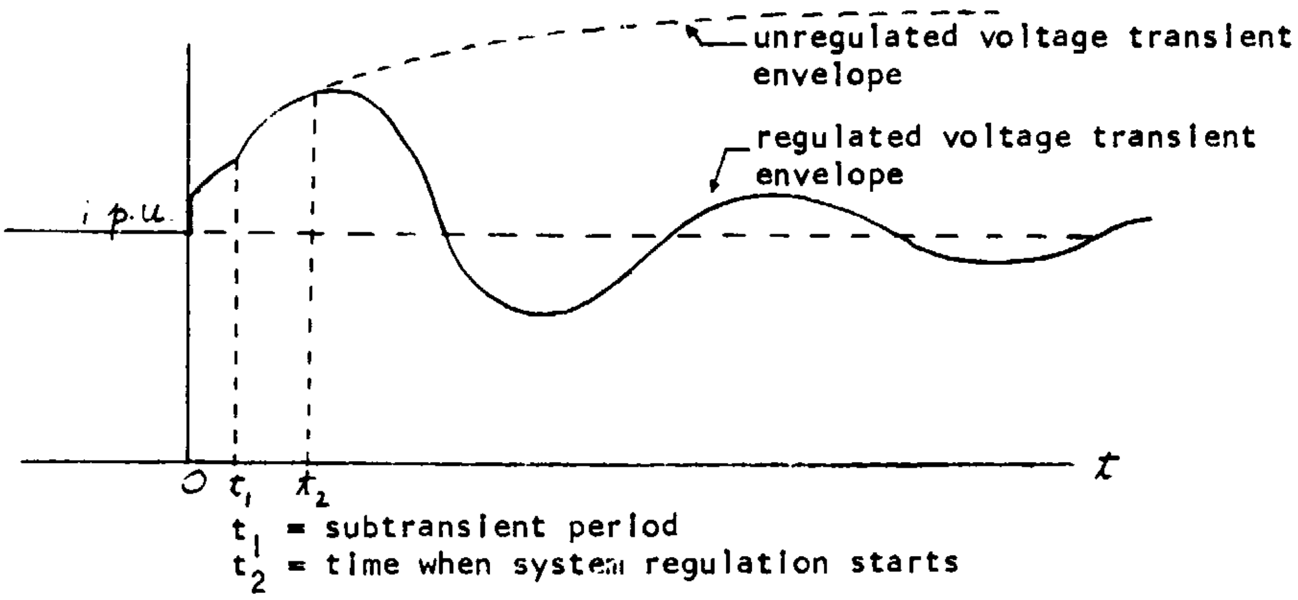

Figure 8

The response of the unregulated generator terminal voltage can be depicted by the phasor diagram in Figure 9. It shows the relationship of the subtransient (E_i''), transient (E_i') and steady-state (E_i) induced voltages. It is a more detailed representation of Figure 4.

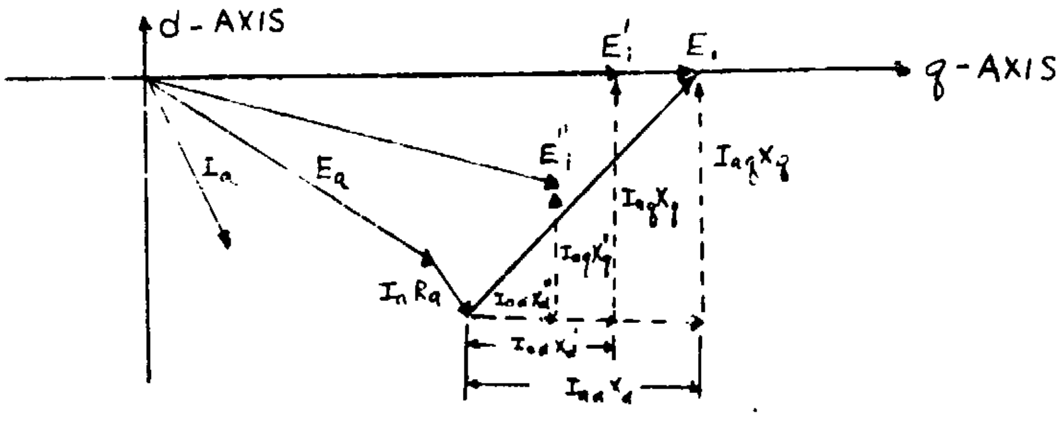

Figure 9

A. Voltage Regulating System - With Series and Shunt Fields and Constant Speed

The regulating system to be studied in this report has both series and shunt field feedbacks. It is shown in Figure 10.

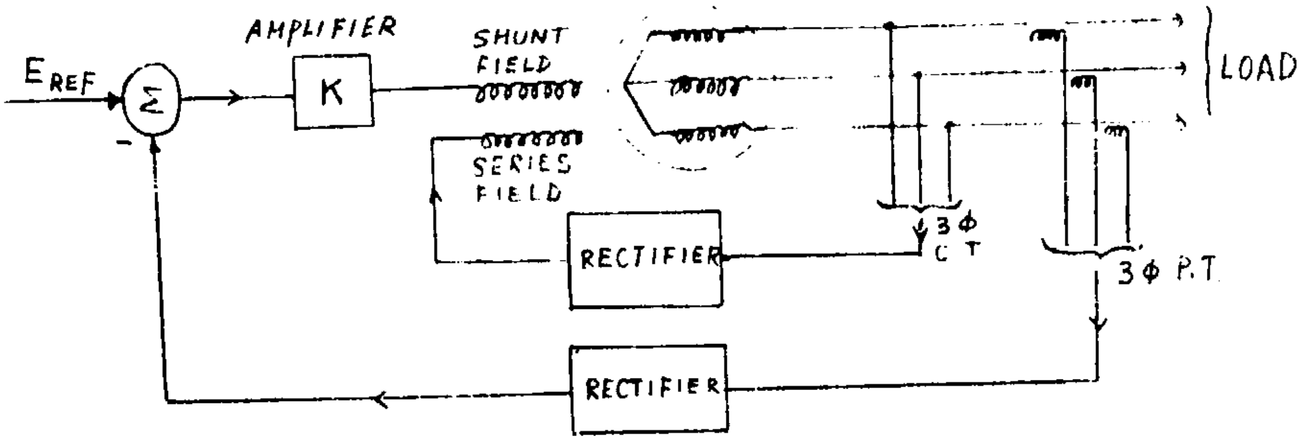

Figure 10

The power transformer has the following transfer function:

$$\frac{1}{1 + pT_p} \qquad (37)^*$$

where T_p is the time constant of the transformer.

Effect of Shunt and Series Fields

The analysis of the regulator system is just like that of a feedback system except the complication of two fields.

---

*The asterisk denotes the equation is valid only in the per unit system

First consider the current transformer as shown in Figure 11.

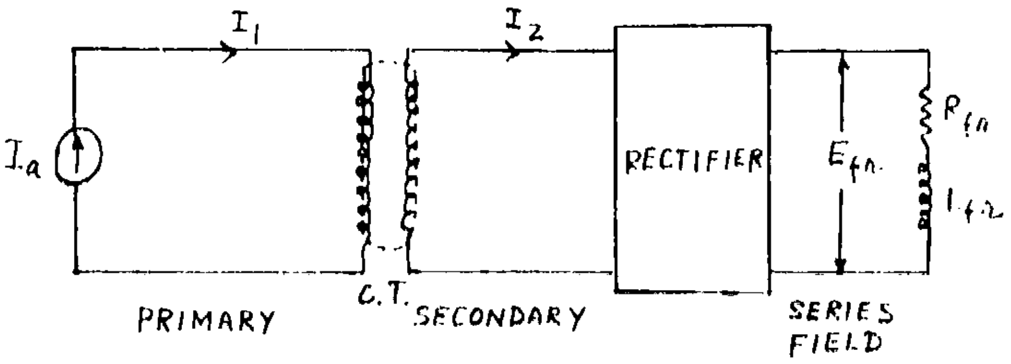

Figure 11

I_1, I_2 = Primary and secondary current

R_{fr}, L_{fr} = Series field resistance and inductance

E_{fr} = Series field voltage

Ideally when the primary current I_1 makes a step change, the secondary current I_2 should also make the same change. However, I_2 cannot change abruptly because of the series field inductance L_{fr}. Thus, most of the excess primary current will be used as magnetizing current, causing a high saturation and a high forcing voltage across the series field. The transfer function is quite complicated.

To make the calculation practical, we can assume I_2 changes exponentially due to a step change of I_1, i.e., the current transformer is replaced by a potential transformer with the voltage across the series field proportional to the primary current. (See Figure 12)

Let the equivalent field current be composed by two parts

$$I_f \cong I_{fd} = I_{fdr} + I_{fdh} \qquad (58)$$

where

I_{fdr}, I_{fdh} = Series and shunt field direct-axis current.

The quad-axis transient currents are assumed negligible.

At no load, 1 p.u. shunt field current I_{fdh} will induce 1 p.u. armature voltage.

1 p.u. shunt field voltage E_{fh} will produce 1 p.u. field current I_f at steady state.

1 p.u. armature current I_a will produce σ p.u. I_{fdr} and σ p.u. E_{fr} at steady state. Thus

$$\sigma = \frac{\text{series field ampere turns with 1 p.u. } I_a \text{ at steady state}}{\text{base shunt field ampere turns}}$$

Let

M_{hr} = Mutual inductance between the shunt and series fields

When there is a rate of change of I_{fr} of 1 p.u./sec, the voltage induced in the shunt field is M_{hr} p.u.

Thus the field current Equation 49 should be modified to include the effect of both fields. Assuming:

$$X_{fdr} = X_{fdh} \tag{59}$$

where

X_{fdr}, X_{fdh} = Series and shunt field reactance.

We have a separate equation for each field current:

$$\frac{E_{fh} - I_{fdh}}{pT'_{doh}} = I_{fdh} + M_{hr} I_{fdr} - (X_d - X'_d)\, I_{ad} + \frac{X_{ad}}{X_{ad} + X_{fd}}\, I_{Dd} \qquad (60)^*$$

$$\frac{\sigma I_a - I_{fdr}}{pT'_{dor}} = I_{fdr} + M_{hr}\, I_{fdh} - (X_d - X'_d)\, I_{ad} + \frac{X_{ad}}{X_{ad} + X_{fd}}\, I_{Dd} \qquad (61)^*$$

where

T'_{dor}, T'_{doh} = Series and shunt field open circuit time constant

E_{fh} = Shunt field excitation voltage

Equation 58 links the two field currents I_{fdh} and I_{fdr}. Under the above assumptions, other equations in Section 4 will remain the same.

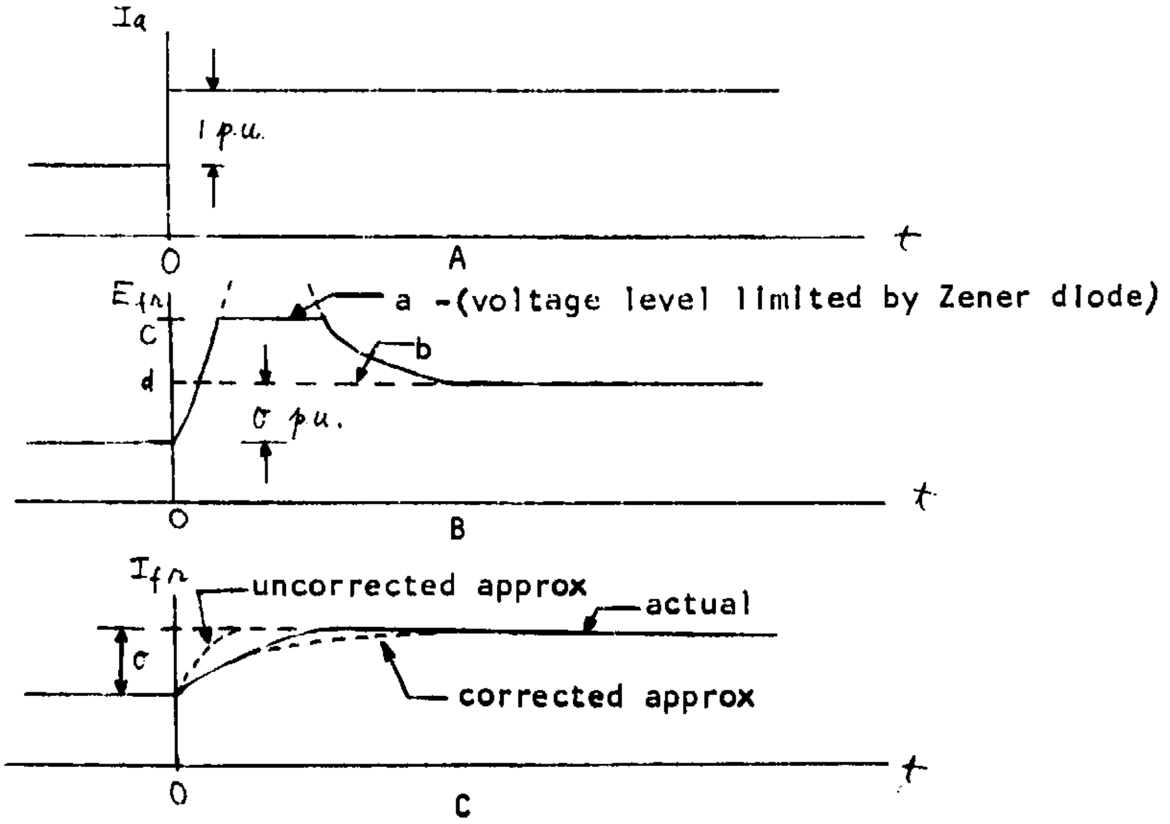

FIGURE 12

---

*The asterisk denotes the equation is valid only in the per unit system

Although E_{fr} is approximated by curve b in Figure 12B, the actual voltage level for the first few cycles is C p.u. which is $c/(1 + \sigma)$ times higher than the approximated level. Hence when we calculate the time constant of the series field, the effect of this high forcing voltage should be considered. The time constant T'_{dor} can therefore be approximated as

$$T'_{dor} = \frac{L_{fr}}{k\ E_{fr}} \qquad (62)$$

where:

k = forcing factor

$$= \frac{\text{initial voltage across series field}}{\text{steady state voltage across series field}}$$

In the example given in Figure 12,

$$k = \frac{c}{d}$$

B. Voltage Regulating System - with Series and Shunt Fields and Variable Speed

When rotor speed changes, the electrical frequency changes correspondingly and all the reactances X_{ad}, X_{fd}, etc. will have no meaning, nor can they be expressed as ωL_{ad}, ωL_{fd}, etc. All inductance voltage drops should be given as p(LI). The generator equations will be more complicated.

To make the analysis simple for practical purpose, all the inductance will be expressed as ωL_{ad}, etc., using the average or base frequency for ω and assume the change in frequency is small enough so that the reactances stay about constant. Only the speed voltage $\omega\lambda$ is assumed to vary with speed.

6. Conclusion

In the regulating system, the load is assumed to have the following impedance function:

$$Z_L = R_L + jX_L \tag{63}$$

where

Z_L, R_L, X_L = Load impedance, resistance and reactance.

Since

$$E_a = I_a Z_L \tag{64}$$

and substituting Equations 14, 15 and 63 into 64, we have

$$\begin{aligned} E_{aq} - jE_{ad} &= (I_{aq} - jI_{ad})(R_L + jX_L) \\ &= (I_{aq}R_L + I_{ad}X_L) - j(I_{ad}R_L - I_{aq}X_L) \end{aligned}$$

Hence

$$E_{ad} = I_{ad}R_L - I_{aq}X_L \tag{65}$$

$$E_{aq} = I_{aq}R_L + I_{ad}X_L \tag{66}$$

Equations 65 and 66 relate armature voltage and current. With the following assumptions:

1. No saturation occurs in the generator
2. Quadrature field current is negligible

$I_{fq} \cong 0$

we have derived a set of 13 equations for the 13 unknowns:

E_a E_{ad} E_{aq}

I_a I_{ad} I_{aq}

I_{fd} I_{fdr} I_{fdh}

I_{Dd} I_{Dq}

λ_{ad} λ_{aq}

The 13 equations are:

$$E_{ad} + r_a I_{ad} + \omega\lambda_{aq} = 0$$

$$E_{aq} + r_a I_{aq} - \omega\lambda_{ad} = 0$$

$$\lambda_{ad} + I_{ad}X_d = I_{Dd} - I_{fd}$$

$$\lambda_{aq} + I_{aq}X_q = I_{Dq}$$

$$\frac{e_{fh} - I_{fdh}}{pT'_{doh}} = I_{fdh} + M_{hr}I_{fdr} - (X_d - X'_d)\ I_{ad} + \frac{X_{ad}}{X_{ad} + X_{fd}}\ I_{Dd}$$

$$-\frac{I_{fdr}}{pT'_{dor}} = I_{fdr} + M_{hr} I_{fdh} - (X_d - X'_d)\, I_{ad} + \frac{X_{ad}}{X_{ad} + X_{fd}}\, I_{Dd}$$

$$I_{fd} = I_{fdh} + I_{fdr}$$

$$-\frac{I_{Dd}}{pT_{Ddo}} = I_{Dd} - \frac{X_{ad}^2}{X_{af} + X_{Dd}}\, I_{ad} + \frac{X_{ad}}{X_{ad} + X_{Dd}}\, I_{fd}$$

$$-\frac{I_{Dq}}{pT_{Dqo}} = I_{Dq} - \frac{X_{aq}^2}{X_{aq} + X_{Dq}}\, I_{aq}$$

$$E_{ad} = I_{ad} R_L - I_{aq} X_L$$

$$E_{aq} = I_{ad} X_L + I_{aq} R_L$$

$$I_a = \sqrt{I_{ad}^2 + I_{aq}^2}$$

$$E_a = \sqrt{E_{ad}^2 + E_{aq}^2}$$

With the aid of the 13 equations, a mathematical model of voltage regulating system shown in Figure 10 is given by the block diagram shown in Figure 13.

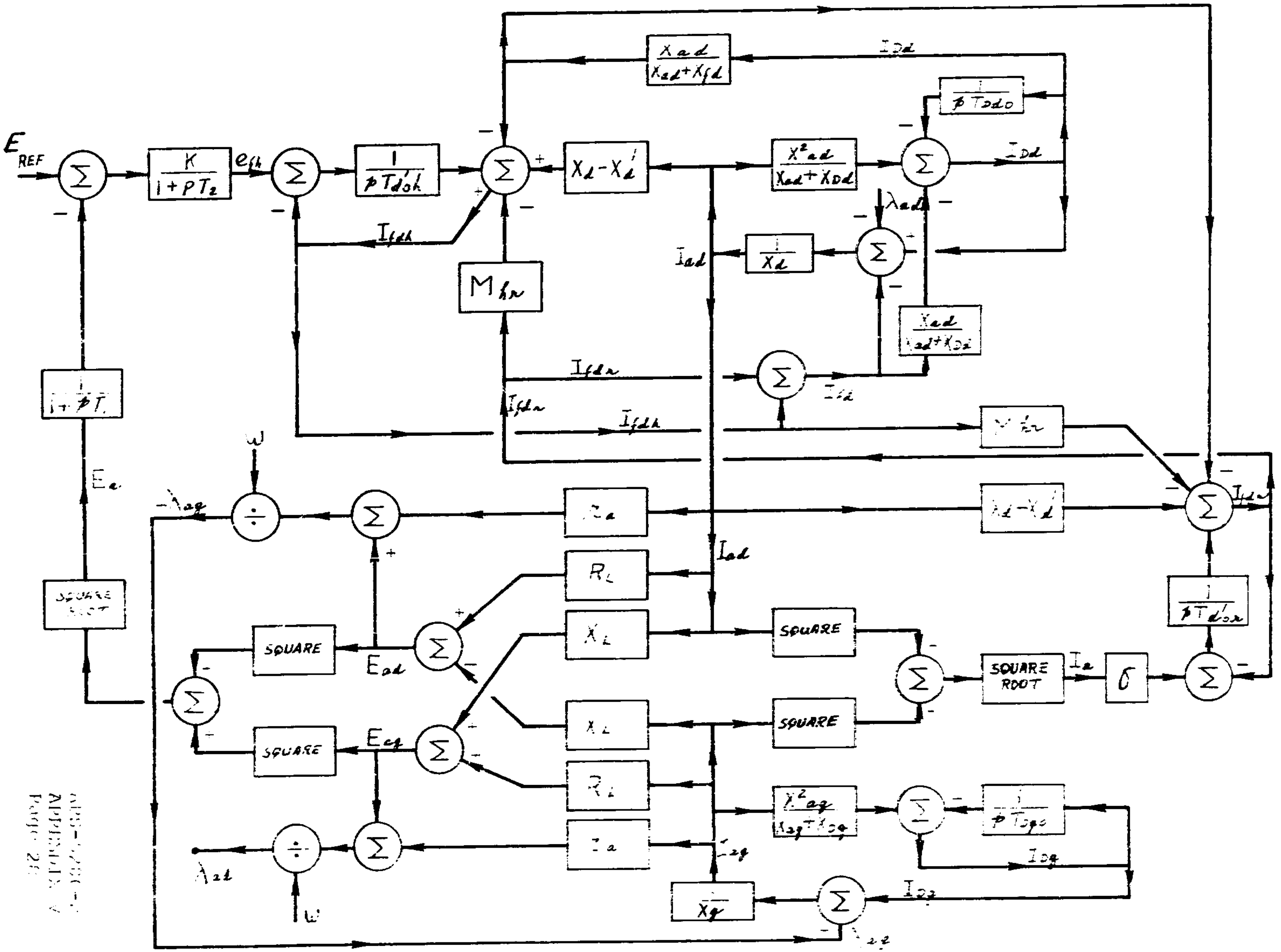
E_{REF}
$\frac{K}{1+pT_2}$
e_{fh}
$\frac{1}{pT'_{doh}}$
$X_d - X'_d$
$\frac{X^2_{ad}}{X_{ad}+X_{Dd}}$
$\frac{1}{pT_{Ddo}}$
$\frac{X_{ad}}{X_{ad}+X_{fd}}$
I_{Dd}
λ_{ad}
$\frac{1}{X_d}$
I_{ad}
$\frac{X_{ad}}{X_{ad}+X_{Dd}}$
I_{fdh}
M_{hr}
I_{fdr}
I_{fd}
X'_{hr}
$X_d - X'_d$
I_{fdr}
$\frac{1}{pT'_{dor}}$
σ
I_a
SQUARE ROOT
SQUARE
SQUARE
$\frac{X^2_{aq}}{X_{aq}+X_{Dq}}$
$\frac{1}{pT_{Dqo}}$
I_{Dq}
I_{aq}
$\frac{1}{X_q}$
λ_{aq}
r_a
R_L
X_L
X_L
R_L
r_a
E_{ad}
E_{aq}
SQUARE
SQUARE
SQUARE ROOT
E_a
$\frac{1}{1+pT_1}$
$-\lambda_{aq}$
λ_{ad}
ω
ω
Σ
$\div$
+
−

FIGURE 13

NOMENCLATURE

E_a = Generator terminal voltage

E_{ad}, E_{aq} = Direct- and quadrature-axis components of E_a

E_f = generator field voltage

E_{fd}, E_{fq} = direct and quadrature axis field voltage

E_{id}, E_{iq} = direct and quadrature axis induced voltage

I_a = generator armature current

I_{ad}, I_{aq} = direct and quadrature axis components of armature current

I_{fd}, I_{fq} = direct and quadrature axis field current of generator

I_{Dd}, I_{Dq} = direct and quadrature axis subtransient current

p = differential operator d/dt

T'_{do}, T'_{qo} = direct and quadrature axis open circuit transient time constants

T''_{do}, T''_{qo} = direct and quadrature axis open circuit subtransient time constants

T'_d, T'_q = direct and quadrature axis short circuit transient time constant

R_a = generator armature resistance

NOMENCLATURE (Cont.)

R_L = load resistance

X_L = load reactance

X_{al} = armature leakage reactance

X_d, X_q = direct and quadrature axis synchronous reactances

X_{ad}, X_{aq} = direct and quadrature axis mutual reactances between stator and rotor circuits, referred to stator.

X'_d, X'_q = direct and quadrature axis transient reactances

X''_d, X''_q = direct and quadrature axis subtransient reactances

X_{fd}, X_{fq} = direct and quadrature axis field circuit leakage reactances

X_{Dd}, X_{Dq} = direct and quadrature axis damper circuit leakage reactances

Z_L = load impedance

λ_{ad}, λ_{aq} = direct and quadrature axis stator flux linkages

ω = speed of the generator

The additional subscript h and r in the field circuit variables denotes shunt or series field.

All voltages, currents, reactances, resistances, impedance, speed and flux linkages are per unit quantities.

APPENDIX A

Blondel's Two-Reactance Method

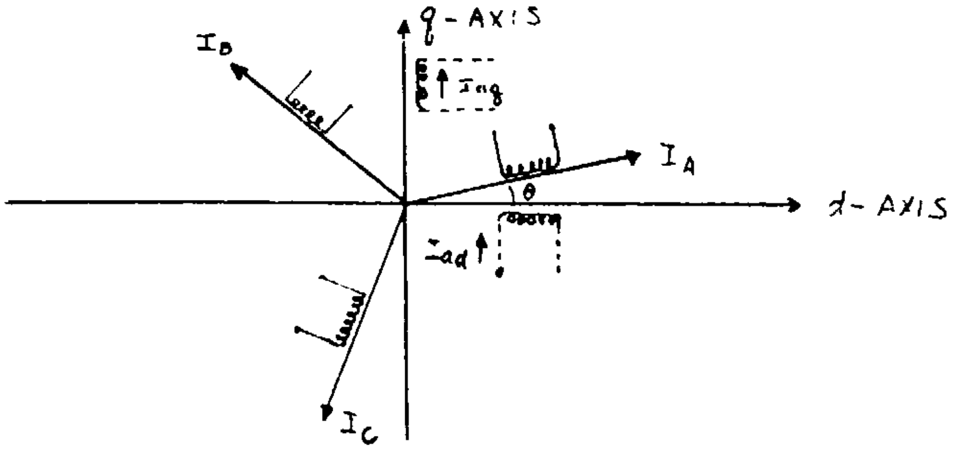

Figure A-1

The phasor diagram of a balanced three-phase current at any instant of time t is shown in Figure A-1.

where

$$\theta = \omega t \tag{A-1}$$

ω = Frequency of the current or speed of generator

Since the armature variables are expressed in three axes (denoted by the capital letters A, B and C), one axis for each phase, and the rotor variables are expressed in two axes (denoted by the small letters d and f), it is desirable to find a transformation to express the three-phase variables by the two-axis variables.

Let two currents I_{ad} and I_{aq} flow through two fictitious coils located at the d and q axis and each having the same number of turns as a phase coil, which would set up the same MMF wave as the actual currents I_A, I_B, I_C. Because of the fact that the three actual coils are replaced by a system of two-axis coils, the unit of current in the axis coils is 3/2 times that of the phase coils.

The d-axis component of MMF in the phase coils due to the I_A is:

$$MMF_{Ad} = N\ I_A\ \text{Cos}\theta \qquad (A-2)$$

where

N = Number of turns in the coil.

The d-axis component of the resultant MMF wave due to the three-phase currents is therefore:

$$MMF_d = I_A\text{Cos}\theta + I_B\text{Cos}(\theta - 2\pi/3) + I_C\text{Cos}(\theta - 4\pi/3) \qquad (A-3)$$

The MMF wave due to current i_{ad} in the axis coil is

$$MMF_d = 3/2\ NI_{ad} \qquad (A-4)$$

The factor 3/2 is inserted to take into account the change in unit of I_d just mentioned. Equating A-3 with A-4 and cancelling the factor N, we have:

$$I_{ad} = \frac{2}{3}\left[I_A\text{Cos}\theta + I_B\text{Cos}(\theta - 2\pi/3) + I_C\text{Cos}(\theta - 4\pi/3)\right] \qquad (A-5)$$

Similarly the q-axis current I_q is given by:

$$I_{aq} = -\frac{2}{3}\left[I_A\text{Sin}\theta + I_B\text{Sin}(\theta - 2\pi/3) + I_C\text{Sin}(\theta - 4\pi/3)\right] \qquad (A-6)$$

If the three-phase currents are to be eliminated, three substitute variables will be required. Hence it is necessary to introduce a third variable I_o, which is called the zero-sequence current in symmetrical component theory, and

$$I_o = \frac{1}{3}(I_A + I_B + I_C) \qquad (A-7)$$

Since I_o produces no flux linking the rotor, it is associated with the stator leakage inductance. In the balanced three-phase condition, the sum of the phase currents is zero, hence

$$I_o = 0 \qquad (A-8)$$

Equations A-5, 6 and 7 can be written in the matrix form as

$$\begin{bmatrix} I_{ad} \\ I_{aq} \\ I_o \end{bmatrix} = (T) \begin{bmatrix} I_a \\ I_b \\ I_c \end{bmatrix} \qquad (A-9)$$

where (T) is the transformation matrix given by

$$(T) = \frac{2}{3} \begin{bmatrix} \cos\theta & \cos(\theta - 2\pi/3) & \cos(\theta - 4\pi/3) \\ -\sin\theta & -\sin(\theta - 2\pi/3) & -\sin(\theta - 4\pi/3) \\ \frac{1}{2} & \frac{1}{2} & \frac{1}{2} \end{bmatrix} \qquad (A-10)$$

The same (T) can be applied to the voltage equations between E_{ad}, E_{aq}, E_o and phase voltages E_A, E_B, E_C as well as between λ_{ad}, λ_{aq}, λ_o and phase flux λ_A, λ_B, λ_C.

In the balanced condition

$$E_o = 0 \qquad (A-11)$$

$$\lambda_o = 0 \qquad (A-12)$$

APPENDIX B

The complete generator circuit is shown in Figure A-2 below.

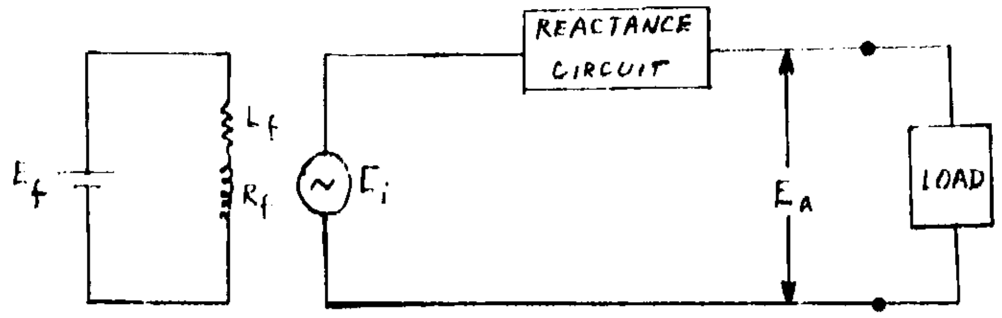

Figure A-2

The equivalent direct axis reactance circuit is shown in Figure A-3.

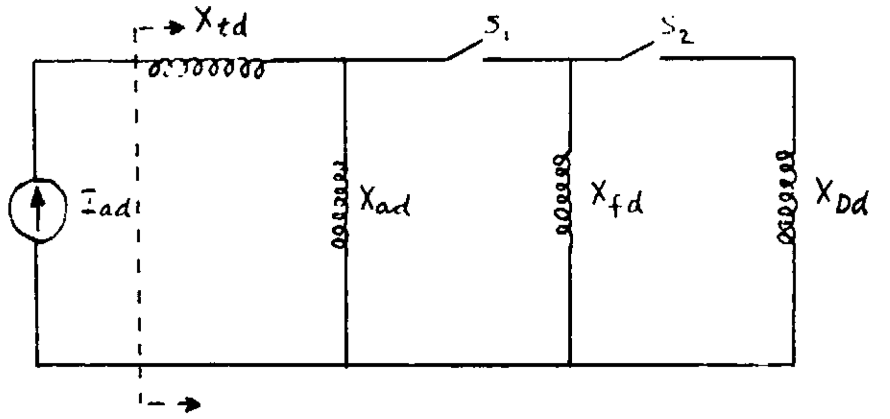

X_{td} = total direct-axis reactance in generator

Figure A-3

When a load is removed or applied to a generator, a transient condition occurs before steady-state is reached. For the first few cycles we have subtransient condition due to the subtransient reactance X_d''. The total reactance is

$$X_{td} = X_d''$$

X''_d is defined in Figure A-3 with switches S_1, S_2 closed.

$$X''_d = X_{al} + \frac{1}{1/X_{ad} + 1/X_{fd} + 1/X_{Dd}}$$

$$= X_{al} + \frac{X_{ad} X_{fd} X_{Dd}}{X_{fd} X_{Dd} + X_{ad} X_{fd} + X_{ad} X_{Dd}} \qquad (A-13)$$

Then we have transient condition due to the transient reactance X'_d. The total reactance becomes

$$X_{td} = X'_d$$

X'_d is defined in Figure A-3 with switch S_1 closed.

$$X'_d = X_{al} + \frac{1}{1/X_{ad} + 1/X_{fd}}$$

$$= X_{al} + \frac{X_{ad} X_{fd}}{X_{ad} + X_{fd}} \qquad (A-14)$$

In steady-state

$$X_{td} = X_d$$

X_d is defined in Figure A-3 with both switches S_1 and S_2 open.

$$X_d = X_{al} + X_{ad} \qquad (A-15)$$

Combining equations A-14 and A-15, we can express X'_d in terms of X_d

$$X'_d = (X_d - X_{ad}) + \frac{X_{ad}X_{fd}}{X_{ad} + X_{fd}}$$

$$= X_d + \frac{-X_{ad}^2 - X_{ad}X_{fd} + X_{ad}X_{fd}}{X_{ad} + X_{fd}}$$

$$= X_d - \frac{X_{ad}^2}{X_{ad} + X_{fd}}$$

$$= X_d - \Delta 1 \qquad \text{(A-16)}$$

$\Delta 1$ is the increase in reactance from transient to steady state period.

Combining equations A-13 and A-15, we can express X''_d in terms of X'_d

$$X''_d = (X_d - X_{ad}) + \frac{X_{ad}X_{fd}X_{Dd}}{X_{fd}X_{Dd} + X_{ad}X_{fd} + X_{ad}X_{Dd}}$$

$$= X_d - \frac{X_{ad}^2\,(X_{fd} + X_{Dd})}{X_{fd}X_{Dd} + X_{ad}X_{fd} + X_{ad}X_{Dd}}$$

$$= X_d - \Delta 2 \qquad \text{(A-17)}$$

$\Delta 2$ is the increase in reactance from subtransient to steady state period.

The equivalent quadrature axis reactance circuit is shown in Figure A-4.

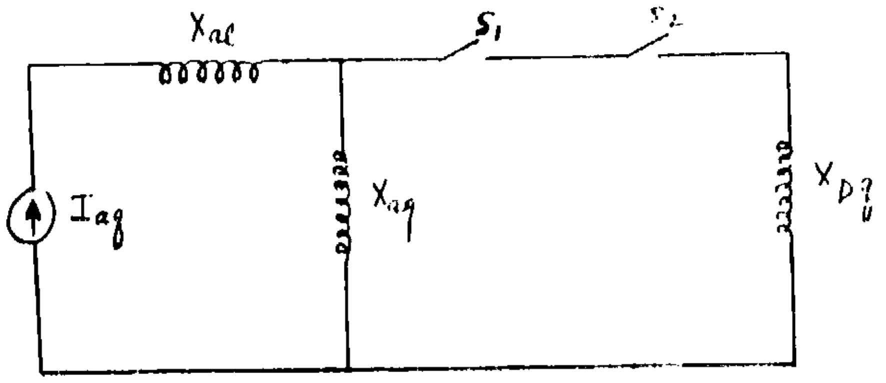

Figure A-4

Figure A-4 is similar to Figure A-4 except X_{fq} is very large (open circuit). Following the previous procedure, we obtain

$$X_q'' = X_{a\ell} + \frac{X_{aq}X_{Dq}}{X_{aq} + X_{Dq}} \tag{A-18}$$

$$X_q = X_q' = X_{a\ell} + X_{aq} \tag{A-19}$$

GARRETT
AIRESEARCH MANUFACTURING COMPANY OF ARIZONA
A DIVISION OF THE GARRETT CORPORATION

APPENDIX VI

ACTIVE FILTER CONSIDERATIONS

(5 pages)

ACTIVE FILTER CONSIDERATIONS

Consideration has been given to the filter problem, since the [illegible]-out tests were performed. It is felt that the system requirements can be reduced to two basic items.

(a) The waveform to the vehicle load should be sinusoidal.
(b) The waveform sensed by the VRE must be sinusoidal.

Previous approaches included:

(a) A speed control filter for reduction of harmonics reflected back on the alternator output due to load-switching (refer to sketch below). This will not completely satisfy requirements (a) and (b) above because the harmonic content of the output of the generator, due to the generator itself, can be 5 percent.

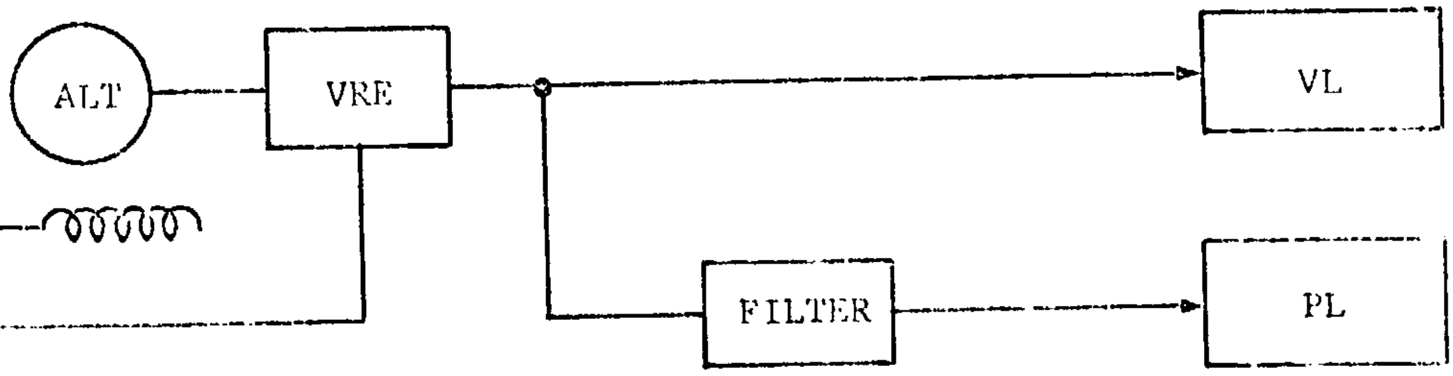

(b) The VRE could be modified to incorporate a small filter or a scheme for sensing RMS voltage. This could be accomplished with a relatively small lightweight package.

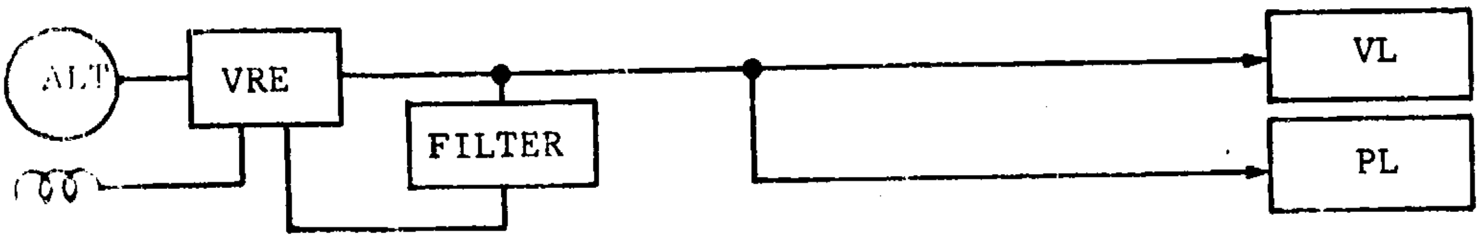

This approach satisfied requirement (b) but not (a). Without knowledge of the details of the entire electrical system and the nature of the vehicle load, judgment cannot be made regarding the adequacy of this approach.

A more direct approach which does satisfy both of the basic requirements is placing a filter on the vehicle load lines with sensing leads for the VRE downstream from this filter.

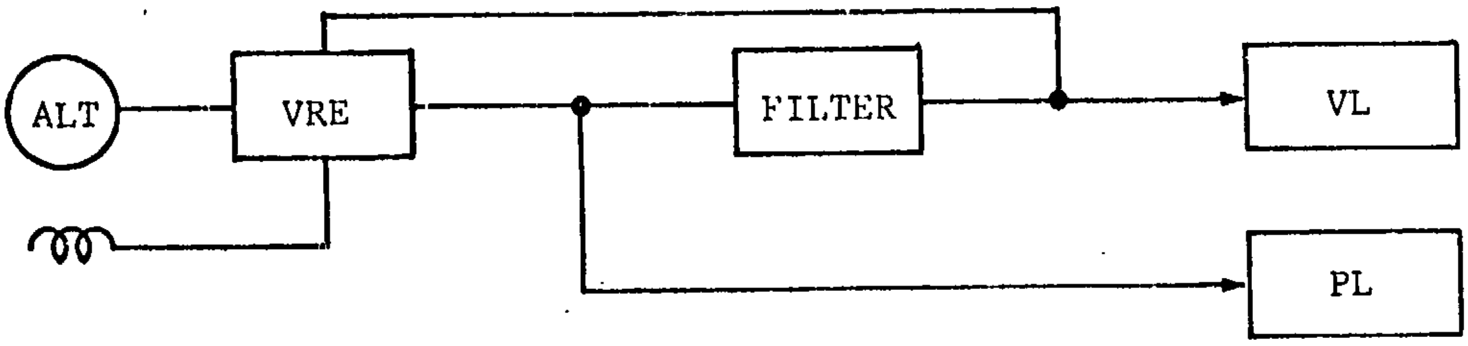

One approach to this filter would be the insertion of reactive components in series and parallel with the load. This would require an accurate description of the load and the design becomes quite difficult if the load power factor is variable. Furthermore, this approach is unattractive because this type of filter must handle the fundamental voltage and load current. Therefore, size and weight become quite large.

It should be noted that the purpose of the filter is to remove the harmonics which, in this case, are all odd and total about 7 percent of the fundamental. An effective approach, utilized by the contractor in production equipment, is to monitor the output and to induce complementary voltages on the line to oppose the harmonics.

By using an active as opposed to a passive element filter, the overall size, weight, and effectivity can be greatly improved. The block diagram (Figure 1) shows the arrangement for an active filter. In this case the harmonic content (distortion) is reduced in proportion to the amplification factors K_1 and K_2. The preamplifier, K_1, is in the audio range and easily kept at a low power level. A high open-loop gain results in a high rejection of the harmonic content. In the power section of this device, the fundamental is not attenuated; the only action of the filter is to oppose the higher harmonics.

Analysis of failure modes show two possibilities. The first and more probable would be a shorted output. This type of failure results in loss of filter action only, that is, no attenuation of the terminal voltage. In the second type of failure, which is an open circuit, there would also be a loss of filter action and a small reduction in the terminal voltage. The actual change in terminal voltage, for this type of failure, would be a function of the volt-second integral of the transformer. This is a constant which is the sum of the volt-second integrals of the harmonic content.

The present distortion is a small fraction of the fundamental (about 7 percent) and consists of odd harmonics.

In reference to this same logic, the power amplifier will only furnish power necessary to eliminate the harmonic content. This is a relatively small amount and can be accurately expressed by the following relationship:

$$P_o = \frac{\left(\sum_{o}^{2\pi} e \sin n\omega t dt \right)^2}{R_L}$$

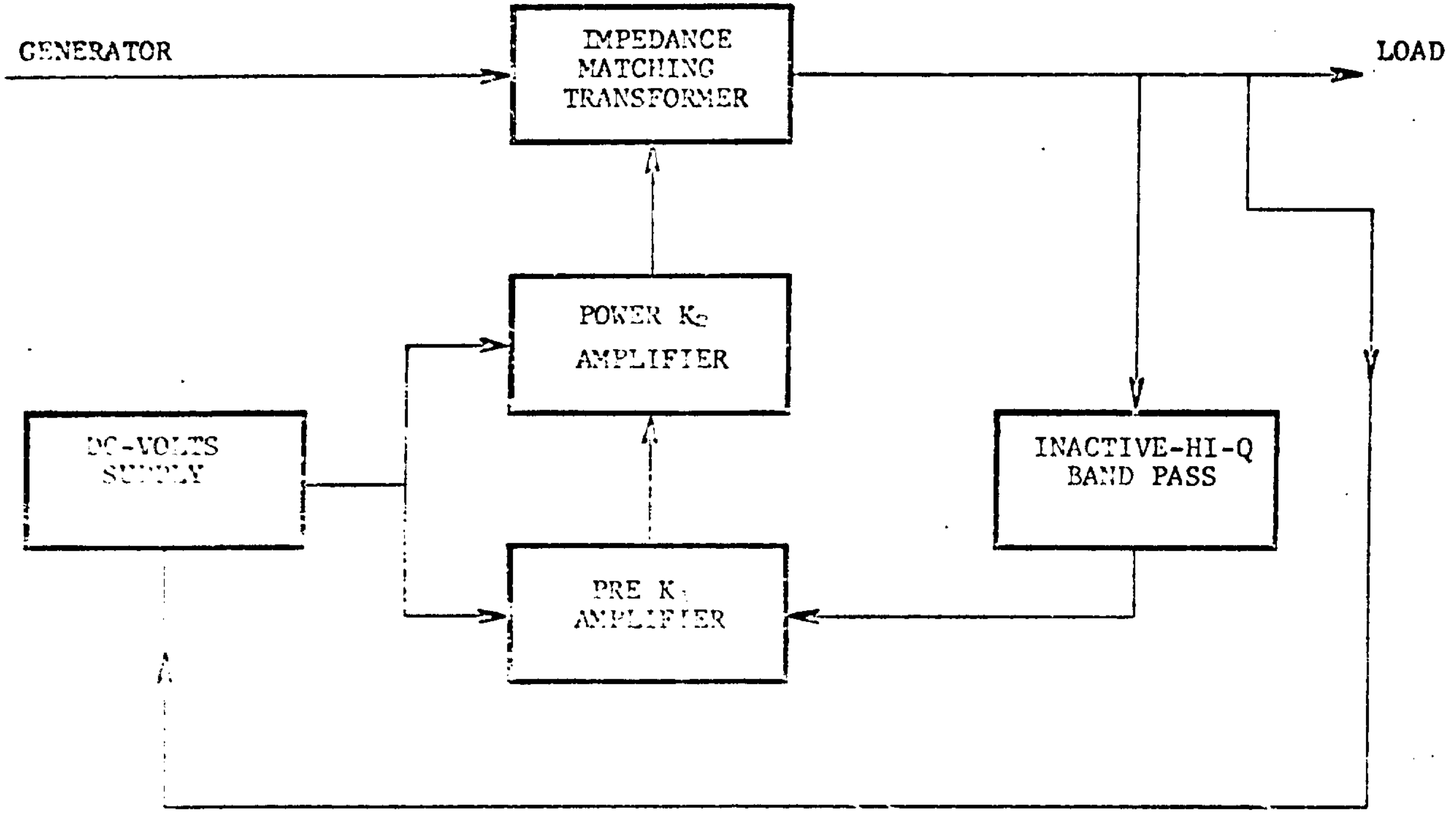

FILTER CIRCUIT FOR REDUCTION OF
HARMONICS GENERATED BY SPEED CONTROL
SWITCHING

FIGURE 1

where "n" represents the odd harmonics and R_L is the bus-bar load. It is assumed that the wave shape is symmetrical about the 0-V axis which eliminates the d-c component and even harmonic distortion.

This type of filtering can be made very efficient for several reasons. First, the filter is designed as an impedance-matching device which offers no rejection to the fundamental. This means a reduction in the magnetics since the flux densities are related to harmonic content only. Second, a different type of magnetics can be used, such as square hysteresis loop material. This fact alone will reduce weight and size as well as increase the efficiency of power transfer. The effective series resistance which results from this filter will be much less because the magnetic requirements are far less demanding than for a passive element.

This type of filter has been used in other applications and represents a proven concept.

AIRESEARCH MANUFACTURING COMPANY OF ARIZONA
A DIVISION OF THE GARRETT CORPORATION

APPENDIX VII

SYSTEMS ANALYSIS

(20 pages)

SYSTEMS ANALYSIS

System Description - Systems at three power levels were simulated, consisting of the complete BRU, VRE, and speed control. Each component was linearized about the appropriate steady-state operating point.

BRU

The BRU unit is described dynamically by deriving linearized perturbation equations about a steady-state operating point. The system under consideration is shown below in Figure 1.

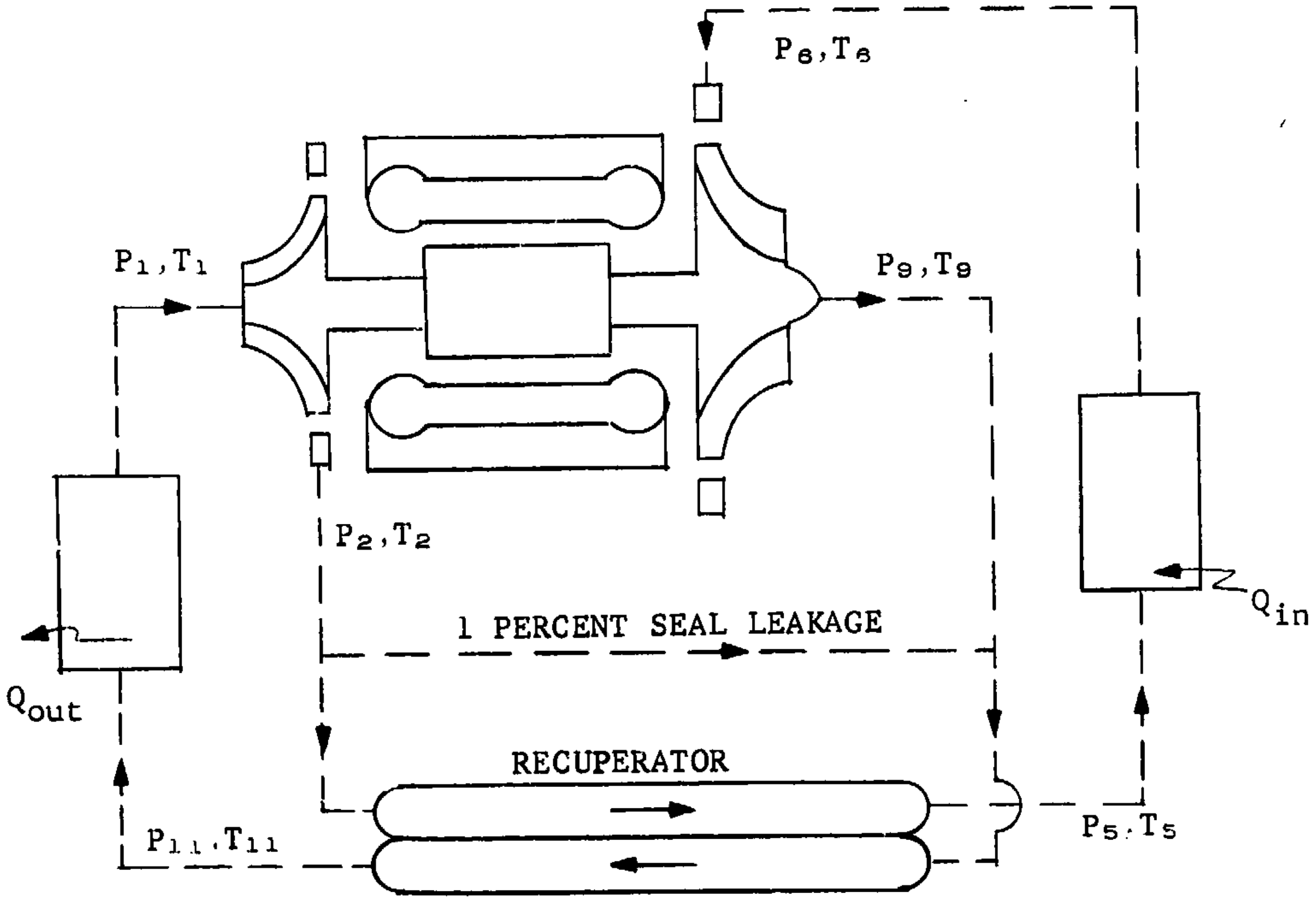

FIGURE 1

The compressor and turbine are described by two maps each. They are corrected-torque (Q/δ) and corrected-weight flow ($W\sqrt{\theta}/\delta$) versus pressure ratio (P_2/P_1) and corrected-speed ($N/\sqrt{\theta}$). Differentiation using lower case letters for perturbated quantities yields:

$$q_c = \frac{\partial Q_c}{\partial P_1} p_1 + \frac{\partial Q_c}{\partial P_2} p_2 + \frac{\partial Q_c}{\partial N} n \tag{1}$$

$$w_{12} = \frac{\partial W_{12}}{\partial P_1} p_1 + \frac{\partial W_{12}}{\partial P_2} p_2 + \frac{\partial W_{12}}{\partial N} n \tag{2}$$

for the compressor and

$$q_t = \frac{\partial Q_t}{\partial P_1} p_1 + \frac{\partial Q_t}{\partial P_2} p_2 + \frac{\partial Q_t}{\partial N} n \tag{3}$$

$$w_{69} = \frac{\partial W_{69}}{\partial P_1} p_1 + \frac{\partial W_{69}}{\partial P_2} p_2 + \frac{\partial W_{69}}{\partial N} n \tag{4}$$

for the turbine, assuming $p_1 = p_9$ and $p_2 = p_6$. Two additional equations relate pressures and flow between components; they are:

$$p_1 = \frac{\gamma R}{(V/T)_1} \frac{[w_{69} - w_{12}]}{S} \tag{5}$$

$$p_2 = \frac{\gamma R}{(V/T)_2} \frac{[w_{12} - w_{69}]}{S} \tag{6}$$

where

$$(V/T)_1 = \frac{V_1}{T_1} + \frac{V_9}{T_9} + \frac{V_{11}}{T_{11}},$$

$$(V/T)_2 = \frac{V_2}{T_2} + \frac{V_5}{T_5} + \frac{V_6}{T_6}$$

γ = specific heat ratio

R = gas constant

V = volume

T = absolute temperature

Combining Eq. (2), (4), (5), and (6) yields:

$$(\tau_1 S + 1)p_1 = \frac{\partial P_1}{\partial P_2} p_2 + \frac{\partial P_1}{\partial N} n \tag{7}$$

$$(\tau_2 S + 1)p_2 = \frac{\partial P_2}{\partial P_1} p_1 + \frac{\partial P_2}{\partial N} n \tag{8}$$

Finally, the turbine, compressor, and absorbed-load torque q_a are equated by:

$$n = \frac{1}{JS} [q_t - q_c - q_a] \tag{9}$$

where

J = rotor inertia

S = Laplace operator

The block diagram illustrated in Figure 2 is the result of combining Eq. (1), (3), (9), and then (7), (8), and (9). An analog diagram is shown in Figure 3.

Alternator and VRE

The alternator and VRE are represented in block diagram form in Figure 4. The system consists of series- and shunt-field loops which influence the alternator voltage output. The series field includes a machine characteristic which internally tends to compensate for alternator load fluctuations. The shunt field circuit is the control loop which modulates the ampere turns (NI) in an effort to maintain constant terminal voltage. The total of alternator ampere turns is physically constrained within limits. The input to this portion of the system is in terms of the alternator perturbation, ΔKVA. The corresponding analog computer diagram is shown in Figure 5.

Speed Control

The speed-control dynamics included in the simulation are given as:

$$\frac{P_p}{n} = \frac{10.5/360}{(0.05S + 1)(0.0157S + 1)^2(0.000825S + 1)^2} \qquad (10)$$

where

P_p = parasitic load change (KW)

n = BRU speed perturbation (rpm)

S = Laplace operator (sec.^{-1})

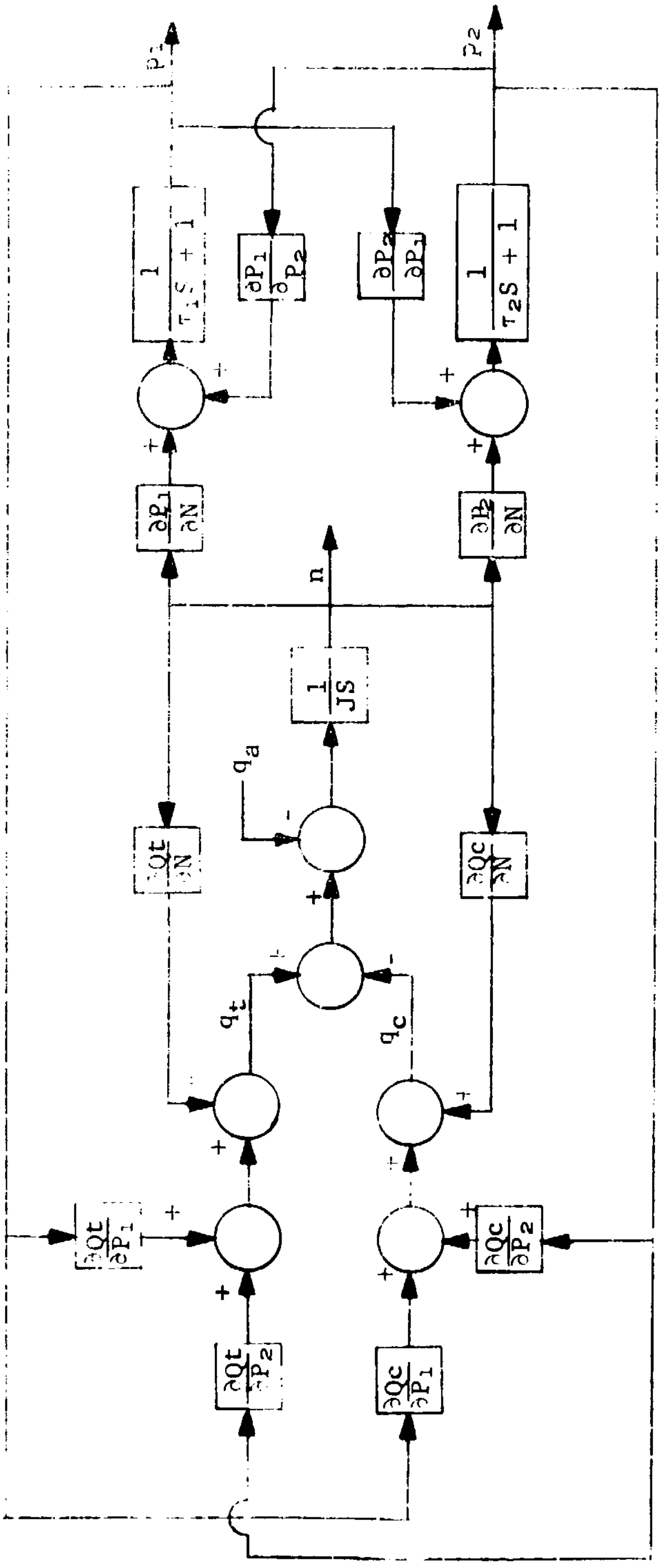

PREPARED	GM	4-67
WRITTEN		
APPROVED		

BLOCK DIAGRAM
NASA BRU

AiResearch Manufacturing Company of Arizona

A40480

FORM P782A-1

FIGURE 2

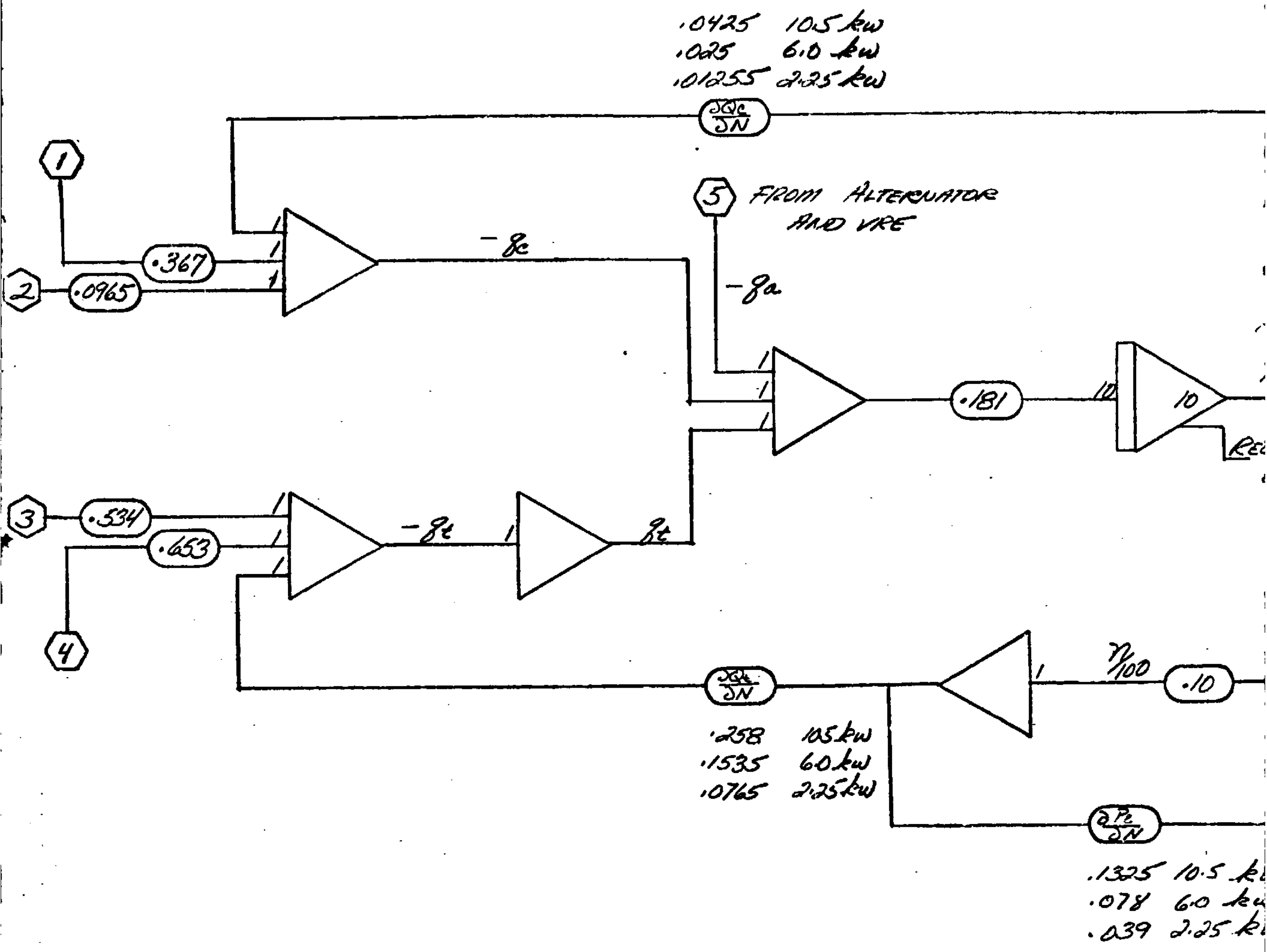
.0425 10.5 kw
.025 6.0 kw
.01255 2.25 kw
∂Qc/∂N
1
2
.367
.0965
1
1
1
-qc
5
FROM ALTERNATOR AND VRE
-qa
1
1
1
.181
10
10
Rec
3
4
.534
.653
1
1
1
-qt
1
qt
∂Qt/∂N
.258 10.5 kw
.1535 6.0 kw
.0765 2.25 kw
1
N/100
.10
∂Pc/∂N
.1325 10.5 k
.078 6.0 k
.039 2.25 k

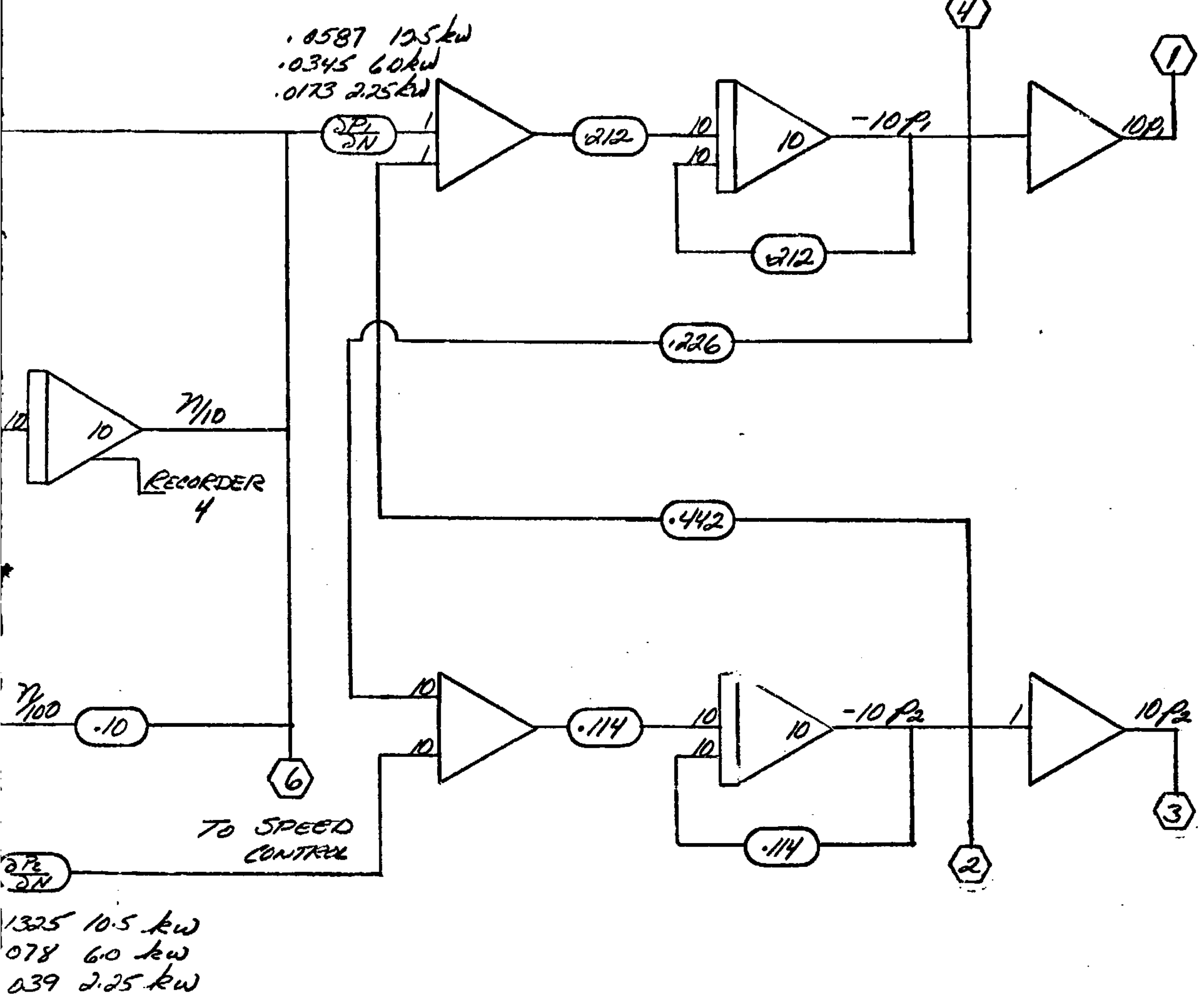

APS-5286-R
APPENDIX VII
Page 6

PREPARED	GM	4-67	ANALOG DIAGRAM NASA BRU	A40481
WRITTEN				
APPROVED	mk	4-67	AiResearch Manufacturing Company of Arizona	

FORM P783A-1

FIGURE 3

FOLDOUT FRAME

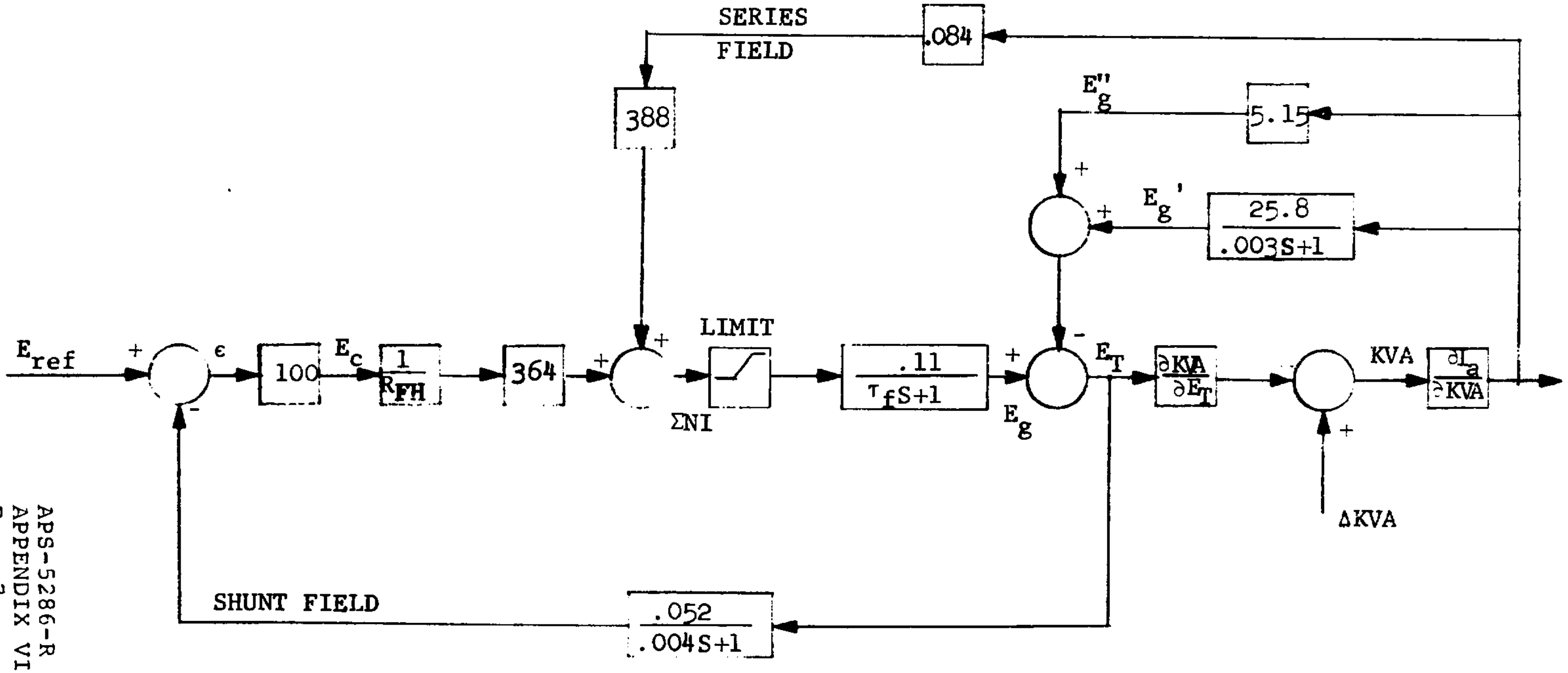

PARAMETERS FOR A HOT ALTERNATOR

E_{ref} = 6.2 VOLTS

R_{fh} - 3.7 OHMS

τ_f 0.1

LOWER LIMIT = 0 AMPERE TURNS

UPPER LIMIT = 4,270 AMPERE TURNS

$$\frac{\partial KVA}{\partial E_T} = \frac{KVA}{E_T}$$

$$\frac{\partial I_a}{\partial KVA} = \frac{I_a}{KVA}$$

PREPARED	GM	4-67	BLOCK DIAGRAM ALTERNATOR AND VRE	A40482
WRITTEN				
APPROVED			AiResearch Manufacturing Company of Arizona	

FORM P793A-1

FIGURE 4

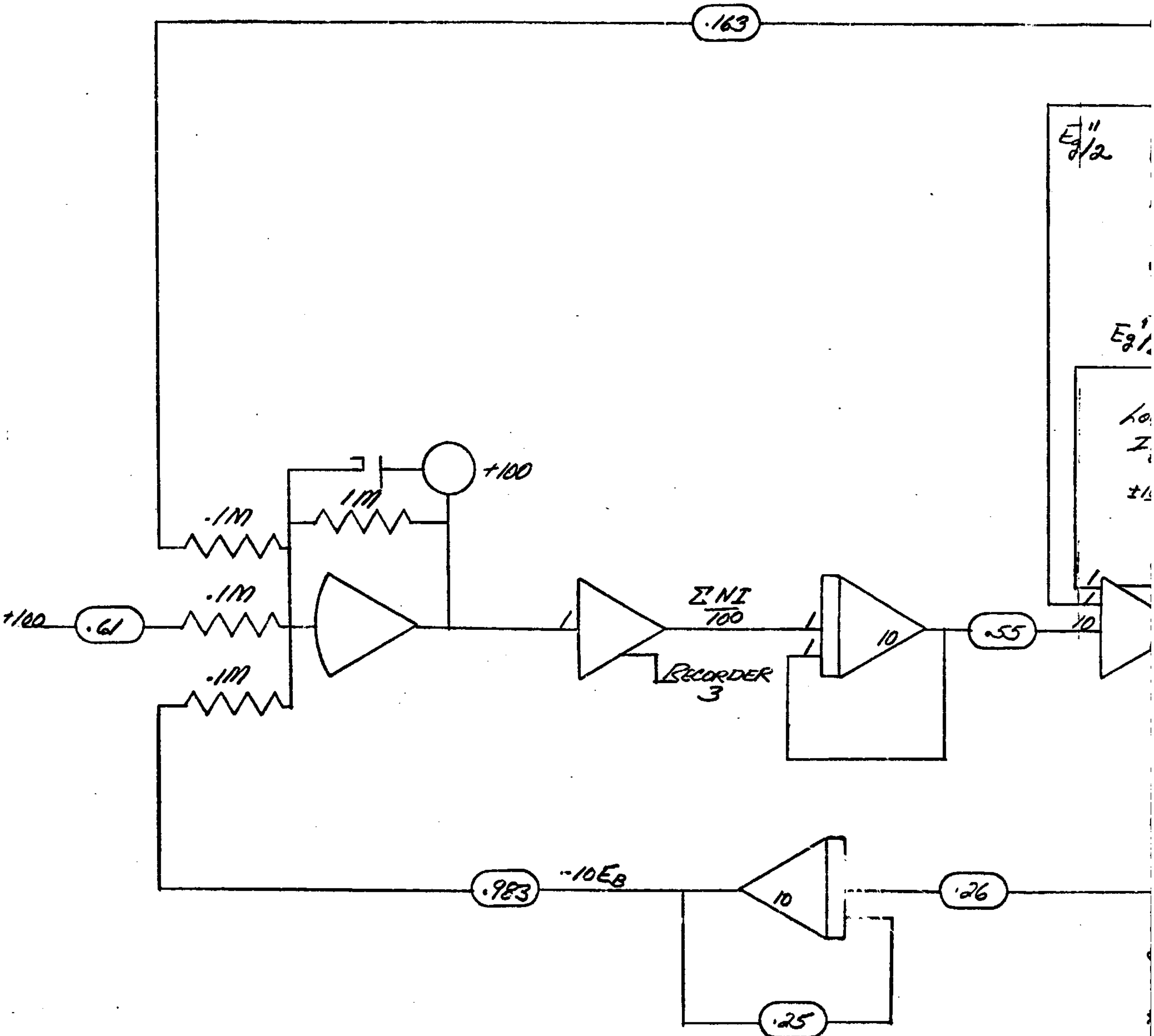
.163
Eg''/2
Eg'/2
+100
1M
.1M
.1M
.1M
+100
.61
1
ΣNI/100
RECORDER 3
1
1
10
.55
1
1
10
-10E_B
.983
10
.26
.25

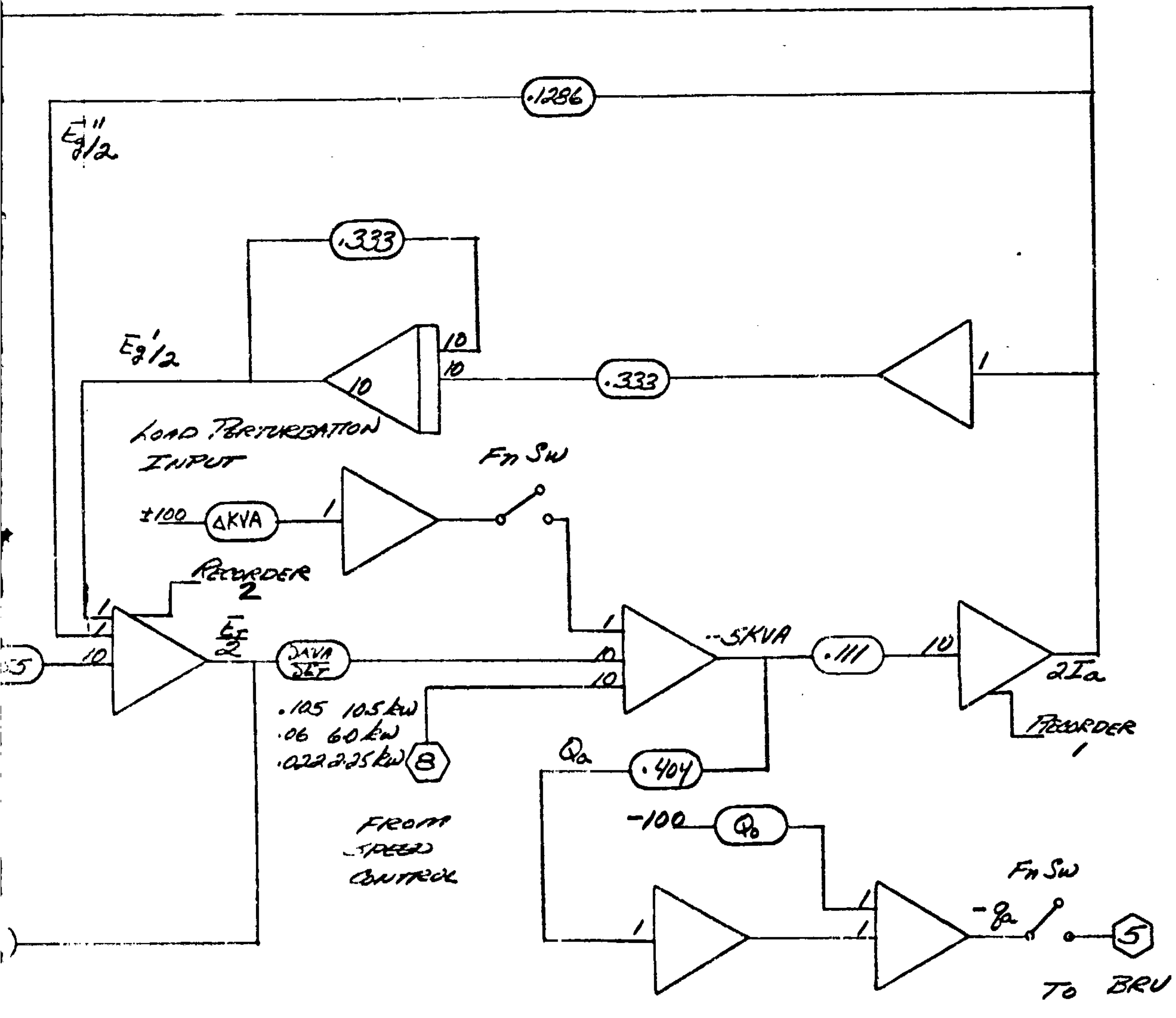

APS-5286-R
APPENDIX VII
Page 8

PREPARED	GM	4-67	ANALOG DIAGRAM ALTERNATOR AND VRE	A40483
WRITTEN				
APPROVED		4-67	AiResearch Manufacturing Company of Arizona	

FORM P7884-1

FIGURE 5

FOLDOUT FRAME

The parasitic load consists of three 6-KW modules incorporated with negligible deadband or overlap. The analog diagram is shown in Figure 6.

Analog Computer Results

The analog computer transient analysis was conducted for three power levels. They were the 10.5-KW full-capacity system and off-design points at 6.0 and 2.25 KW. BRU component parameters at each of these design points are summarized below:

Net Generator Output, KW	2.25	6.0	10.5
Turbine Inlet Temperature, °R	2060	2060	2060
Compressor Inlet Temperature, °R	540	540	540
Shaft Speed, rpm	36,000	36,000	36,000
Compressor Mass Flow, lb/sec	0.377	0.756	1.28
Compressor Inlet Pressure, psia	6.76	13.5	22.9
Compressor Pressure Ratio, lb/sec.	1.9	1.9	1.9
Turbine Inlet Pressure, psia	12.45	25.0	42.1
Turbine Pressure Ratio	1.75	1.75	1.75

Results of this study are shown in Figures 7 through 13. These curves show line current (I_a), terminal voltage (E_t), alternator ampere turns (ΣNI), speed (n), and parasitic load (P_p) as a function of time following a step-load change. Speed is given in terms of a perturbated quantity where zero corresponds to 36,000 rpm or 100 percent. In each case, the system was subjected to full-load step-changes. A discussion on the computer traces follows.

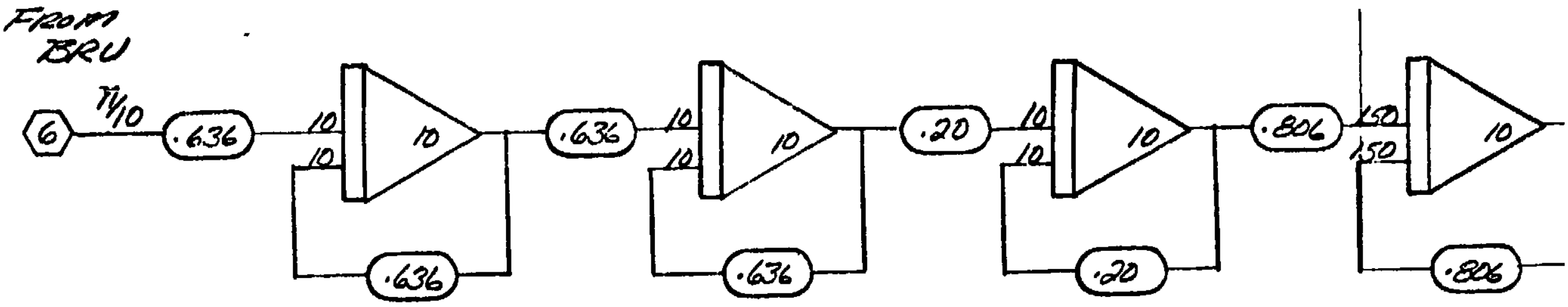

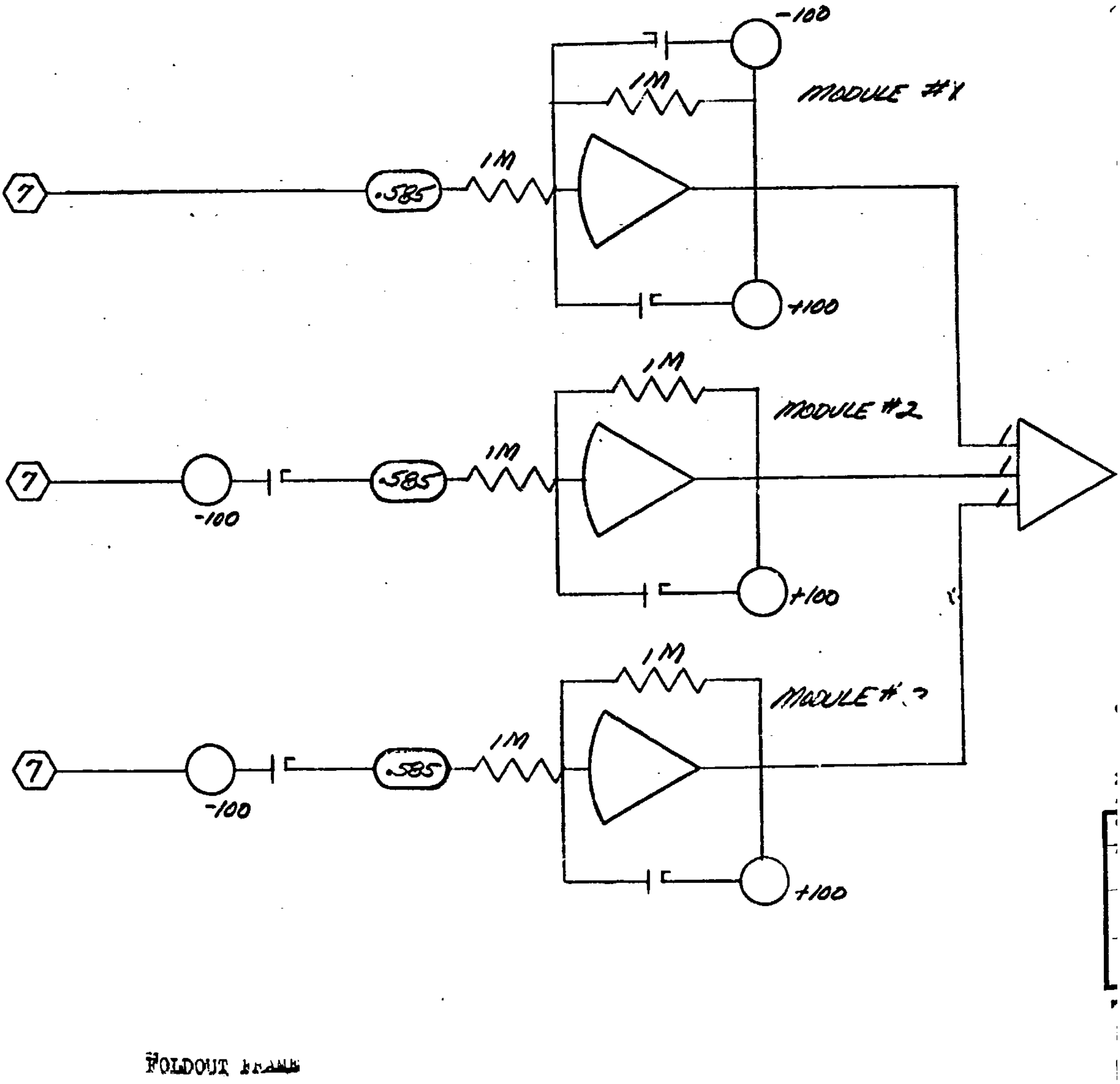

FOLDOUT FRAME

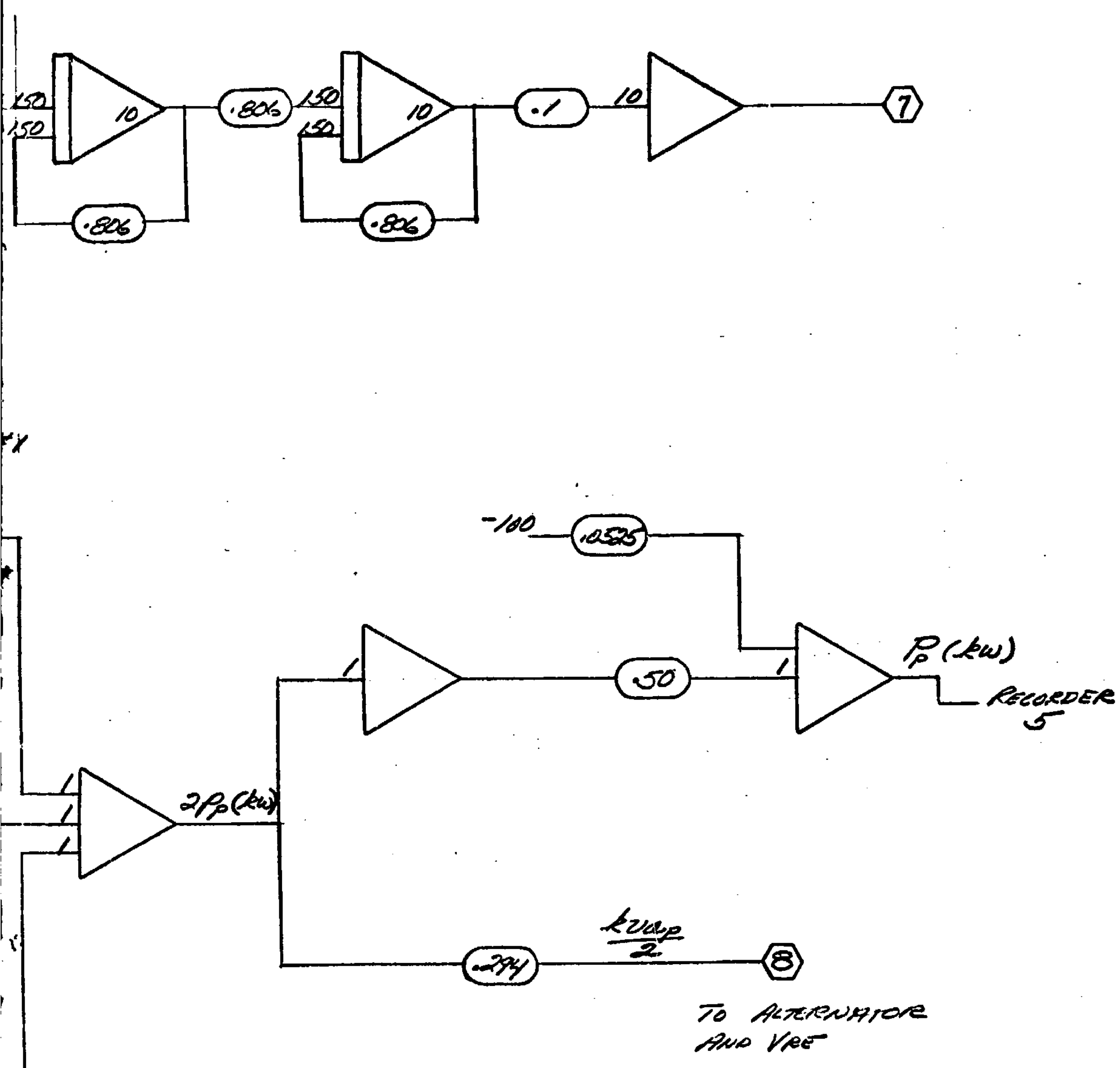

PREPARED	GM	4-67	ANALOG DIAGRAM SPEED CONTROL	A40484
WRITTEN				
APPROVED	M.K.	4-67	AiResearch Manufacturing Company of Arizona	

FORM P703A-1

FIGURE 6

FOLDOUT FRAME

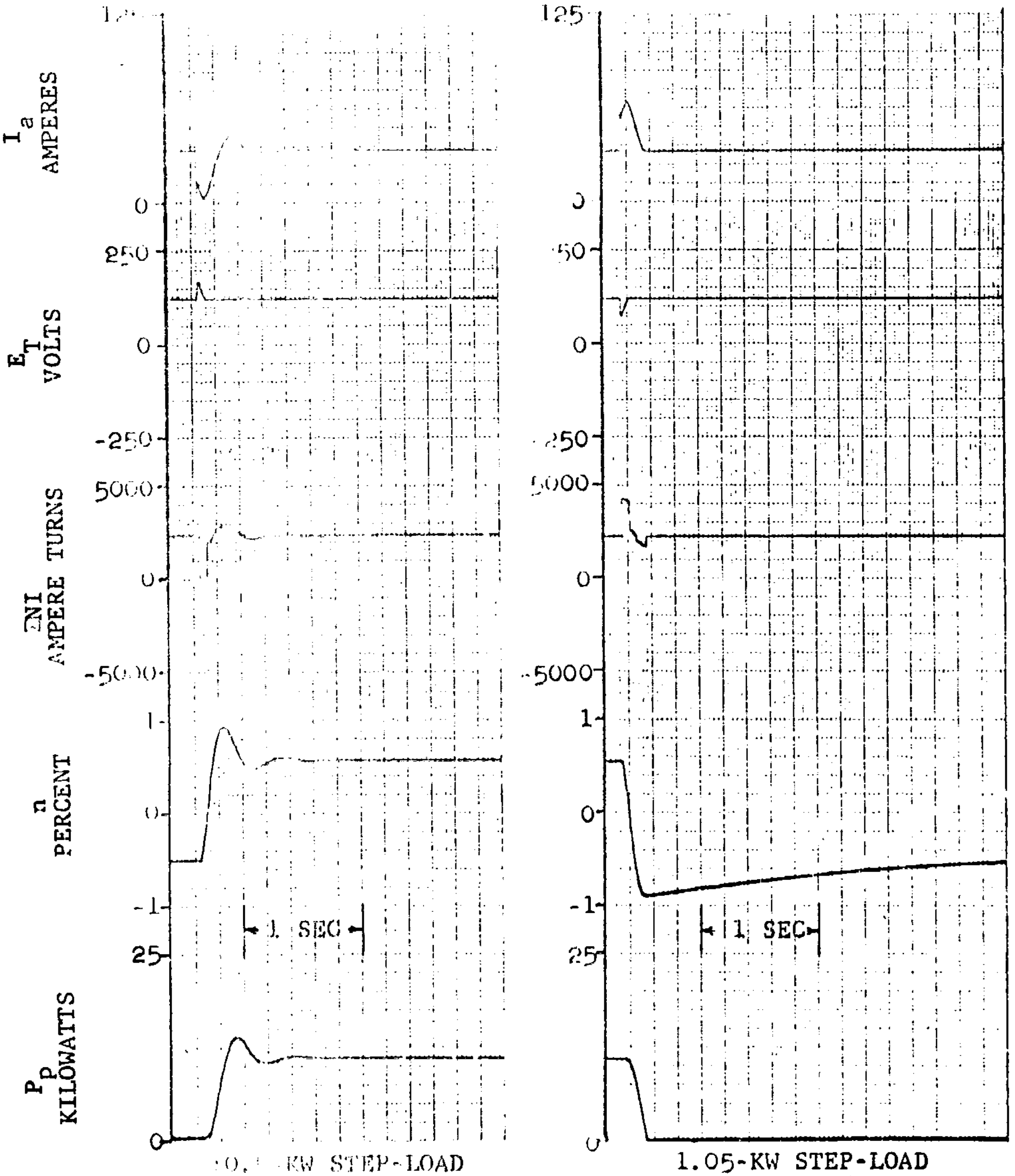

10.5-KW STEP-LOAD DECREASE

1.05-KW STEP-LOAD INCREASE

CONTROL GAIN = 10.5 KW PER 1 PERCENT SPEED ERROR

PREPARED	GM	4-67	NASA BRU WITH VRE AND SPEED CONTROL 10.5-KW SYSTEM	A40485
WRITTEN				APS-5286-R
APPROVED		4-67	AiResearch Manufacturing Company of Arizona	Page 11

FORM P728A-1

FIGURE 7

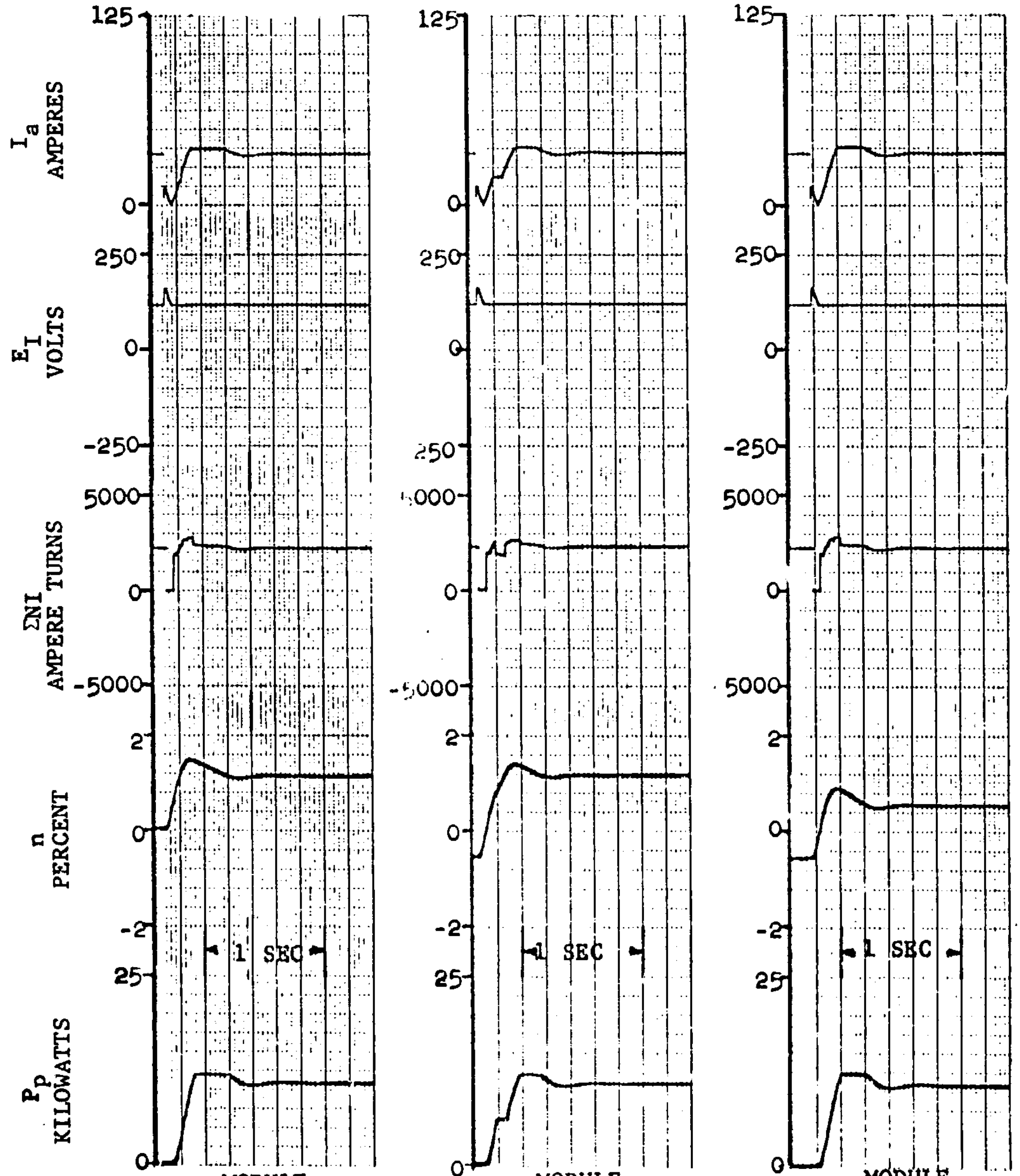

MODULE 1 FAULTED

MODULE 2 FAULTED

MODULE 3 FAULTED

10.5-KW STEP-LOAD DECREASE

CONTROL GAIN = 10.5 KW PER 1 PERCENT SPEED ERROR

PREPARED	GM	4-67	NASA BRU WITH VPE AND SPEED CONTROL 10.5-KW SYSTEM	A40486
WRITTEN				
APPROVED	m.K.	4-67	AiResearch Manufacturing Company of Arizona	APS-5286-R Page 12

FORM P782A-1

FIGURE 8

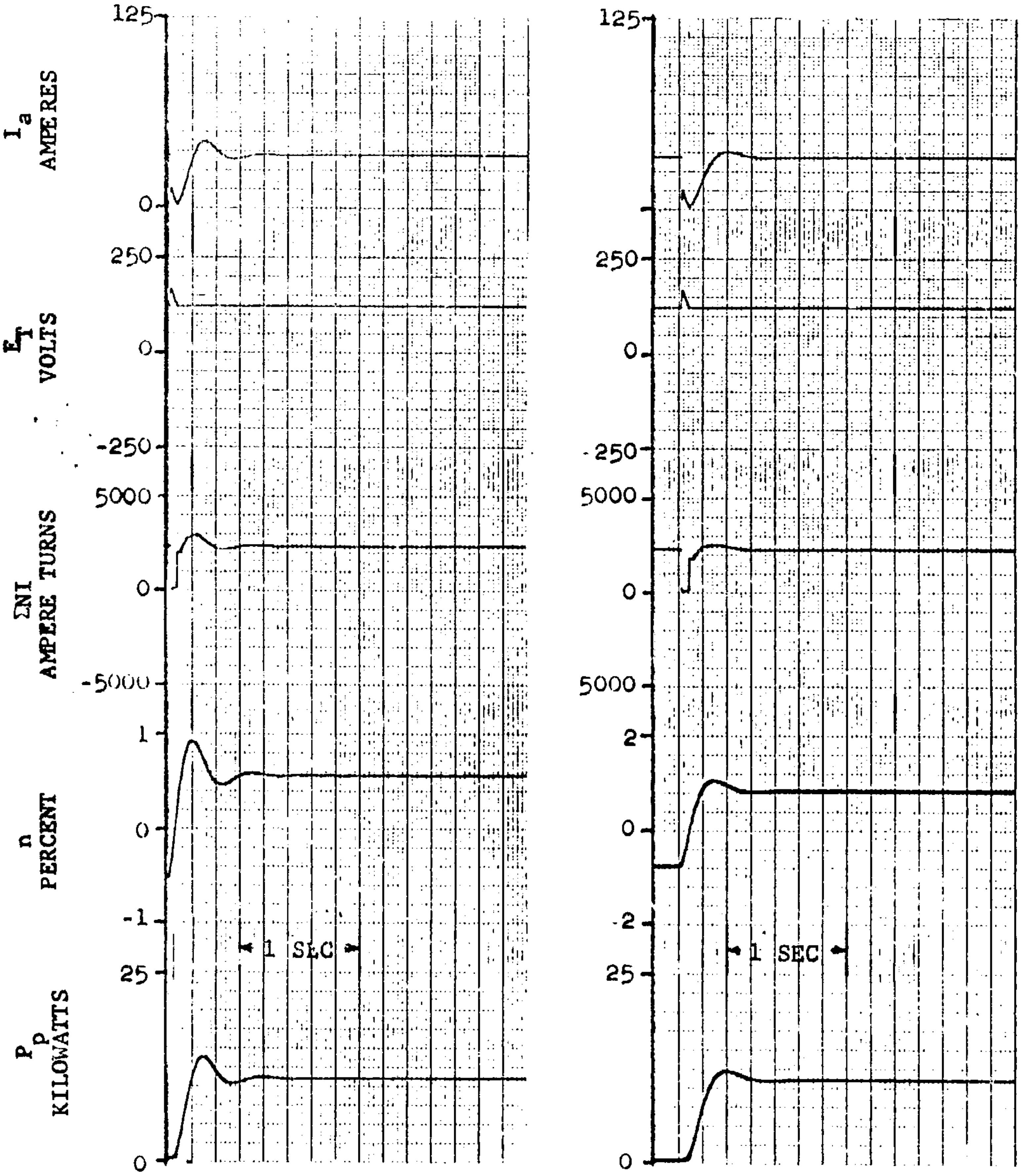

CONTROL GAIN 10.5 KW PER 1 PERCENT SPEED ERROR

CONTROL GAIN - 7.0 KW PER 1 PERCENT SPEED ERROR

10.5 KW STEP-LOAD DECREASE

PREPARED	GM	4-67	NASA BRU WITH VRE AND SPEED CONTROL 10.5-KW SYSTEM	A40487
WRITTEN				
APPROVED	m. k.	4-67	AiResearch Manufacturing Company of Arizona	APS-5286-R Page 13

FORM P7884-1

FIGURE 9

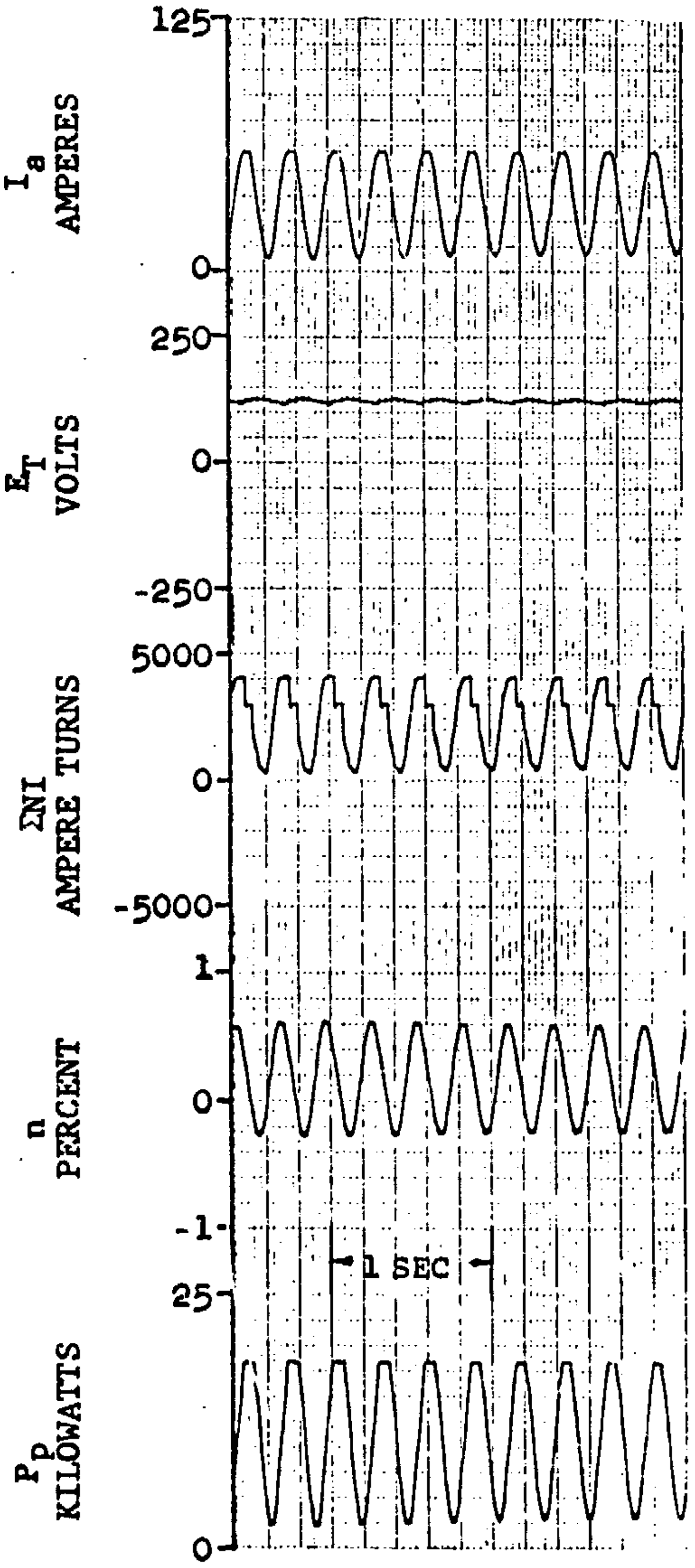

CONTROL GAIN 31.5 KW PER 1 PERCENT SPEED ERROR

PREPARED	GM	4-67	NASA BRU WITH VRE AND SPEED CONTROL 10.5-KW SYSTEM	A40488
WRITTEN				
APPROVED	m. K.	4-67	AiResearch Manufacturing Company of Arizona	

FORM P788A-1

FIGURE 10

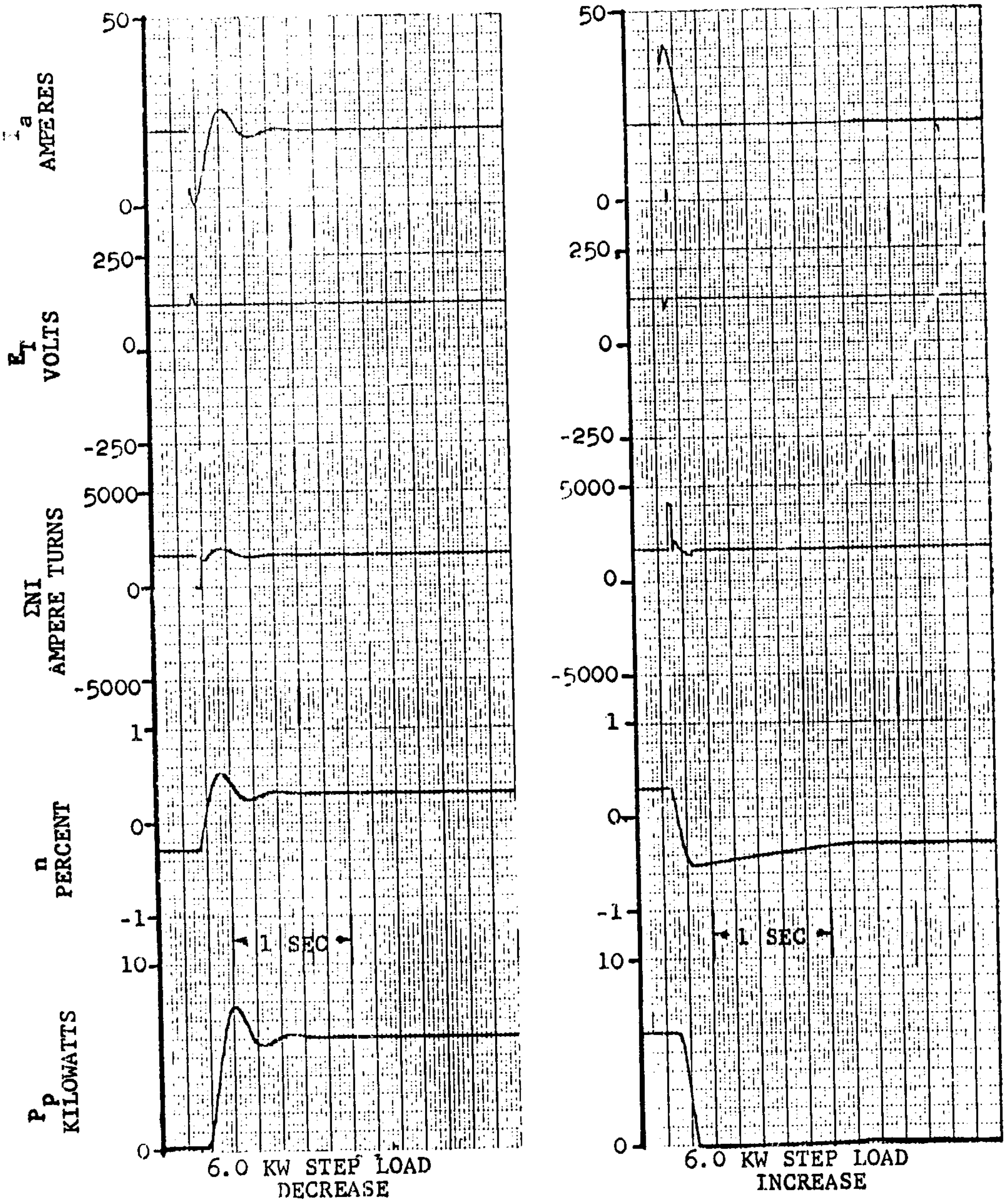

6.0 KW STEP LOAD
DECREASE

6.0 KW STEP LOAD
INCREASE

CONTROL GAIN : 10.5 KW PER 1 PERCENT SPEED ERROR

PREPARED	GM	4-67	NASA BRU WITH VRE AND SPEED CONTROL 6.0-KW SYSTEM	A40489
WRITTEN				
APPROVED	M.K.	4-67	AiResearch Manufacturing Company of Arizona	APS-5286-R Page 15

FORM [illegible]A-1

FIGURE 11

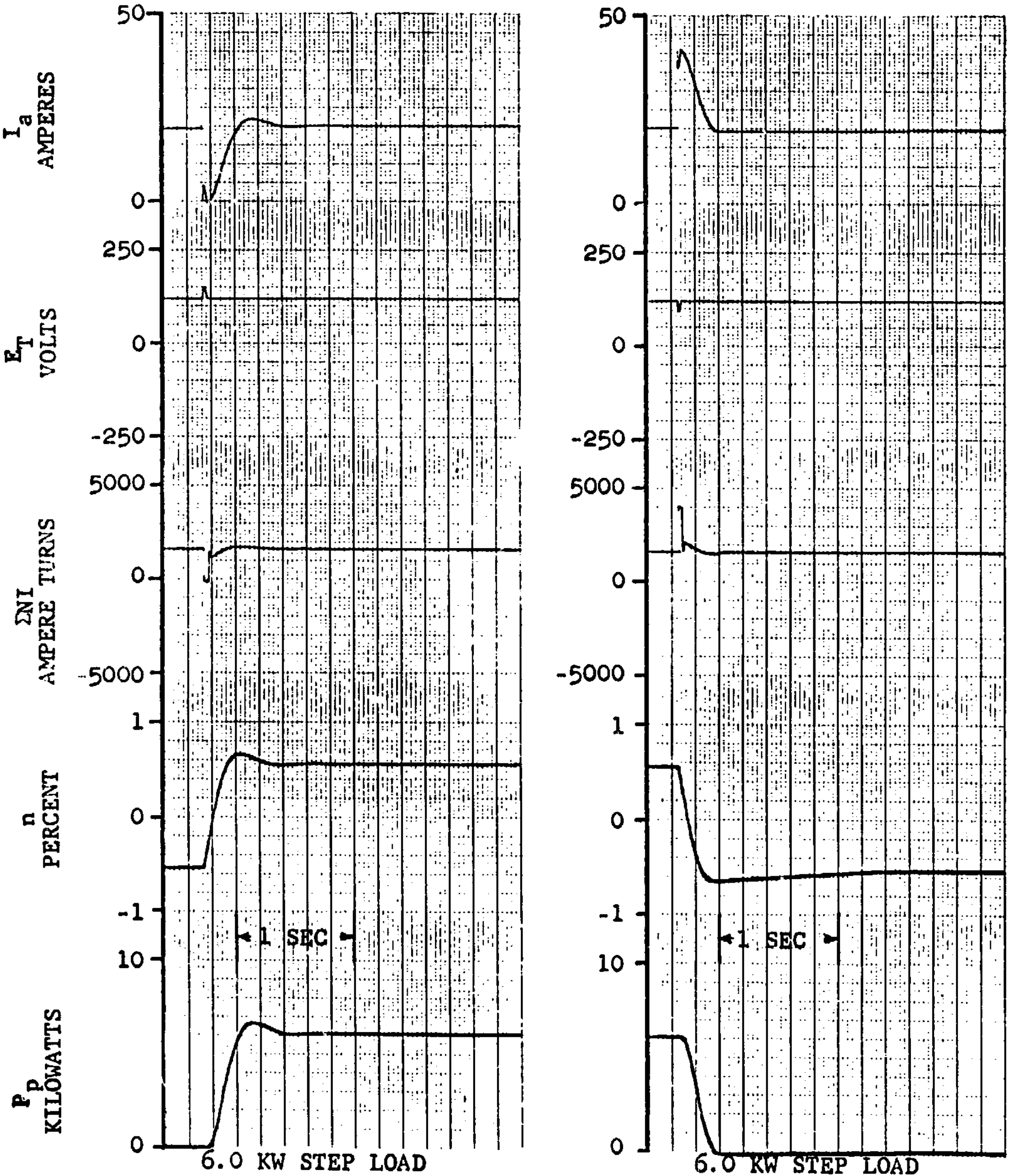

6.0 KW STEP LOAD DECREASE

6.0 KW STEP LOAD INCREASE

CONTROL GAIN = 7.0 KW PER 1 PERCENT SPEED ERROR

PREPARED	GM	4-67	NASA BRU WITH VRE AND SPEED CONTROL 6.0-KW SYSTEM	A40490
WRITTEN				
APPROVED	M.K.	4-67	AiResearch Manufacturing Company of Arizona	APS-5286-R Page 16

FIGURE 12

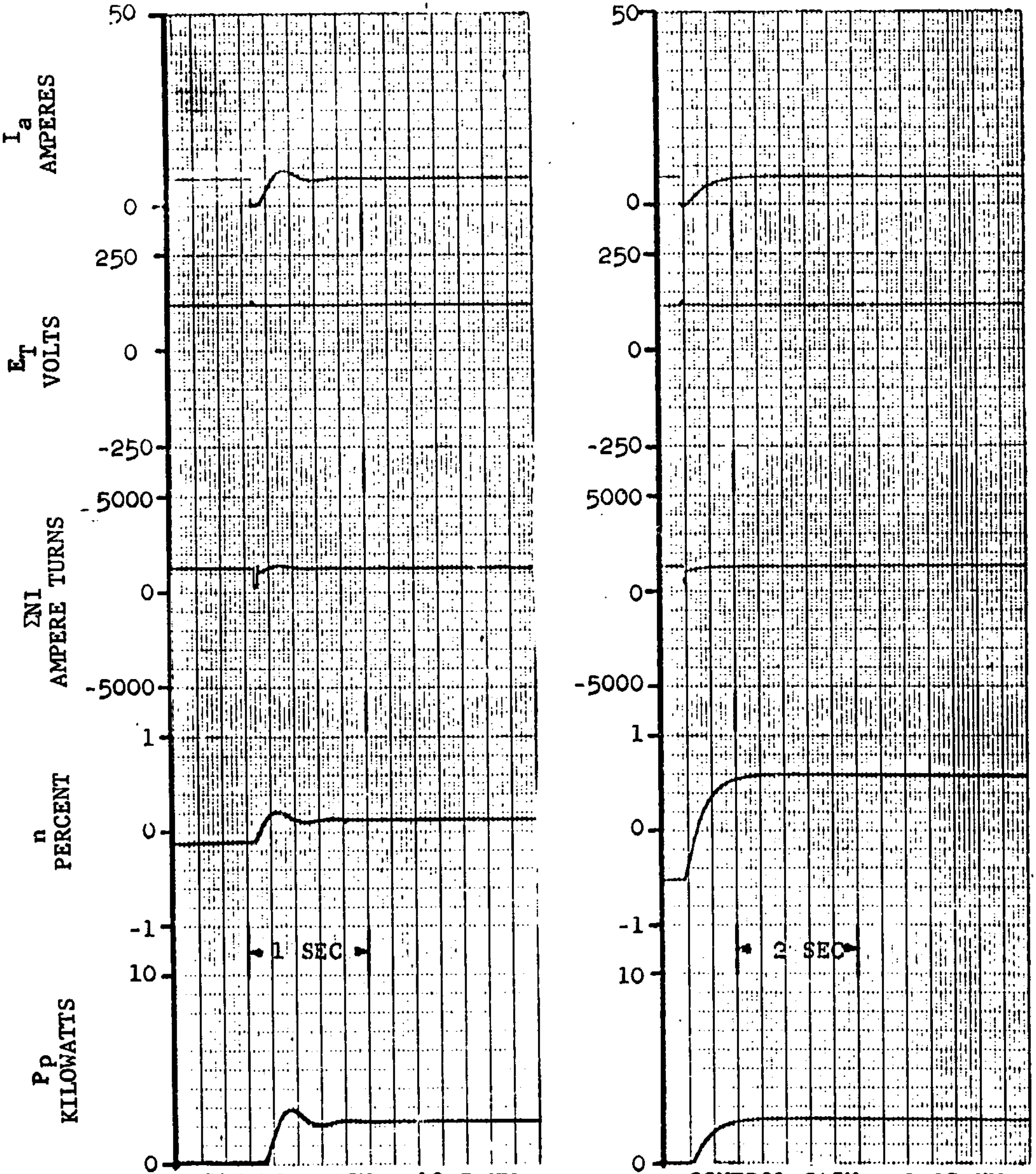

CONTROL GAIN = 10.5 KW PER 1 PERCENT SPEED ERROR

CONTROL GAIN 2.25 KW PER 1 PERCENT SPEED ERROR

2.25 KW STEP-LOAD DECREASE

PREPARED	GM	4-67	NASA BRU WITH VRE AND SPEED CONTROL 2.25-KW SYSTEM	A40491
WRITTEN				
APPROVED		4-67	AiResearch Manufacturing Company of Arizona	APS-5286-R Page 17

FORM P793A-1

FIGURE 13

10.5-Kilowatt System

The system response to instantaneous full-load (10.5 KW) change is shown in Figure 7. The maximum speed excursion is equal to 0.9 percent for increasing and decreasing load. Steady-state is attained within 1.0 sec. following load removal and within 3.2 sec. following load addition. The system responds very quickly to load removals because the parasitic load changes to regulate speed without saturation. When full-load is added, the parasitic load is reduced proportionally to speed error. Upon saturation of the control at 0 KW, the vehicle response then resembles that of an open-loop system. The transient voltage pulse is ±50.0 for a duration of less than 0.08 sec. The steady-state voltage error is imperceptible.

Figure 8 illustrates speed transients following 10.5-KW step-load decreases, assuming one of the three speed control modules has failed. Initially, the vehicle load is 10.5 KW and parasitic load is 0 KW. When the vehicle load is reduced to zero the parasitic load saturates at 12.0 KW, as the speed is sufficiently large. When the following speed reduction is sufficient to demand less than 12.0-KW parasitic load, the control functions in its normal manner, arriving at a steady-state value of 10.5 KW. The speed response is consistent with the control configuration as depicted under each trace. The maximum speed-error is well within the 2-percent design goal, and the time to attain steady-state is less than 1.0 sec.

The effect of control gain is illustrated in Figure 9. Each system is subjected to a 10.5-KW load removal. The higher gain system (10.5 KW/1 percent speed-error) limits the maximum speed-error to 0.9 percent but does not attain steady-state until 1.0 sec. has elapsed. The system with 7 KW/1 percent gain overshoots to approximately 1.05 percent and reaches steady-state within 0.6 sec. However, the steady-state speed-error is 0.8 percent compared with approximately 0.5 percent. Seven KW/1 percent speed-error control gain appeared to be optimum with regard to minimum settling time without yielding excessive speed overshoots. It would be advantageous to fabricate the breadboard speed control so that this gain is adjustable and an optimum value is obtained by experimentation with the actual hardware.

Limit-cycle operation is shown in Figure 10 with a control gain of 31.5 KW/1 percent speed-error. This gain is just sufficient to cause the system to become unstable. The gain margin is, therefore, 31.5/10.5 = 3.0 KW. The period for one cycle is 0.3 sec. which corresponds to a frequency of 3.33 Hz.

2.5- and 6.0-Kilowatt System

Generally, the above comments also apply to the 6.0- and 2.25 KW-systems. Speed overshoots, voltage fluctuations, and response times at the lower power levels are less than those existing at the 10.5-KW level. Typical transient responses of the 6.0-KW system are shown in Figures 11 and 12.

Figure 13 illustrates the full-load transient speed response for the 2.25-KW system with gains of 10.5 and 2.25 KW/1 percent speed-error. This system is characterized by minor voltage fluctuations as a result of small-load perturbations. The speed response is reasonably fast when the standard 10.5-KW/1 percent gain is employed and substantially overdamped and slow with the 2.25-KW/1 percent speed-control gain.

Conclusions

The transient analysis of the speed control, including the effect of interactions between the speed-control and the VRE systems, has been completed and the results are very encouraging. It appears that the system, as presently defined, will meet the design specification; namely, "Transient frequency excursions shall remain within ±2 percent of 1200 Hz with a recovery time of 1 sec., with no sustained oscillations, when step-load changes of one per unit-load are made."

To summarize the results of the study:

(a) For the 10.5-KW system, having a speed-control gain in the range of 10.5 to 7.0 KW/1 percent speed-error, the transient specification can be met.

(b) The 10.5-KW system is the worst-case over the power level range of interest.

(c) Although the specification does not cover speed-control module faults, they were investigated in the study. It was found that the speed excursion remained within 2 percent of the nominal, even though a fault should occur in any one of the three speed-control modules.

(d) The speed-control gain can be increased to about 31.5 KW/1 percent speed-error before system instability results. However, for speed-control gain values above 10.5 KW/1 percent speed-error, oscillations are sustained for increasing lengths of time.